به‌نام خدا

سیستم‌های شاسی و بدنه خودرو

مفاهیم و روابط مقدماتی سیستم ترمز

دوره کارشناسی ارشد مهندسی خودرو
دانشگاه علم و صنعت ایران

پاییز ۹۵

AutoLibrary

Braking System

Braking system must accomplish three different tasks:

- *To stop the vehicle completely.*
- *To control speed*
- *To keep the vehicle stopped on a slope.*

Other than the design of the system itself, the performance of the system is conditioned by factors outside the system, such as:

- Payload and its distribution in the vehicle
- Road slope
- Longitudinal acceleration

Braking System

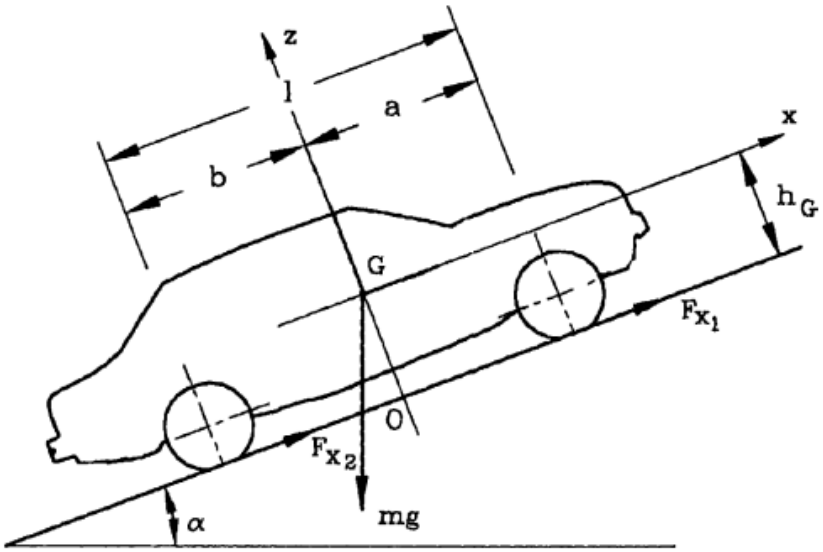

- Maximum braking forces are determined by *m, b, a, h_G (load conditions).*
- *These forces are also determined by the braking deceleration ax.*
- *Braking force distribution between the two axles is also determined by the* obtained longitudinal acceleration.

Braking System

These functions are accomplished in a vehicle by three different systems:

- Service braking system (normal driving conditions)
- Emergency or secondary braking system (in case of failure of the normal brake)
- Parking braking system (for parking and slopes)

Braking System

- On a perfectly paved road, this stopping distance must be obtained:

$$s \leq 0.1V + \frac{V^2}{150}$$

s is the stopping distance (m)

V is the car speed (km/h) at the onset of braking

- an increased distance is allowed when one of the circuits is broken (only the emergency system is functional)

$$s \leq 0.1V + \frac{2V^2}{150}$$

Braking System

For a service circuit, an average deceleration

$$a \geq 2.9\ m/s^2$$

With the emergency circuit it can be increased to

$$a \geq 5.8\ m/s^2$$

- A further condition applies to the control force needed to achieve such a stopping distance. This force, applied to the pedal by the driver's foot, must be:

$$F_p \leq 500\ N$$

Braking System

Parking system:

- The parking braking system must be designed to keep the vehicle stopped on a slope of:

$$i \geq 18\%$$

- or to reduce its speed, on a flat road, by an acceleration of:

$$a \geq 1.5\ m/s^2$$

- after having applied on the control a force:

$$F_p \leq 500\ N\ ;\ F_m \leq 400N$$

Braking System

Disc brakes:

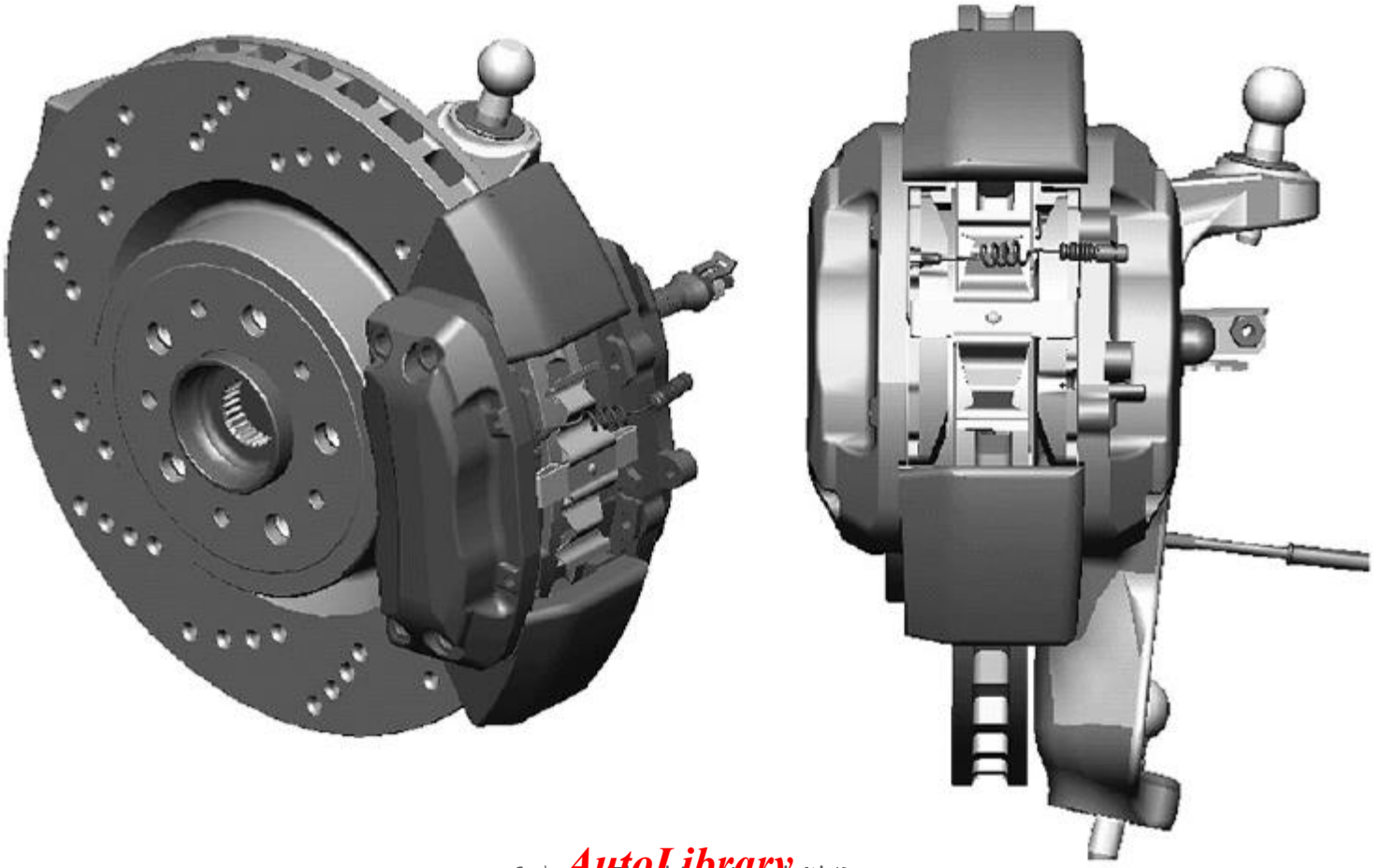

Braking System

Drum brakes:

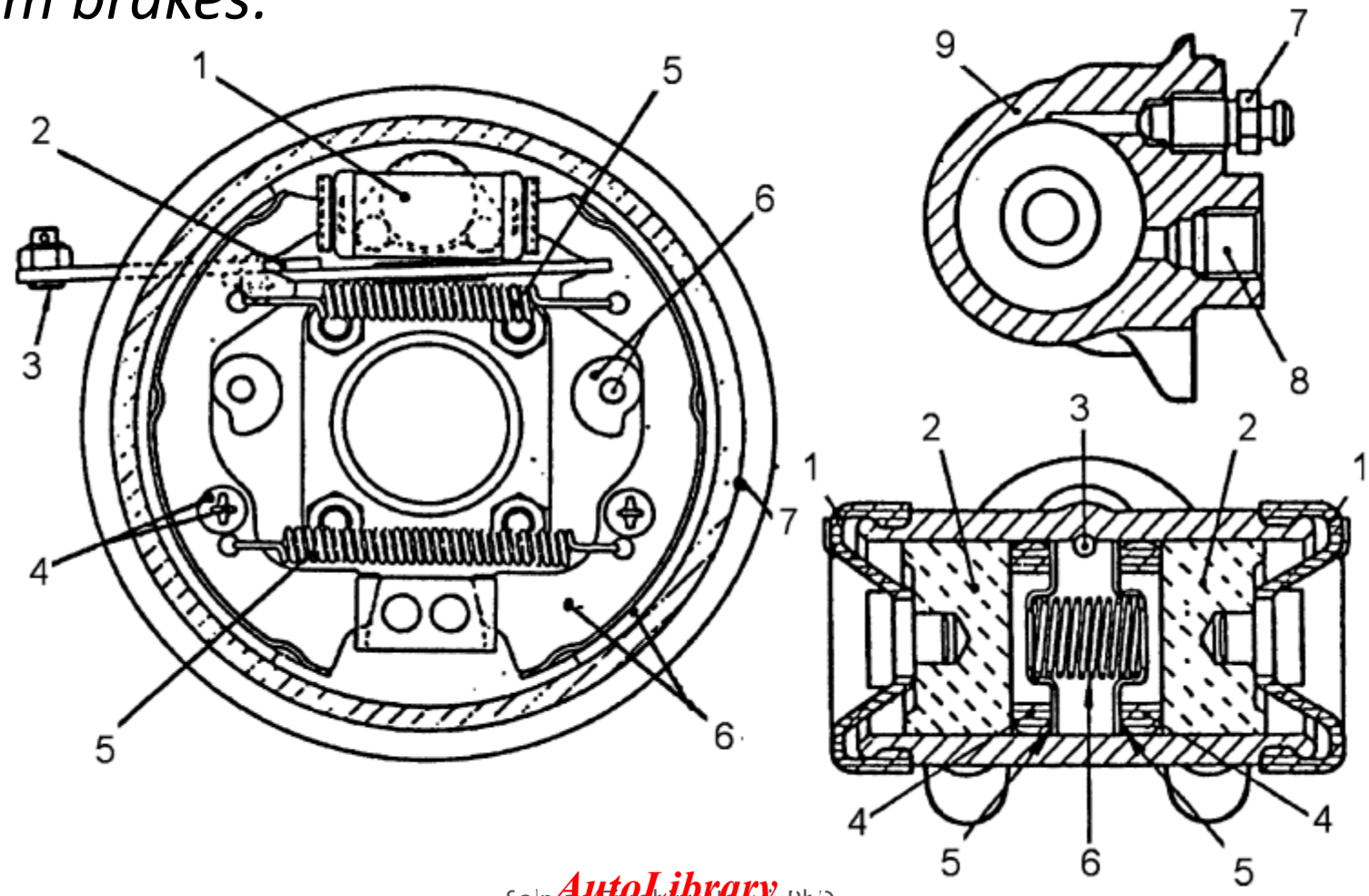

Braking System

Control system components:

- Pump
- Braking fluid
- Distributor

Braking System

INDUSTRIAL VEHICLE BRAKES*:*

- European homologation regulations impose on commercial or industrial vehicles a minimum stopping distance

$$s \leq 0.15V + \frac{V^2}{103,5}$$

- With the emergency brake, the stopping distance can rise to:

$$s \leq 0.15V + \frac{2V^2}{c}$$

- where *c is 115 for industrial and commercial vehicles for transportation of goods* and 130 for buses

Braking System

- With the emergency circuit the accepted mean deceleration is:

$$a \geq 2.2 - 2.5\ m/s^2\ ,$$

- while for the service circuit it is:

$$a \geq 4.0\ m/s^2$$

Braking System Design for Passenger Cars

ISO coordinate system

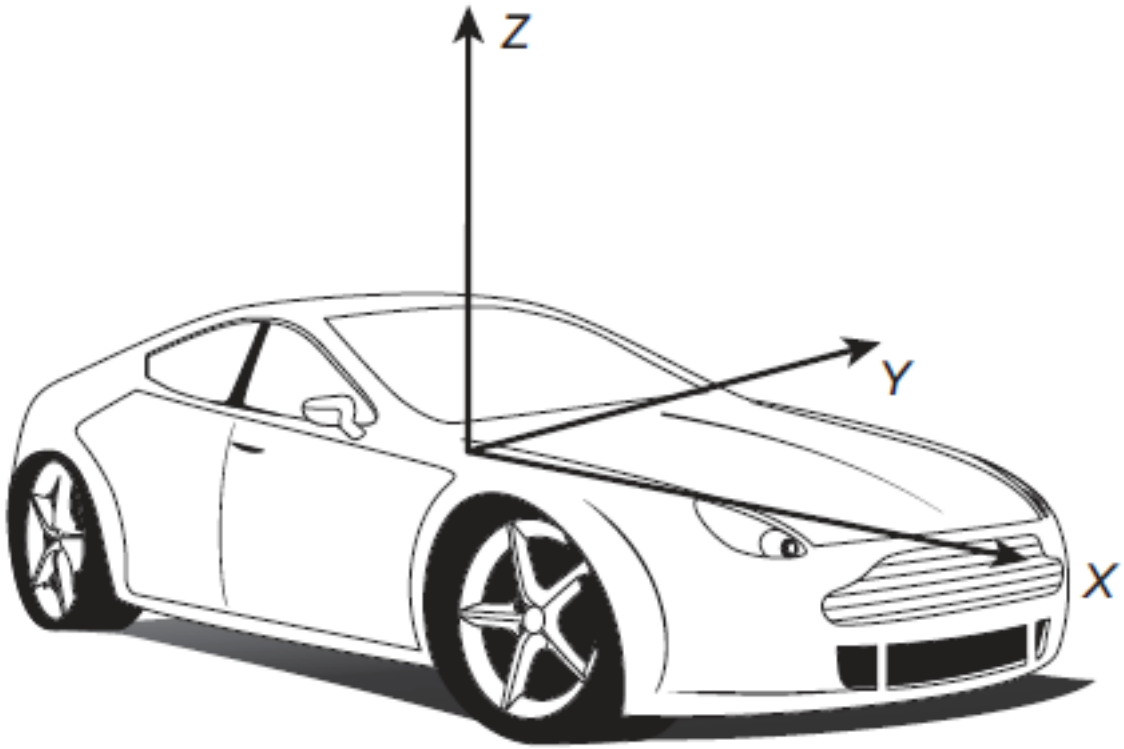

Braking System Design for Passenger Cars

A 'free-body' diagram of a two-axle, four-wheel rigid passenger car in dynamic equilibrium

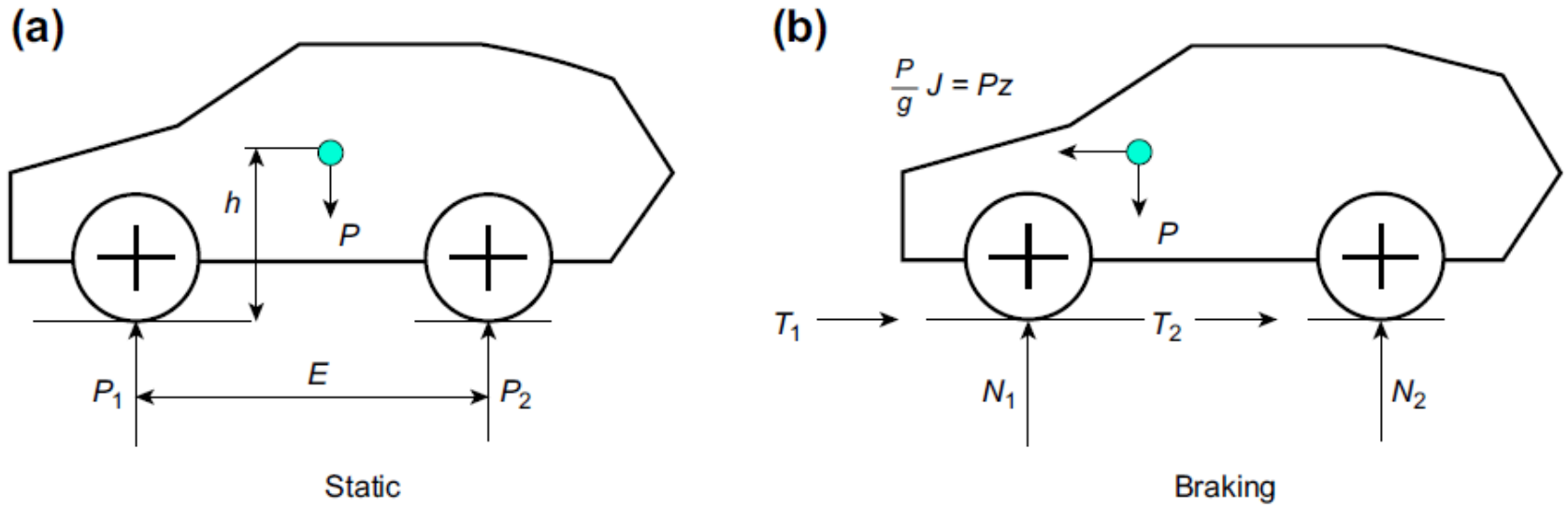

Figure 3.2: 2D Road Vehicle Force System Under Static (a) and Dynamic (b) Braking Conditions.

Braking System Design for Passenger Cars

A 'free-body' diagram of a two-axle, four-wheel rigid passenger car in dynamic equilibrium

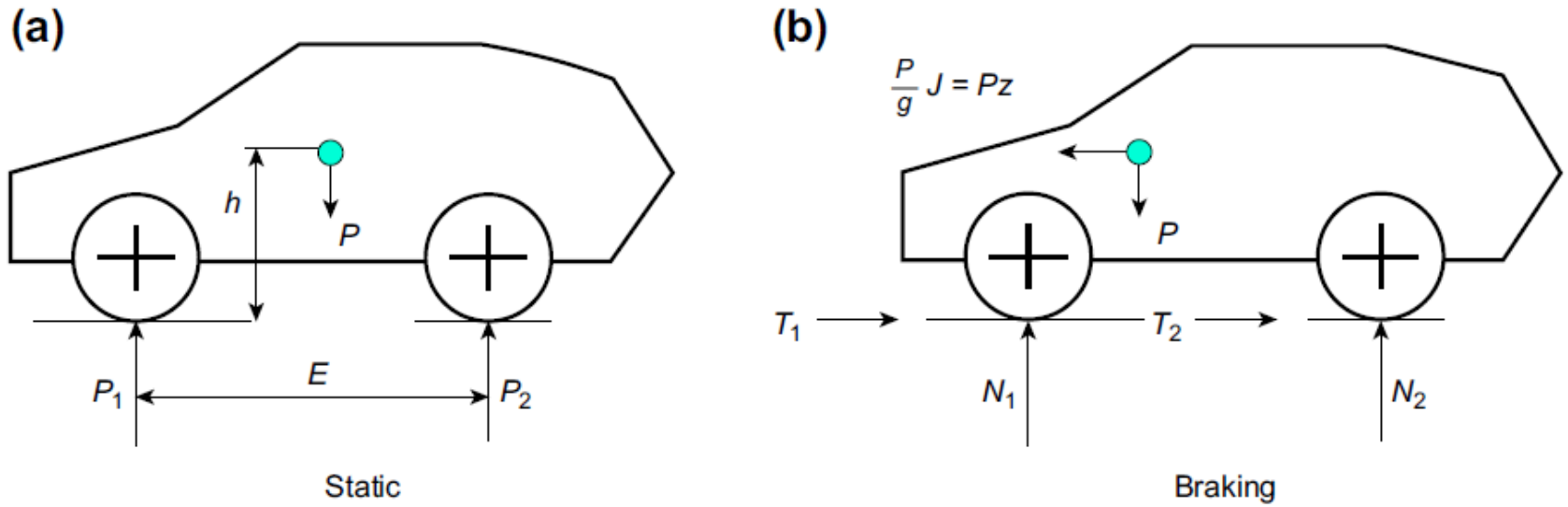

Figure 3.2: 2D Road Vehicle Force System Under Static (a) and Dynamic (b) Braking Conditions.

Braking System Design for Passenger Cars

taking moments about the instantaneous point of contact of the rear wheels

$$L_1 + L_2 = E$$

$$N_1(L_1 + L_2) - PL_2 - Pzh = 0$$

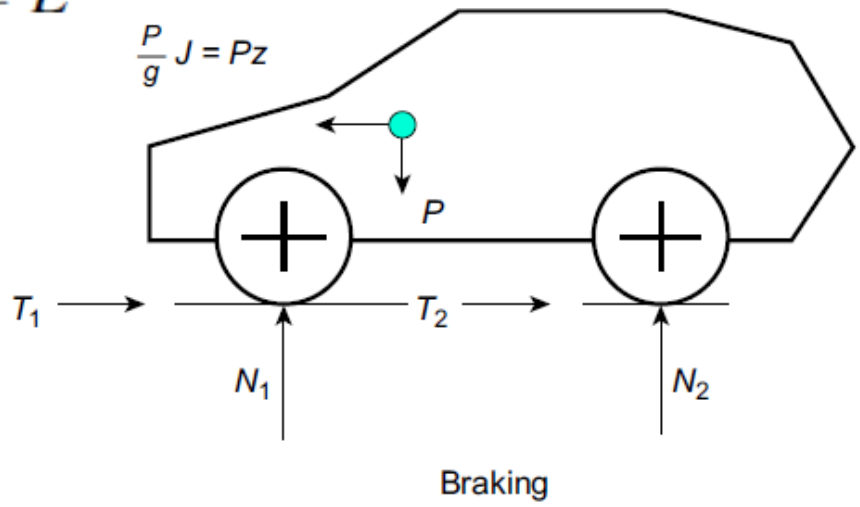

Braking

$$J = 0; \quad P_1 = \frac{PL_2}{L_1 + L_2}$$

$$N_1 = P\left[\frac{L_2}{L_1 + L_2} + \frac{zh}{(L_1 + L_2)}\right] = P_1 + \frac{Pzh}{E}$$

Braking System Design for Passenger Cars

taking moments about the instantaneous point of contact of the front wheels, we have for the rear wheels:

$$N_2 = P\left[\frac{L_1}{L_1 + L_2} - \frac{zh}{(L_1 + L_2)}\right] = P_2 - \frac{Pzh}{E}$$

$$N_1 + N_2 = P \quad \text{and} \quad L_1 + L_2 = E$$

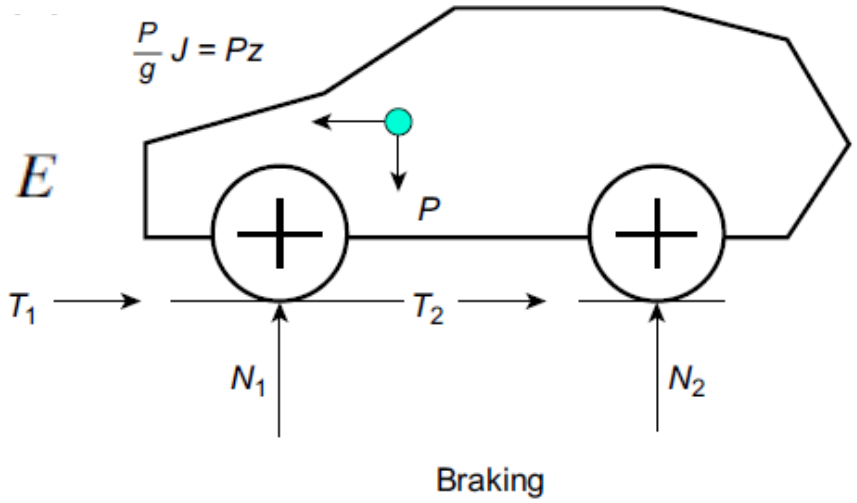

Braking

Braking System Design for Passenger Cars

Effect of Braking Weight Transfer on Normal Wheel Reactions

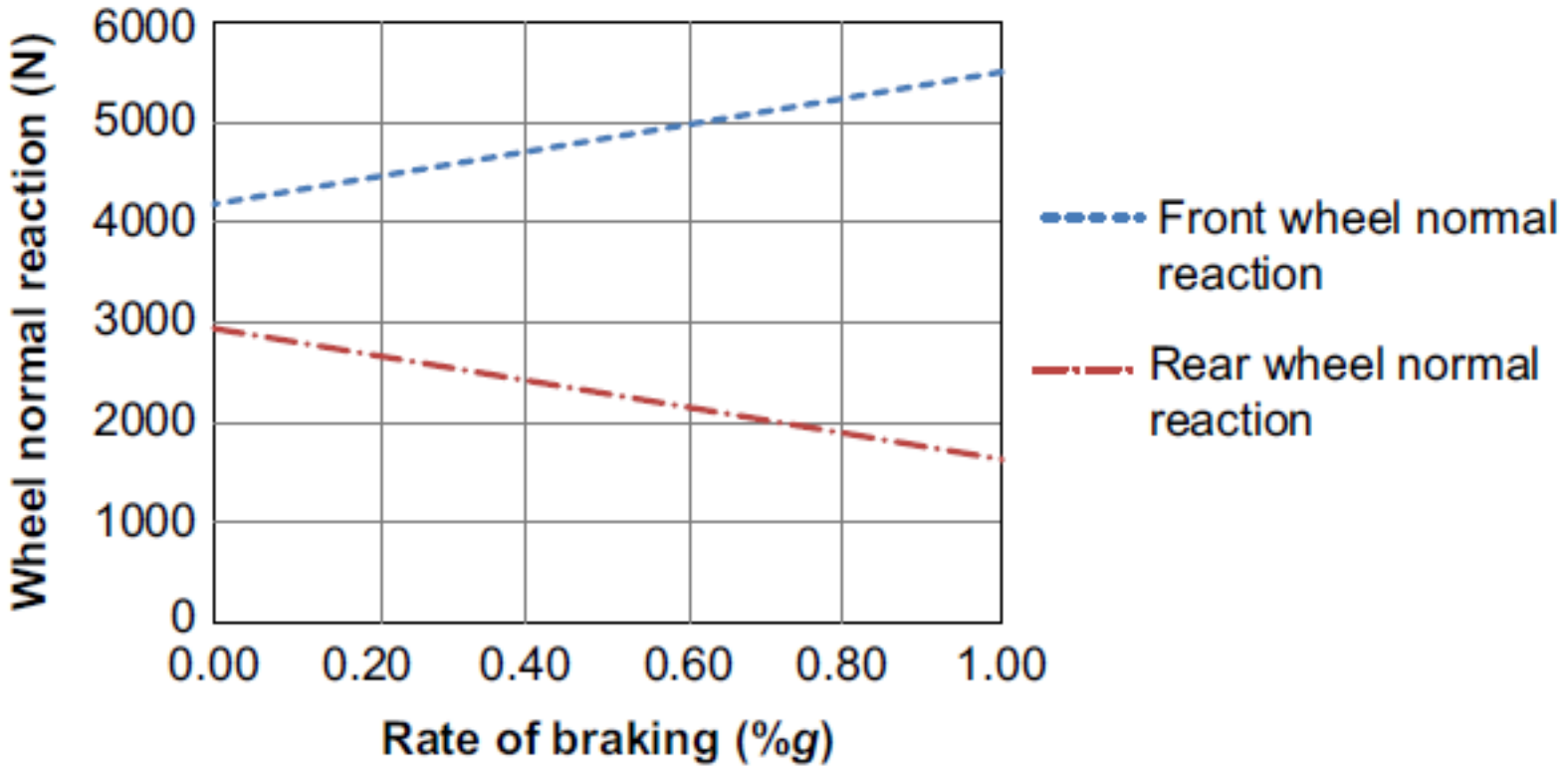

Braking System Design for Passenger Cars

Example Passenger Car Design Specification

Design Parameter	Specification (DoW)	Specification (GVW)
Wheelbase, $E = L_1 + L_2$ (mm)	2750	2750
Centre of gravity height, h (mm)	500	575
Position of centre of gravity behind the front axle, L_1 (mm)	1130	1300
Vehicle mass, M (kg)	1450	1950
Vehicle weight, P (N) $= Mg = 1450 \times 9.81 =$	14,225	19,130
Front/rear braking ratio (X_1/X_2)	70/30	70/30

Braking System Design for Passenger Cars

Vehicle Skidding (Sliding) on a Horizontal Road with all Wheels Locked

$$P = N_1 + N_2 = Mg$$

$$F_1 + F_2 = MJ$$

$$(F_1 + F_2) = \mu_t (N_1 + N_2)$$

$$\frac{(F_1 + F_2)}{(N_1 + N_2)} = \mu_t = \frac{J}{g} = z$$

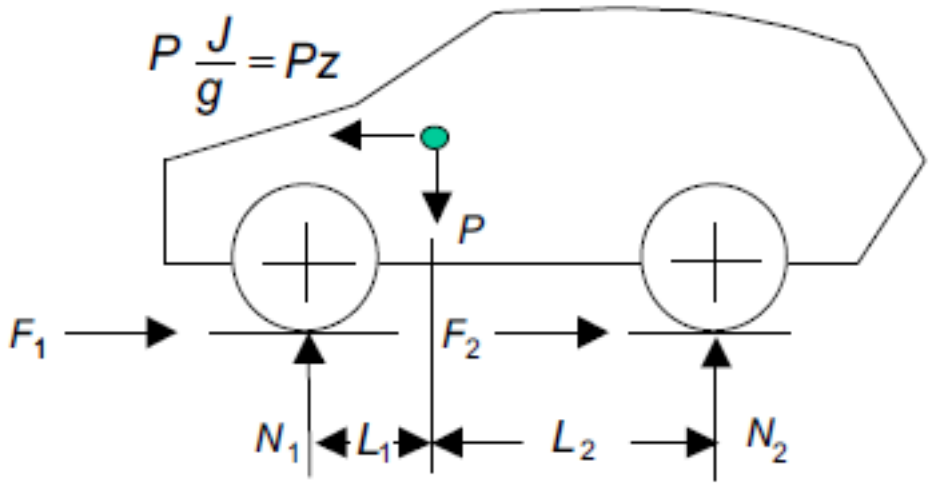

Braking System Design for Passenger Cars

Car Cornering on a Horizontal Road; (a) Stationary. (b) Cornering

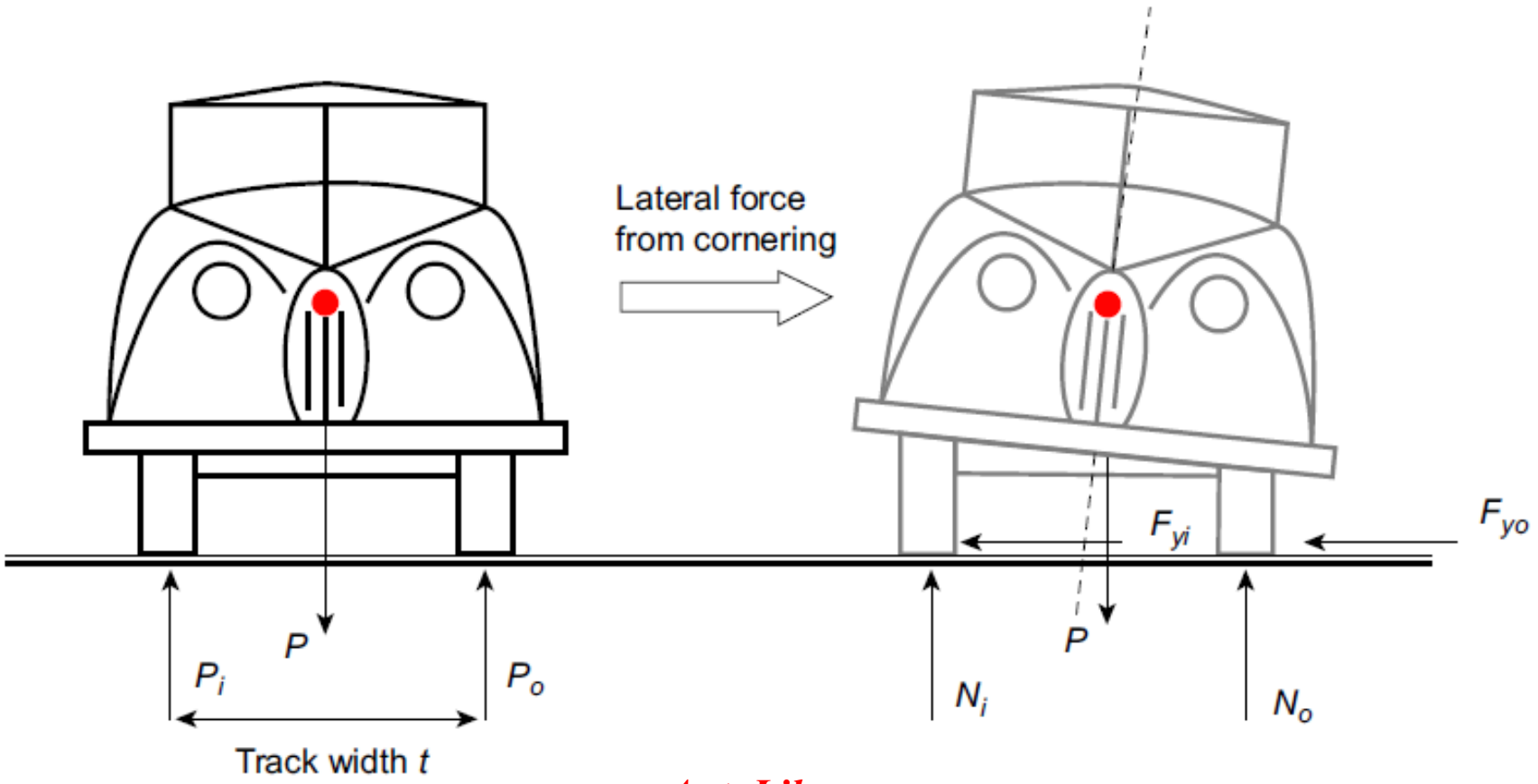

Braking System Design for Passenger Cars

Taking moments about the outside tyre contact patch:

$$F_c = mv^2/R$$

$$N_i t - P\frac{t}{2} + hF = 0$$

$$N_i = \frac{P}{2} - \frac{hF}{t}$$

$$N_o = \frac{P}{2} + \frac{hF}{t}$$

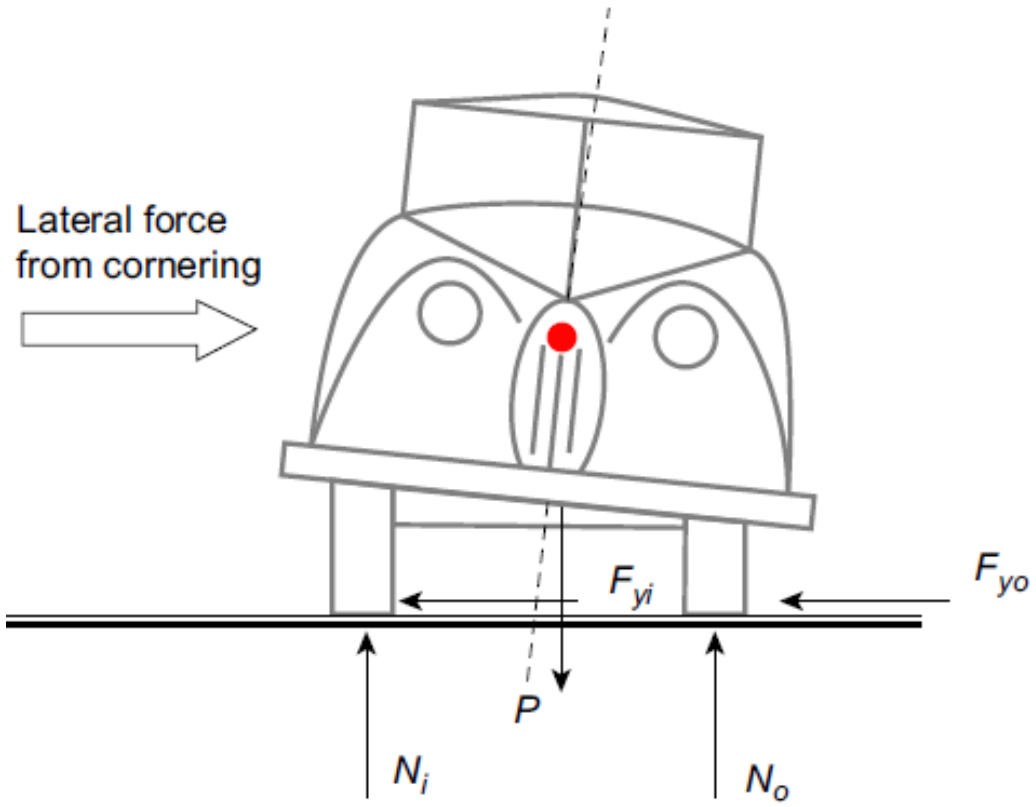

Braking System Design for Passenger Cars

Effect of Lateral Weight Transfer on the Front and Rear Wheel Normal Reactions

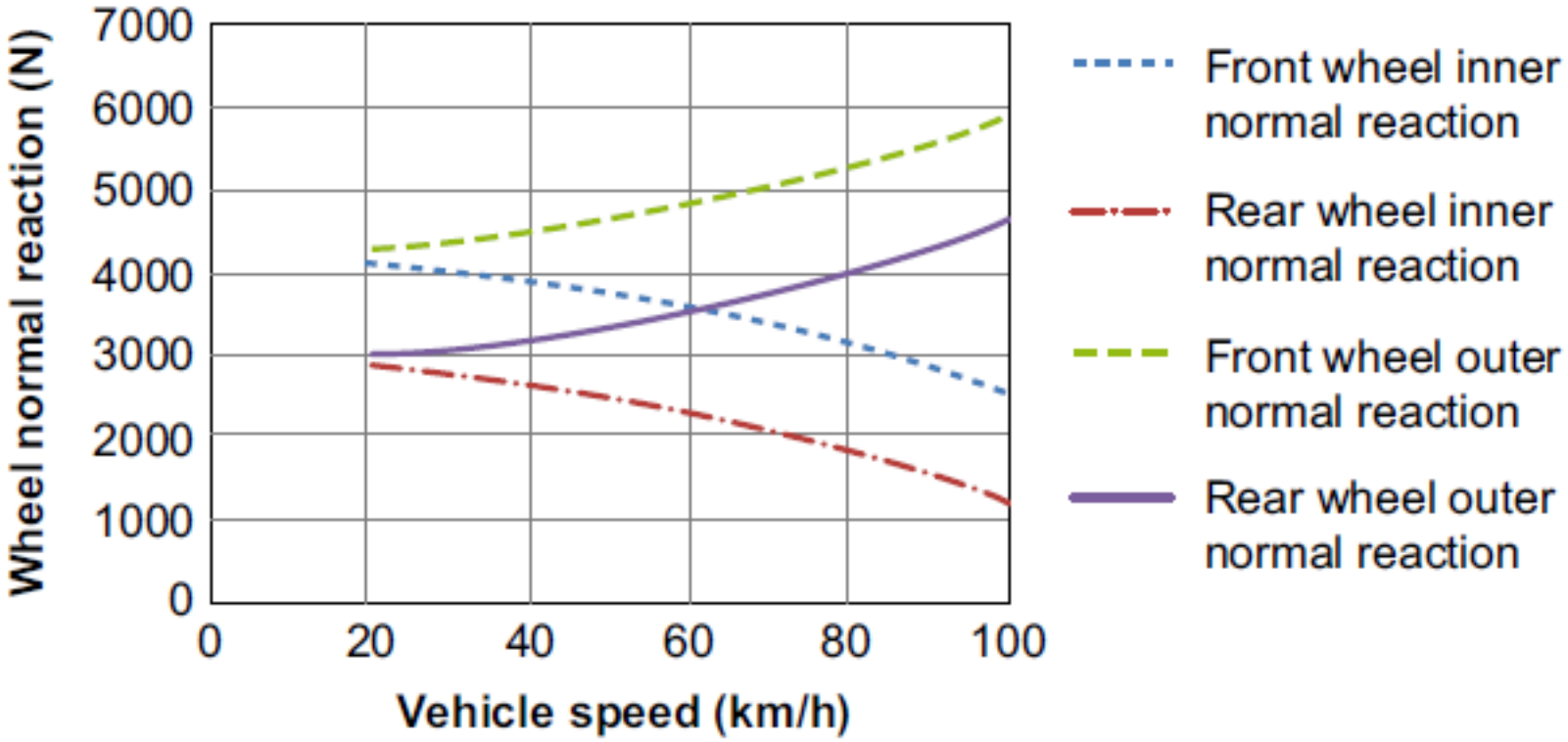

Braking System Design for Passenger Cars

Wheel slip is defined in terms of the ratio of the actual speed of rotation of the road wheel to the free-rolling speed of rotation

$$\text{Wheel slip} = (V - \omega r_r)/V$$

V = vehicle forward speed (m/s)
ω = tyre rotational speed (rad/s)
r_r = rolling radius of the tyre (m).

Braking System Design for Passenger Cars

$$\text{BFC} = \text{Braking force on the wheel} / \text{Dynamic wheel load}$$

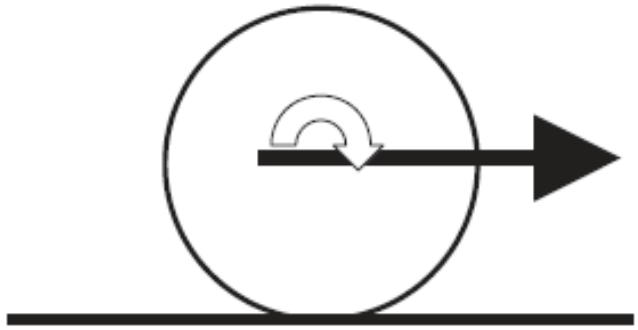

(a) Vehicle accelerating – wheel rotating faster than free rolling speed.

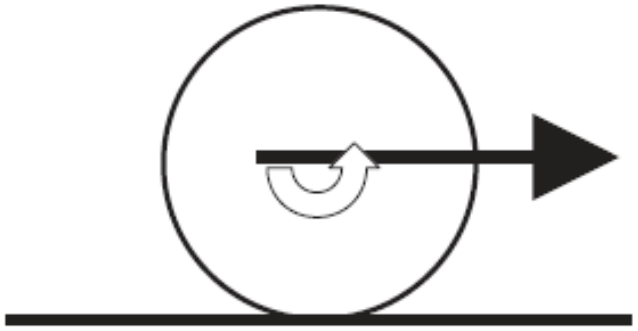

(b) Vehicle decelerating – wheel rotating slower than free rolling speed.

Direction of Wheel Slip in Acceleration (a) and Braking (b)

Braking System Design for Passenger Cars

A. Free rolling (no braking)
B. Stable slip zone
C. Peak adhesion
D. Wheel lock.

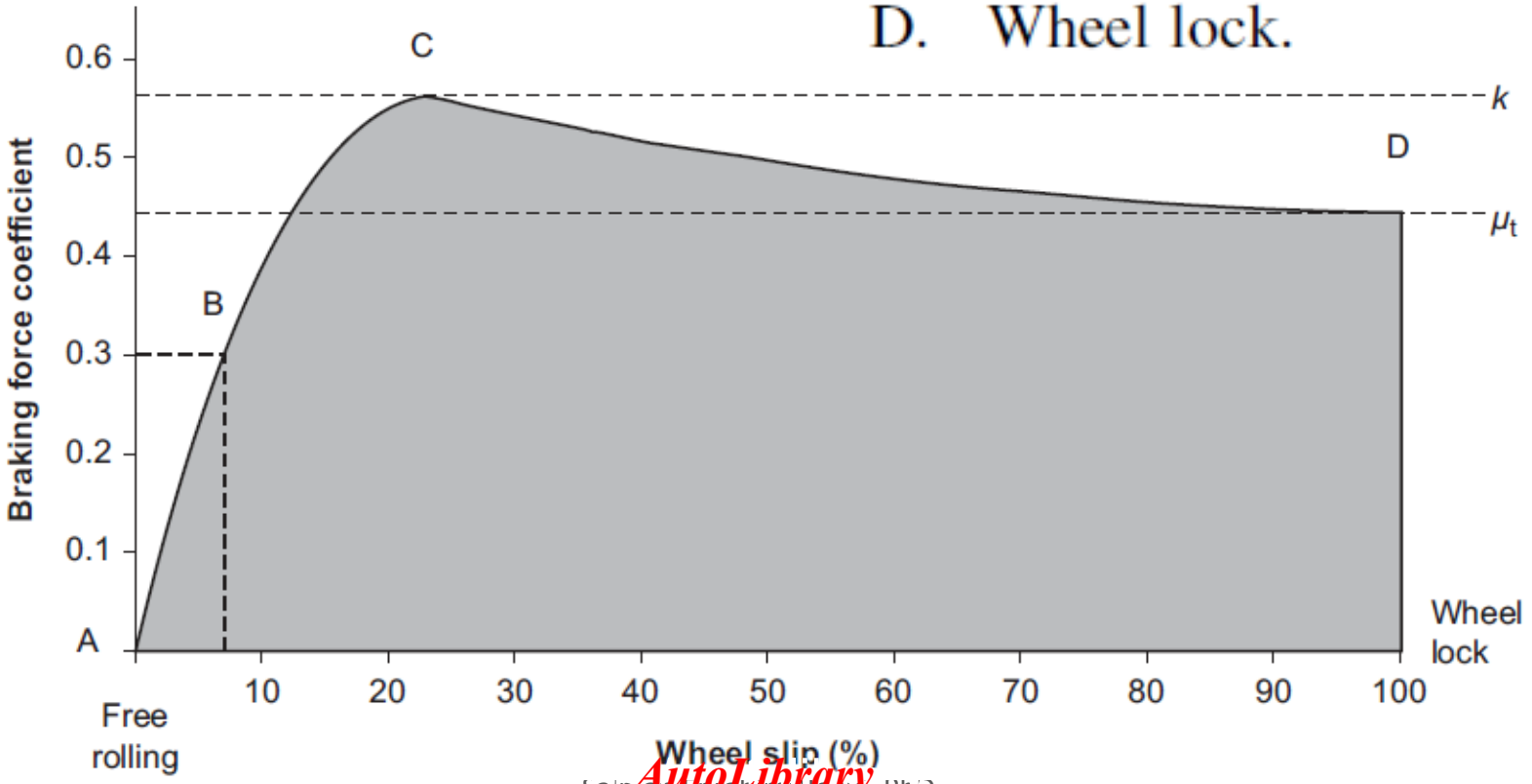

Braking System Design for Passenger Cars

$$\text{SFC} = \text{Lateral force}/\text{Dynamic wheel load}$$

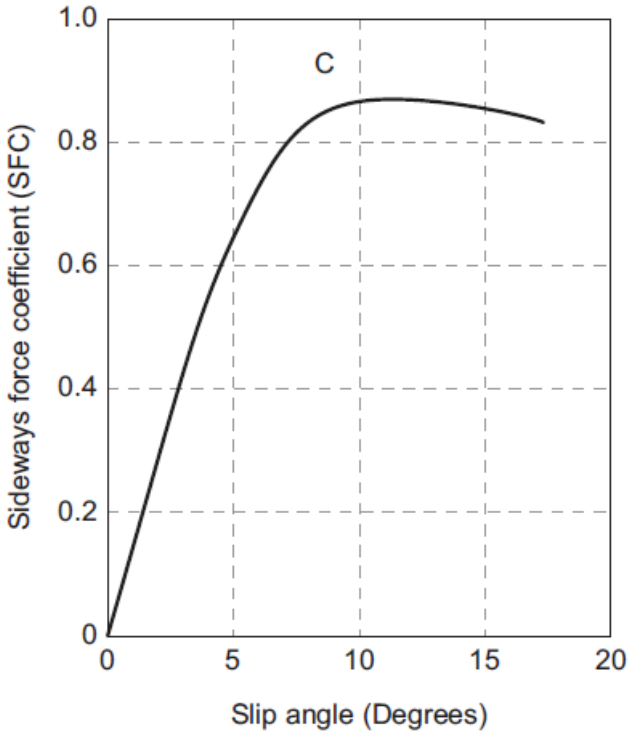

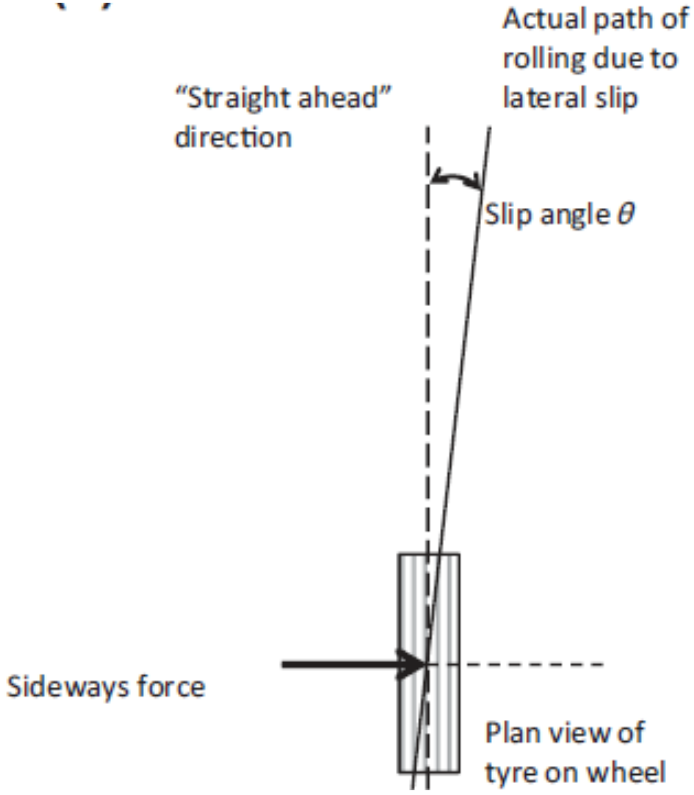

SFC vs. Slip Angle

Braking System Design for Passenger Cars

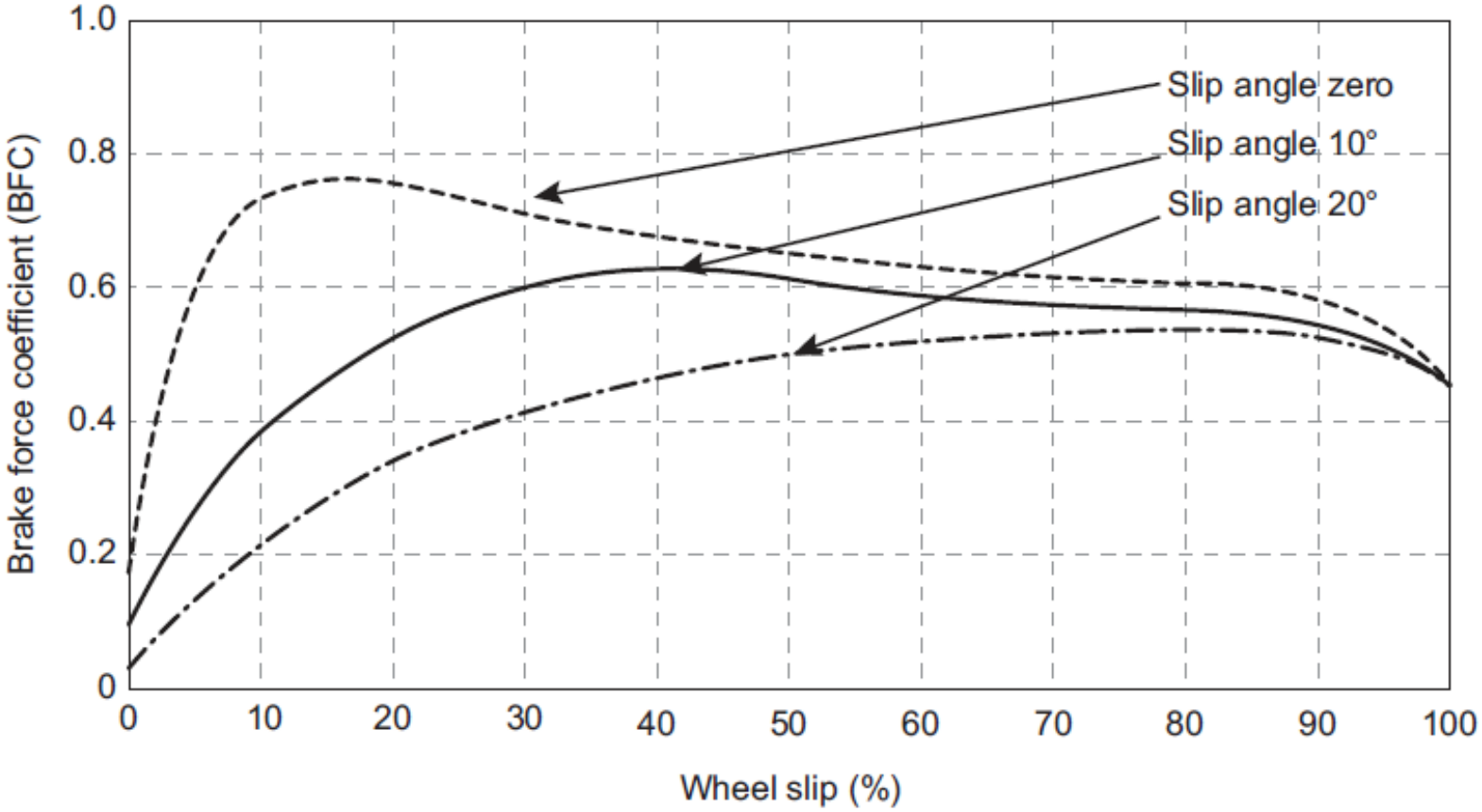

Figure 3.15: Effect of Slip Angle on BFC—Wheel Slip Relationship.

Brake Force Distribution

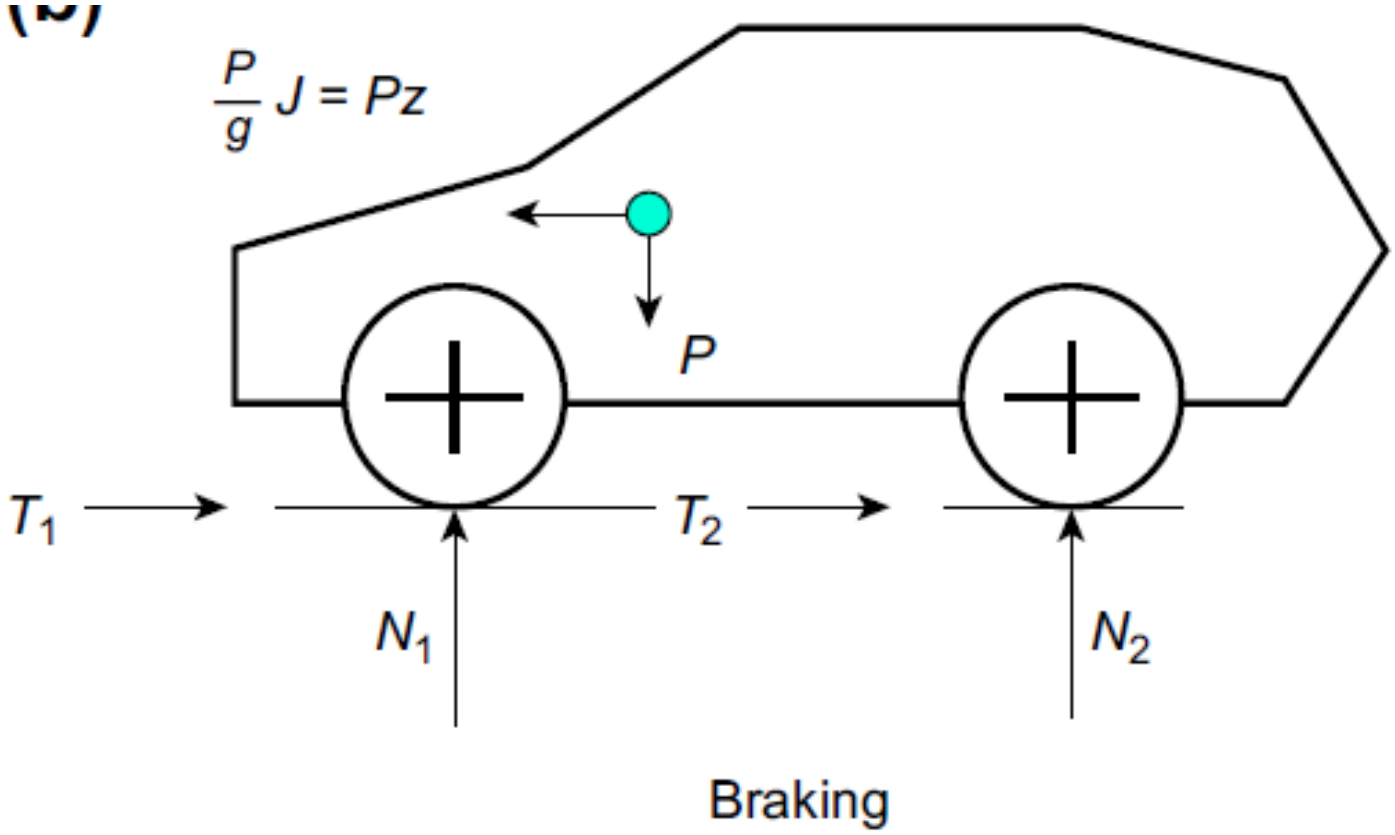

Brake Force Distribution

All wheels braking but not locked

$$\text{Total braking force} = \text{Mass} \times \text{Deceleration} = \frac{PJ}{g} = Pz$$

$$Pz = T_1 + T_2$$

$$Pz_{max} = kP$$

$$z_{max} = k$$

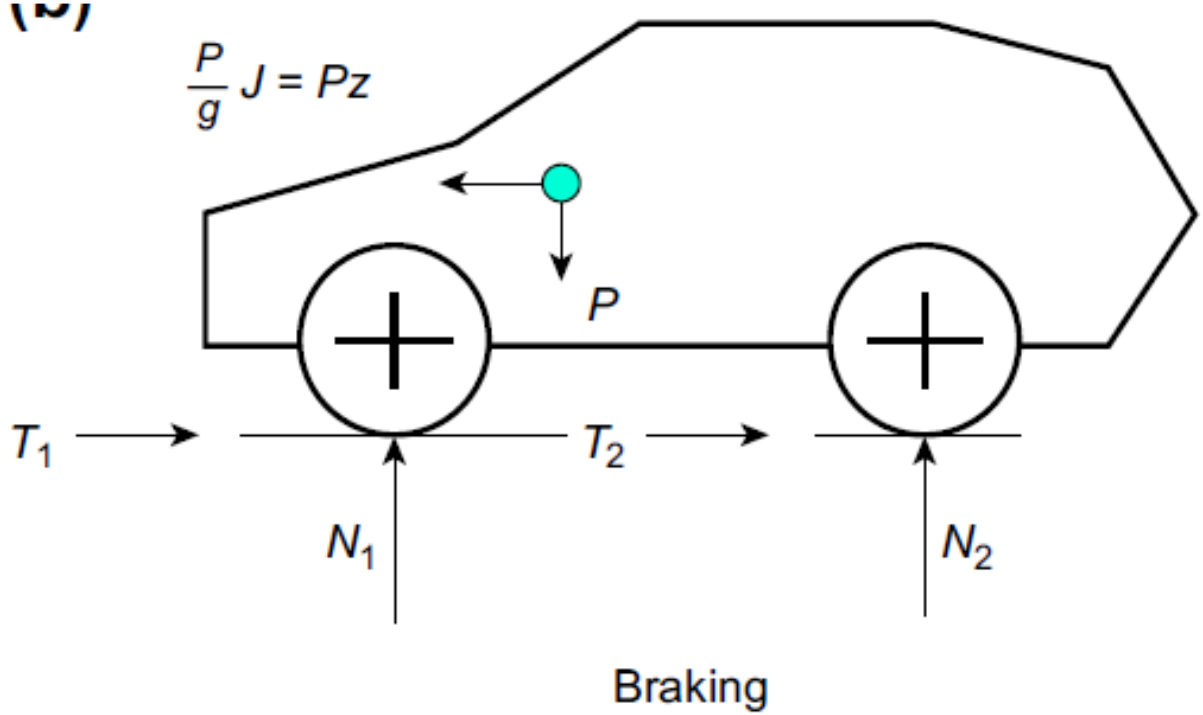

Braking

Brake Force Distribution

For all wheels to be on the point of locking simultaneously, the braking force at each wheel must be in proportion to the dynamic normal reaction at that wheel

$$T_1/T_2 = N_1/N_2$$

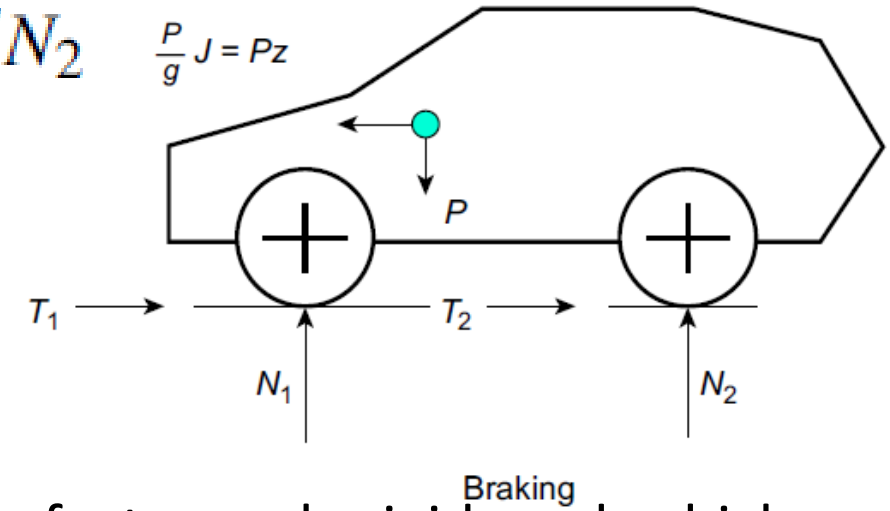

The braking force ratio of a two-axle rigid road vehicle can be specified as the ratio X1/X2, where X1 and X2 are the proportion of the vehicle's total braking force generated at the front and rear axles respectively.

Brake Force Distribution

$$T_1/T_2 = X_1/X_2 \text{ and } X_1 + X_2 = 1$$

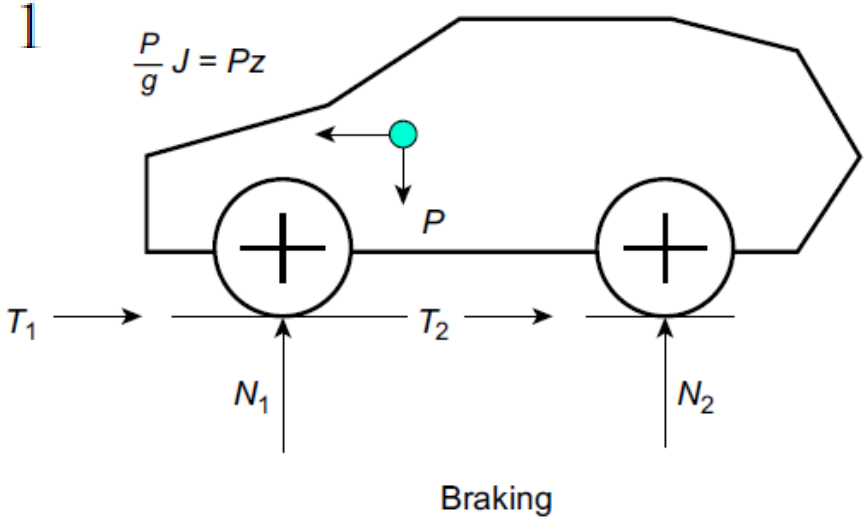

Braking

$$T_1 + T_2 = PzX_1 + PzX_2 = Pz(X_1 + X_2) = Pz$$

$$T_1 = X_1Pz$$

$$T_2 = X_2Pz$$

$$T_n = X_nPz$$

Brake Force Distribution

For a two-axle rigid vehicle with a fixed brake distribution which is designed so that the front wheels will lock first:

$$X_1/X_2 = \text{constant}$$

$$N_1 = P_1 + \frac{Pzh}{E} \quad \text{and} \quad N_2 = P_2 - \frac{Pzh}{E}$$

Brake Force Distribution

The braking force at the front axle when the front wheels are about to lock

$$T_1 = kN_1 = k\left\{P_1 + \frac{Pzh}{E}\right\} \qquad T_2 = k\left\{P_1 + \frac{Pzh}{E}\right\}\frac{X_2}{X_1}$$

$$T_1 + T_2 = Pz = k\left\{P_1 + \frac{Pzh}{E}\right\} + k\left\{P_1 + \frac{Pzh}{E}\right\}\frac{X_2}{X_1} = k\left(1 + \frac{X_2}{X_1}\right)\left\{P_1 + \frac{Pzh}{E}\right\}$$

$$= k\left(\frac{X_1 + X_2}{X_1}\right)\left\{P_1 + \frac{Pzh}{E}\right\} = k\left(\frac{1}{X_1}\right)\left\{P_1 + \frac{Pzh}{E}\right\}$$

$$z = \frac{k}{P}\left(\frac{1}{X_1}\right)\left\{P_1 + \frac{Pzh}{E}\right\} = \frac{k}{P}\left(\frac{P_1}{X_1} + \frac{Pzh}{EX_1}\right)$$

$$z = \frac{kP_1}{PX_1}\left(\frac{EX_1}{EX_1 - kh}\right) = \frac{kEP_1}{P(EX_1 - kh)}$$

Brake Force Distribution

When the rear wheels are about to lock

$$z = \frac{kEP_2}{P(EX_2 + kh)}$$

Simultaneous front and rear wheel lock

$$z_{crit} = k = \left(X_1 - \frac{P_1}{P}\right)\frac{E}{h}$$

$$z_{crit} = k = \left(\frac{P_2}{P} - X_2\right)\frac{E}{h}$$

Brake Force Distribution

the front wheels locked (μ_t) but the rear wheels at peak adhesion k

$$Pz = \mu_t \left\{ P_1 + \frac{Pzh}{E} \right\} + k \left\{ P_2 - \frac{Pzh}{E} \right\}$$

$$\mu_t = 0.7k.$$

$$z = k \left\{ \frac{0.7P_1 + P_2}{1 + 0.3k\frac{h}{E}} \right\}$$

Brake Force Distribution

To achieve the 'ideal' braking distribution through a variable braking ratio, the braking distribution must be continuously adjustable to match the dynamic weight distribution for all values of z

$$N_1 = P_1 + \frac{Pzh}{E}$$

$$N_2 = P_2 - \frac{Pzh}{E}$$

$$\frac{X_1^{var}}{X_2^{var}} = \frac{P_1 + \frac{Pzh}{E}}{P_2 - \frac{Pzh}{E}} \quad \text{for all values of } z$$

$$X_1^{var} = \frac{N_1}{P} = \frac{P_1}{P} + \frac{zh}{E}$$

$$X_2^{var} = \frac{N_2}{P} = \frac{P_2}{P} - \frac{zh}{E}$$

Chapter six

Brake System Layout Design

Previous chapters have shown how the braking forces generated at the road wheels of a vehicle must be designed to maximize the vehicle's ability to decelerate with acceptable driver effort and maximum stability, and how foundation brakes are designed to generate the required braking torque.

In this chapter these aspects are brought together in the design or layout of the braking system. Two of the most commonly used actuation systems are studied: the hydraulic system used on most passenger cars and light commercial vehicles (vans), and the pneumatic system used on most heavy commercial vehicles.

vehicle braking system layout design process

The vehicle braking system layout design process can proceed as summarized in the following four-step brake system design procedure:

Step 1. Design the basic braking system parameters based on the vehicle configuration:

1.1. Calculate the basic braking ratio for the worst case vehicle

1.2. Calculate the maximum brake torque required at each brake

1.3. Calculate the maximum power dissipation at each brake.

vehicle braking system layout design process

Step 2. Specify the foundation brakes:

2.1. Determine the rotor type and size

2.2. Determine the thermal mass of the rotor

2.3. Confirm the brake factor or C* (ηC*)

2.4. Confirm the friction material size in terms of thermal and mechanical loading.

vehicle braking system layout design process

Step 3. Design the actuation system:

3.1. Specify the actuation mechanism, e.g. hydraulic or pneumatic

3.2. Design the brake actuators (hydraulic cylinder sizes, air actuator sizes, slack adjuster lever lengths)

3.3. Design the 'master actuator' (brake pedal) system:

3.3.1. Hydraulic systems: pedal configuration, master cylinder piston size and stroke, servo boost ratio and knee point, fluid 'consumption'

3.3.2. Air systems: maximum pressure, response time, air reserve.

vehicle braking system layout design process

Step 4. Verify the design and check compliance with legislative requirements (e.g. UN Regulations 13 and/or 13H):

4.1. Intact system

4.2. Partial system failure

4.3. Parking.

Each step is explained below, and two examples are fully worked through for a passenger car (a two-axle rigid vehicle e Chapter 3) and a commercial vehicle (an articulated commercial vehicle comprising a tractor and semi-trailer e Chapter 4). After completing the design of the vehicle braking system, there are four more steps that will be covered in later chapters:

vehicle braking system layout design process

Step 5. Evaluate operational effects: loading and usage; heat and temperature; wear and durability; environmental; consistency and stability.

Step 6. Refine and optimize: system response and pedal feel; noise and vibration; cost and weight; manufacturability.

Step 7. Integrate with safety systems: ABS; ESC; traction control; automated emergency braking; etc.

Step 8. Brake performance verification by testing.

Step 1.1 Design the Basic Braking System Parameters Based on the Vehicle Configuration -Calculate the Basic Braking Ratio for the Worst Case Vehicle

The analyses derived in Chapter 3 (two-axle rigid vehicles, e.g. passenger cars and light commercial vehicles) and Chapter 4 (multi-axle commercial vehicle combinations including towing vehicles and full trailers o.r semi-trailers) are used in this step.

Step 1.2 Design the Basic Braking System Parameters Based on the Vehicle Configuration-Calculate the Maximum Brake Torque Required at Each Wheel

Assuming no lateral variation in brake torque, for each wheel on the axle the brake torque is calculated from

$$\tau_{wi} = T_{wi} r_r = T_i r_r / 2 \qquad (6.1a)$$

as illustrated in Figure 6.1

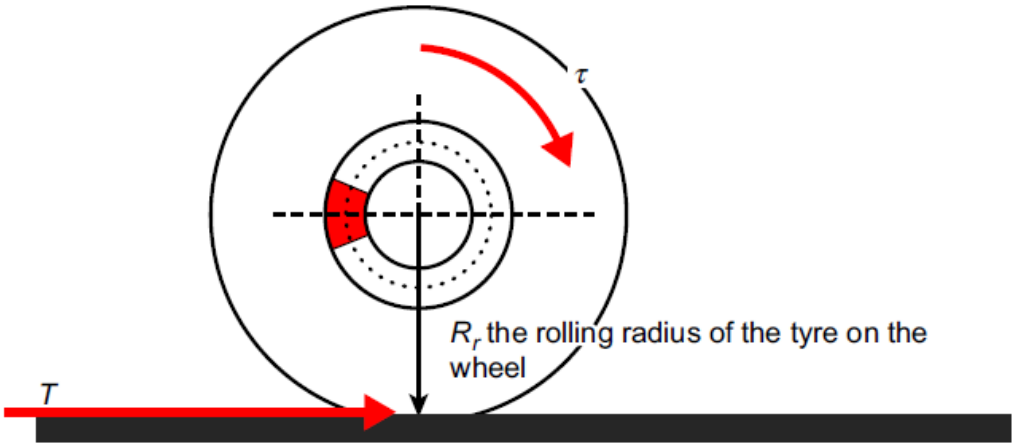

Figure 6.1: Disc Brake on Road Wheel Showing the Braking Force at the Tyre/Road Interface.

for two-axle rigid vehicles such as cars and light vans:

$$\tau_{w1} = T_{w1} r_r = X_1 P z r_r / 2 \qquad (6.1b)$$

$$\tau_{w2} = T_{w2} r_r = X_2 P_z r_r / 2 \qquad (6.1c)$$

where for a vehicle with ‘n’ axles:

$$\tau_{wi} = T_{wi} r_r = X_i P z r_r / 2 \qquad (6.1d)$$

Alternatively the brake torque required to decelerate a maximum axle load of N_{imax} at the required maximum deceleration

$$\tau_{wi} = T_{wimax} r_r = N_{imax} z_{max} r_r / 2 \qquad (6.1e)$$

For passenger cars the worst case for the front brakes is usually at least gross vehicle weight (GVW) with the DoW braking ratio, at a target rate of braking of z =1

The rear brakes worst case is also usually at least GVW but with the GVW braking ratio, at the same target rate of braking of z =1

The polar moment of inertia of a disc of radius r rotating about the axis perpendicular to its plane (the 'Z-axis') is:

$$I_{zz} = \tfrac{1}{2} mr^2 \qquad (6.2)$$

For a ventilated disc of outer diameter 355 mm, thickness 20 mm, made from cast iron with a density of 7100 kg/m3, the equivalent thickness is 16 mm and the estimated polar moment of inertia is 0.18 kg m2.

A brake drum can be modelled in two parts: the flange as a circular plate and the wall as a cylinder, both of the same outer diameter. The polar moment of inertia of a cylinder rotating about its longitudinal axis (the 'Z-axis') is:

$$I_{zz} = mr^2 \qquad (6.3)$$

Step 1.3 Design the Basic Braking System Parameters Based on the Vehicle Configuration e Calculate the Maximum Power Dissipation at Each Brake

In addition to being specified in terms of maximum braking torque, brakes may also have a specified power dissipation, the instantaneous power dissipated in a brake ‘i’ is:

$$\dot{Q}_i = \tau_{wi}\omega \qquad (6.4)$$

where u is the instantaneous angular velocity (rotational speed) of the wheel and brake.

Over a single brake application from one speed (v1) to another, lower, speed (v2), the wheel rotational speeds are u1 (initial rotational speed) and u2 (final rotational speed) and the mean power dissipation is calculated from:

$$\dot{\bar{Q}}_i = \tau_{wi}\frac{(\omega_1 + \omega_2)}{2} \qquad (6.5)$$

The total energy Qi dissipated in such a brake application can be estimated from:

$$Q_i = \dot{\bar{Q}}_i t \qquad (6.6)$$

where t is the duration of the brake application

The energy dissipated by the brake (Qi) can be compared with that estimated from the proportion of vehicle kinetic energy dissipated by the brake based on the braking ratio:

$$Q_i = \tfrac{1}{2} m V^2 X_i / 2 \qquad (6.7)$$

This is used in Step 2.2 to calculate the single-stop temperature rise.

Step 2

Step 2.1 Specify the Foundation Brakes e Determine the Rotor Type and Size

Considerations that influence rotor size include:

1. Torque and power rating (see Step 1)
2. Packaging constraints
3. Single-stop temperature rise calculations
4. Fade and Alpine descent temperature prediction
5. Benchmarking.

The brake assembly must fit inside the wheel rim, which therefore limits its overall diameter. With a disc brake, the caliper has to fit over the disc, so the rotor outer radius is limited by the radial thickness of the caliper plus necessary clearance, as illustrated in Figure 6.2

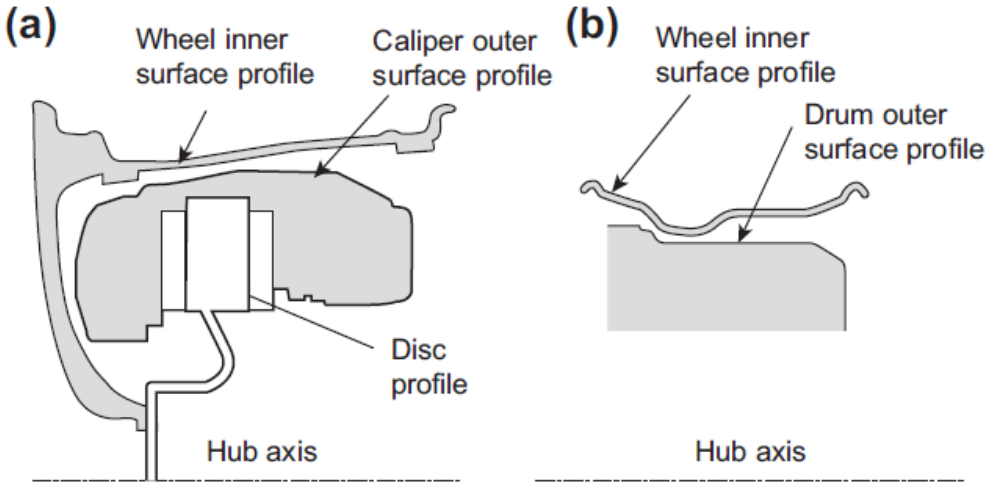

Figure 6.2: Brake Assembly and Wheel Packaging.
(a) Disc brake. (b) Drum brake.

For a disc brake, having determined the maximum disc outer diameter and thus the outer radius ro, the inner radius ri of the rubbing path can be determined from the 'good practice' rule of ro/ri≤1.5, as explained in Chapter 5. The disc effective radius (re) should be as large as possible, and the final design depends upon the pad surface area and aspect ratio. **For a drum brake**, re is the inner radius of the brake drum and depends upon the clearance between the drum outer circumference and the wheel as explained above, and the wall thickness of the drum, which is determined by thermal and mechanical strength and wear considerations.

Step 2.2 Specify the Foundation Brakes e Determine the Thermal Mass of the Rotor

The thermal mass of the rotor is an important design parameter that should be included in the brake system design process at this early stage. It defines the 'single-stop temperature rise' (SSTR e explained in Chapter 7), which assumes that in a single brake application (under specified loading and speed conditions) the proportion of kinetic energy dissipated by any particular brake is entirely converted to heat and absorbed by the rotor assembly as there is no time for heat flow to the free surfaces for surface heat loss.

Step 2.3 Confirm the Brake Factor (or ηC^*)

The term ‘brake factor’ is usually used by passenger car and light commercial vehicle manufacturers for hydraulically actuated brake systems, while the parameter ηC^*(which includes the effect of actuator efficiency) is usually quoted by commercial vehicle manufacturers for pneumatically actuated systems.

Here, the term ‘brake factor’ is used generically to indicate the relationship between the brake actuation force (*Pa*) and the braking force generated at the tyre/road interface (*Ti*).

Table 6.1: Typical Guidelines for Single-Stop Temperature Rise (SSTR)

Rotor Type	SSTR (°C)
Drum	350–400
Solid disc	550
Vented disc	600–650

For a disc brake, assuming that the actuation force Pa is the same as the resultant normal force at the pad/disc interface (Nc), the torque sw generated by a disc brake is:

$$\tau_w = 2\mu P_a r_e \qquad (5.4b)$$

Substituting BFdisc= 2μ, the brake force Tw at the tyre/road interface of one wheel is:

$$T_w = \mathrm{BF}_{disc} P_a r_e / r_r \qquad (6.8a)$$

For axles with a disc brake on each end, the total braking force is:

$$T_i = 2\mathrm{BF}_{disc} P_a r_e / r_r \qquad (6.9a)$$

Similarly, the torque generated by a drum brake is:

$$\tau_{drum} = (F_1 + F_2)r_e = (S_1 + S_2)P_a r_e \qquad (5.21)$$

using the combined shoe factor (S1 + S2) as the brake factor (BF), Equation (6.8a) also applies to the drum brake:

$$T_w = \mathrm{BF}_{drum} P_a r_e / r_r \qquad (6.8b)$$

For axles with a drum brake on each end, the total braking force is:

$$T_i = 2\mathrm{BF}_{drum} P_a r_e / r_r \qquad (6.9b)$$

The equivalent parameter to BF as used above is ηC^* (when the efficiency of the internal actuation system is included), and thus Equations (6.8) and (6.9) for commercial vehicle brakes and axles respectively become:

$$T_w = \eta C^* P_a r_e / r_r \qquad (6.8c)$$

and the total axle braking force is:

$$T = 2\eta C^* P_a r_e / r_r \qquad (6.9c)$$

Step 2.4 Confirm the Friction Material Size, Thermal and Mechanical Loading

Although friction force is, according to Amontons' law, independent of the apparent friction area defined by the surface area of the brake pad or lining, the friction material may suffer mechanical or thermal failure if it is too small.

Shear loading refers to the friction force per unit area of the brake pad or lining, as illustrated in Figure 6.3

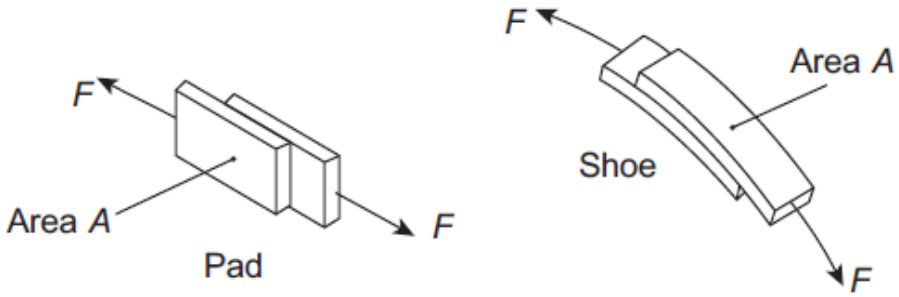

Figure 6.3: Friction Material Shear Loading.

Assuming that the wheels do not lock, this can be calculated from the braking force at the tyre/road interface (T_i; see Chapters 3 and 4). For an axle with two disc brakes each with two pads of friction surface area *Ap*:

$$\text{Shear loading(pad)} = T_i\left(r_r/r_e \cdot 4A_p\right) \qquad (6.10)$$

For an axle with two Simplex drum brakes (floating actuator) each with leading shoe factor S1, trailing shoe factor S2, and brake factor = combined shoe factor (CSF = S1 +S2), the lining loading on each leading shoe (surface area A_l) is:

$$\text{Shear loading(leading shoe)} = T_i(S_1/\text{CSF})r_r/(r_e \cdot 2A_1) \qquad (6.11)$$

(only the leading shoe is considered because $S_1 > S_2$).

Typical design target values for a front wheel drive passenger car are 1.4 MPa for front disc brakes and 0.3 MPa for rear drum brakes for a rate of braking z = 0.5 g at GVW. A high-performance car may reach 1.75 MPa at z = 1, at GVW.

For an S-cam drum brake fitted to a heavy commercial vehicle axle, the design target value may lie in the region of 0.75 MPa for z = 0.6 g. The friction materials must retain sufficient shear strength to meet these targets at high temperature, e.g. repeated high-duty braking at GVW and high speed, or continuous (drag) braking.

The mean power dissipation $\dot{\bar{Q}}_i$ associated with a vehicle axle (which has two brakes) may be calculated in terms of the mean angular velocity during the brake application, as previously explained from Equation (6.5).

This may also be calculated in terms of the mean vehicle speed as indicated in Equation (6.12):

$$\dot{\bar{Q}}_i = T_i(v_1 - v_2) \qquad (6.12a)$$

where v1 and v2 are in units of m/s.

The mean power dissipation in decelerating a vehicle from road speed V1 to V2 km/h at a rate of braking of z is (the factor of 3.6 converts km/h to m/s):

$$\dot{\bar{Q}}_i = \frac{zPX_i(V_2 - V_1)}{3.6} \qquad (6.12b)$$

Assuming again that the wheel does not lock, the mean power density for each individual pad of friction surface area *Ap* in a disc brake is $\dot{\bar{Q}}_i/4Ap$.

Typical values of mean power density for a front wheel drive car during a 0.5 g deceleration to rest at GVW from 90% of vehicle maximum speed are:

- 8.5 MW/$m^2$for front disc brakes;
- 1.2 MW/$m^2$for rear drum brakes.

High-performance cars may reach higher power dissipations, e.g. at 1 g deceleration from Vmax at GVW:

- Mean pad work rate 20 W/mm^2;
- Pad shear loading 1.75 MPa.

When steps 1 and 2 have been completed it is often useful to undertake ‘benchmarking’ to compare the proposed foundation brake specifications with those of competitor vehicles on the basis of size, weight, maximum speed, engine power, etc.

Steps 3 and 4

Step 3 (design the actuation system) and Step 4 (verify the design and check compliance with legislative requirements) both depend strongly on the type of vehicle

Passenger Car and Light Commercial Vehicle Braking Systems with Hydraulic Actuation

The design of a hydraulic actuation system for a two-axle rigid vehicle such as a passenger car or light commercial vehicle is explained here, based on a passenger car with the specifications shown in Table 6.2.

Table 6.2: Example Vehicle Data

	DoW	GVW
Wheelbase, $E = L_1 + L_2$ (mm)	2800	2800
Centre of gravity height, h (mm)	675	650
Position of centre of gravity behind the front axle, L_1 (mm)	1120	1486
Position of centre of gravity in front of the rear axle, L_2 (mm)	1680	1314
Vehicle mass, M (kg)	1750	2450
Tyre dynamic (rolling) radius, r_r (mm)	325	325

From ***Step 1.1***:

Front/rear braking ratio(X_1/X_2) for $z_{crit} = 0.6$: DoW 74/26, GVW 61/39

For the front brakes on the example vehicle at *zcrit* ¼ 0.6, the braking distribution X1/X2 is 74/26 (DoW loading condition), which is the worst case for the front brakes. The maximum worst case front brake torque at GVW and z = 1 is (including a correction factor of 1.05 for rotational inertia) τ_{w1max}= 3050 Nm.

For the example vehicle at *zcrit*= 0.6, the braking distribution X1/X2 is 61/39 (GVW loading condition), which is the worst case for the rear brakes. The maximum worst case rear brake torque at GVW and z = 1 is (including a correction factor of 1.05 for rotational inertia) τ_{w2max}= 1600 Nm.

The maximum and mean power dissipations at each brake (Step 1.3) from an initial road speed of 145 km/h to rest for this vehicle are calculated from Equations (6.4) and (6.5):

Power Dissipation	Peak (kW)	Mean (kW)
Front brake	287	144
Rear brake	151	75

In the example vehicle the smallest wheel rim inner diameter is 200 mm, and the maximum front brake disc outer radius to allow clearance for the caliper within the wheel rim is 150 mm

giving an effective radius (*re* = *rm*) of 125 mm. The ratio *ro*/*ri* is thus 1.50

In ***Step 2.3***, having designed the front and rear brake rotors in the example given, the brake factor of the disc brakes to be used is confirmed by specifying a suitable coefficient of friction μ.

For this vehicle the front and the rear disc brake factors are initially specified as 0.76 (μ=0.38).

Step 2.4 confirms the friction material size based on the thermal and mechanical loading. Based on the typical limits of shear loading and mean work rate discussed earlier (1.4 MPa and 8.5 MW/m2 respectively for disc brake pads in a 0.5 g stop at maximum GVW from 145 km/h, which is assumed to be 90% of this vehicle's maximum speed),

The estimated pad areas are shown in Table 6.3. The limiting factor is the mean work rate

Table 6.3: Estimated Values of Shear Loading and Mean Work Rate for Disc Brake Pads on the Example Vehicle in a 0.5 g Deceleration to Rest at Maximum GVW from 145 km/h

Axle	Pad Width (mm)	Pad Length (mm)	Pad Area (mm^2)	Shear Loading (MPa)	Mean Work Rate (MW/m^2)
Front	50	110	5500	1.06	8.6
Rear	40	75	3000	1.02	8.3

Assuming the maximum road speed of this vehicle is 160 km/h, the design worst case for the front and rear brakes at 1 g deceleration from V_{max} at GVW is summarized in Table 6.4

Table 6.4: Estimated Values of Shear Loading and Work Rate for the Same Area Disc Brake Pads on the Example Vehicle in a 1 *g* Deceleration to Rest at Maximum GVW from 160 km/h

Axle	Pad Width (mm)	Pad Length (mm)	Pad Area (mm^2)	Shear Loading (MPa)	Mean Work Rate (MW/m^2)
Front	50	110	5500	2.12	17.2
Rear	40	75	3000	2.0	16.6

Step 3 Design the Hydraulic Actuation System

Step 3.1 Specify the Actuation Mechanism (Hydraulic System)

Since the foundation brake design has now been defined for this vehicle, the brake system design can proceed to the design of the selected hydraulic actuation system. The brakes on most modern passenger cars and light commercial vehicles are actuated via a hydraulic actuation system that uses 'muscular' energy (i.e. the driver effort or force applied to the brake pedal) to create hydraulic pressure in the brake fluid to provide the required actuation forces at the foundation brakes.

The basic components of the hydraulic actuation system are illustrated in Figure 6.4, and include the brake pedal, booster (if fitted), master cylinder, hydraulic lines (pipes, tubes, hoses, etc.) and slave cylinders at the brakes.

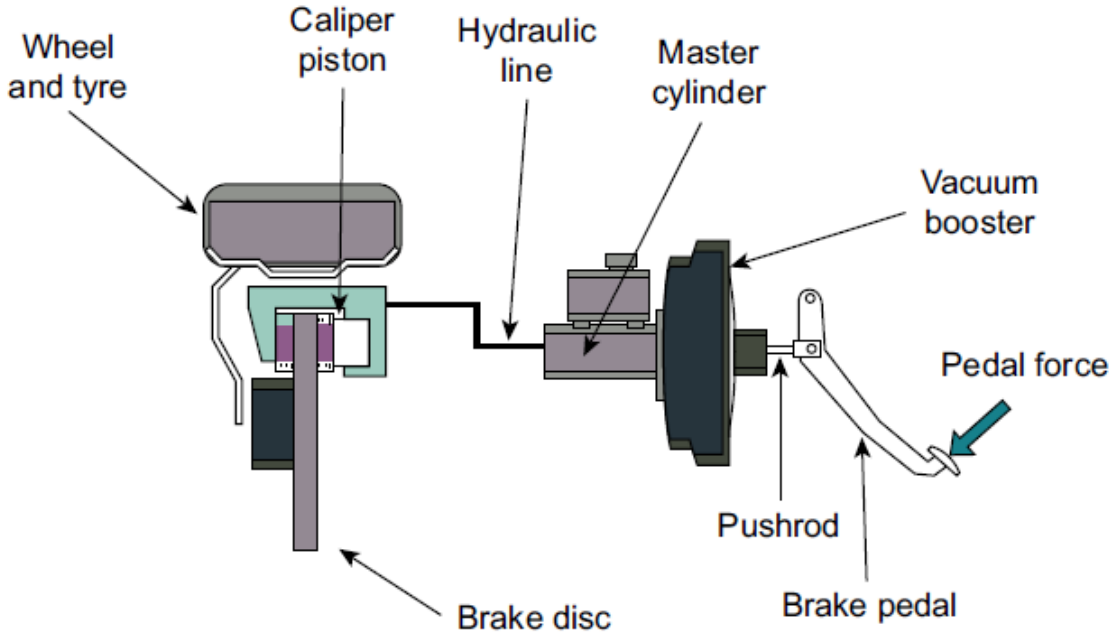

Figure 6.4: Basic Components of a Hydraulic Braking System for a Passenger Car or Light Van.

It is a legislative requirement (UN Regulations 13 and 13H; see Chapter 8) that every road vehicle has at least two separate brake actuation circuits, as illustrated in Figure 6.5

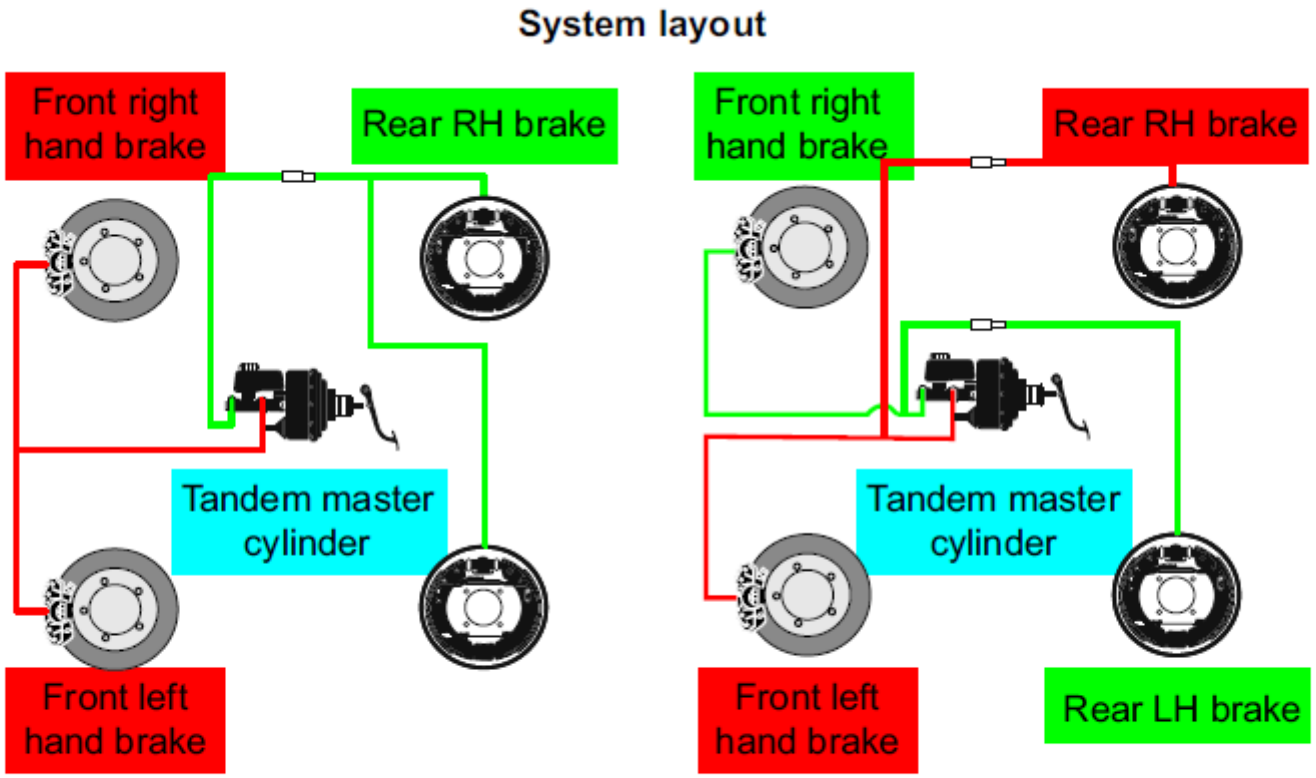

Figure 6.5: 'Split' Configurations for Passenger Cars and Light Commercial Vehicles with Hydraulic Braking Systems.

The simplest configuration for a two-axle rigid vehicle is a ‘vertical split’, where the front brakes are on one circuit and the rear brakes are on the other.

The vertical split can be satisfactory for rear wheel drive (RWD) and four-wheel drive (4WD) vehicles, but is usually not satisfactory for front wheel drive (FWD) vehicles because their weight distribution is concentrated on the front axle, especially when unladen.

For FWD cars and light commercial vehicles the ‘diagonal split’ is better. This ensures that braking is always available at one front and one rear wheel, each on opposite sides of the vehicle

Step 3.2 Design the Brake Actuators (Hydraulic System)

Referring to Figure 6.4, the hydraulic pressure generated by the master cylinder is transmitted via the hydraulic brake lines to the slave cylinders, which provide the actuation force at each brake. For the example vehicle the required maximum brake torque calculated in ***Step 1.1*** is

$\tau_{w1max} = 3050$ Nm and $\tau_{w2max} = 1600$ Nm. From Equation (5.4b) the required maximum clamp force N_{cmax} is:

$$N_{cmax} = \tau_w/(2\mu r_e) \tag{6.13a}$$

On the basis of Equation (5.4e) where disc BF $= 2\mu$:

$$N_{cmax} = \tau_w/(r_e \mathrm{BF}) \tag{6.13b}$$

Assuming that the actuation force P_{ai} is the same as the clamp force N_{ci}, for the example vehicle the required actuation forces are P_{a1} = 30.9 kN and P_{a2} =16.3 kN. A good starting point in sizing the brake slave cylinders is to specify a maximum line pressure in the hydraulic system, for example 100 bar (10 MPa). This would initially propose the following actuator sizes for this example vehicle:

Front disc brakes: 1 X 63 mm diameter piston (or 2 X 45 mm diameter pistons);

Rear disc brakes: 1 X 48 mm diameter piston.

The braking performance of the whole vehicle with the initially proposed braking system must now be examined, using the analysis of vehicle braking distribution and adhesion utilization presented in Chapter 3.

The ratio X1/X2 is calculated using Equations (3.19) (for the moment ignoring the effect of threshold pressure):

$$X_1 = T_1/Pz = \mathrm{BF}_1 P_a r_{e1}/r_{r1} \qquad (6.14a)$$

$$X_2 = T_2/Pz = \mathrm{BF}_2 P_a r_{e2}/r_{r2} \qquad (6.14b)$$

Using the proposed slave piston sizes (front disc brakes 2 X 45 mm or 1 X 63 mm diameter pistons; rear disc brakes 1 X 48 mm diameter piston):

$$X_1/X_2 = 65/35 = 1.83$$

which can be compared with the initial value (from ***Step 1.1***) of X1/X2 = 74/26 (DoW) or 61/39 (GVW) based on z_{crit} ¼ 0.6. As illustrated in Figure 6.6, this indicates that the rear wheels are 'over-braked' in the unladen condition so it is necessary to adjust the actuation design to meet the requirement of $z_{crit} \leq 0.6$ in this condition

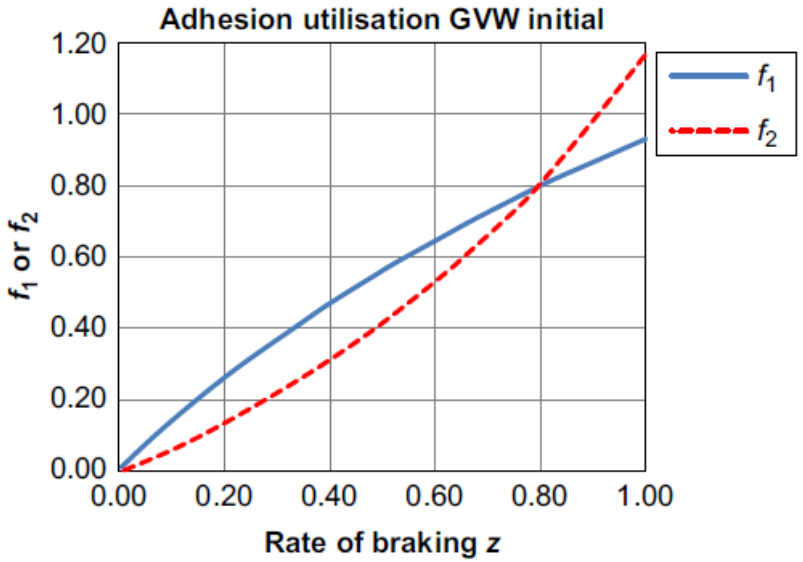

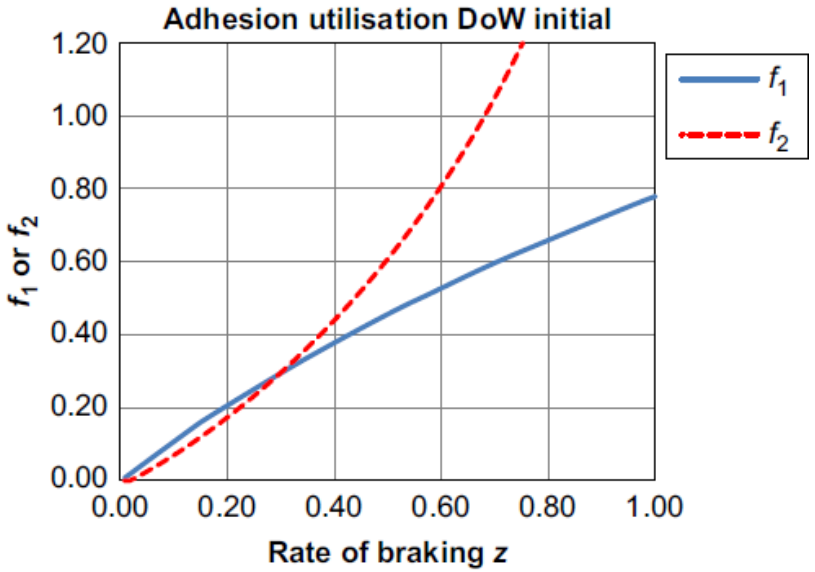

Figure 6.6: Adhesion Utilisation Curves for First Proposed Design Showing Premature RWL, $z_{crit} < 0.6$.

Reducing the rear brake slave cylinder from 48 mm diameter to 38 mm achieves z_{crit} = 0.6, as illustrated in Figure 6.7.

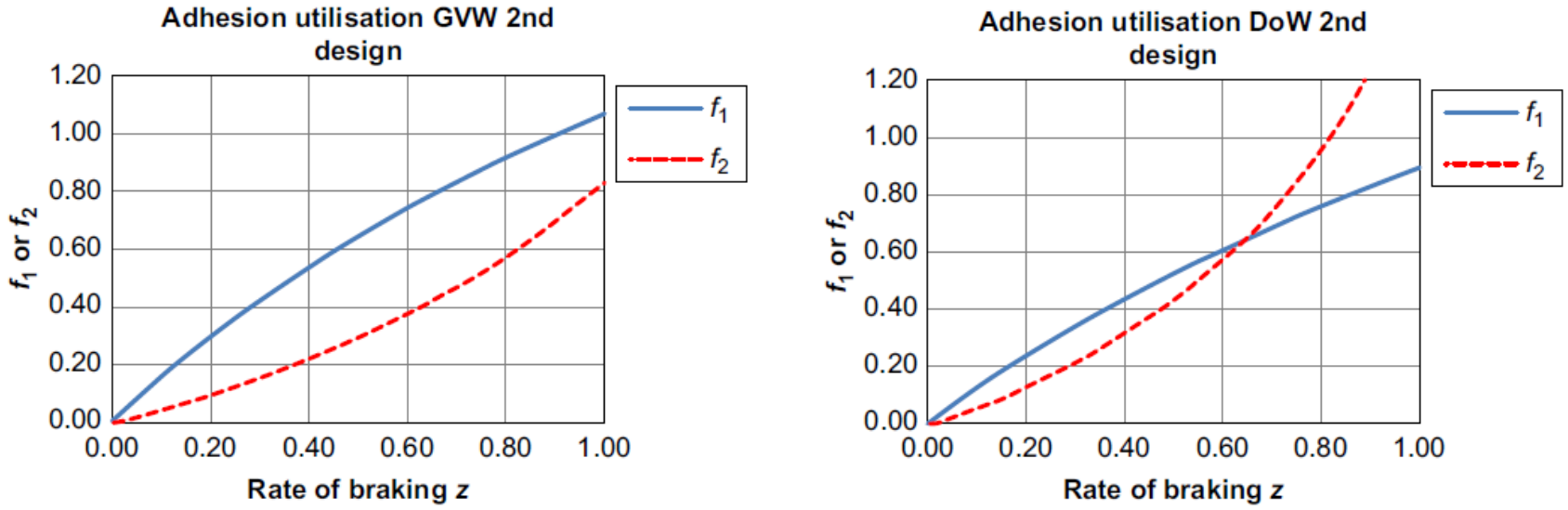

Figure 6.7: Adhesion Utilisation Curves for Second Proposed Design Showing $z_{crit} \geq 0.6$.

the optimized actuation pressures for ideal braking distribution in the GVW and DoW loading conditions are shown in Figure 6.8.

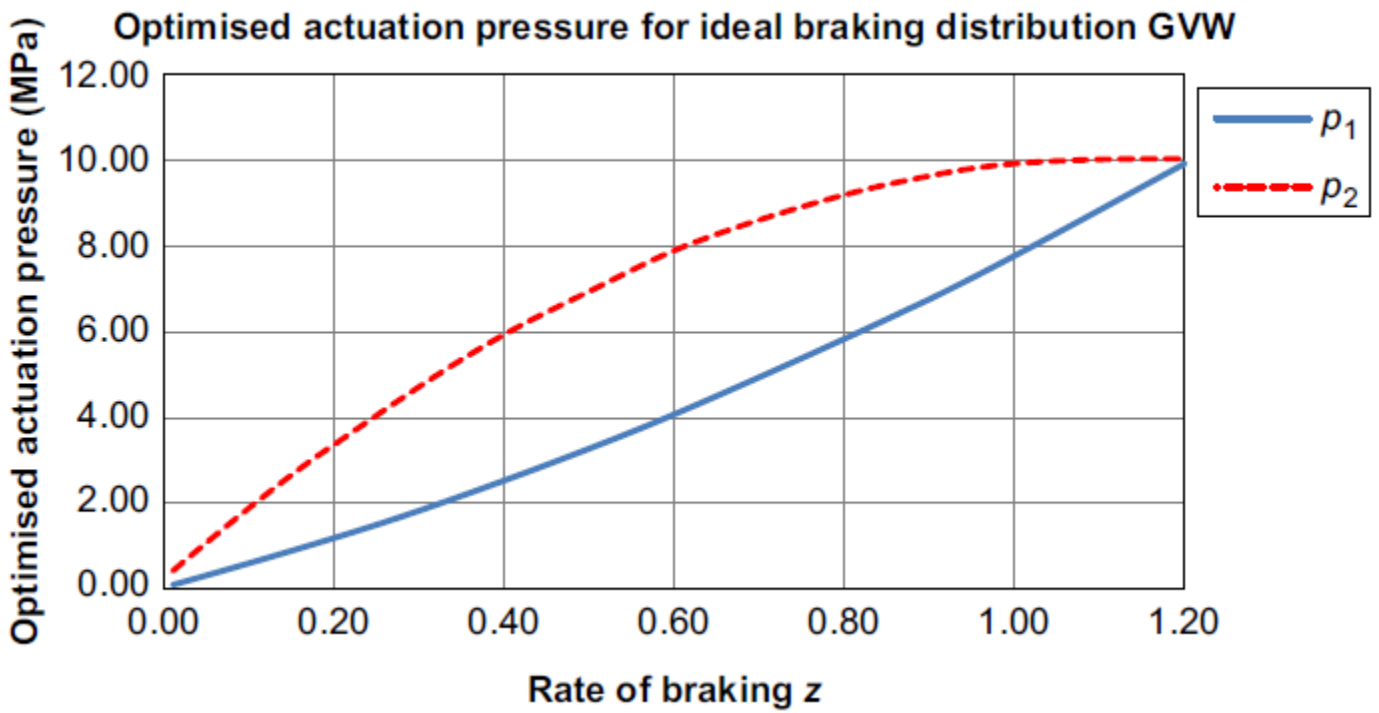

Figure 6.8: Optimised Actuation Pressures for Ideal Braking Distribution in the GVW and DoW Loading Conditions.

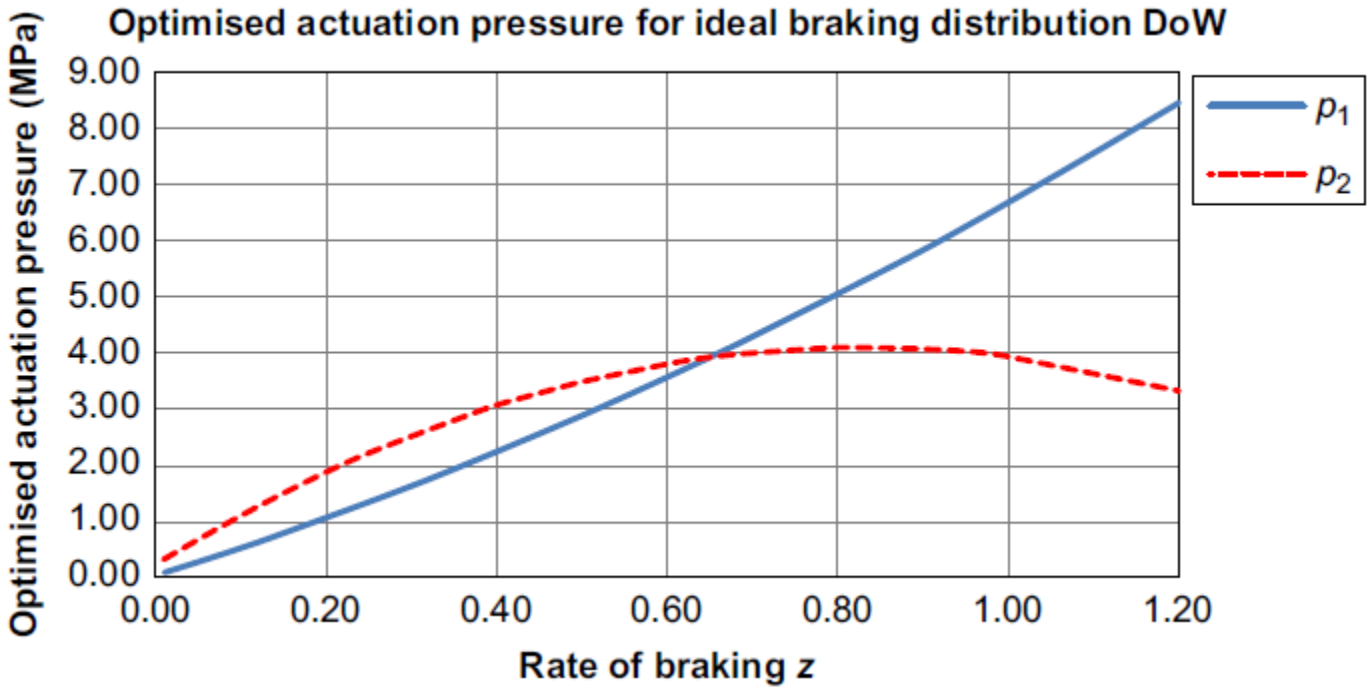

Figure 6.8: Optimised Actuation Pressures for Ideal Braking Distribution in the GVW and DoW Loading Conditions.

In the DoW condition the actuation pressure to the rear brake must be lower than that to the front brakes, while in the GVW condition the actuation pressure to the rear brakes must be higher than that to the front brakes in order to take advantage of the greater adhesion on the rear axle in the GVW condition.

However, to achieve the 'ideal' ratio X1/X2, the master cylinder pressure can only be reduced to give the required actuation pressure at the front or rear brakes

Step 3.3 Design the 'Master Actuator' (Brake Pedal) System (Hydraulic System)

Step 3.3.1 is to design the brake pedal system, including the pedal configuration, master cylinder piston size and stroke, servo boost ratio and knee point, and fluid consumption.

The EU legislative requirement (UN, Feb 2014) is for a minimum vehicle deceleration in the booster fail condition of z =0.25 with the driver effort (Fd) between 6.5 and 50 daN (see Chapter 8).The master cylinder can therefore only be designed in conjunction with the brake pedal design.

Brake Pedal

The brake pedal is one of the primary ‘driver interfaces’ between the customer and the vehicle. The response (deceleration) of the vehicle to the force applied to the brake pedal by the driver must be consistent and confidence-inspiring.

First, the force system must be designed so that the force (F_d) applied by the driver's foot to the brake pedal (the 'driver effort') is multiplied by the brake pedal lever ratio (R_p) to give the pedal output force (F_p), which is also called the 'pushrod force':

$$F_p = R_p F_d \qquad (6.15)$$

This ratio is initially specified as indicated in Figure 6.9

This ratio is initially specified as indicated in Figure 6.9

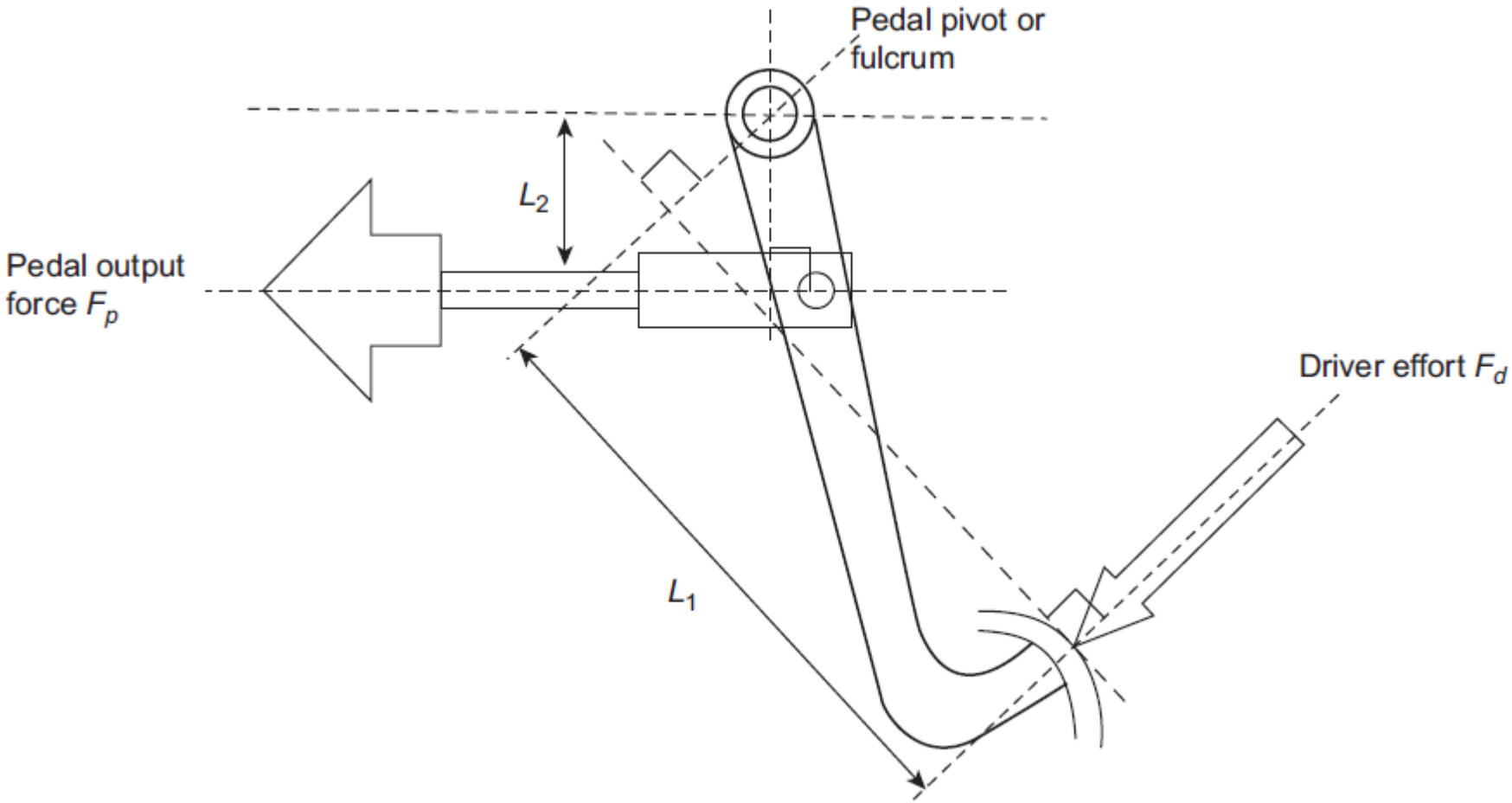

Figure 6.9: Brake Pedal.

as the perpendicular distance from the pedal pivot to the centre of the pressure pad on which the driver's foot acts (L_1), to the perpendicular distance from the pedal pivot to the clevis pin where the pushrod is attached (L_2)

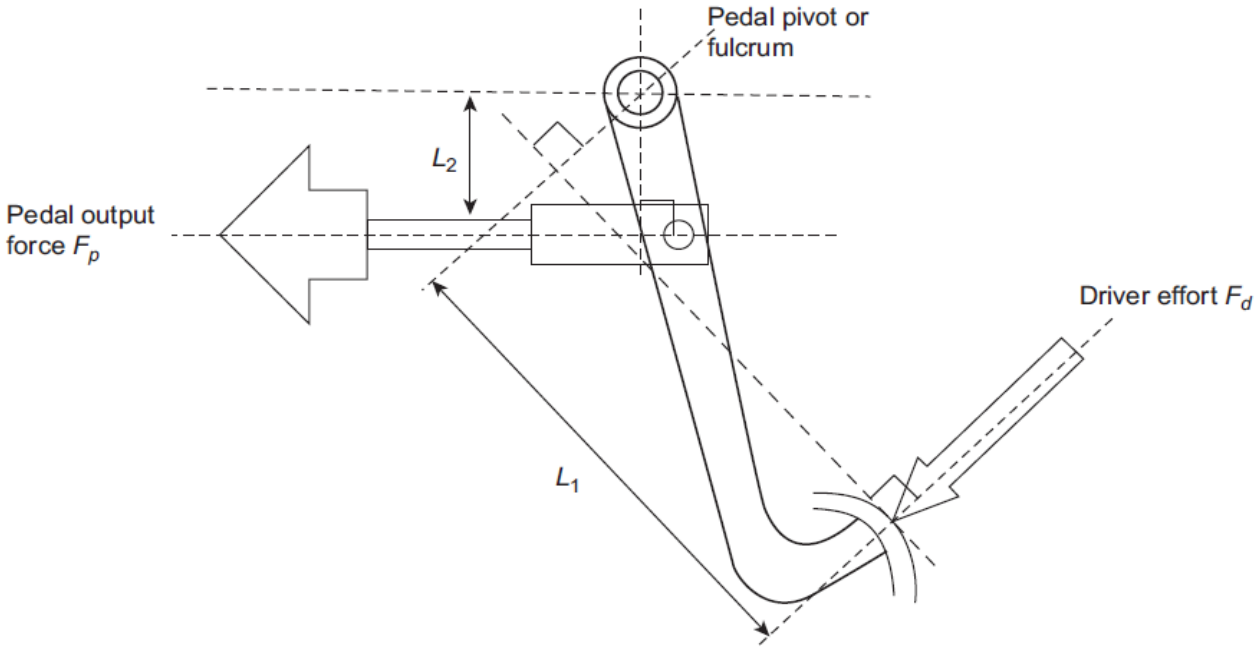

Figure 6.9: Brake Pedal.

The limiting factors on brake pedal design are:

- The available package space between the firewall, instrument cluster and the driver's legs for accessibility reasons.
- The effective pedal ratio in combination with the servo boost ratio, actuation design, and brake factor.
- Crashworthiness-related safety requirements, e.g. avoiding pedal intrusion into the driver's leg-room, which may require a pedal retraction feature.
- Ergonomic requirements to define the limits of travel and effort, the spacing between the pedals, and the trajectory of the brake pedal relative to the driver's seating position.

The last factor includes the 'step-over' height between the accelerator and brake pedals relative to the lateral separation of the pedals and any footrest that might be fitted, as illustrated in Figure 6.10.

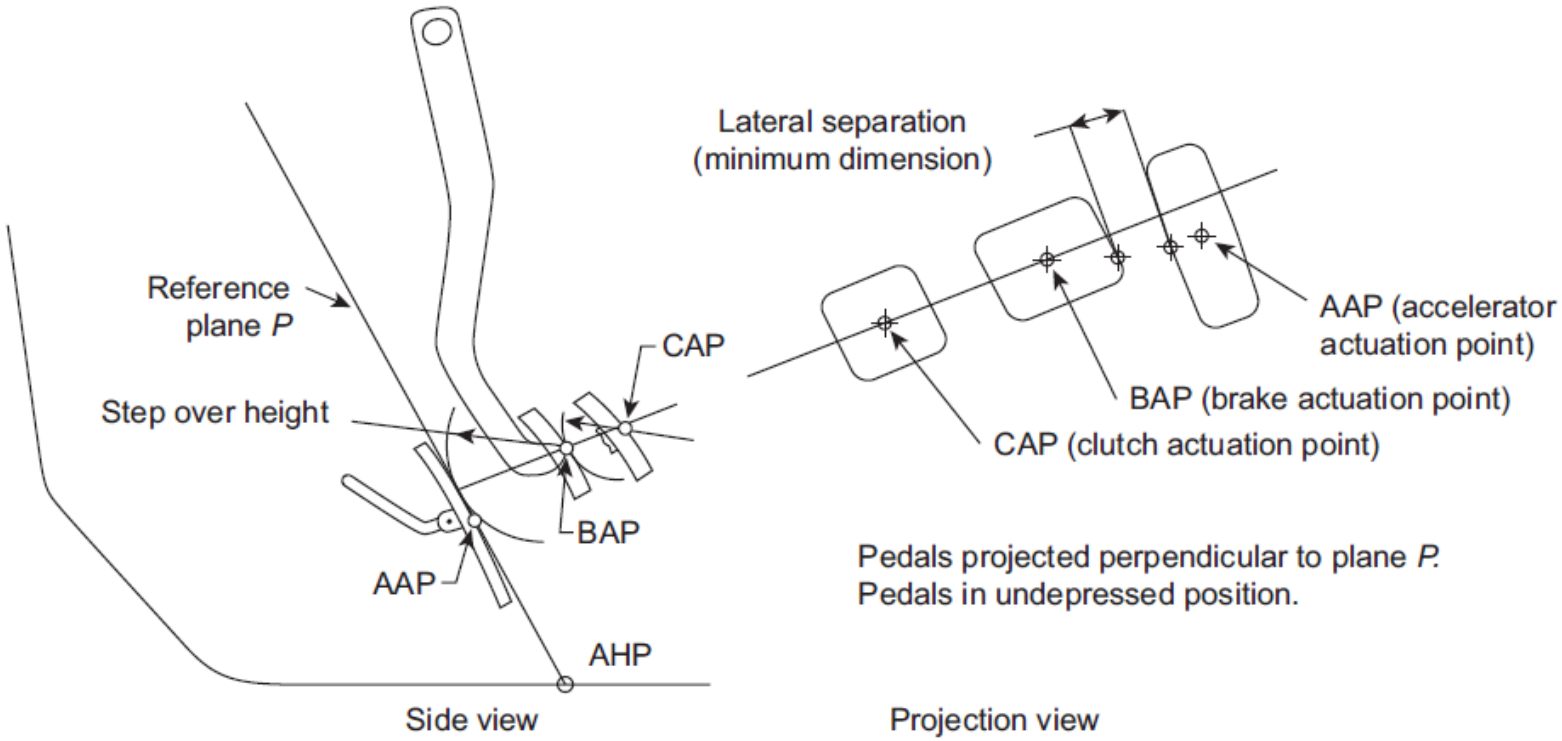

Figure 6.10: Nominal Dimensional Relationship Between Brake Pedal and Accelerator Pedal (Svensson, 2013).

Parameters to be considered for a good pedal feel include:

- Initial ‘dead’ travel before deceleration is perceived
- Relationship between deceleration and pedal effort
  Relationship between deceleration and pedal travel
- Relationship between pedal travel and effort
- Deceleration consistency
- Static and dynamic hysteresis
- Time delay between the application of the driver effort and the deceleration response of the vehicle.

The maximum pushrod travel or full stroke depends upon the pedal travel and the pedal ratio (R_p) as shown in Equation (6.16) and must not exceed the maximum length of piston travel of the master cylinder, which is usually specified by its manufacturer:

$$\text{Full stroke} = x_{pmax}/R_p \qquad (6.16)$$

If the maximum pedal travel (x_{pmax}) is 100 mm and R_p =4, the full stroke of the master cylinder would be 25 mm and the maximum length of piston travel of the master cylinder would in practice usually be specified as significantly more (e.g. 36 mm) to accommodate deformation and deflections of the system components under actuation forces.

Master Cylinder

The master cylinder converts the pushrod force (F_p) into brake circuit hydraulic pressure. Separate master cylinder functions are required for each circuit in case one fails. The necessary two functions are incorporated into a dual master cylinder, which is usually a 'tandem' design, in which two pistons share a single cylinder as illustrated in Figure 6.11(a).

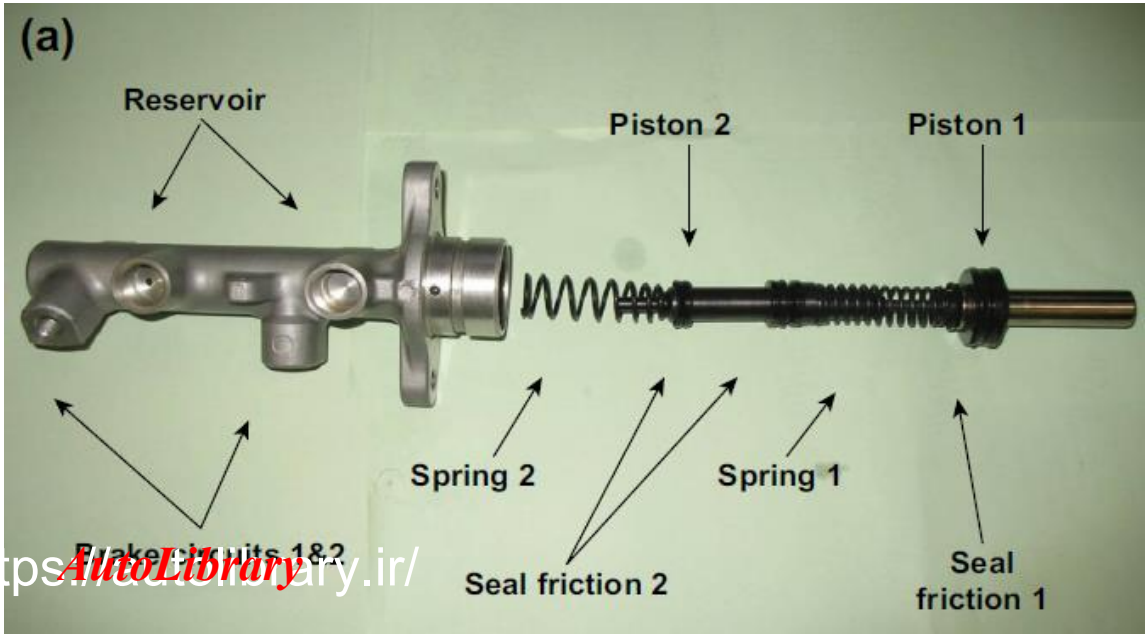

Figure 6.11: Master Cylinder Designs.

(a) Tandem master cylinder design.

Many modern systems now use the 'centre valve' design of master cylinder as shown in Figure 6.11(b).

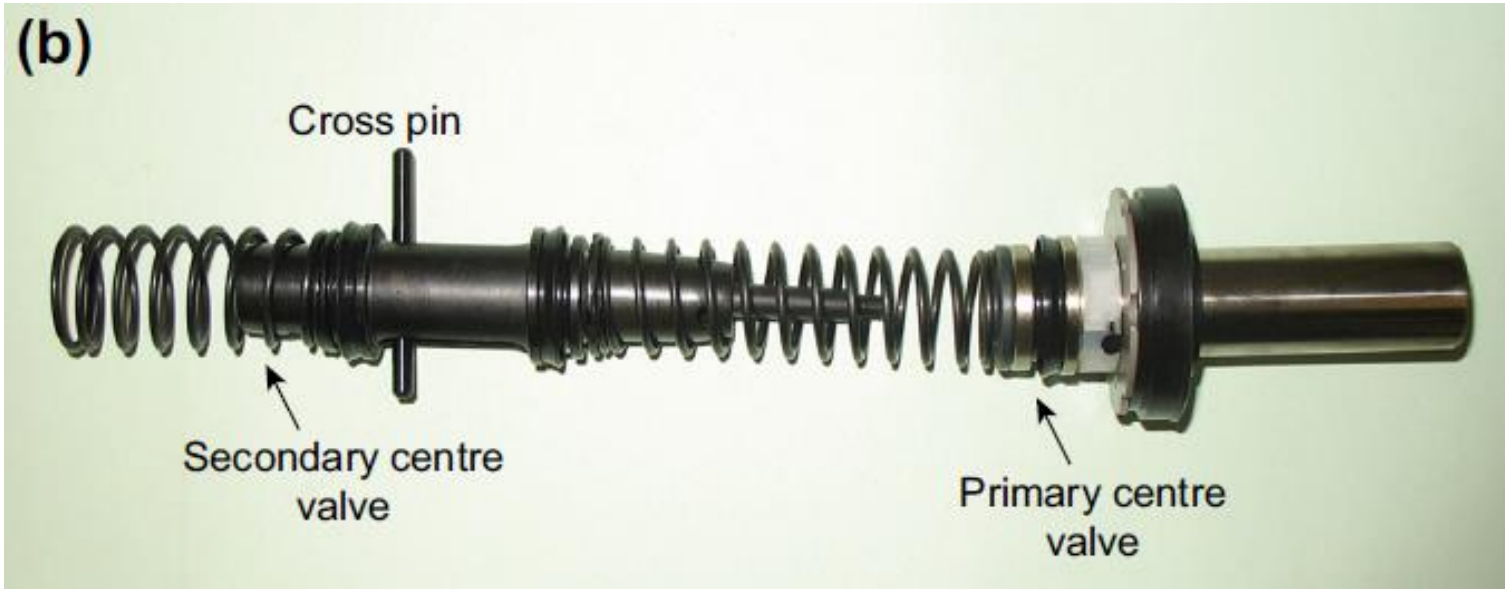

Figure 6.11: Master Cylinder Designs.
(a) Tandem master cylinder design. (b) Centre valve design (Ho, 2009).

If p_1 and p_2 are the hydraulic pressures generated in the primary and secondary chambers respectively by the input force P_{mc} (Gerdes et al., 1995):

$$p_1 = \left(P_{\text{mc}} - P_{k1} - F_{f1} - P_{c1}\right)/A_{mc1} \qquad (6.17a)$$

$$p_2 = p_1 - \left(P_{k2} + F_{f2} + P_{c2}\right)/A_{\text{mc2}} \qquad (6.17b)$$

where:

A_{mc1} and A_{mc2} are the cross-sectional areas of the primary and secondary pistons respectively;
F_{f1} and F_{f2} are the seal friction forces of the primary and secondary pistons respectively;
P_{k1} and P_{k2} are the spring pre-load forces on the return springs;
P_{c1} and P_{c2} are damping forces arising from the viscosity of the hydraulic fluid.

For braking system layout outline design, a useful approximation to Equations (6.17) is:

$$p = p_1 = p_2 = \eta_{mc} P_{mc} / A_{\mathrm{mc}} \qquad (6.18)$$

ηmc is an efficiency factor associated with hydraulic actuators (cylinders); typically for a brake master cylinder it is approximately 0.95

Brake Servo (Booster)

Drivers expect to be able to achieve high rates of braking at relatively low pedal efforts, which means that some form of servo or booster is usually incorporated to amplify the pushrod force (F_p) from the brake pedal. The most common type of servo device used on passenger cars and light vans is the 'vacuum' booster, although electrical boosters are becoming available. UN Regulation 13H (UN, Feb 2014) allows relatively high pedal effort to meet the braking performance prescribed for the booster fail condition (z =0.25 equivalent to J =2.44 m/s2 for driver effort (F_p) between 6.5 and 50 daN) so back-up servo assistance is not usually designed into hydraulic braking systems.

The vacuum booster total output force that actuates the master cylinder (P_{mc}) is therefore the sum of the input force from the brake pedal (F_p) and the servo assistance force generated by the pressure differential across the booster diaphragm (= pressure differential X booster diaphragm effective area), so that:

$$P_{mc} = F_p R_b \qquad (6.19)$$

The vacuum booster (Figure 6.12), requires air depression up to about 0.8 bar below atmospheric pressure.

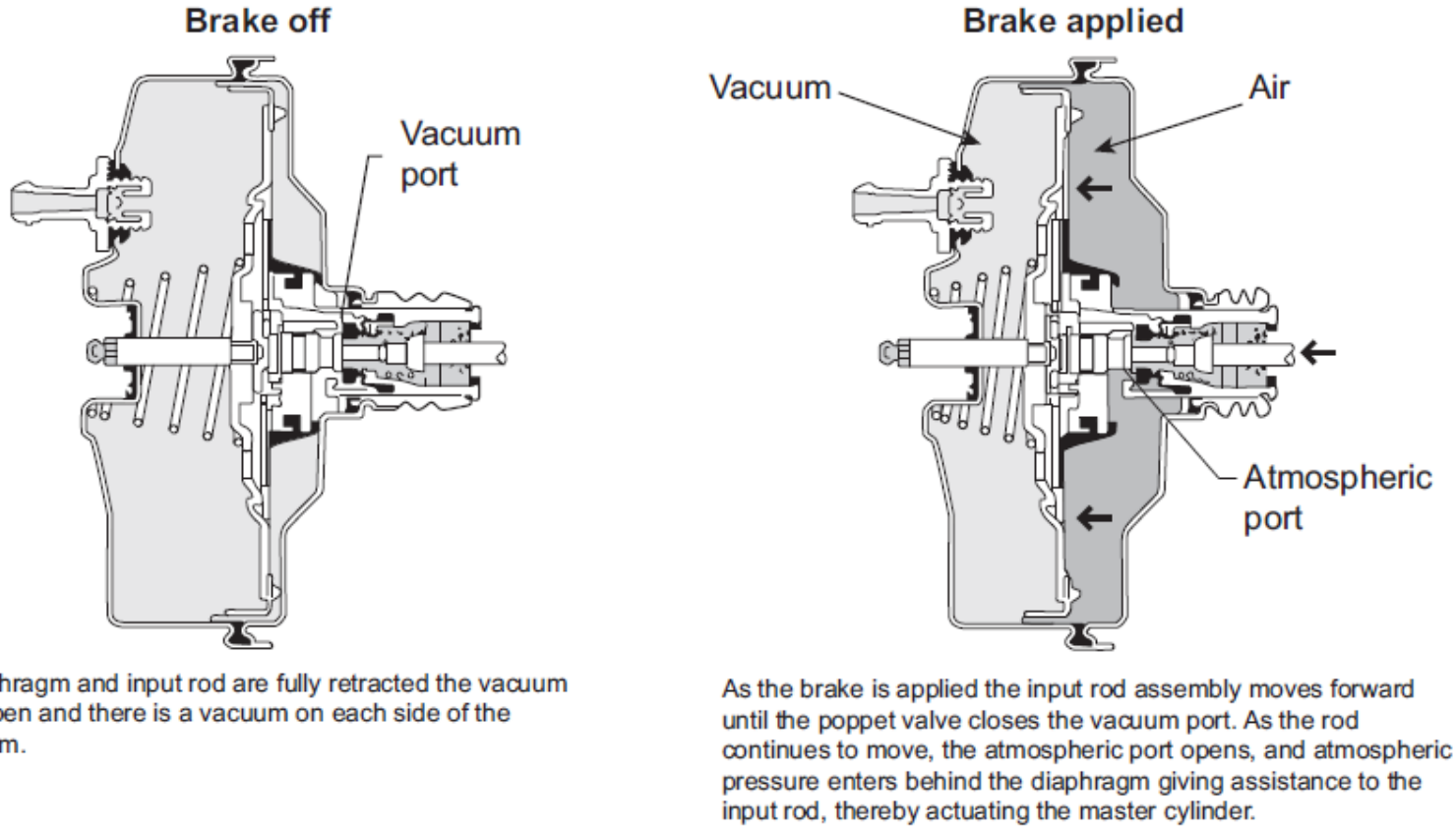

Figure 6.12: Vacuum Servo.

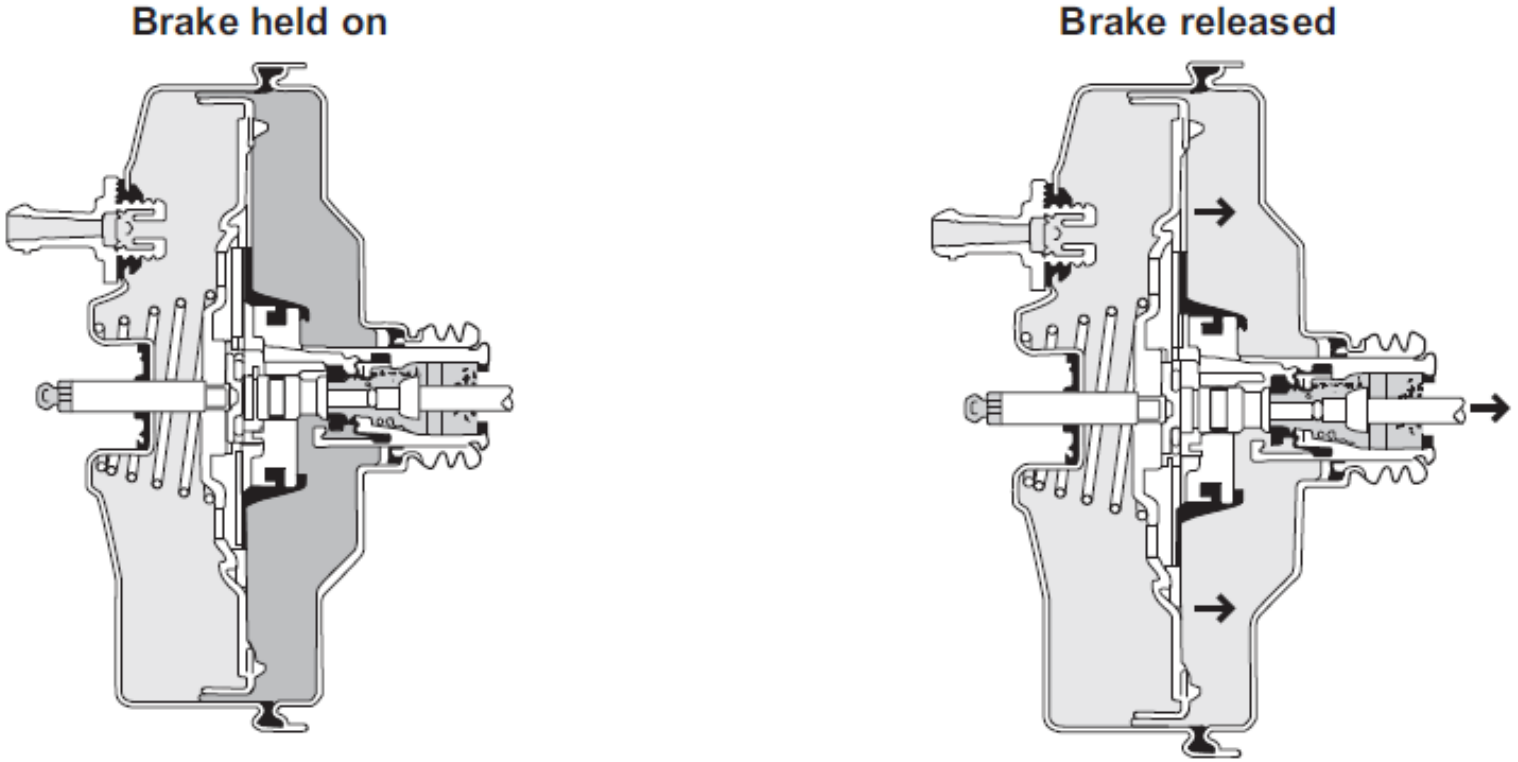

Figure 6.12: Vacuum Servo.

The total force amplification from the brake pedal to the master cylinder is the combination of the pedal ratio (Equation (6.15)) and the boost ratio (Equation (6.19)):

$$P_{mc} = R_p F_d R_b \qquad (6.20)$$

In the event of failure of the vacuum booster for any reason, R_b =1 because the pushrod force from the brake pedal (F_p) is transmitted to the master cylinder unchanged

Figure 6.13 shows the output line pressure generated by the master cylinder (p) vs. the input force to the booster (F_p).

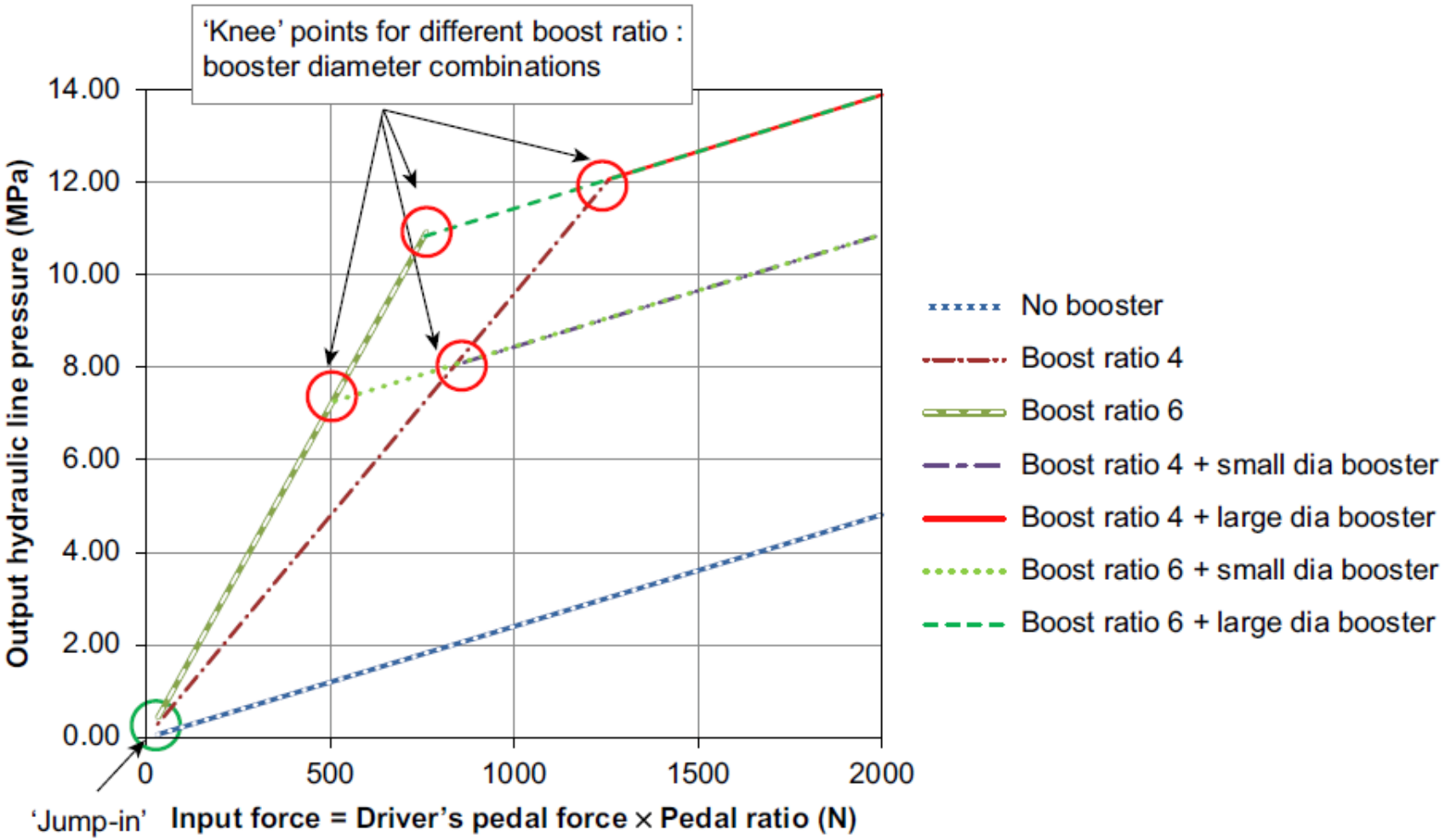

Figure 6.13: Vacuum Booster Boost Ratio and Knee Point.

Combining Equations (6.18) and (6.20) defines the basic relationship between the driver effort (F_d) and the generated master cylinder pressure (p):

$$p = \eta_{mc} R_p F_d R_b / A_{mc} \qquad (6.21a)$$

For the example vehicle an initial estimate of the required master cylinder size in the servo-fail condition, when the boost ratio R_b =1, can be found from Equation (6.21b):

$$A_{mc} = \eta_{mc} R_p F_d R_b / p \qquad (6.21b)$$

To meet the requirements of UN Regulation 13H in this condition (F_{dmax} =500 N, z = 0.25, R_b =1), an initial proposed design of the brake pedal (R_p) and the master cylinder diameter (D_{mc}) could be:

$$\text{Brake pedal lever ratio}\left(R_p\right) = 4:1$$

Operational factors including the effect of temperature on brake torque (fade) is approximately 3 MPa:

$$A_{mc} = 0.95 \times 4 \times 500 \times 1/3 \times 1\text{E}6 = 630\ \text{mm}^2$$

$$\text{Master cylinder diameter } D_{mc} = 28\ \text{mm}$$

Many master cylinder manufacturers offer standard bore sizes, and 27 mm diameter is taken as the nearest standard size. The boost ratio and knee point can now be designed to achieve the desired relationship between the driver effort (F_d) and the vehicle deceleration. Equation (6.21a) can be rearranged to:

$$F_d = pA_{mc} / (\eta_{mc} R_p R_b) \qquad (6.21c)$$

The system equation for the hydraulic brake actuation system can be formed by combining the individual component equations in Step 3.1, which are summarized below. It is assumed (see Chapter 5) that the pad actuation force (P_{ai}) is the same as the clamp force at the pad/disc interface (N_{ci}).

$$\text{Wheel brake torque: } \tau_{wi} = \text{BF}(p_i - p_{ti})A_{ai}\eta_i r_{ei} \tag{5.6b}$$

$$\text{Master cylinder pressure: } p_i = \eta_{mc}P_{mc}/A_{mc} \tag{6.22}$$

$$\text{Force amplification from the brake pedal to the master cylinder: } P_{mc} = R_p F_d R_b \tag{6.23}$$

Combining these gives the general brake hydraulic actuation system equation for the brake torque and the braking force generated at each wheel when the driver applies a force to the brake pedal (pedal effort F_d):

$$\tau_{wi} = \mathrm{BF}_i\left(\left(\eta_{mc} R_p F_d R_b / A_{mc}\right) - p_{ti}\right)\left(A_{ai}\eta_i r_{ei}\right) \qquad (6.24)$$

The wheel braking force is:

$$T_{wi} = \mathrm{BF}_i\left(\left(\eta_{mc} R_p F_d R_b / A_{mc}\right) - p_{ti}\right)\left(A_{ai}\eta_i r_{ei}\right)/R_r \qquad (6.25)$$

and the axle braking force is:

$$T_i = 2\mathrm{BF}_i\left(\left(\eta_{mc} R_p F_d R_b / A_{mc}\right) - p_{ti}\right)\left(A_{ai}\eta_i r_{ei}\right)/R_r \qquad (6.26)$$

For the whole vehicle the total braking force (T =T1+ T2) is given by Equation (6.27).

$$\begin{aligned} T &= (T_1 + T_2) \\ &= 2\mathrm{BF}_1\left(\left(\eta_{mc} R_p F_d R_b / A_{mc}\right) - p_{ti}\right)\left(A_{sc1}\eta_{sc1} r_{e1}\right)/r_{r1} + 2\mathrm{BF}_2\left(\left(\eta_{mc} R_p F_d R_b / A_{mc}\right) - p_{ti}\right) \\ &\quad \times \left(A_{a1}\eta_1 r_{e2}\right)/r_{r2} \end{aligned} \qquad (6.27)$$

Brake Pedal Feel and Fluid Consumption

Brake pedal feel is very important in modern passenger car brake system design, and is primarily determined by the relationship between the driver effort (force applied on the pedal by the driver's foot) and the pedal travel (movement), as indicated in Figure 6.14

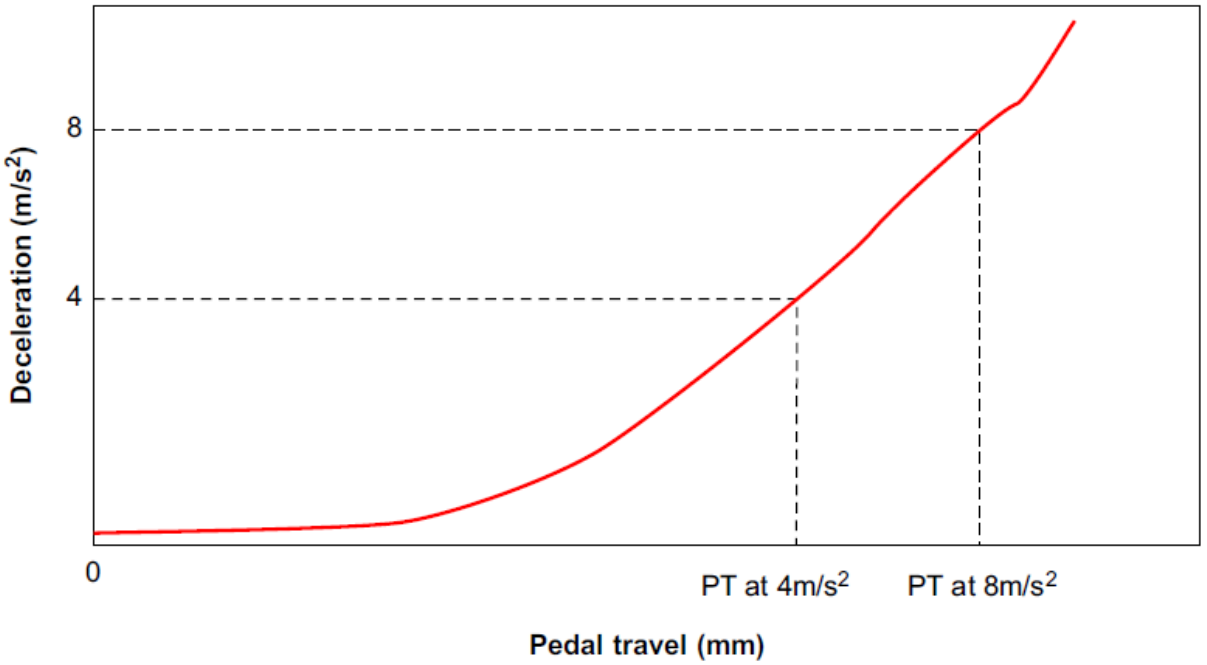

Figure 6.14: Brake Pedal Feel Example Characteristic.

The factors that influence pedal travel include:

- Brake pedal and mounting (bulkhead) clearance, deflection and deformation
- Servo (booster) valve clearances, spring settings and reaction disc deformation
- Master cylinder bore and seal deformation, and valve clearances (c_{mc})
- ABS/ESC system valve clearances and internal deformation
- Brake pipe and flexible hose deformation (cbp and c_{bh})

- Slave cylinder bore and seal deformation (c_{sc})
- Brake fluid compression (c_{bf})
- Pad/disc or lining/drum clearances
- Brake pad or brake shoe assembly compression, deflection and wear
- Stator deformation e disc brake caliper and drum brake anchor plate
- Rotor deformation and deflection e disc and drum.

The purpose is to avoid a situation where the extra movement to compensate for the fluid consumption causes the pedal to reach the limit of its travel before the required hydraulic pressure is generated. It should be noted that the term 'fluid consumption' does not imply that any hydraulic fluid is lost from the system, and the term 'fluid reserve' does not refer to the amount of brake fluid in the reservoir of the master cylinder, but to the volume (V_{mc}) of brake fluid of the master cylinder, as defined in Equation (6.22):

$$V_{mc} = A_{mc} \cdot \text{Full stroke} = A_{mc} x_{pmax} / R_p \qquad (6.28)$$

A typical design target could be 50% fluid reserve at z =1, GVW (at a specified worst case operational condition, which may mean high brake operating temperatures after repeated braking), i.e.:

$$\frac{\text{Volume of brake fluid displaced to achieve } z = 1}{\text{Volume } (V_{mc}) \text{ of brake fluid in the master cylinder stroke}} \leq 0.5 \qquad (6.29)$$

This is illustrated in Figure 6.15.

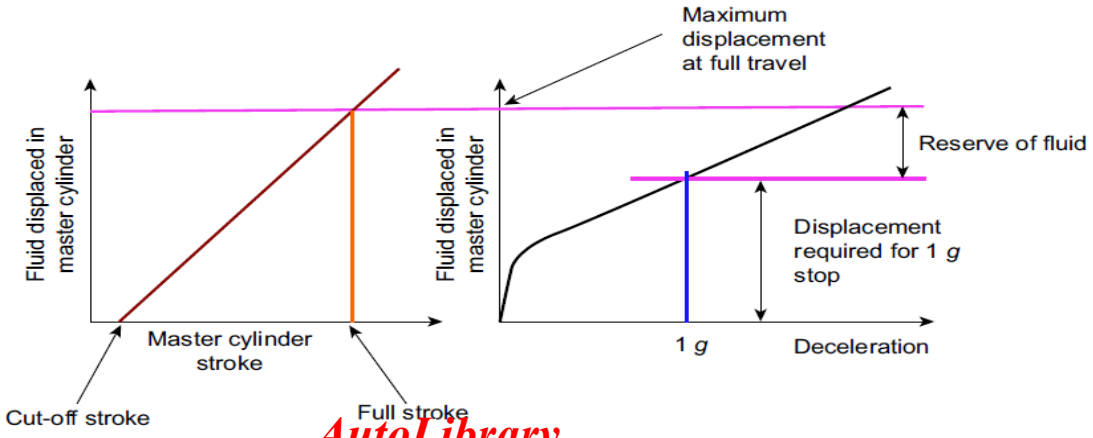

Figure 6.13: Brake Fluid Consumption Design Target.
(a) Fluid volume displaced vs. stroke. (b) Fluid volume displaced vs. deceleration.

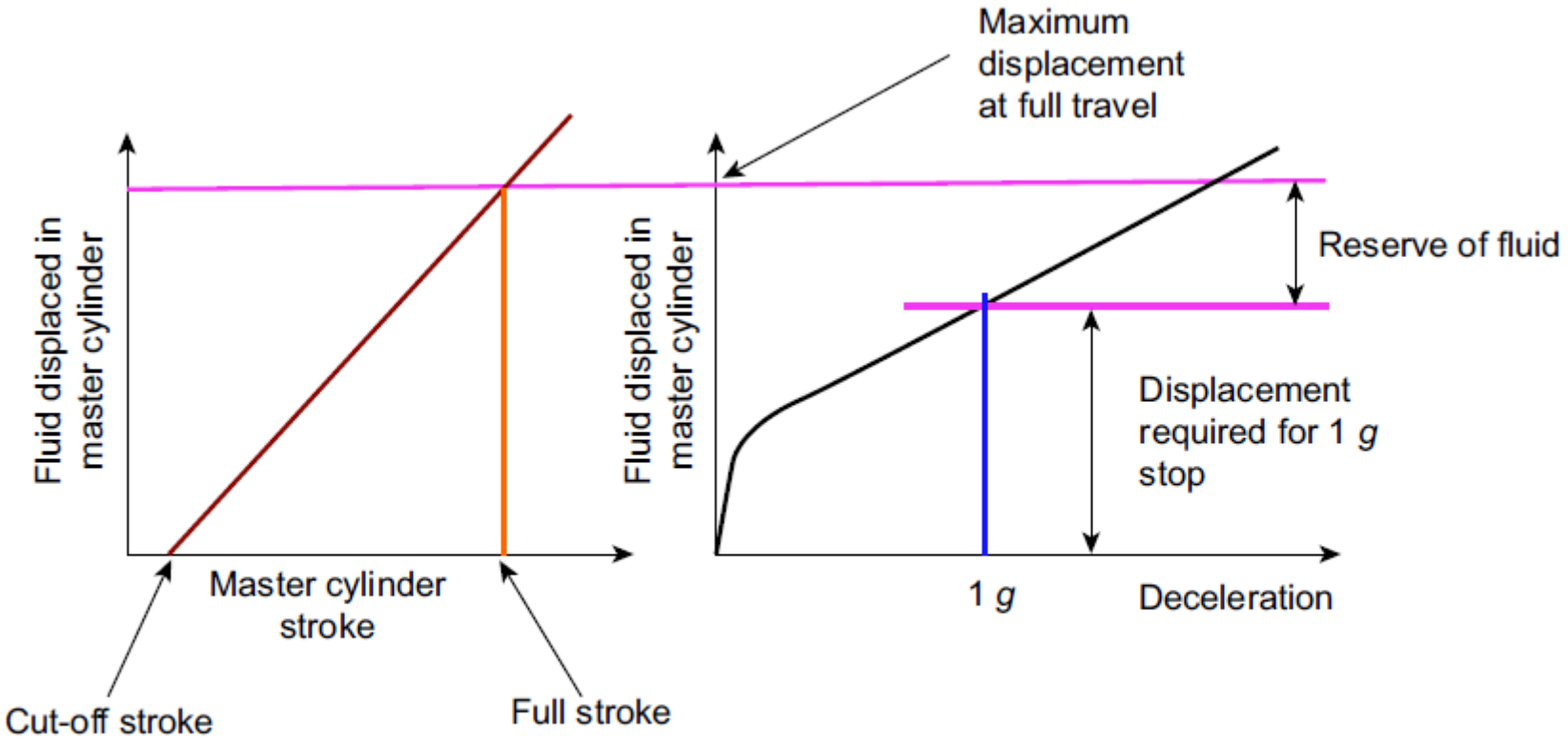

Figure 6.15: Brake Fluid Consumption Design Target.
(a) Fluid volume displaced vs. stroke. (b) Fluid volume displaced vs. deceleration.

Brake Pedal and Mounting (Bulkhead) Clearance, Deflection and Deformation

As previously stated, deflection and deformation of the brake pedal, pedal box and the vehicle bulkhead should be minimized to achieve the stiffest system possible. This is achieved by CAE analysis. Although brake pedal and mounting clearance, deflection and deformation affects pedal travel, it is external to the master cylinder and the effect can be quantified separately and added to pedal travel resulting from the master cylinder movement.

Servo (Booster) Valve Clearances, Spring Settings and Reaction Disc Deformation

ratio (and ultimately the knee point) directly influence the driver effort (pedal force) required to generate the required line pressure in the brake actuation system and hence the vehicle deceleration. Additionally there are other components in a vacuum booster that affect the relationship between the pedal force and the line pressure, and thus the pedal feel; in particular, the valves must be sensitive and controllable enough to provide proportional assistance even at very low pedal force under all driving conditions.

An example characteristic of master cylinder pressure vs. pedal travel for a car brake actuation system (three datasets) is shown in Figure 6.16.

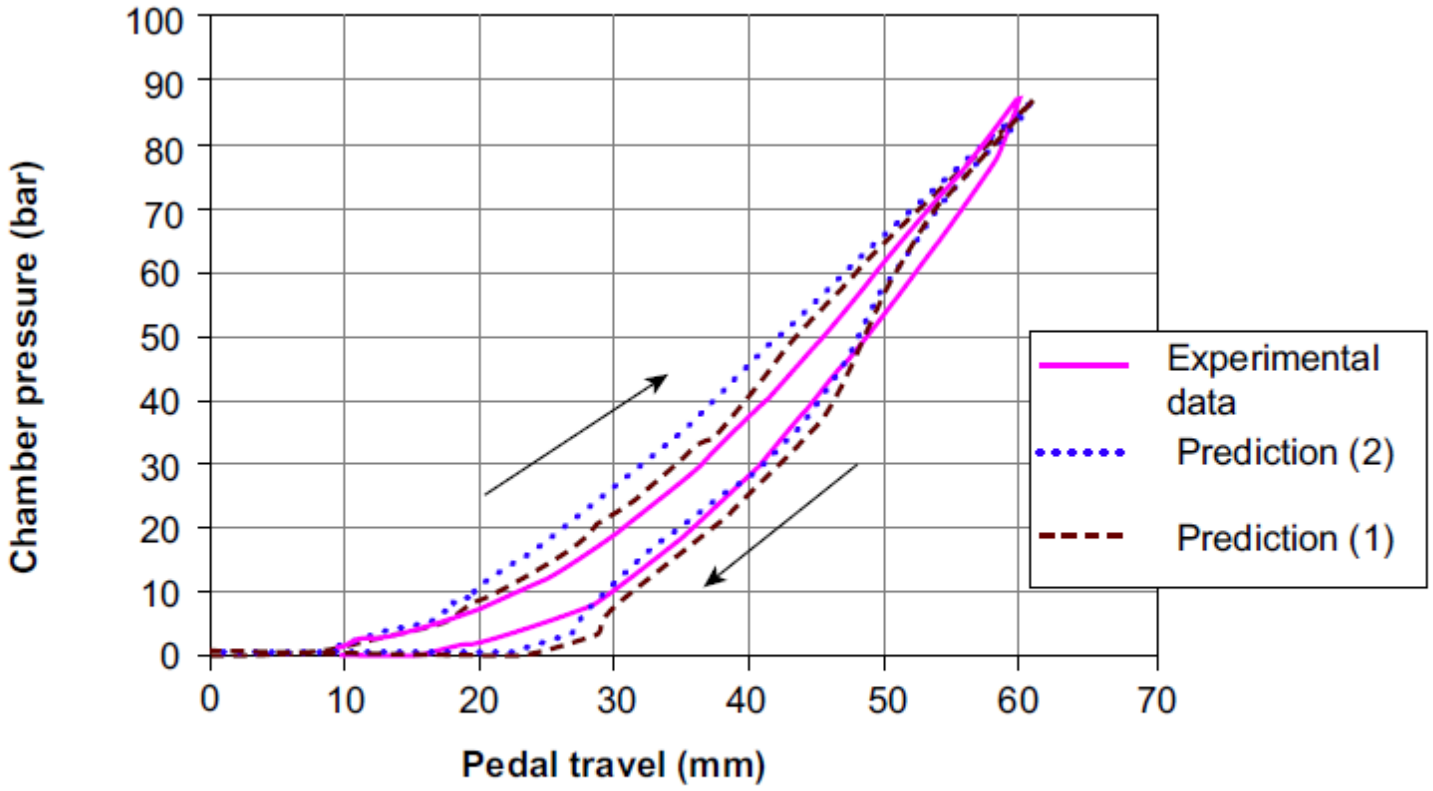

Figure 6.16: Vacuum Servo Characteristic Example: Master Cylinder Pressure vs. Pedal Travel (Three Datasets Shown).

Master Cylinder Bore and Seal Deformation, and Valve Clearances (c_{mc})

The radial expansion (u_r) of the master cylinder bore under hydraulic pressure p can be calculated from thick walled pressure vessel theory (Lame´'s equations):

$$u_r = \frac{r_a}{E\left(r_b^2 - r_a^2\right)}\left[(1-\nu)pr_a^2 + (1+\nu)pr_b^2\right] \qquad (6.30)$$

r_a and r_b are the tube inner and outer radii respectively.

Using Equation (6.22) a comparison of the estimated expansion of the bore of different master cylinder designs and materials is shown in Table 6.5.

Table 6.5: Comparison of the Estimated Expansion of the Bore of Different Master Cylinder Designs and Materials

Material	Cast Iron	Steel	Aluminium Alloy
Bore diameter (mm)	20.64	20.64	20.64
Wall thickness (mm)	5	3	7
Young's modulus (GPa)	175	200	75
Poisson's ratio	0.25	0.29	0.33
Hydraulic pressure (MPa)	10	10	10
Radial expansion (mm)	0.0013	0.0017	0.0028
c_{mc} (mm^3/MPa) (assuming a 25 mm stroke)	0.22	0.27	0.46
Fluid 'consumption' at 10 MPa (100 bar) (mm^3)	2.2	2.7	4.6

Together with the piston travel to actuate the valves, this suggests that the fluid consumption coefficient c_{mc} (mm3 / MPa) for a 20.64 mm diameter centre valve master cylinder at hydraulic pressure p_{mc} (MPa) could be:

$$c_{mc} = 580 + (2.2p_{mc}) \qquad (6.31)$$

This is an example that depends on the size specification, design and manufacture of the master cylinder. Design improvements in master cylinder valves continue to be made to reduce the actuation movement needed.

ABS/ESC System Valve Clearances and Internal Deformation

As explained in Chapter 11, ABS/ESC systems are designed to be neutral in terms of brake system performance including pedal feel when they are not operational. During operation they are designed to minimize transient dynamic effects (pulsing) on the brake pedal.

Brake Pipe and Flexible Hose Deformation (cbp and cbh)

Hydraulic brake lines are thick walled steel tubes, and thick-walled composite flexible hoses made from reinforced rubber where flexibility is required to connect parts that move relative to each other, e.g. from a subframe to a caliper. The radial expansion of thick-walled steel brake lines can also be predicted from Equation (6.21), and for a typical brake line at 100 bar the fluid consumption can be around 1.5 mm3 per metre length. Hence c_{bp} = 0.15 mm3/MPa $ m. The composite hoses have a much higher flexibility, and a typical value of fluid consumption estimated from manufacturers' expansion data is c_{bh} = 30 mm3/MPa . m.

Slave Cylinder Bore and Seal Deformation (c_{sc})

As explained in Chapter 5, slave cylinders and pistons provide the actuation force at the foundation brake (disc or drum) in a hydraulically actuated braking system. In drum brakes the slave piston acts directly on the shoe tip, and in disc brakes there may be one, two or more pistons acting on each pad to ensure that the actuation force is as uniformly distributed as possible over the pad/disc friction interface. The relationship between the applied hydraulic pressure and the actuation force generated by the slave cylinder piston is defined by Equation (5.5).

Brake Fluid Compression (c_{bf})

The compressibility of brake fluid is affected by temperature and the presence of trapped air and moisture. Vehicle manufacturers use vacuum fill techniques for charging the hydraulic brake system on the vehicle assembly line, and annual replacement of the fluid is recommended to minimize the effects of moisture (moisture content also affects vaporization point).

The physical and chemical properties of brake fluid are closely specified, and Figure 6.17 indicates the dependence of fluid compressibility (*cbf*) on temperature for different types of brake fluid.

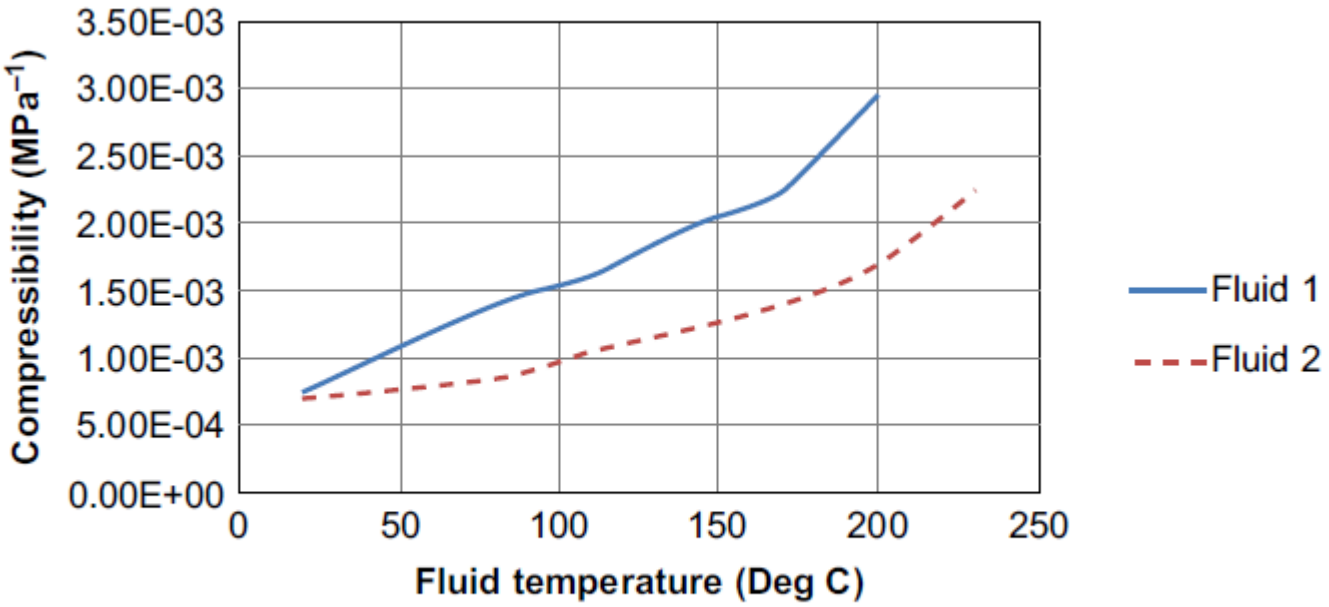

Figure 6.17: Brake Fluid Compressibility vs. Temperature (Internet Source).

Pad/Disc or Lining/Drum Clearances

In order to minimize residual drag forces (parasitic losses), running clearances between the rotor and stator friction elements must be maintained when the brake is not being used. As explained in Chapter 5, a threshold force is required to overcome the retraction forces generated by the 'pull-off' springs in drum brakes and the seal 'roll-back' in disc brakes. Then piston movement is required to close the running clearance.

Brake Pad or Brake Shoe Assembly Compression, Deflection and Wear

Brake pad compression is influenced by the compressive stiffness of the friction material, and the flexure of the backplate as explained in Chapter 5 referring to friction interface pressure distribution.

Stator Deformation e Disc Brake Caliper and Drum Brake Anchor Plate

Disc brake caliper deflection was briefly discussed in Chapter 5; deformation, displacement and distortion of the caliper arise from caliper deflection under clamp load, caliper twisting under friction drag loading, and thermal deformation. Deformation and deflection of the anchor plate of the type of Simplex drum brake fitted to most passenger cars and light vans are not considered to affect fluid consumption significantly.

Rotor Deformation and Deflection e Disc and Drum

Good detail design of brake discs is essential to minimize fluid consumption arising from the deformation and deflection of brake rotors. A new brake can be manufactured and assembled with minimum deformation and deflection, but as soon as it is used, the disc will deform and deflect as a result of the thermomechanical loads imposed on it by braking friction.

Factors which influence the generation of DTV include:

- Disc design for minimal coning
- Stable disc material with temperature
- Disc and hub manufacture with tight tolerances on runout
- Assembly processes designed to minimise ‘bolt-up’ distortion
- Rigid stator (caliper) with minimum deflection and distortion under operational loads.

Experimental measurement of brake line pressure vs. pedal travel from a static bench test rig is shown in Figure 6.18, which indicates a contribution of different parts of the hydraulic actuation system to fluid consumption.

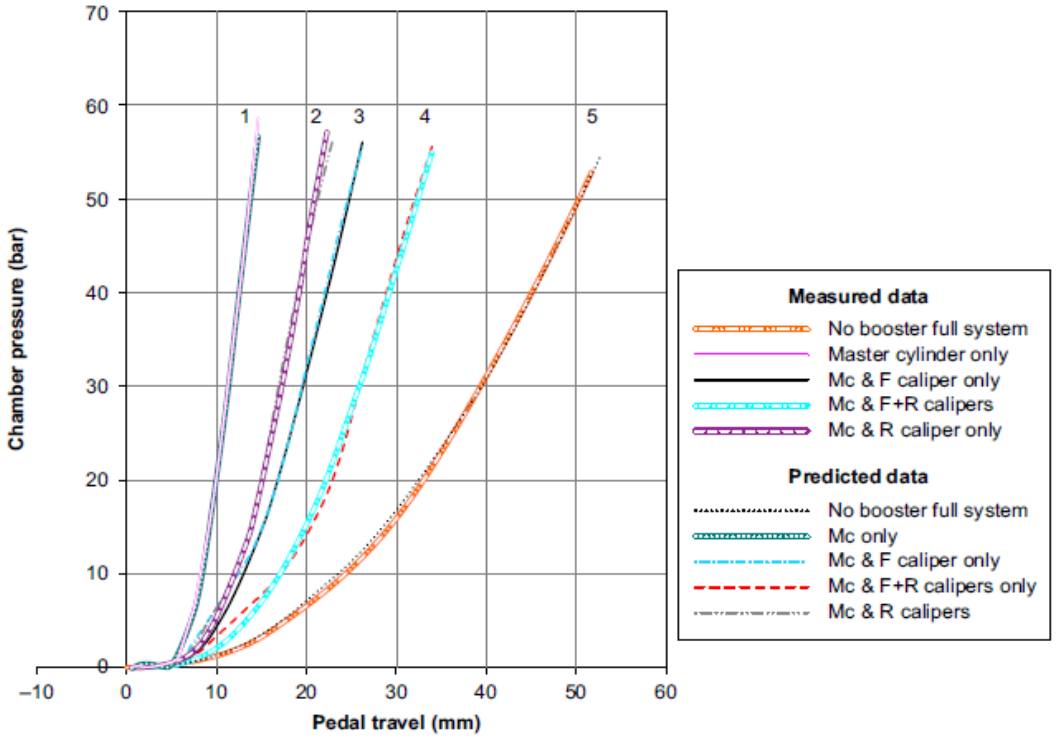

Figure 6.18: Contribution of Different Parts of the Hydraulic Actuation System to Fluid Consumption as indicated by the change in the relationship between master cylinder chamber pressure and pedal travel. (Ho, 2009).

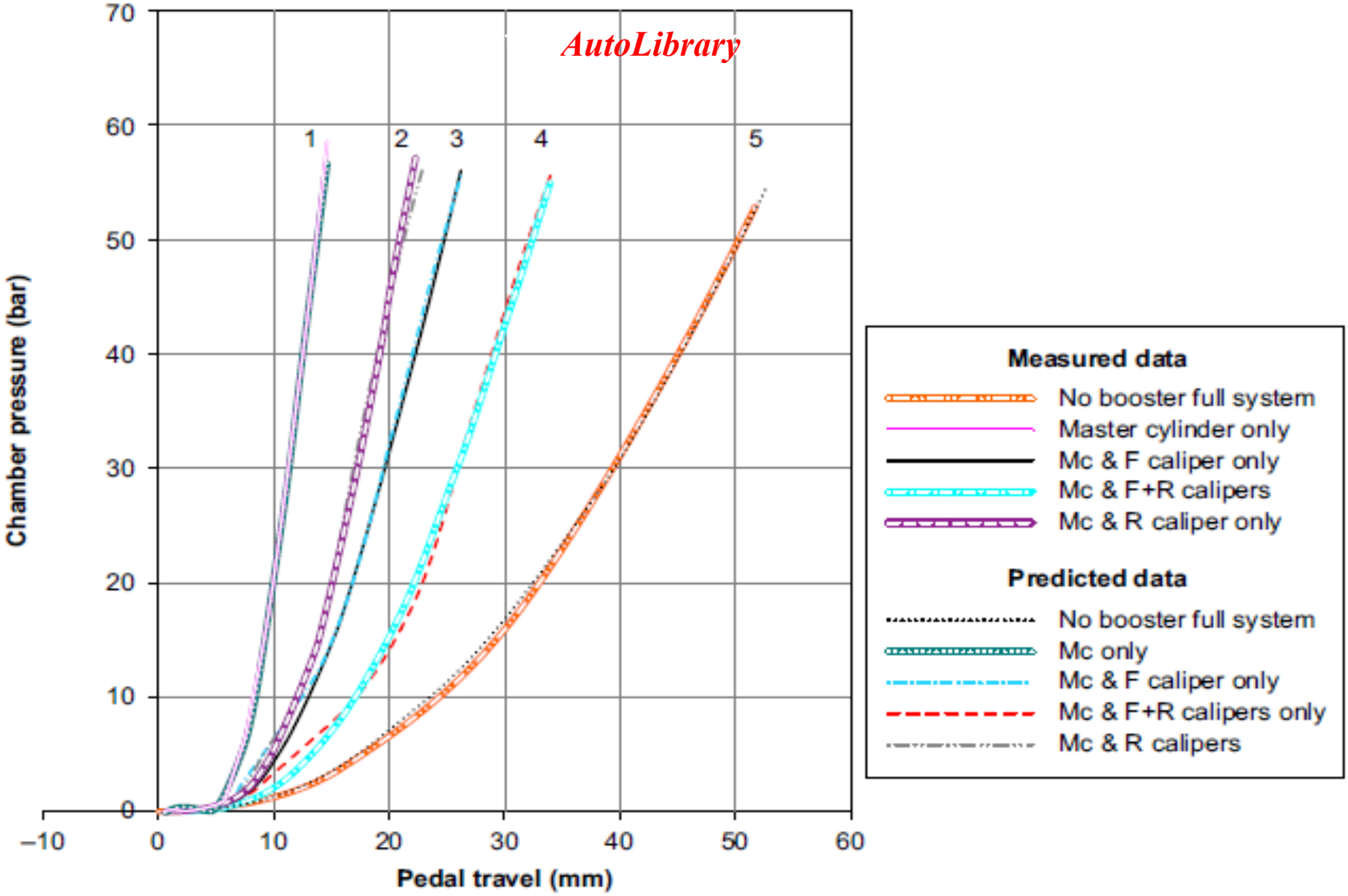

Figure 6.18: Contribution of Different Parts of the Hydraulic Actuation System to Fluid Consumption as indicated by the change in the relationship between master cylinder chamber pressure and [illegible] travel. (Ho, 2009).

Step 4 Verify the Design and Check Compliance with Legislative Requirements (UN Regulation 13H)

Steps 1-3 above describe the brake system design procedure for the example passenger car defined in Table 6.2, and the typical design targets that must be verified for the braking system on this type of vehicle include:

- Compliance with all legal requirements.
- Brake pedal feel: the subjective perception of brake pedal force and travel to achieve the required vehicle deceleration should meet the manufacturer's targets.

- Stopping distance: the vehicle must be capable of achieving the minimum stopping distance and/or mean fully developed deceleration (MFDD).
- Stability and adhesion utilization: the vehicle must decelerate without deviation or imbalance between axles.
- The vehicle must decelerate without generating noise, judder and vibration.
- Wear and durability: the life of the brake rotors and stators must meet customer expectations.

Equation (6.27) is used to calculate the design braking performance of the vehicle specified in Table 6.2 with the additional designed system data summarized in Table 6.7.

Table 6.7: Hydraulic Braking System Design Specification

Design Parameter	Design Value
Brake pedal ratio	4.0
Boost ratio	4.0
Booster diameter	Large
Brake master cylinder diameter	27 mm
Master cylinder efficiency	0.95
Brake master stroke	36 mm
Foundation brakes:	
Front brake factor ($BF = 2\mu$)	0.76
Rear brake factor $BF = 2\mu$ for a disc brake (BF = combined shoe factor $= S_1 + S_2$ for a drum brake)	0.76
Front disc effective radius	125 mm
Rear disc effective radius	130 mm
Front slave cylinder diameter	1×63 mm
Front slave cylinder threshold pressure	0.05 MPa
Front slave cylinder efficiency	0.95
Rear slave cylinder diameter	1×38 mm
Rear slave cylinder threshold pressure	0.25 MPa
Rear slave cylinder efficiency	0.95

Step 4.1 Intact System

Annex 3 of UN Regulation 13H (see Chapter 8) requires minimum levels of vehicle deceleration to be verified by tests. The prescribed performance is based on the stopping distance and the mean fully developed deceleration, MFDD. (Note that the symbol used in this book for MFDD is *Jm*, while that used in UN Regulations 13H and 13 is *dm*) with the vehicle in the laden condition as specified by the manufacturer.

Step 4.2 Partial System Failure

The braking system performance in the booster fail condition as specified in UN Regulation 13H requires vehicle deceleration (J_m) > 2.44 m/s2 (z = 0.25) from 100 km/h with the driver effort (F_d) not exceeding 500 N. A line pressure of approximately 2.65 MPa is required to achieve z = 0.25, and using Equation (6.21c) with R_b set to 1 for the servo-fail condition; this requirement is met with the required pedal force Fd = 403 N.

If one brake circuit fails, e.g. by rupture of the brake hydraulic pipe, UN Regulation 13H requires $J_m \geq 2.44$ m/s2 (z = 0.25) from 100 km/h with F_d not exceeding 500 N. To simulate this in the calculation, the system failure can be simulated for each type of braking system split:

X-split: multiply BF_1 and BF_2 by 0.5: $F_d = 258$ N
Front–rear split: set the corresponding value of BF to 0
Front brake system failure ($BF_1 = 0$): $F_d = 384$ N
Rear brake system failure ($BF_2 = 0$): $F_d = 133$ N.

Step 4.3 Parking

UN Regulation 13H also requires that the parking braking system must be capable of holding a fully laden vehicle stationary on a 20% up or down gradient (angle of inclination = 11.3) with a manually applied force to the control of ≤ 400 N. This requirement usually determines the design and specification of the parking brake, and very often the rear brake effective radius r_e is maximized in order to maximize the torque for any specified actuation system design.

EPB systems are becoming increasingly popular because of the advantages summarized below:

- Improved operational safety
- Simple operation, including hill hold capacity independent of driver skill
- Simpler packaging; no hand or foot lever to intrude into the occupant area
- Integral diagnostic system with an emergency braking function via the service brake system in connection with ESP if the service brake system fails
- Easier installation
- Enhanced safety by automatic application, reduced risk of vehicle ‘roll-away’
- Potential integration into anti-theft system.

Comment on Verification Against Legislative Requirements e Hydraulic Braking Systems

Legislative requirements represent the minimum level of performance required of a road vehicle braking system, and vehicle manufacturers always aim to exceed this level of braking performance, often by a considerable margin. Additional ‘in-house’ braking performance standards are specified by individual vehicle and component manufacturers relating to many aspects of braking, e.g. the fluid consumption discussed earlier.

Two alternative brake actuation system designs considered for a medium sized passenger car, which are summarized in Table 6.8

Table 6.8: Comparison of Alternative Brake Actuation System Designs for a Medium-Sized Passenger Car (Svensson, 2013)

Design Specification	Design 1	Design 2
	Brake Pedal Ratio	
Actuation unit	4	2.65
Diaphragm size	8 & 9 inch (tandem)	8 & 9 inch (tandem)
Brake master cylinder diameter (mm)	27	22.2
Brake master stroke (mm)	36	46
	Foundation Brakes	
Front effective radius (mm)	125	125
Rear effective radius (mm)	130	130
Front disc effective mass (kg)	6.0	6.0
Rear disc effective mass (kg)	2.8	2.8

with the same wheel cylinder diameter for each design (60 mm), the mechanical ratios for the two systems were the same:

$$\frac{\text{Wheel cylinder area}}{\text{Master cylinder area}} \cdot r_p = \left[\frac{60^2}{27^2}\right] \cdot 4 = \left[\frac{60^2}{22.2^2}\right] \cdot 2.65 = 19.7$$

Both designs satisfied the requirements of UN Regulation 13H, e.g.:

- Booster fail ($J_m > 2.44$ m/s^2): $J_m = 3.05$ and 2.70.
- Adhesion utilisation for $J \geq 5.15$ m/s^2 ($f_i \leq 0.85$): $f_i = 0.72$ (both designs).

Commercial Vehicle Braking Systems with Pneumatic Actuation

Commercial vehicle braking systems have several complicating features that are not present on passenger cars, and some of these are discussed here before dealing with the actuation system design. First, because of their large size and large mass, commercial vehicles present a very high demand on their foundation brakes to achieve safe and reliable braking. For this reason, many commercial vehicles are fitted with retarders that provide braking torque through the vehicle driveline and supplement the retardation provided by the foundation brakes, thereby reducing the braking duty on the foundation brakes.

for a commercial vehicle the laden condition is the worst case for all axles. Equation (6.1d) requires the braking distribution Xi to be calculated for each axle as explained in Chapter 4, which for the laden case at z =0.5 is 0.254/0.263/0.483. Equation (6.1d) then gives the following maximum brake torque requirements at each axle at the design maximum rate of braking of 0.8:

$$\text{Tractor front axle: } \tau_{w1max} = T_{w1max} r_r = X_1 P z r_{r1}/2 = 19.8 \text{ kNm}$$
$$\text{Tractor rear axle: } \tau_{w2max} = T_{w2max} r_r = X_2 P z r_{r2}/2 = 20.6 \text{ kNm}$$
$$\text{Tractor rear axle: } \tau_{w3max} = T_{w3max} r_r = X_3 P z r_{r3}/2 = 12.6 \text{ kNm}$$

(based on a three-axle bogie; see below)

As previously explained, for commercial vehicles the brakes on each axle should provide sufficient braking force to provide the required maximum deceleration for the maximum weight being carried on that axle. On this basis the maximum brake torque requirements at each axle at a design maximum rate of braking of 0.8 are comparable:

$$\text{Tractor front axle: } \tau_{w1max} = 19.4 \text{ kNm}$$
$$\text{Tractor rear axle: } \tau_{w2max} = 22.3 \text{ kNm}$$
$$\text{Semi-trailer axles: } \tau_{w3max} = 19.4 \text{ kNm}$$

The maximum and mean power dissipations at each brake (Step 1.3) from an initial road speed of 96 km/h (legal maximum throughout the EU) to rest for this vehicle are calculated from Equations (6.4) and (6.5). (Generally, vehicle manufacturers test to the vehicle design speed irrespective of any speed limits as these may change and therefore influence an existing type approval.)

Power Dissipation	Peak (kW)	Mean (kW)
Tractor front brake	1072	536
Tractor rear brake	1114	557
Trailer brake	671	335

From ***Step 2.1*** (specify the foundation brakes, determine the rotor type and size), ventilated discs are selected for the front and rear brakes of the tractor, with S-cam drum brakes on the trailer axles (disc brakes would also be an option for semi-trailers). For commercial vehicles there is a standard range of wheel rim sizes, e.g. 17.5, 19.5, 22.5 and 22.5 inches, and brake manufacturers specify brakes for each of these.

For ***Step 2.3***, the brake factor (or ηC^*) of the brakes is specified by the brake manufacturer (see Chapter 5). From Equation (5.47) the brake factor in the form of the specific torque of a cam actuated disc brake was estimated to be 26, and for an S-cam drum brake the brake factor was estimated to be 11 (Equation (5.45)).

Step 2.4 is intended to confirm the friction material size based on the thermal and mechanical loading. The typical limits of shear loading and mean work rate discussed earlier relate to cars and light vans, not commercial vehicles. Manufacturers of brakes for commercial vehicles provide a complete foundation brake unit including pads or lined shoes, for which the shear loading and work rate have been extensively proven, so commercial vehicle designers do not usually use thermal and mechanical loading e this is the responsibility of the brake manufacturer

Step 3 Design the Pneumatic Actuation System

Step 3.1 Specify the Actuation Mechanism (Pneumatic System)

The brake system design for this commercial vehicle can now proceed to the design of the pneumatic actuation system, which for most modern heavy commercial vehicles uses compressed air up to a maximum of about 8.5 bar (0.85 MPa) to create an actuation force at the foundation brake, which is converted to an actuation torque via a lever. With drum brakes, especially the S-cam type specified here for the semi-trailer axles, this lever incorporates a ‘slack adjuster’ that provides automatic adjustment to cater for wear (see Figure 5.23)

The layout of the pneumatic actuation system is illustrated in Figure 6.19

(a) Towing vehicle braking system

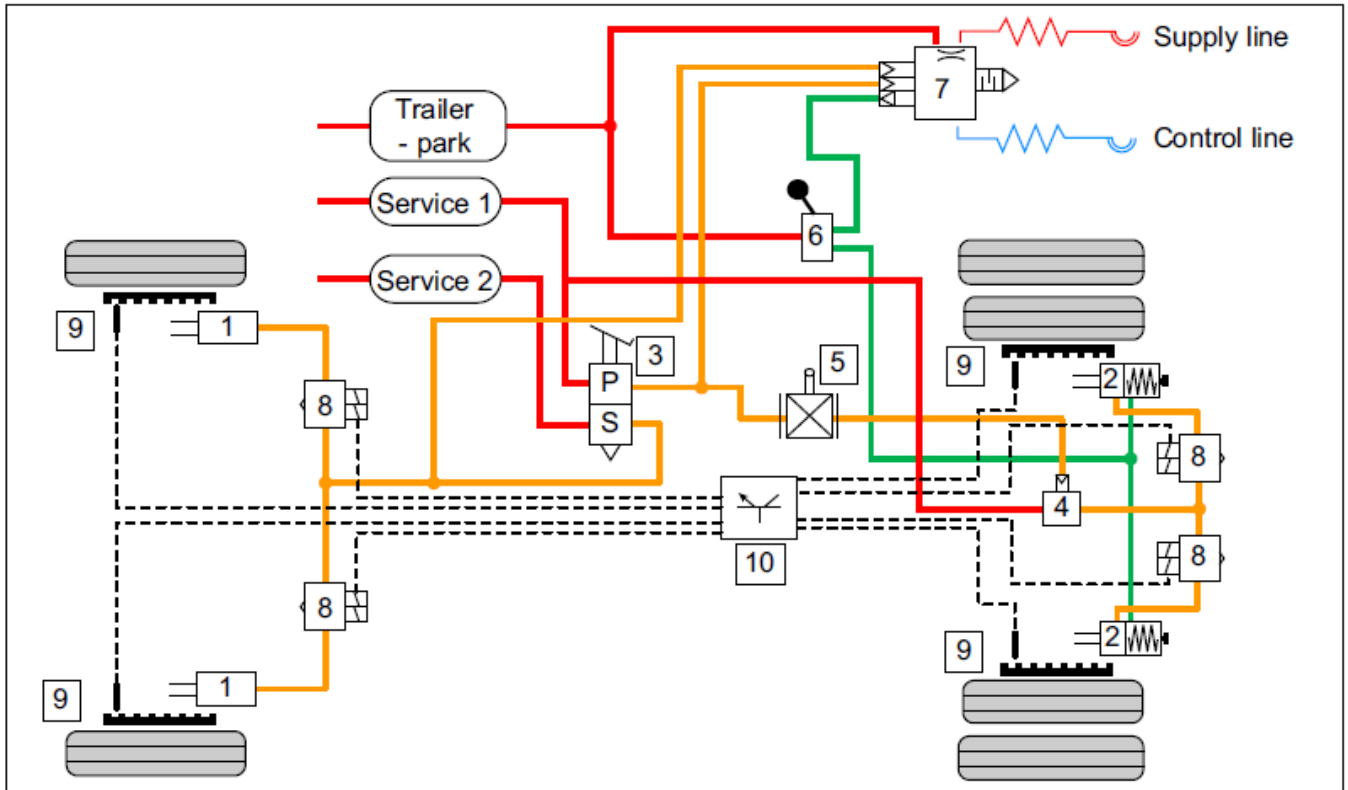

Ref	Description	Ref	Description	Ref	Description	Ref	Description
1	Brake actuator	4	Relay valve	7	Trailer control valve	10	ABS ECU
2	Spring brake actuator	5	Load sensing valve	8	ABS pressure modulators		
3	Footbrake valve	6	Hand control valve	9	Wheel speed sensors		

Figure 6.19: (a) Two Line/Dual Circuit Pneumatic Braking System with ABS for a Two-Axle Rigid Commercial Vehicle. (b) Two Line/Dual Circuit Pneumatic Braking System with ABS for a Semi-Trailer (Ross, 2013).

(b) Trailer braking system

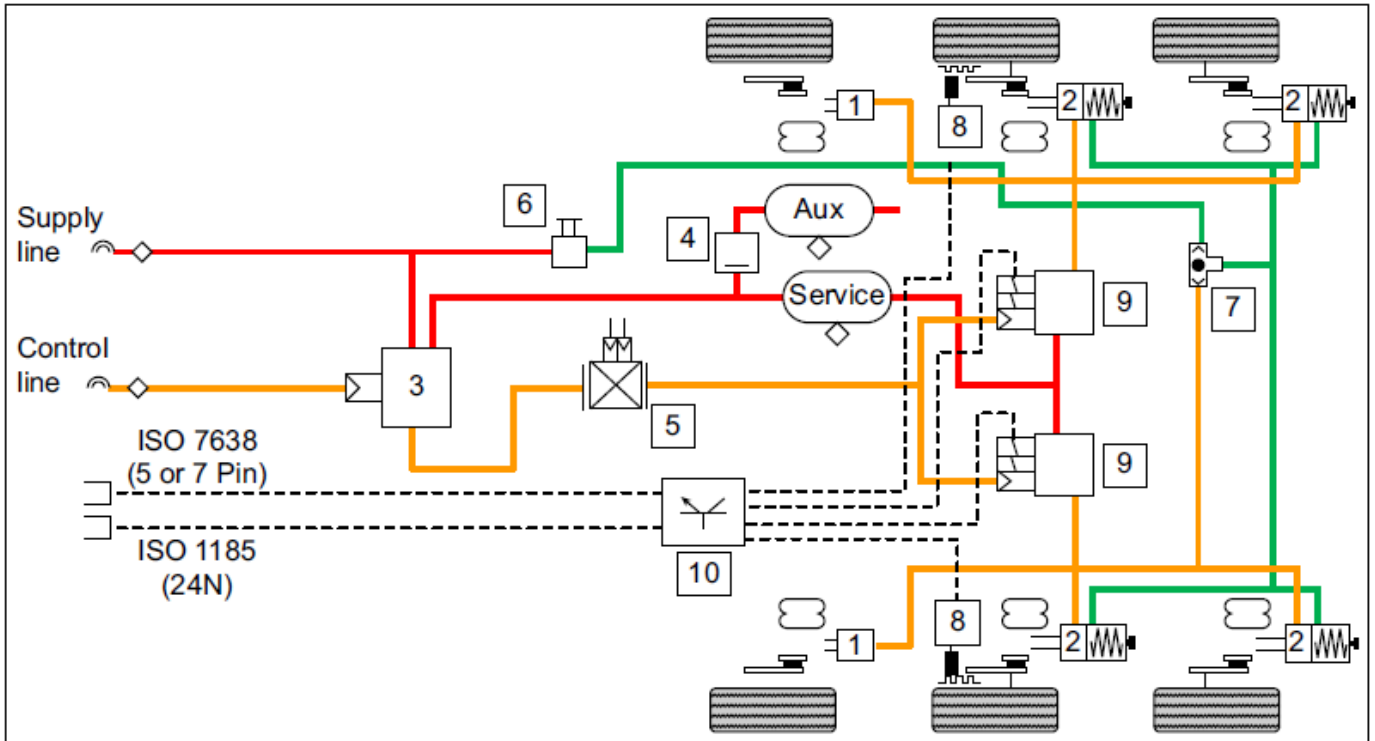

Ref	Description	Ref	Description	Ref	Description	Ref	Description
1	Brake actuator	4	Charging valve	7	Double check valve	10	ABS ECU
2	Spring brake actuator	5	Load sensing valve	8	Wheel speed sensors		
3	Emergency relay valve	6	Hand control valve	9	Pressure modulator		

Figure 6.19: (a) Two Line/Dual Circuit Pneumatic Braking System with ABS for a Two-Axle Rigid Commercial Vehicle. (b) Two Line/Dual Circuit Pneumatic Braking System with ABS for a Semi-Trailer (Ross, 2013).

and includes the brake actuator and lever components, as illustrated in Figure 6.20.

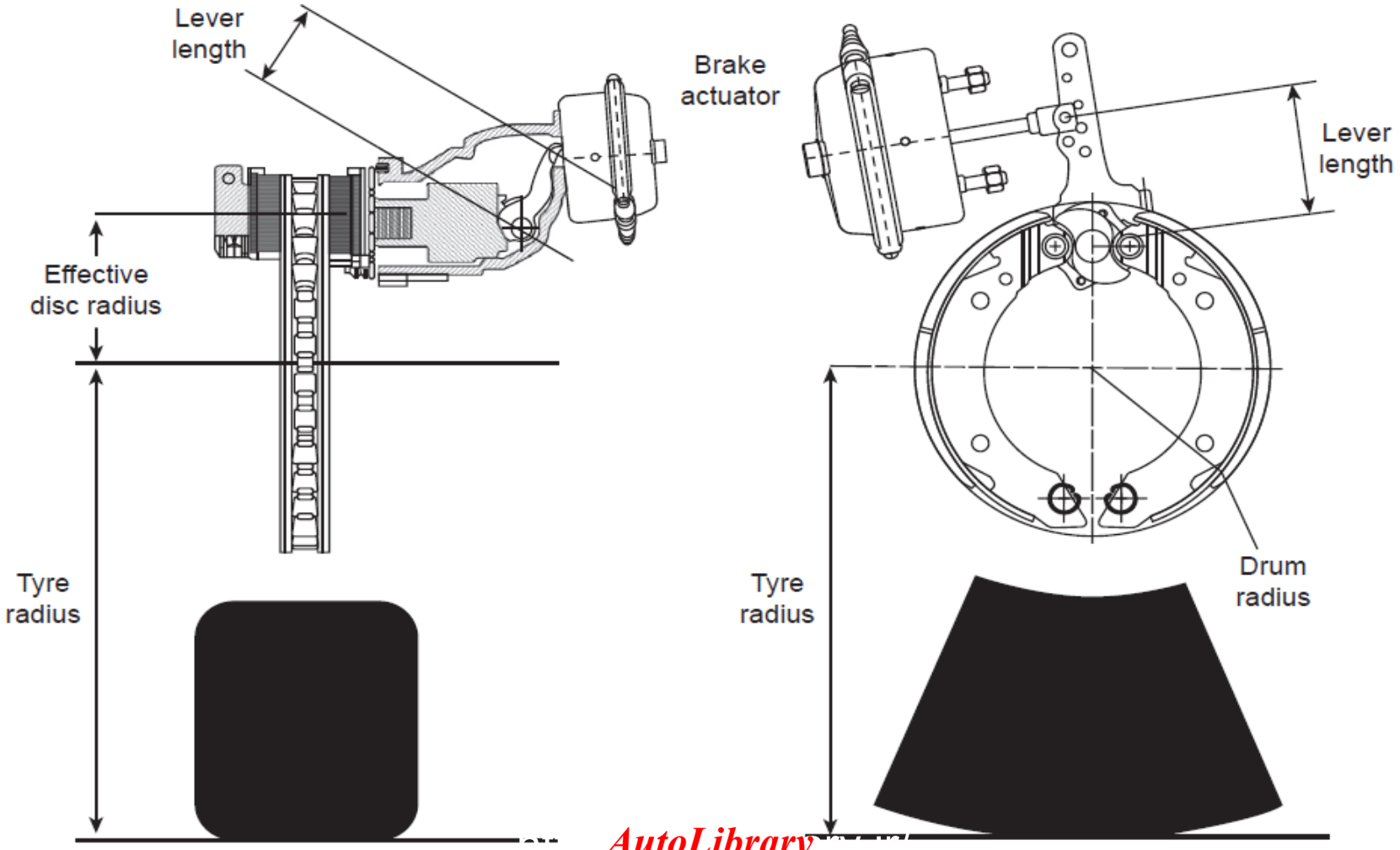

Figure 6.20: Pneumatic Brake Actuation (Ross 2013).

Step 3.2 Design the Brake Actuators

For a pneumatically actuated braking system the brake actuator design includes the pneumatic actuator size and stroke and the lever length. The input torque to an air actuated brake was defined in Equation (5.32):

$$\tau_a = P_a l = (p - p_t) A_a \eta l \qquad (5.32)$$

Each brake on the rear axle of the tractor is required to generate T_{max} = 20.6 kNm braking torque and from Equation (5.40) (ignoring threshold torque):

$$\tau = \tau_a \mathrm{BF} \qquad (5.40)$$

Manufacturers provide formulae for each type of air actuator from which the output force for any actuation air pressure can be calculated as indicated in Table 6.9

Table 6.9: Air Brake Actuator Formulae (Pneumatic Actuation Pressure p is Specified in MPa)

Actuator Type/Size	Disc Brakes Output Force P_a (N)	Drum Brakes Output Force P_a (N)
16	$P_a = 107.5p - 34.5$	$P_a = 104.5p - 19.0$
18	$P_a = 112.1p - 37.6$	
20	$P_a = 120.8p - 35.7$	$P_a = 124.0p - 24.0$
22	$P_a = 128.2p - 37.1$	
24	$P_a = 141.6p - 31.2$	$P_a = 143.0p - 28.5$
27		$P_a = 169.0p - 34.0$
30		$P_a = 196.0p - 39.0$

There are two design parameters in this equation that must be decided: the actuation lever length l (see Figure 6.20) and the air actuator size (area) A_a (see Figure 6.21).

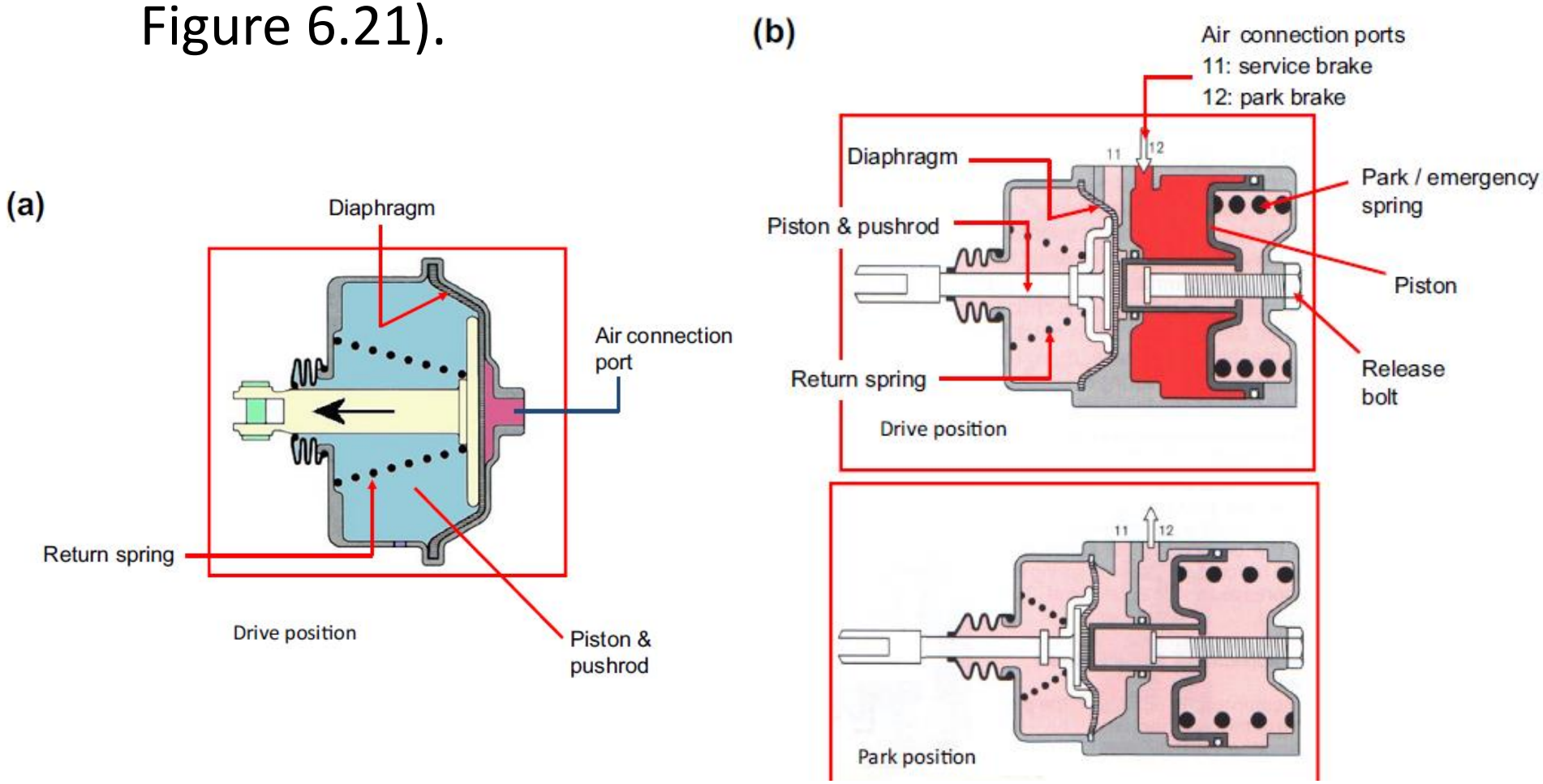

Figure 6.21: Pneumatic Actuators (Courtesy Arfesan).
(a) Standard actuator. (b) Spring brake actuator: (i) drive position; (ii) park position.

S-cam drum brake. The actuator manufacturer's formulae are used to calculate the output force net of the threshold force, and then the brake torque is calculated taking account of the brake threshold actuation torque according to Equation (5.40), which yields:

$$\tau_i = (\tau_{ai} - \tau_{ti})\mathrm{BF} \qquad (6.32)$$

The torque generated by each brake when the driver applies an air pressure of p (MPa) in the actuation system via the foot or hand valve is therefore:

$$\tau_{wi} = (((p_i - p_{ti})A_{ai}\eta_i l_i)\tau_{ti})\mathrm{BF}_i \qquad (6.33a)$$

where p_{ti} is the actuator threshold pressure (see Table 6.9) and s_{ti} is the brake threshold torque. Alternatively the brake threshold force p_{ti} may be specified, in which case Equation (6.33b) is used:

$$\tau_{wi} = (((p_i - p_{ti})A_{ai}\eta_i) - P_{ti})l_i \mathrm{BF}_i \qquad (6.33b)$$

The wheel braking force is:

$$T_{wi} = (((p_i - p_{ti})A_{ai}\eta_i l_i)\tau_{ti})\mathrm{BF}_i / r_{ri} \qquad (6.34a)$$

$$T_{wi} = (((p_i - p_{ti})A_{ai}\eta_i - P_{ti})l_i \mathrm{BF}_i / r_{ri} \qquad (6.34b)$$

Commercial vehicles may have more than one axle to carry the required normal load, e.g. in the form of a bogie on a semi-trailer. Where ‘n’ is the number of axles carrying the normal load at any specific location on the vehicle or trailer, the ‘axle braking force’ is:

$$T_i = 2n_i T_{wi} \qquad (6.35)$$

Step 3.3 Design the 'Master Actuator' (Brake Pedal) System (Pneumatic System)

In a pneumatically actuated braking system, the brake pedal takes the form of a proportional valve that increases the pneumatic actuation control pressure in response to the driver's demand. Although the valve may basically depend upon movement to determine the pneumatic pressure, modern foot valves for commercial vehicles are designed with force feedback to provide pedal feel to the driver in the same way that a hydraulically actuated car system does.

Step 4 Verify the Design and Check Compliance with Legislative Requirements (UN Regulation 13)

***Steps 1-3* above describe the brake system design procedure for the commercial vehicle defined in Table 4.6, and the typical design targets that must be verified for the braking system on this vehicle include:**

- Compliance with all legal requirements including a reserve of travel in the brake actuation system.
- Pneumatic actuation system pressure and reserve, e.g. UN Regulation 13; the capacity of the energy reservoirs must be sufficient to enable the vehicle to be brought to a halt after the eighth brake application as prescribed for secondary braking.

- Stopping distance: the vehicle must be capable of achieving the minimum stopping distance and/or MFDD.
- Stability and adhesion utilization: the solo vehicle and the vehicle combination must decelerate without deviation or imbalance between axles.
- The vehicle must decelerate without generating noise, judder and vibration.
- Wear and durability: the life of the brake rotors and stators must meet customer expectations.

It can also accommodate different pneumatic actuation pressures to the different axles by inserting factors to modify the actuation pressure to the brakes (see Figure 6.23(a, b)).

$$\begin{aligned} T &= (T_1 + T_2 + T_3 + T_4 \text{ etc.}) \\ &= [2n_1(((p_1 - p_{t1})A_{a1}\eta_1 l_1)\tau_{t1})\mathrm{BF}_1/r_{r1}] + [2n_2(((p_2 - p_{t2})A_{a2}\eta_2 l_2)\tau_{t2})\mathrm{BF}_2/r_{r2}] \\ &\quad + [2n_3(((p_3 - p_{t3})A_{a3}\eta_3 l_3)\tau_{t3})\mathrm{BF}_3/r_{r3}] + [2n_4(((p_4 - p_{t4})A_{a4}\eta_4 l_4)\tau_{t4})\mathrm{BF}_4/r_{r4}] \text{ etc.} \end{aligned} \tag{6.36}$$

Equation (6.36) is used to calculate the design braking performance of the vehicle specified in Table 4.6 with the designed system data summarized in Table 6.10.

Table 6.10: Pneumatic Braking System Design Specification for an Articulated Tractor/Semi-Trailer Combination

Design Parameter	Design Value
Tractor: front axle(s) (#1)	
Number of axles (n_1)	1
Type of foundation brake	Air-actuated disc brake
Effective radius (r_{e1})	173 mm
Brake factor (BF_1)	26
Threshold force (P_{t1})	131N
Air actuator size	Type 24
Equation (Table 6.9)	$1416p - 312$
Lever length (l_1)	76 mm
Tractor: rear axle(s) (#2)	
Number of axles (n_2)	1
Type of foundation brake	Air-actuated disc brake
Effective radius (r_{e2})	173 mm
Brake factor (BF_2)	26
Threshold force (P_{t2})	131 N
Air actuator size	Type 24
Equation (Table 6.9)	$1416p - 312$
Lever length (l_2)	76 mm
Trailer: axle(s) (#3)	Semi-trailer
Number of axles (n_3)	3
Type of foundation brake	Air actuated S-cam drum brake
Effective radius (r_{e3})	210 mm
Brake factor (BF_3)	11
Threshold torque (τ_{t3})	23 Nm
Air actuator size	Type 20
Equation (Table 6.9)	$1240p - 240$
Lever length (l_3)	135 mm
Trailer: axle(s) (#4)	Not applicable to this example
Number of axles (n_4)	0

The service brakes of a commercial vehicle are applied by a foot-operated control valve ('pedal'); the secondary and park controls may be via a hand-operated valve. The following performance requirement principles apply:

- 'Service braking performance': the defined performance is required when no faults are present and must be achieved when the driver has both hands on the steering control.

- ‘Secondary braking performance’: the defined performance is required when a ‘single’ defect is present and must be achieved when the driver has at least one hand on the steering control.
- ‘Residual braking performance’: the defined performance is required when there is a failure within a service braking circuit.

As explained in Chapter 8, compatibility between towing vehicles and trailers is ensured by examining the calculated values of T_m / P_m, where T_M is the total force developed by the towing vehicle's brakes and Pm is the simulated tractor weight (=M + Ms) . g). When plotted against the coupling head air pressure, P_M, must lie within the compatibility bands as shown for a tractor / semi-trailer combination in Figure 6.22

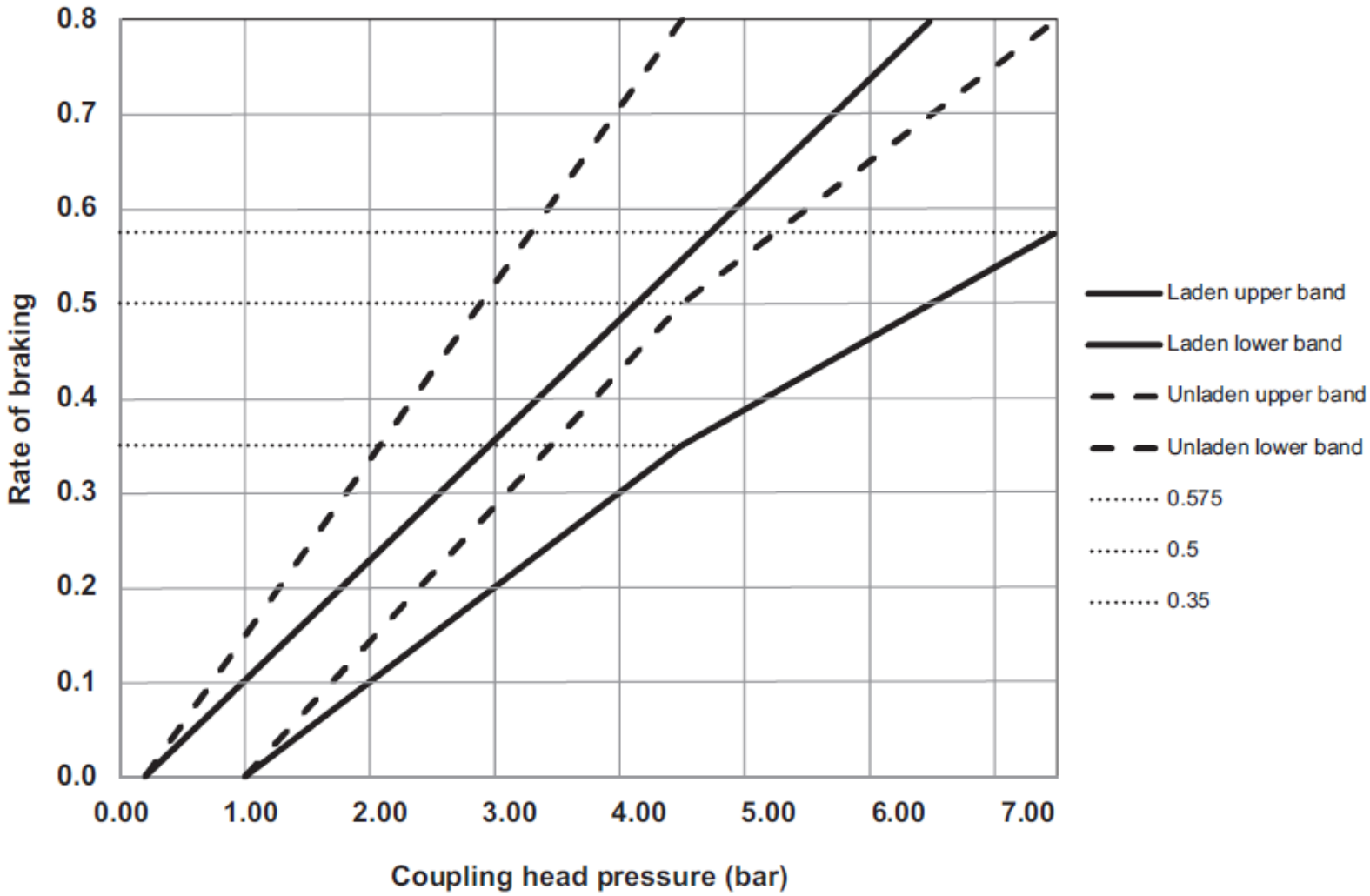

Figure 6.22: Compatibility Bands for Tractors with Semi-Trailers.

Fully laden (GVW) condition is shown in Figure 6.23(a), and the effect of load sensing can be seen in Figure 6.23(b), where the air pressure to the tractor rear brakes and the semi-trailer brakes is reduced to control the braking distribution in the unladen

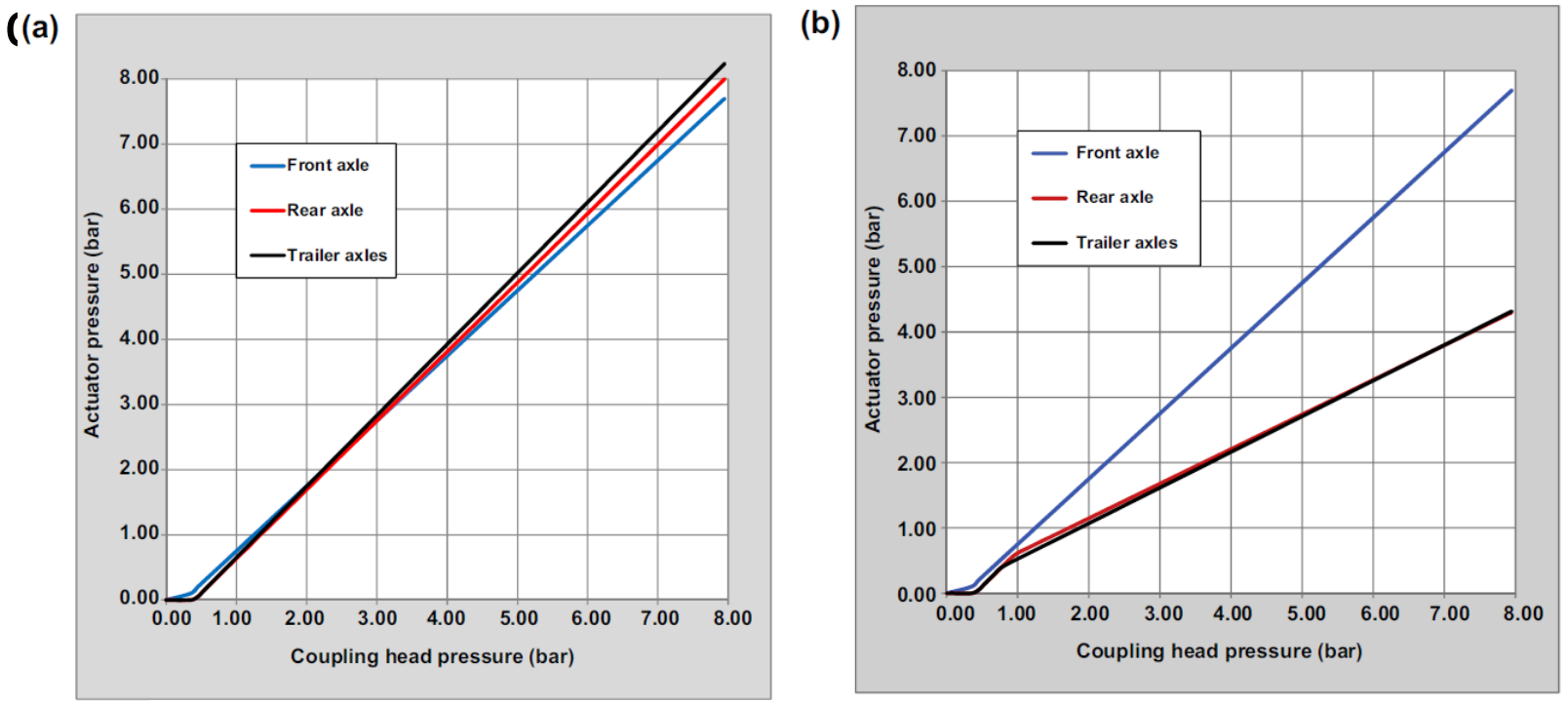

Figure 6.23: Articulated Commercial Vehicle Combination Braking System Pressure Characteristics (Bass, 2013).
(a) Laden. (b) Unladen.

Step 4.2 Partial System Failure

For partial system failure, secondary braking can be simulated, e.g. by setting the front brakes to be inoperative, in which case J = 2.2 m/s2 is achieved with an actuation air pressure of about 3.3 bar, which is also satisfactory.

Step 4.3 Parking

As for passenger cars, the parking brake system on commercial vehicle can actuate the brakes of any axles depending on the vehicle and brake configuration in order to meet the UN Regulation 13H requirements (see Chapter 8).

Comment on Verification Against Legislative Requirements -Pneumatic Braking Systems

As for passenger cars, legislative requirements for the braking of commercial vehicles represent the minimum level of performance required of a road vehicle braking system, and commercial vehicle manufacturers always aim to exceed this level of braking performance, often by a considerable margin.

Developments in Road Vehicle Brake Actuation Systems

This chapter has shown how braking systems can be designed for conventional hydraulically actuated brakes fitted to a passenger car or light van, and for conventional pneumatically actuated brakes fitted to commercial vehicles. Although hydraulic and pneumatic braking systems are still almost universally used on these vehicles, new designs of braking systems are likely to become more widely utilized in the near future, especially in electric and hybrid vehicles. These systems include (Moore, 2013) Electro-Hydraulic Brake (EHB) systems, which for passenger cars include:

- **Electronic control unit**
- **Electronic pedal with pedal-feel simulator and sensors for monitoring driver settings.**

The other claimed advantages of EHB systems include:

- Shorter braking and stopping distances
- Optimized pedal feel, braking and stability behavior
- No pedal vibration during ABS operation
- Improved packaging for crashworthiness and easier vehicle assembly
- Compatibility with all required braking and stability functions.
- Compatibility for networking with future traffic management systems.

A Hybrid Braking System (HBS) for passenger cars operates the front brakes via a conventional hydraulic system, and the rear brakes via electric actuators with an integrated electric parking brake, so it is essentially a two-circuit system and an alternative to full EHB. It avoids the need for long hydraulic lines and handbrake cables to the rear axle.

The components of HBS include:

- Two hydraulic wheel brakes on the front axle
- Two electromechanical wheel brake modules at the rear axle

- Integrated Electric Parking Brake (EPB) at the rear axle
- Electronic Braking Systems (EBS) hydraulic unit including Electronic Control Unit (ECU)
- Pedal/booster unit with small booster.

The advantages of an HBS are claimed to include:

- Cheaper and cleaner electric actuation to the rear brakes, operating on a conventional 12 V system
- Easily combined with Electric Parking Brake (EPB) and Hill Launch Assist
- Easily combined with regenerative braking technology on rear wheel drive vehicles.

An Electromechanical Brake (EMB) system for passenger cars is a full ‘brake-by-wire’ system, which eliminates brake fluid and hydraulic lines completely and generates the demanded braking force directly at each wheel.

The components of the EMB include:

- Wheel brake actuation modules
- An ECU, which includes all brake and stability functions
- Electronic pedal module with a pedal feel simulator and sensors for interpreting driver demand.

The advantages of the EMB system are claimed to include:

- No hydraulic systems; and consequent packaging, environmental, assembly and maintenance benefits
- Easier implementation of braking and stability functions, including EPB, automatic hill hold and parking brake, and adjustable pedal feel characteristics
- Improved crash safety performance through elimination of the booster and master cylinder assembly and decoupling from pedal box

- Fully optimized braking giving shortest stopping distances and optimal stability
- Increased comfort with silent operation, adjustable brake pedal
- Can be easily networked with future traffic management systems, e.g. autonomous cruise control, and collision prevention systems.

Chapter seven

Thermal Effects in Friction Brakes

The rotor and stator components of a brake friction pair (disc and pads, or drum and linings) operate in sliding contact under the applied actuation forces to generate friction forces that oppose the direction of relative sliding to create the retarding torque required to decelerate the vehicle. Friction brakes are required to transform large amounts of kinetic energy into heat over very short time periods and in the process they create high temperatures, steep temperature gradients and substantial thermal stresses.

If the brakes become too hot, deterioration in brake performance and ultimately premature failure may result from a number of causes, such as:

- Brake fade, when the coefficient of friction between rotor and stator is reduced (see Chapter 2).
- Excessive thermal distortion, which can also affect the torque output from a brake (see Chapter 5).
- High thermal stresses at the metal rotor surface resulting in surface cracking.
- Reduction in mechanical strength and other property changes in the rotor material.

- Increased wear of the friction material
- Increased risk of fluid vaporization and deterioration of rubber seals in the brake hydraulic actuation cylinders.

As explained in Chapter 6, thermal analysis is an essential part of the vehicle braking system layout design process (Steps 2.2 and 2.4 of the four-step brake system design procedure) and require calculations or predictions of the following parameters:

- Friction pair surface temperatures and temperature distributions
- Thermal and thermo mechanical stresses

- Thermal deformations and deflections
- Cooling characteristics
- Brake fluid temperatures
- Temperatures of seals, bearings and associated brake components.

Heat Energy and Power in Friction Brakes

Drivers use the brakes on their vehicle in many different and unpredictable ways. In previous chapters, the maximum torque from any brake on a vehicle was calculated and used to design the vehicle's braking system based on the vehicle manufacturer's standards and legislative requirements relating to the required vehicle deceleration. The parameters that affect the thermal loading of a vehicle's brakes include initial and final road speeds, initial brake temperature, deceleration, environmental conditions (ambient temperature, wind), resistance to vehicle motion (engine braking, retarder, aerodynamic drag, tyre/ transmission rolling resistance), topography (downhill braking) and additional loads (trailer).

The three types of braking conditions that can be defined for brake thermal performance analysis in road vehicles are:

1. Single application of the vehicle's brakes; often termed 'stops' (to rest) or 'snubs' (from an initial road speed to a final road speed).
2. Repeated application of the vehicle's brakes; often associated with fade tests.
3. Continuous application of the vehicle's brakes, often called drag braking; usually associated with the maintenance of a constant speed on a long downhill gradient.

The energy associated with a moving road vehicle of mass M (kg) travelling at a speed of v (m/s) is the 'translational kinetic energy' Q_{ke} (J), where:

$$\text{Translational kinetic energy} = Q_{ke} = \frac{1}{2}Mv^2 \qquad (7.1)$$

Note that in this book, 'vehicle road speed' is defined as V (km/h), and 'linear speed' is defined as v (m/s).

Note that although deceleration by a vehicle during braking is negative acceleration, for convenience in this book deceleration (J m/s2) is always taken as positive, and v1 > v2:

$$\Delta Q_{ke} = \frac{1}{2} M \left(v_1^2 - v_2^2 \right) \qquad (7.2)$$

The 'braking energy', DQ_b, that is dissipated by the brakes of this road vehicle during a single brake application when it decelerates from v1 to v2 (m/s), is the part of the total kinetic energy that is not absorbed or dissipated by other retarding forces on the vehicle.

This can include wind and tyre rolling resistance (Q_{wr} and Q_{rr}), transmission losses (Q_{tr}), engine braking (Q_{eng}), retarder (Q_{ret}) and regenerative braking (Q_{reg} - if fitted) estimated from the work done by the forces associated with each of these over the distance travelled by the vehicle during the brake application. Additionally, the effect of road gradient must be included; if driving uphill, kinetic energy is converted into potential energy (Q_g), which is effectively reducing the duty on the brakes, and vice versa if driving downhill when the duty on the brakes is increased. Thus, the braking energy can be estimated as:

$$\Delta Q_b = \Delta Q_{ke} - \Delta Q_{rr} - \Delta Q_{wr} - \Delta Q_{tr} - \Delta Q_{eng} - \Delta Q_{ret} - \Delta Q_{reg} \pm \Delta Q_g \qquad (7.3)$$

Assuming constant deceleration, the energy dissipated by wind and tyre rolling resistance and transmission losses during the brake application at deceleration J (m/s2) can be calculated from:

$$\Delta Q_{rr} + \Delta Q_{wr} + \Delta Q_{tr} = \frac{1}{2} m \left(v_1^2 - v_2^2 \right) (J_{rr}/J) \qquad (7.4)$$

Based on the example passenger car previously examined in Chapters 3 and 6, using Equation (7.3) the braking energy has been calculated for a rate of braking z =0.5 from a road speed of V1 =80 km/h to V2 =20 km/h, ignoring engine braking and assuming that no retarder or regenerative braking is fitted to the vehicle. In the laden condition (GVW =2450 kg):

Total KE $(Q_{ke}) = 567$ kJ

$(\Delta Q_{rr} + \Delta Q_{wr} + \Delta Q_{tr}) = 34$ kJ

$\Delta Q_g = 113$ kJ

(For a 10% uphill gradient $\Delta Q_b = 448$ kJ)

(For a 10% downhill gradient $\Delta Q_b = 675$ kJ)

In this example DQ_g is approximately 6% of Q_{ke} and since this represents the kinetic energy that is not dissipated through the brakes, it approximately offsets the rotational kinetic energy of the vehicle engine and driveline, plus the wheels and brake rotors, which was previously broadly estimated as 5%.

In a drag braking application when a constant vehicle speed is maintained on a downward slope for a distance L (m) at a constant gradient of angle a using the friction brakes and including an appropriate value of engine braking and rolling resistance, the potential vehicle energy change *DQpe* is:

$$\Delta Q_{pe} = Mg\Delta H = MgL \sin \alpha \qquad (7.5)$$

where M is the vehicle mass, g is the acceleration due to gravity (= 9.81 m/s2) and ΔH (m) (=L sinα) is the vertical height difference between the start and finish of the drag brake application.

To predict the thermal performance of individual brakes, the proportion of the total vehicle braking energy must be evaluated at each brake. This can be done by using the vehicle braking distribution (see Chapter 6), which defines the brake force generated by each brake (*i*) to achieve the desired vehicle deceleration, and hence the work done by each brake during vehicle braking. A convenient way to do this is to define the equivalent mass M_i associated with each wheel:

$$m_i = X_i M \tag{7.6}$$

From Equation (7.2) therefore:

$$\Delta Q_{kei} = \frac{1}{2} X_i M \left(v_1^2 - v_2^2 \right) \tag{7.7}$$

In a single brake application to bring a vehicle to rest it can be assumed that if T_{wi} remains constant then the angular velocity ω of the wheel at any instant (time =t) decreases linearly with time to rest from an initial angular velocity ω_1. The rate of heat generation Q_i at time t is then as shown in Equation (7.8):

$$\dot{Q}_i = \tau_{wi} \omega \tag{6.4}$$

$$\dot{Q}_i = \tau_{wi} \omega = \tau_{wi} \omega_1 \left(1 - \frac{t}{(t_2 - t_1)} \right) \tag{7.8}$$

The braking torque takes time to develop when the brake is actuated, so the braking power change during braking has a typical form as shown in Figure 7.1.

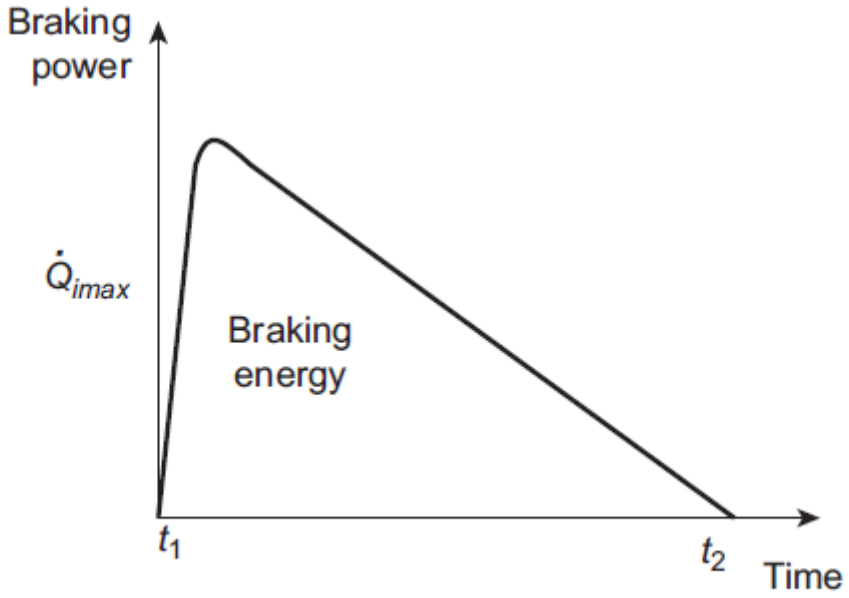

Figure 7.1: Braking Power in a Single Brake Application.

Where the braking power is not constant with time, the area under the braking power curve represents the braking energy for brake *i*, which can be determined by integration:

$$\int_{t_1}^{t_2} \delta E_i = \int_{t_1}^{t_2} \dot{Q}_i \delta t \qquad (7.9)$$

The brake power generation or heat input to the brake may be further simplified as shown in Figure 7.2(a, b)

Figure 7.2(a) shows the maximum braking power as being instantly developed at the start of the brake application and then declining linearly to zero at the end.

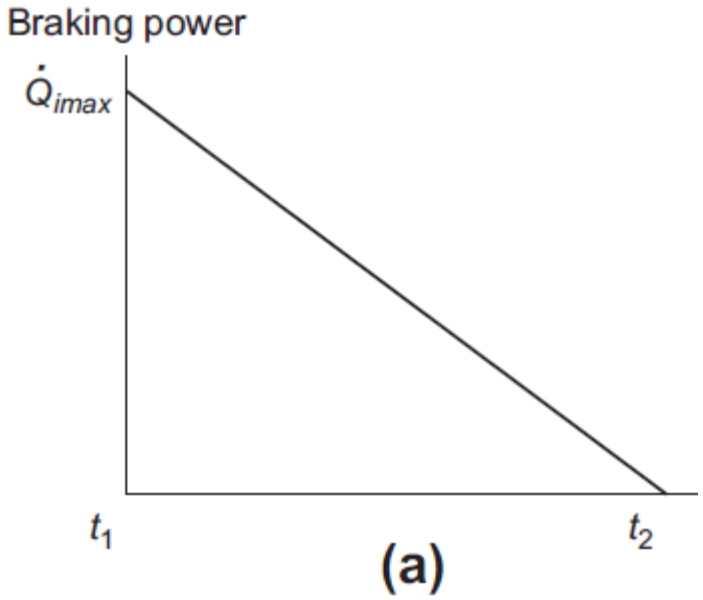

Figure 7.2: Idealised Braking vs. Time Characteristic.

In Figure 7.2(b) the braking power is ramped up at a rate determined by the system response characteristics and is closer to the real brake application (Figure 7.1).

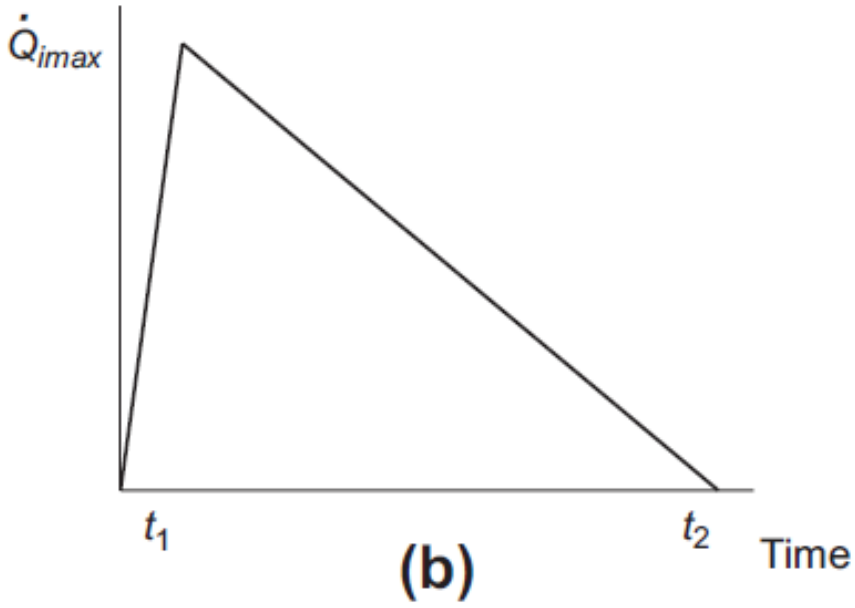

Figure 7.2: Idealised Braking vs. Time Characteristic.

The mean power dissipation Qi is calculated from

$$\dot{\overline{Q}}_i = \frac{1}{2}\dot{Q}_{max} \qquad (7.10)$$

or as indicated in Chapter 6, Equation (6.5):

$$\dot{\overline{Q}}_i = \tau_{wi}\frac{(\omega_1 + \omega_2)}{2} \qquad (6.5)$$

The braking energy dissipated during the brake application is calculated from Equation (7.11), where t1 is the time of the start of the brake application and t2 is the time of the end of the brake application:

$$Q_i = \frac{1}{2}\dot{\overline{Q}}_{imax}(t_2 - t_1) \qquad (7.11)$$

Ignoring the time taken to actuate the brake, the braking energy in a long drag brake application from time t1 to t2 (s) can be calculated from:

$$Q_i = \dot{Q}_i(t_2 - t_1) \qquad (7.12)$$

The braking power vs. time for a series of repeated brake applications with non-zero final speeds is shown in Figure 7.3.

The braking power vs. time for a series of repeated brake applications with non-zero final speeds is shown in Figure 7.3.

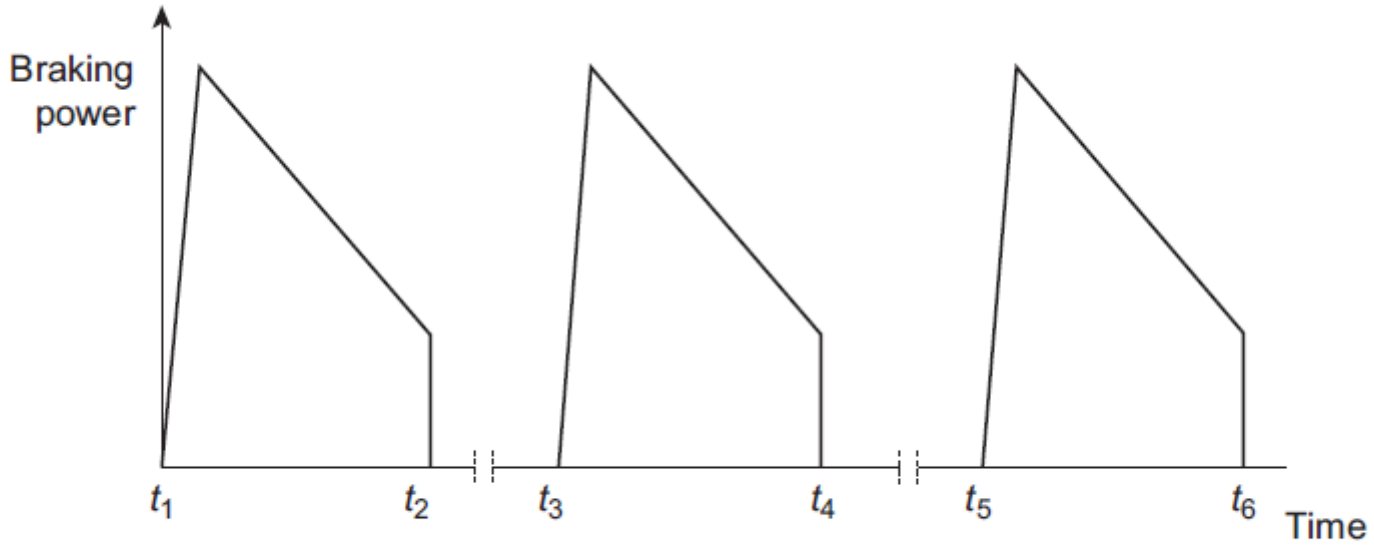

Figure 7.3: Repeated Braking vs. Time Characteristic with Non-Zero Final Speeds.

For drag braking at constant speed (Figure 7.4) the braking torque is constant and thus braking power Q remains constant after the initial rise.

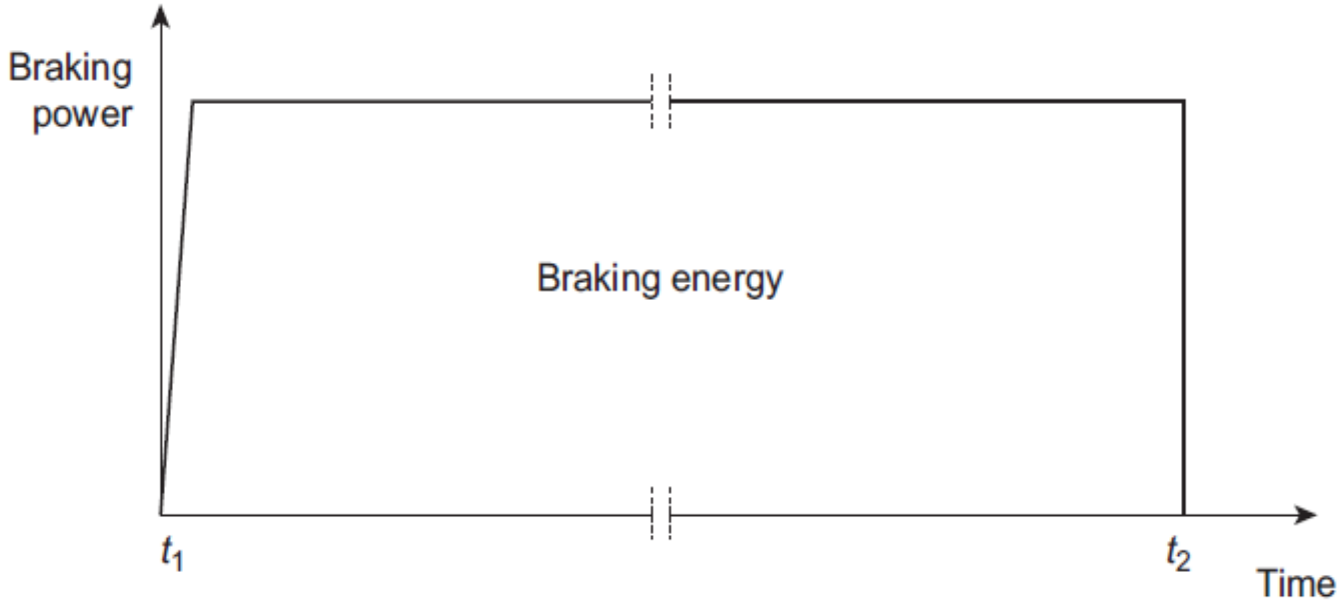

Figure 7.4: Drag braking vs. Time Characteristic, Constant Speed.

Braking Energy Management and Materials

The kinetic energy that a brake will be required to convert to heat and dissipate on a vehicle determines first whether a disc or drum brake should be selected, and then its size. The advantages of disc brakes over drum brakes have already been discussed in Chapter 5, and brake sizing has been presented in Chapter 6 in terms of brake torque and braking force requirements on vehicles.

Brake rotor design must take account of the limited mechanical properties:

- Low ductility e maximum tensile strain is less than 0.5%
- Low impact strength and high notch sensitivity because the graphite flakes act as stress

raisers

- Low fatigue strengths because of the effects of the graphite flakes on crack initiation.

Grey cast irons maintain their mechanical properties up to approximately 500C, above which the mechanical properties decrease significantly. The thermal properties for a typical automotive grey cast iron (e.g. ISO Grade 250, ultimate tensile strength 250 MPa; see e.g. Ihm, 2003) are indicated below (usually the properties reduce as bulk temperature increases):

- Density, 7200 kg/m^3
- Specific heat, 450–550 J/kg K
- Thermal conductivity, 45–54 W/m K
- Coefficient of thermal expansion, $12 \times 10^{-6}\ K^{-1}$
- Melt temperature, 1145°C.

Brake Thermal Analysis

Brake thermal analysis is needed for the foundation brake design and for the brake system layout design stage (see Chapter 6), in Steps 1.3, 2.2 and 2.4. Additionally brake thermal analysis is an essential part of Step 5 (part of the brake system layout design process in Chapter 5, and covered in detail here): to evaluate operational effects including loading and usage, heat and temperature, wear and durability, consistency and stability.

Bulk thermal effects relate to large-scale global temperature rise, which can be analyzed as follows:

1. Prediction of the bulk temperature rise of brake components, including the brake disc or drum, brake pad or shoe and lining assembly, and other associated components such as the caliper, wheel bearings and suspension components.
2. Prediction of temperature distributions within the friction pair (disc/drum and pad/ lining) and the prediction of thermal stresses.
3. Detailed thermo mechanical analysis usually by computational methods such as the finite element (FE) method.

Bulk temperature rise Δθ can be estimated from the energy Q entering the brake component, the portion of the brake component mass (m) that is expected to be heated during braking, and its specific heat (C_p):

$$\Delta\theta = Q/mC_p \qquad (7.13)$$

An example is the calculation of the ‘single-stop temperature rise’ (SSTR) of a brake disc or drum, as introduced in Chapter 6. The kinetic energy input to each brake on the vehicle during a single-stop brake application from its designed maximum speed to rest is calculated using Equation (7.7) with v2=0. Using Equation (7.13) the bulk temperature rise is calculated for the part of the disc or drum that is in contact with the stators; in the case of a brake disc this is the mass of the friction ring, i.e.

the mass of the disc less the hub flange and hat region, and in the case of a brake drum it is the mass of the friction cylinder, i.e. the mass of the drum less the flange (see Figure 7.5).

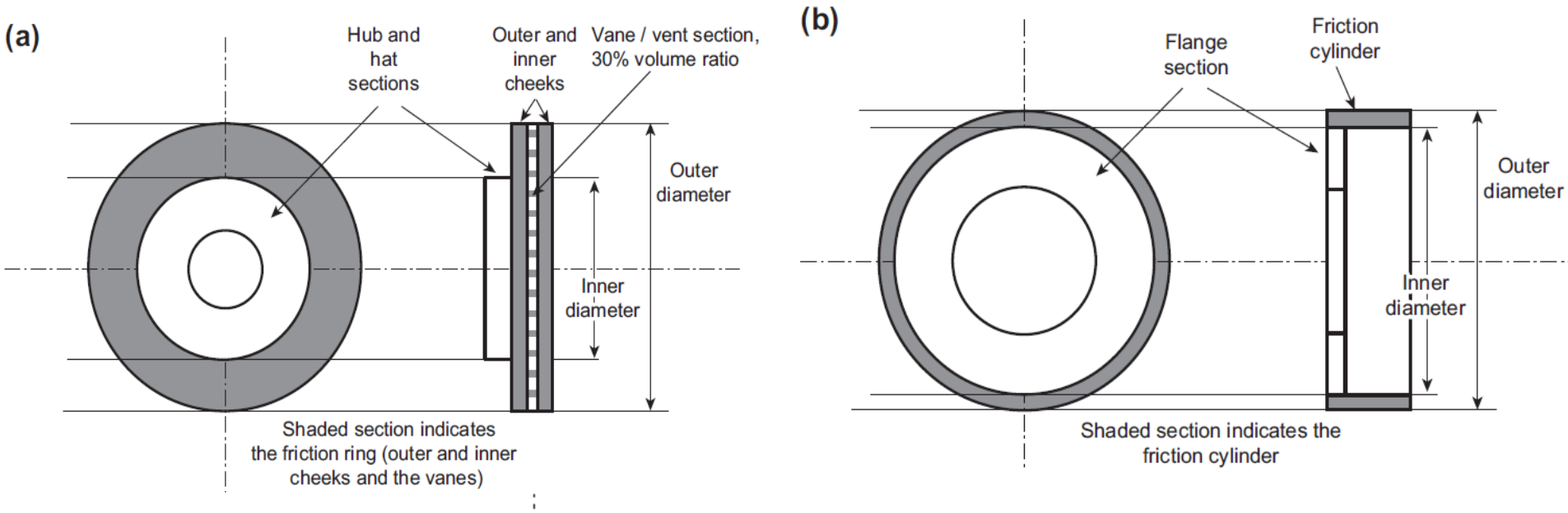

Figure 7.5: (a) Friction Ring of a Brake Disc. (b) Friction Cylinder of a Brake Drum.

This approach to the heat partition at a sliding contact was originally presented by Jaeger (1942) and is based on the assumption that the temperature on the rotor friction surface is the same as the temperature on the stator friction surface, an assumption that is discussed later. For the rotor:

$$Q_{\mathrm{r}} = Q_i \left[\frac{A_{sr}\sqrt{k_r \rho_r c_{pr}}}{A_{\mathrm{sr}}\sqrt{\left(k_r \rho_r c_{pr}\right)} + A_{\mathrm{ss}}\sqrt{\left(k_s \rho_s c_{ps}\right)}} \right] \qquad (7.14a)$$

and for the stator:

$$Q_{\mathrm{s}} = Q_i \left[\frac{A_{ss}\sqrt{k_s \rho_s c_{ps}}}{A_{ss}\sqrt{\left(k_s \rho_s c_{ps}\right)} + A_{sr}\sqrt{\left(k_r \rho_r c_{pr}\right)}} \right] \qquad (7.14b)$$

$$Q_{\mathrm{r}} = Q_i \left[\frac{A_{sr}\sqrt{k_r \rho_r c_{pr}}}{A_{\mathrm{sr}}\sqrt{\left(k_r \rho_r c_{pr}\right)} + A_{\mathrm{ss}}\sqrt{\left(k_s \rho_s c_{ps}\right)}} \right] \tag{7.14a}$$

$$Q_{\mathrm{s}} = Q_i \left[\frac{A_{ss}\sqrt{k_s \rho_s c_{ps}}}{A_{ss}\sqrt{\left(k_s \rho_s c_{ps}\right)} + A_{sr}\sqrt{\left(k_r \rho_r c_{pr}\right)}} \right] \tag{7.14b}$$

where:

A_{sr}, A_{ss} = Friction surface area of the rotor and stator respectively (m^2);
k = Thermal conductivity (W/m K);
ρ = Mass density (kg/m^3);
C_p = Specific heat at constant volume (J/kg K).

Friction Surface Temperature Prediction Using Analytical Methods

Analytical methods for predicting brake friction surface temperatures have been used for many years, usually treating the friction pair components as semi-infinite bodies. The most widely used formulae are those proposed by Newcomb and Spurr (1967) and Limpert (2011), which are suitable for basic design calculations. Assuming that the frictional contact area (rubbing path) is a continuous band on the disc surface and the frictional heat is generated uniformly over this band, a 2D heat equation can be formulated to find the temperatures within a disc or drum.

Considering a brake disc that has axial symmetry the heat equation in cylindrical coordinates is:

$$\frac{\partial \theta}{\partial t} = \alpha_1 \left(\frac{\partial^2 \theta}{\partial r^2} + \frac{1}{r} \frac{\partial \theta}{\partial r} + \frac{\partial^2 \theta}{\partial z^2} \right) \qquad (7.15)$$

where a1 is the thermal diffusivity of the rotor material = k/ρcp (m2/s), and the domain $r_i \leq r \leq r_o$ and $0 \leq z \leq$ d1 where d_1 is the semi-thickness of the (solid) rotor. The boundary conditions are that the temperature gradient is zero at the centre plane of the disc (z = d1):

$$\frac{\partial \theta}{\partial z} = 0 \quad \text{at} \quad z = d_1 \qquad (7.16)$$

and over the other surfaces the heat flux input is:

$$k_1 \frac{\partial \theta}{\partial r} + h(\theta - \theta_o) = -\dot{q}_{i1}(t) \qquad (7.17)$$

where h is a heat transfer coefficient (W/m^2 K) that defines the heat transfer from the exposed surfaces of the rotor, as explained later in this chapter. For the non-rubbing path surfaces of the disc the value of $\dot{q}_{i1}$ (t) is zero.

The form of the analytical solution depends on the value of the parameter $\lambda = d_1/\sqrt{\alpha_1 t_s}$, where d_1 is the brake drum thickness or the semi-thickness of the brake disc and α_1 is the thermal diffusivity of the rotor. If $\lambda \leq 1.21$ the body can be considered to be infinitely thick and the mean temperature rise θ at the friction surface is given by:

$$\theta = \frac{2\dot{q}_1 t^{1/2}}{\pi^{1/2}(k_1 p_1 c_1)^{1/2}}\left(1 - \frac{2}{3}\frac{t}{t_s}\right) \qquad (7.18)$$

The temperature rises rapidly and reaches a maximum value at t = ts /2, and then reduces because of the reduction in braking energy input as the vehicle slows down. The maximum temperature (θ max) is given by Equation (7.19), which shows the importance of having rotor materials with high thermal property values (k1, p1, c1) to reduce maximum temperatures:

$$\theta_{\max} = 0.53\dot{q}_1 \left(\frac{t_s}{k_1 p_1 c_1} \right)^{1/2} \qquad (7.19)$$

If $\lambda < 1.21$ the body cannot be considered to be infinitely thick and the temperature is given by:

$$\theta = \frac{\alpha_1 \dot{q}_1}{d_1 k_1} \left\{ \left(1 - \frac{t}{2t_s}\right) + \frac{d_1^2}{3\alpha_1} \left(1 - \frac{t}{t_s}\right) + \frac{d_1^4}{45\alpha_1^2 t_s} \right\} \qquad (7.20)$$

The maximum temperature calculated from Equation (7.20) is greater than that calculated from Equation (7.19) and occurs nearer the end of the brake application. This is because the thermal capacity of the body is finite, and because there is no surface heat transfer from it, the resultant temperature is higher.

Brake Temperature, Stress and Deformation Prediction Using Computational Methods

Brake thermal analysis using computational methods such as the FE method enables the prediction of bulk component temperature, stress, and deformation profiles and distributions to a much higher accuracy and realism than by using analytical methods. The advantages of FE analysis include the realistic modelling of component geometry, material properties and boundary conditions.

Ultimately the hot areas may substantially reduce local interface pressures and even lose contact in a cyclic process that is broadly known as ‘thermoelastic instability’ (Barber, 1969).

$$q = \mu p v \qquad (7.21)$$

In hot spots and hot bands, friction surface temperatures can be much higher than those predicted using any assumption of uniform heat flux distribution across the friction interface.

FE analysis starts with the generation of a ‘mesh’ of ‘elements’, which in modern FE analysis software systems is generated automatically. The type of element used must follow the FE system supplier’s recommendations and verification examples should be completed before predictions are started. The element size and refinement of the mesh must be appropriate to the geometry of the part(s) being modelled, and their thermophysical properties, and the quality of the mesh must always be checked.

For example, because the friction material has a low thermal conductivity, smaller elements (in the predominant direction of heat flow) must be specified to accommodate the steeper temperature gradient. This can be checked using the 'Fourier number' (Fo):

$$Fo = \alpha \Delta t / \Delta x^2 \qquad (7.22)$$

where α is the thermal diffusivity of the friction material, Δ_t is the FE solution time increment and Δ_x is the element size thickness in the predominant direction of heat flow, usually normal to the friction interface.

It is usual to specify an initial temperature distribution in the components that is the same as the surrounding or ambient temperature. Two types of temperature prediction analysis can be generated:

- Steady-state temperature prediction, which calculates the temperature distribution when equilibrium has been reached.
- Transient temperature prediction, which calculates the temperature distributions at different times as the heat flows through the components.

The method for the prediction of brake disc temperatures, stresses and deformations using the FE method was demonstrated by Day et al. (1991). For a single brake application on a solid disc rotor of a passenger car front brake (vehicle and brake data are summarized in Table 7.1-next page), the calculated maximum heat flux over the whole rubbing path (both sides of the disc) is approximately 1.5 MW/m^2 and the SSTR is 171^0C.

Table 7.1: Vehicle and Brake Data

Vehicle Characteristics	
Vehicle mass	1300 kg
Brake force distribution X_1/X_2	66:34
Brake Application Characteristics	
Initial vehicle speed	100 km/h (28 m/s)
Final vehicle speed	0
Duration of brake application	4 s
Average deceleration	7 m/s^2 (0.7 g)
Initial brake temperature	20°C
Front Brake Discs (Solid)	
Disc outer diameter	227 mm
Disc ring inner diameter	127 mm
Disc thickness	11 mm
Total disc mass	3 kg
Disc ring mass	2.2 kg

This is a simple design that was quickly modelled using the 2D axisymmetric FE mesh design illustrated in Figure 7.6 (Day et al., 1991).

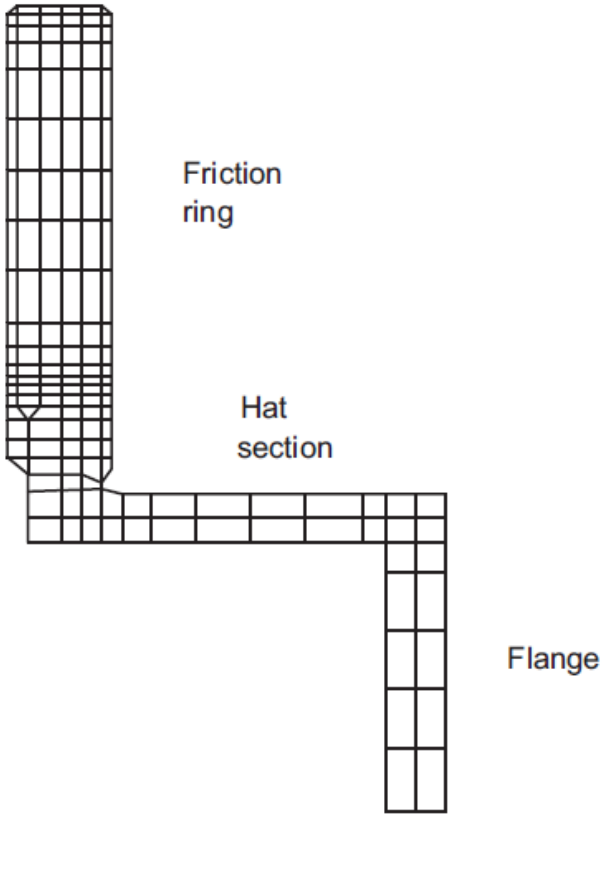

Figure 7.6: 2D Axisymmetric FE Brake Disc Model (Day et al., 1991).

Example results from the FE analysis of a ventilated brake disc (from the front axle of a medium-sized passenger car) are shown in Figure 7.7.

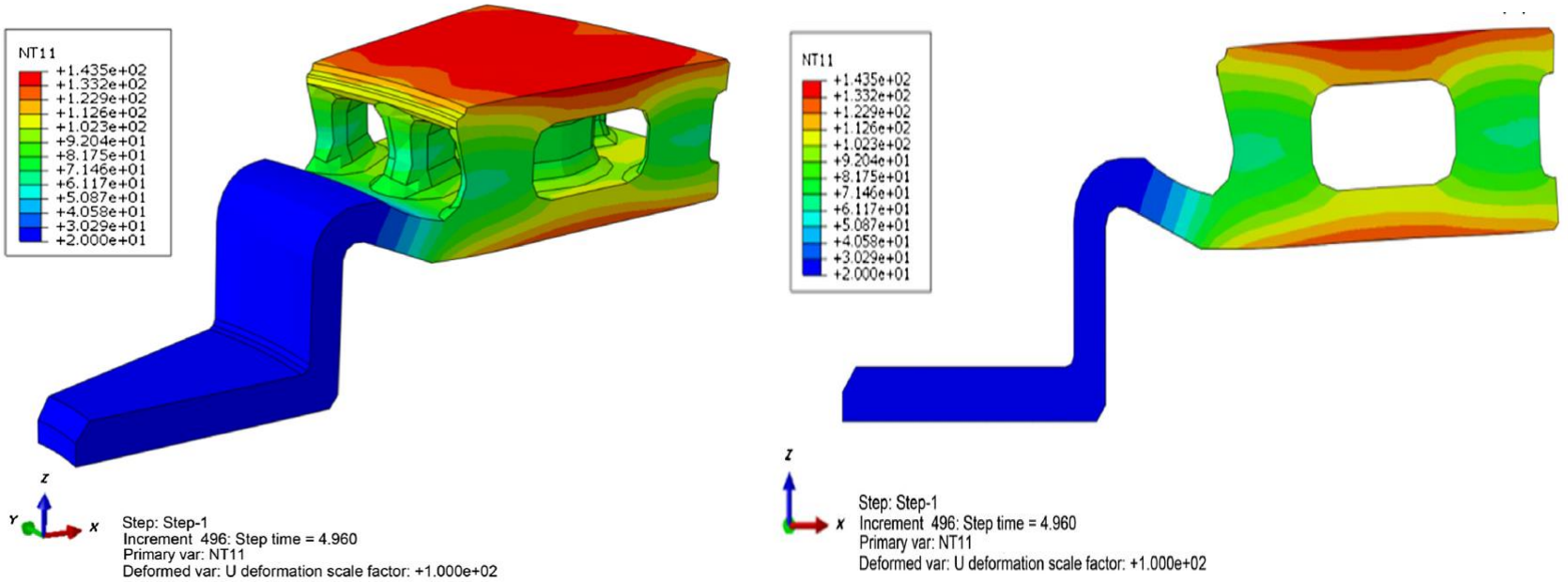

Figure 7.7: (a) 3D Sector Model of a Brake Disc Showing the Predicted Transient Temperature Distribution for a 0.4 *g* Brake Application. (b) The Same Transient Temperature Distribution Showing the Coning Distortion of the Friction Ring (Tang, private communication).

based on a 3D FE modelling procedure that utilizes a ‘sector’ model, with symmetrical boundaries on radial planes either side of a complete vane region. For thermal analysis the assumption is that there is no heat flow across the boundary planes, and for stress analysis a plane strain boundary condition applies. Figure 7.7(a) shows the FE model with the predicted transient temperature distribution halfway through a single 0.4 g brake application, and Figure 7.7(b) illustrates the same temperature distribution superimposed on the deflected shape, i.e. the shape of the thermal deformation predicted for this temperature distribution.

the disc surface temperature also varies circumferentially, as illustrated in Figure 7.8 (Tirovic, 2013).

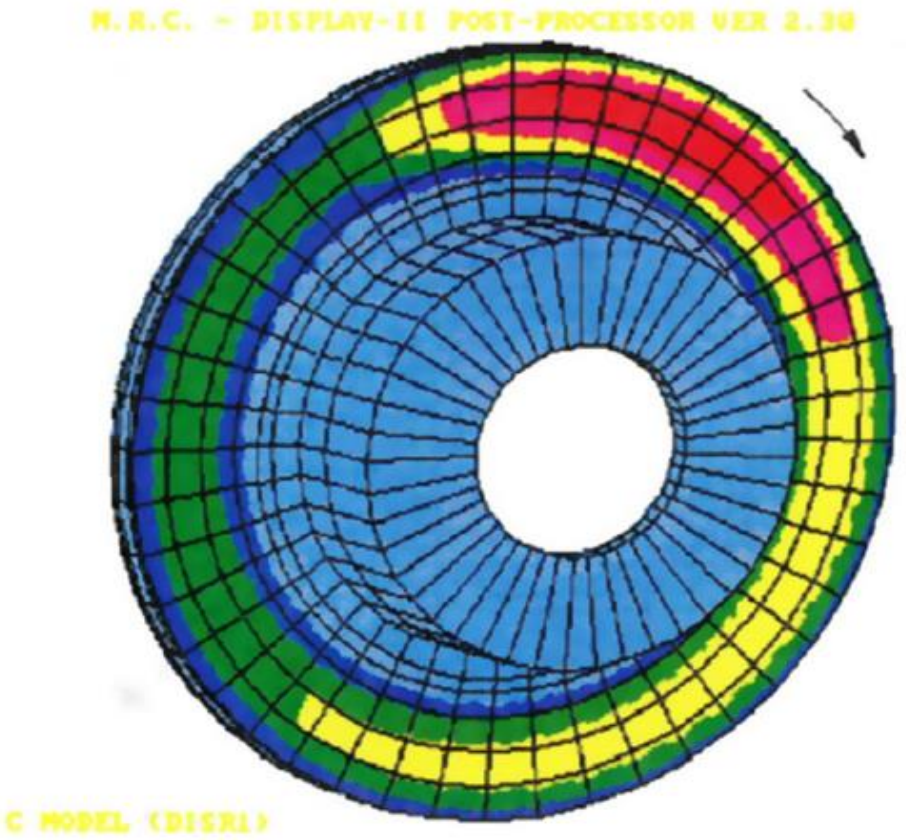

Figure 7.8: Circumferential Variation in the Surface Temperature of a Rotating Brake Disc (Tirovic, 2013).

Radial cracks or crazing on the rubbing path of a brake disc is termed thermal cracking (see Figure 7.9) and is a brake disc failure mode resulting from stresses created by elastoplastic deformation of the cast iron during the heating cycle, which in turn generates residual tensile stresses during cooling.

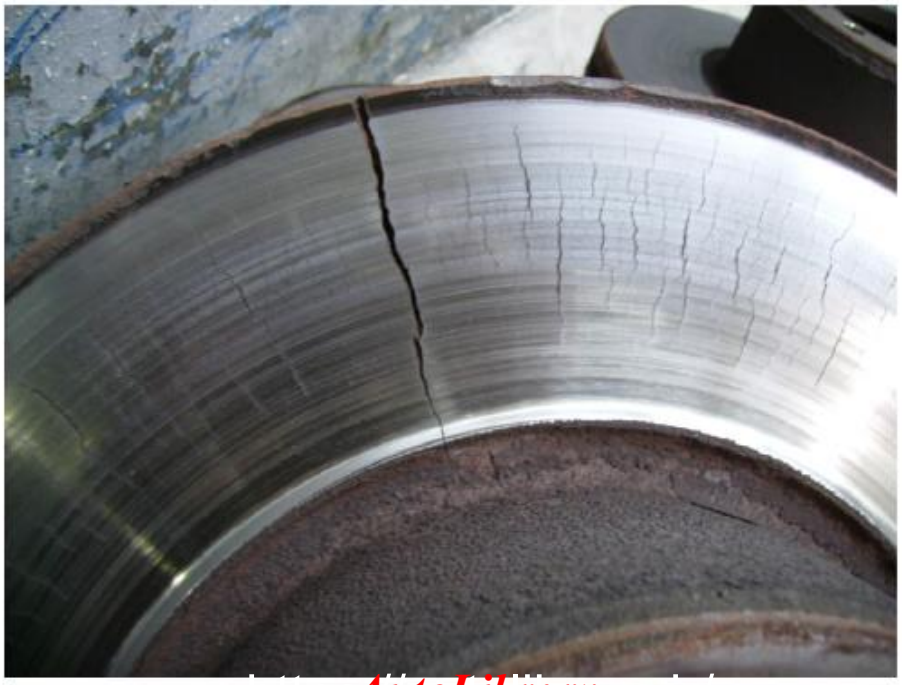

Figure 7.9: Disc Thermal Cracking.

Good disc brake design should therefore aim to keep the braking energy input as even as possible, radially and circumferentially, so particular attention should be paid to the following factors:

- Design the disc for minimal coning.
- Design the disc and hub assembly for minimal runout and bolt-up distortion.
- Use a good quality and consistent disc material.
- Design the calipers and their mounting to be as rigid as possible.

Heat Dissipation in Brakes

It has already been established that heat dissipation is essential in brake system design. Heat is dissipated from brakes by three modes of heat transfer: conduction, convection and radiation. For brake designs and braking duties on most road vehicles, convection is the prime mode of heat dissipation; however, because modern brakes are designed to operate at high temperatures the other two modes (conduction and radiation) should also be considered in brake thermal analyses to enable the accurate prediction of temperatures.

Effective brake cooling ducts can be designed, but normally increase aerodynamic drag and therefore are not always acceptable to vehicle manufacturers.

$$(\theta_t - \theta_0) = (\theta_{t_1} - \theta_0)e^{(-bt)} \qquad (7.23)$$

where:

θ_0 = ambient temperature (°C);
θ_t = bulk temperature of rotor at time t (°C);
θ_{t_1} = bulk temperature of rotor at the start of cooling (°C);
t = time (s);
b = cooling rate (s^{-1}).

The standard procedure for determining brake cooling rates is to drive the vehicle at constant speed and monitor the decay in rotor bulk temperature over time. Equation (7.23) can be written as the following:

$$\ln \frac{(\theta_t - \theta_0)}{(\theta_{t_1} - \theta_0)} = -bt \qquad (7.24)$$

The slope of a graph of ln (natural log) of $(\theta_t\text{-}\theta_0)/(\theta_{t1}\text{-}\theta_0)$ vs. time (t) gives the cooling coefficient (b), which depends upon the vehicle, the type of brake, the wheels and many other parameters, including the road speed.

The parameters *b0* and C also depend upon the vehicle, the type of brake, the wheels and many other parameters, and in the past have been best determined experimentally.

$$b = b_0 + Cv^{0.8} \qquad (7.25)$$

The braking power (heat) dissipated from the exposed surface of the rotor ($\dot{Q}$) can be estimated from Equation (7.26), where As is the exposed surface area of the rotor and the parameter h is a heat transfer coefficient (W/m^2 K)

$$\dot{Q} = -hA_s(\theta_t - \theta_0) \qquad (7.26)$$

During a brake application, if the braking energy flows into the rotor and creates a bulk temperature rise of Δ_θ, and is then transferred through the rotor to be dissipated by surface heat transfer (e.g. convection) from its exposed surfaces:

$$Q = mC_p\Delta\theta \qquad (7.27)$$

Combining Equations (7.26) and (7.27):

$$\dot{Q} = mC_p\frac{\mathrm{d}\theta}{\mathrm{d}t} = -hA_s(\theta_t - \theta_0) \qquad (7.28)$$

and thus

$$\frac{\mathrm{d}\theta}{\mathrm{d}t} = -\frac{hA_s}{mC_p}(\theta_t - \theta_0) \tag{7.29}$$

which when integrated has the solution:

$$\theta(t) = \theta_0 + \mathrm{e}^{-\left(\frac{hA_s}{mC_p}\right)t}(\theta_{t_1} - \theta_0) \tag{7.30}$$

Equation (7.30) is the same form as Equation (7.23) and thus:

$$b = \left(\frac{hA_s}{mC_p}\right) \tag{7.31}$$

and therefore:

$$h = \frac{bmC_p}{A_s} \tag{7.32}$$

For repeated braking of a regular time interval Δ_t, Newcomb and Spurr (1967) showed that the average temperature of a brake rotor before the 'nth' brake application is:

$$\theta_{t_n} = \theta_0 + \Delta\theta\left\{\frac{e^{(-b\Delta t)} - e^{(-nb\Delta t)}}{1 - e^{(-b\Delta t)}}\right\} \qquad (7.33)$$

and after the '*n*th' brake application is:

$$\theta_{t_{n+1}} = \theta_0 + \Delta\theta\left\{\frac{1 - e^{(-nb\Delta t)}}{1 - e^{(-b\Delta t)}}\right\} \qquad (7.34)$$

Some experimental data for disc brake cooling at constant speed are shown in Figure 7.10 in terms of in $(\theta_t\text{-}\theta_0)/(\theta_{t1}\text{-}\theta_0)$ vs. time (t) for a solid and a ventilated disc. The cooling rate increases with the rotational speed of the disc, for the solid disc (Figure 7.10(a)) from 1.3 x 10^{-3} s^{-1}at 450 rev/min to 2.6 2.6 x 10^{-3} s^{-1}at 1200 rev/min (equivalent road speeds of 55 and 150 km/h). For the ventilated disc (Figure 7.10(b)) the cooling rate increases from 2.88 x 10^{-3} to 4.44 x 10^{-3} s^{-1} between the same speeds, demonstrating the advantage of a ventilated disc design over a solid disc.

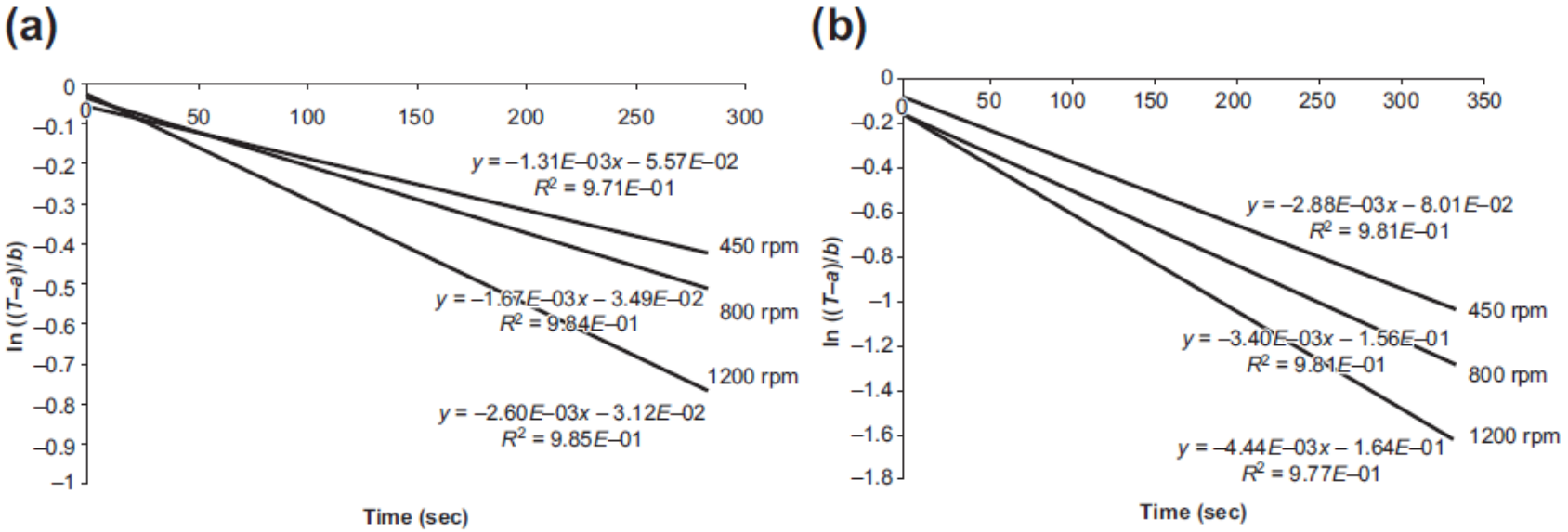

Figure 7.10: Cooling Curves for a Disc Brake.
(a) Solid. (b) Ventilated.

When a steady state is reached with repeated braking:

$$\theta_{t_{n+1}} = \theta_0 + \frac{\Delta\theta}{b\Delta t} \qquad (7.35)$$

These analytical methods can only provide approximations but are useful for basic design purposes. The use of computational, especially FE, and also computational fluid dynamics (CFD), methods for brake thermal analysis has enabled predictions of temperatures in brakes on road vehicles to be made with great accuracy, provided that the thermophysical properties of the materials involved are known, and the boundary conditions are realistically applied.

Convective Heat Transfer

Heat transfer from the exposed surfaces of a body such as a brake rotor to the environment is governed by Equation (7.26), where the local heat transfer coefficient from a surface of temperature $\theta_{\mathrm{st}}$is h_{conv} (W/m^2 K). Airflow is the main influencing factor on convective heat dissipation; a stationary brake disc or drum in still air dissipates heat only by natural convection, but if it is rotating, the heat dissipation increases as the convective cooling becomes 'forced' because of the airflow over the free surfaces, and this increase is more pronounced if the disc or drum is exposed to cross flow of air, e.g. from a side wind.

Convective heat dissipation from the brake disc was predicted by FE and CFD analyses using the type of model shown in Figure 7.11.

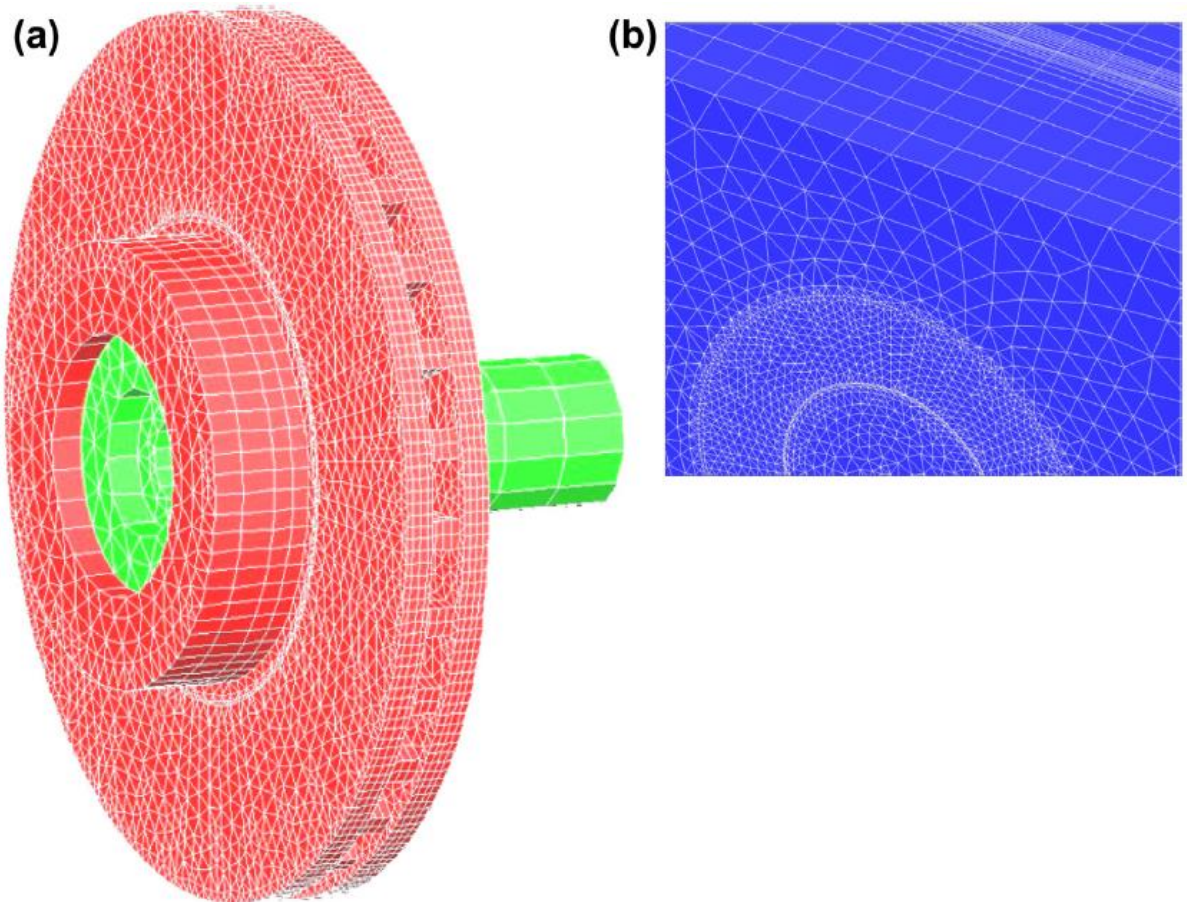

Figure 7.11: Examples of FE Mesh for Brake Disc Thermal Analysis (a) and CFD Mesh for Airflow and Convection Analysis (b) (Tirovic, 2013).

The CFD flow analysis predicted the airflow through the disc vanes and disc cooling, e.g. as indicated in Figure 7.12 for a disc at 100C rotating at 450 rev/min in an environment at ambient temperature of 20^0C.

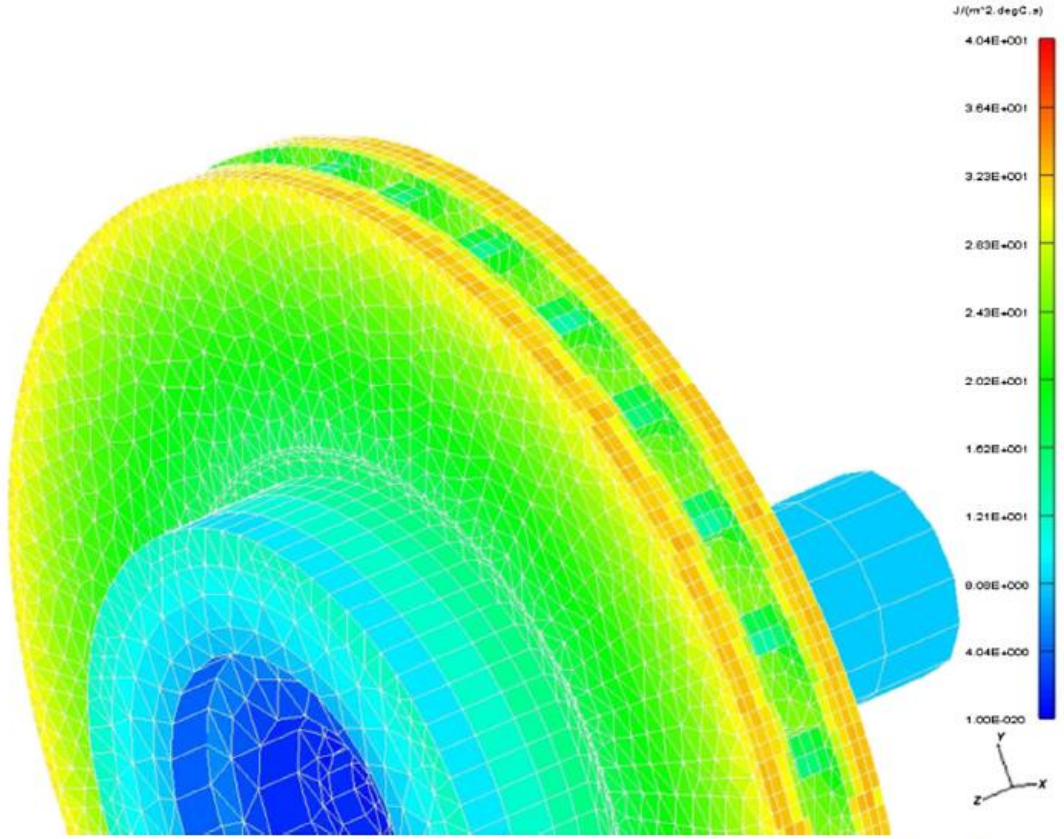

Figure 7.12: Brake Disc Surface Heat Transfer Coefficient Values Predicted by CFD for a Disc Rotating at 450 rev/min at 100°C in an Environment at Ambient Temperature of 20°C (Tirovic, 2013).

The maximum air exit temperature was 30^0C at the exit from the vanes at the disc outer periphery, so the maximum air temperature rise was only 10^0C. Flow stagnation and increase of air temperatures at the hat/friction ring transition region can also be seen. Predicted local convective heat transfer coefficients (h_{conv}) for the same disc rotating in the same environment ranged between 4 and 40 W/m^2 K, and were lowest in the hat area and highest at the air inlet into the channels (at the disc inner radius).

High values were also predicted at the disc outer periphery. At the friction surfaces of the disc, the heat transfer coefficient increased in the radial direction outwards, from approximately 10 to 30 W/m^2 K. The average values of heat transfer coefficients were also calculated from the CFD analyses, and the relationship between average heat transfer coefficients and disc rotational speed is shown in Figure 7.13.

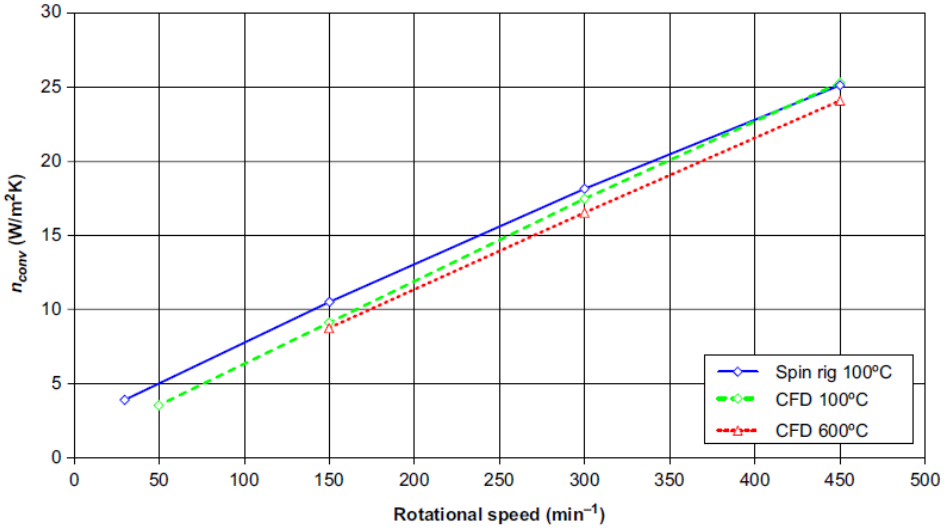

Figure 7.13: Average Brake Disc Surface Heat Transfer Coefficient Values Predicted by CFD and Compared with Experimental (Test Rig) Data, for a Disc Rotating at 450 rev/min at 100°C, in an Environment at Ambient Temperature of 20°C (Tirovic, 2013).

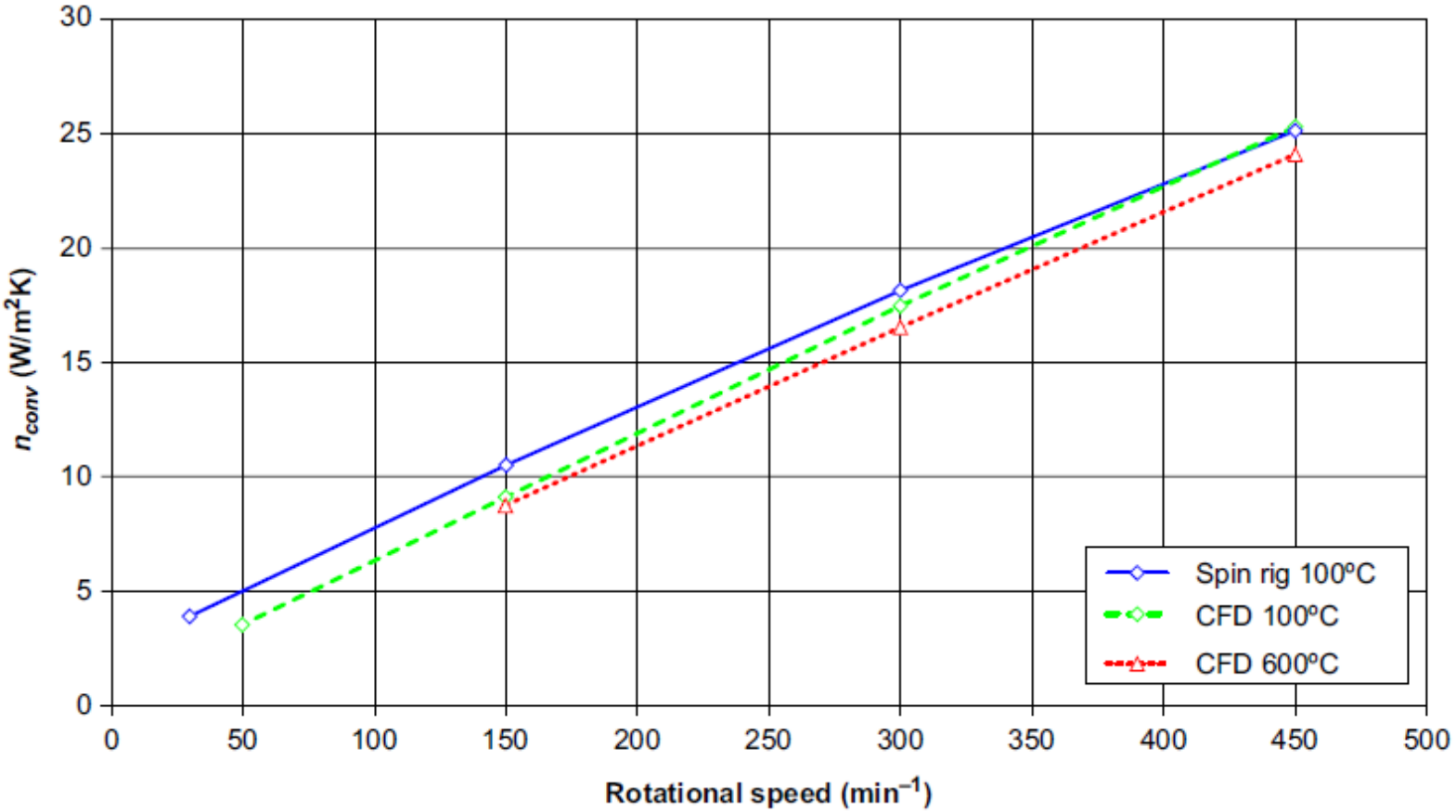

Figure 7.13: Average Brake Disc Surface Heat Transfer Coefficient Values Predicted by CFD and Compared with Experimental (Test Rig) Data, for a Disc Rotating at 450 rev/min at 100°C, in an Environment at Ambient Temperature of 20°C (Tirovic, 2013).

The influence of the wheel on convective heat transfer coefficients was also investigated by Voller et al. (2003) for the same environment (still air). A brake disc design in which the outboard friction cheek was attached to the hat showed very little change in the convective heat transfer coefficient with the wheel in place. This was because the air flowed into the vents from the inboard side, as indicated in Figure 7.14(a).

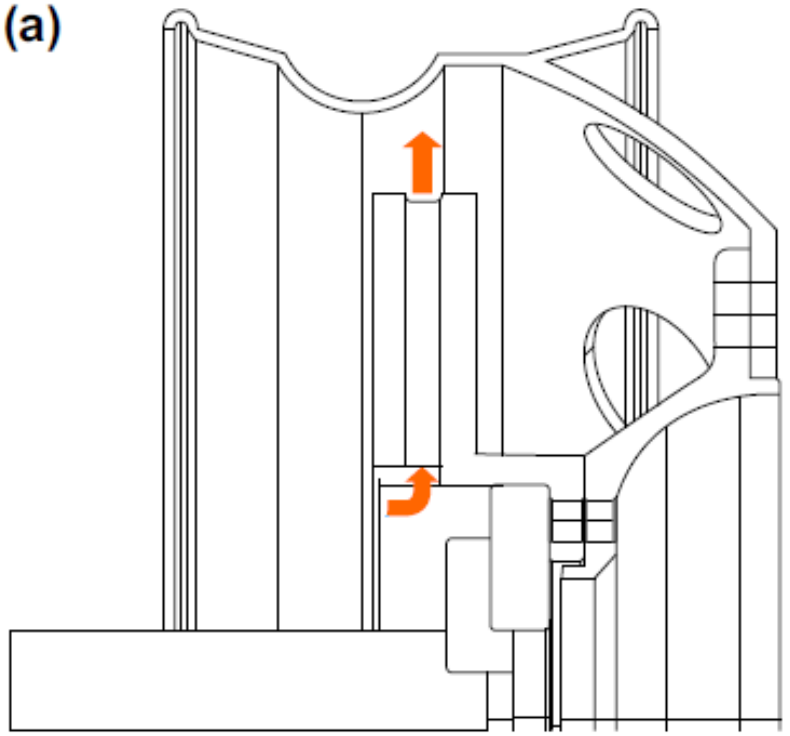

Figure 7.14: Cooling Airflow for Two Different Designs of Brake Disc (Tirovic, 2013).
(a) Outboard attachment. (b) Inboard attachment (reverse ventilated).

A second design of brake disc, a reverse ventilated design with the inboard friction cheek attached to the hat (Figure 7.14(b)), showed similar cooling characteristics for the disc alone to the first design of brake in still air. However, when assembled with the wheel, the convective heat transfer coefficients reduced substantially because the wheel assembly restricted the supply of air into the vents from inside the wheel, not from the outside.

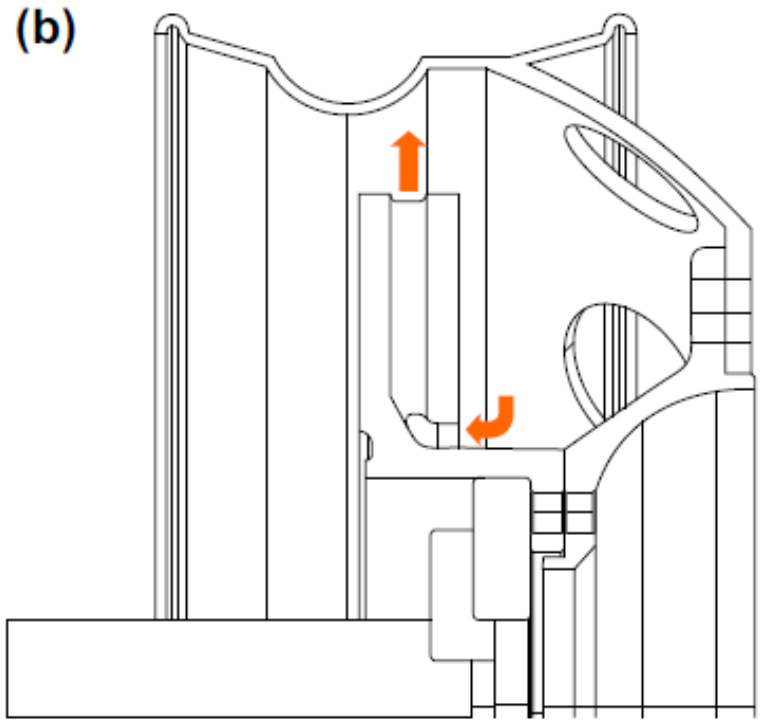

Figure 7.14: Cooling Airflow for Two Different Designs of Brake Disc (Tirovic, 2013)
(a) Outboard attachment. (b) Inboard attachment (reverse ventilated).

The second design of ventilated brake disc (Figure 7.14(b)) is desirable because it is known to reduce coning deformation, so, in order to improve cooling, the airflow into the vents was increased by piercing the wheel carrier, as illustrated in Figure 7.15.

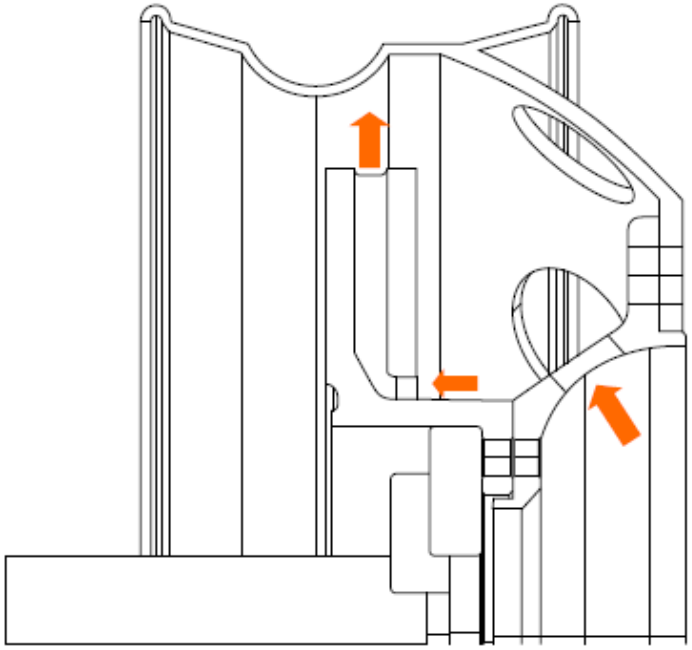

Figure 7.15: Anti-Coning Brake Disc and Pierced Wheel Carrier (Tirovic, 2013).

Figure 7.16 summarizes the predicted heat transfer coefficients for the second design of brake disc and the two different wheel carriers. The brake disc with the pierced carrier wheel assembly had cooling reduced from the disc alone (no wheel), but is significantly higher than for the solid carrier.

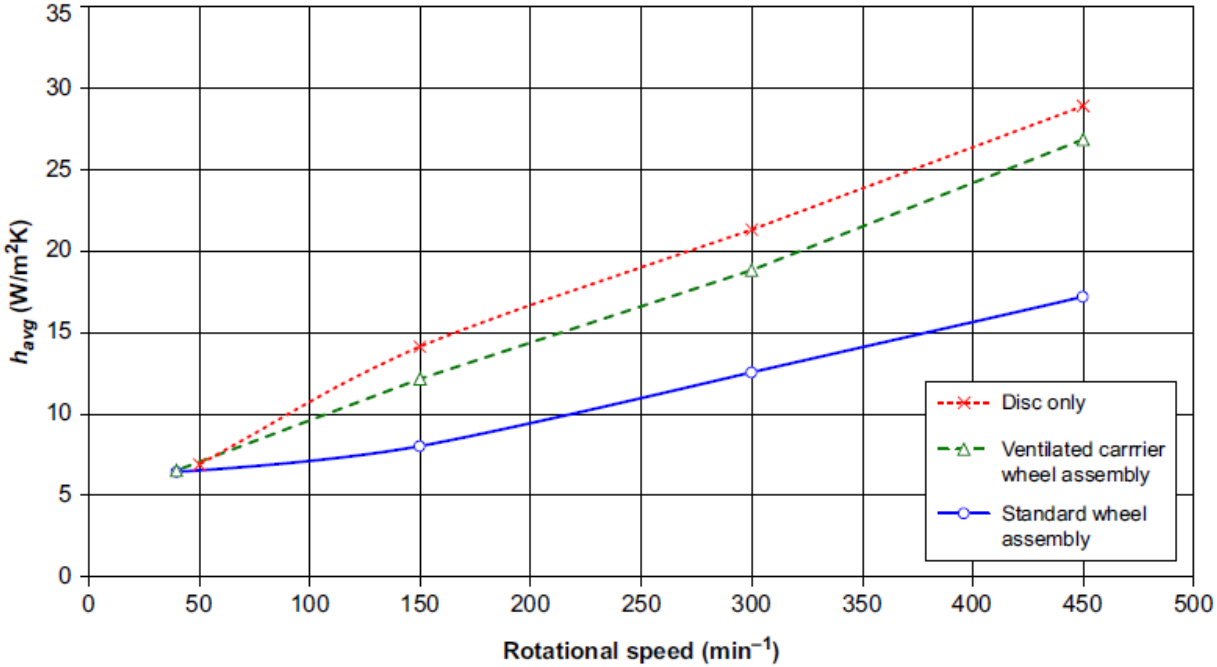

Figure 7.16: Average Heat Transfer Coefficient Values for the Second Design of Brake Disc Rotating at 100°C, in an Environment at Ambient Temperature of 20°C (Tirovic, 2013).

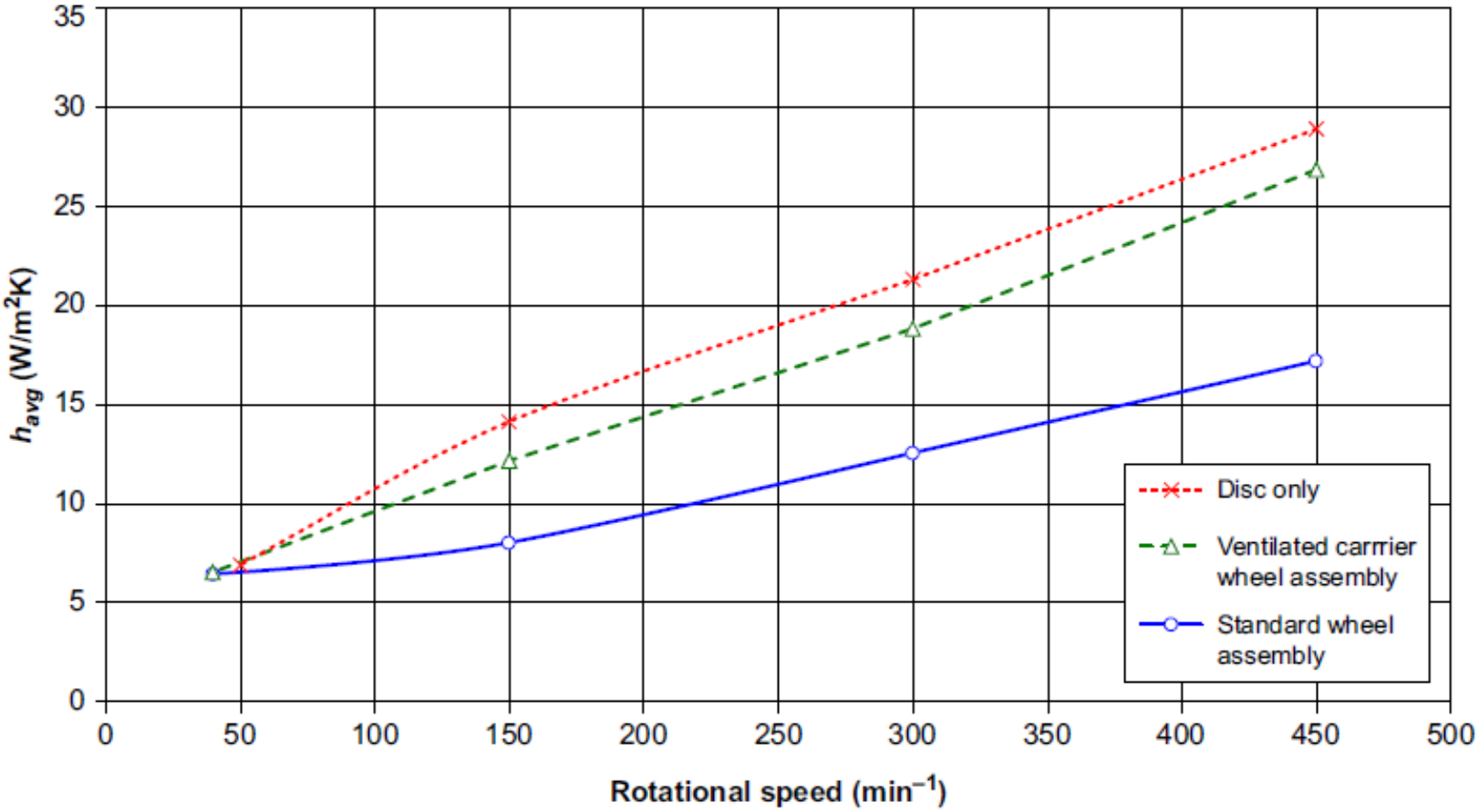

Figure 7.16: Average Heat Transfer Coefficient Values for the Second Design of Brake Disc Rotating at 100°C, in an Environment at Ambient Temperature of 20°C (Tirovic, 2013).

Conductive Heat Transfer

Heat transfer by conduction from the disc to the hub and the wheel is important in brake cooling, and involves heat transfer across interfaces between such components that are in contact, e.g. the disc is bolted to the hub flange, and the wheel is also bolted to this assembly. Conductive heat transfer also occurs at the interface of all other brake components, such as the pad, piston and caliper, and across all of these interfaces there is additional resistance to heat flow because of the ‘interface contact resistance’.

A typical steady-state temperature profile in two contacting solid bodies of cross-sectional area A (m^2) with heat flow through them is shown in Figure 7.17.

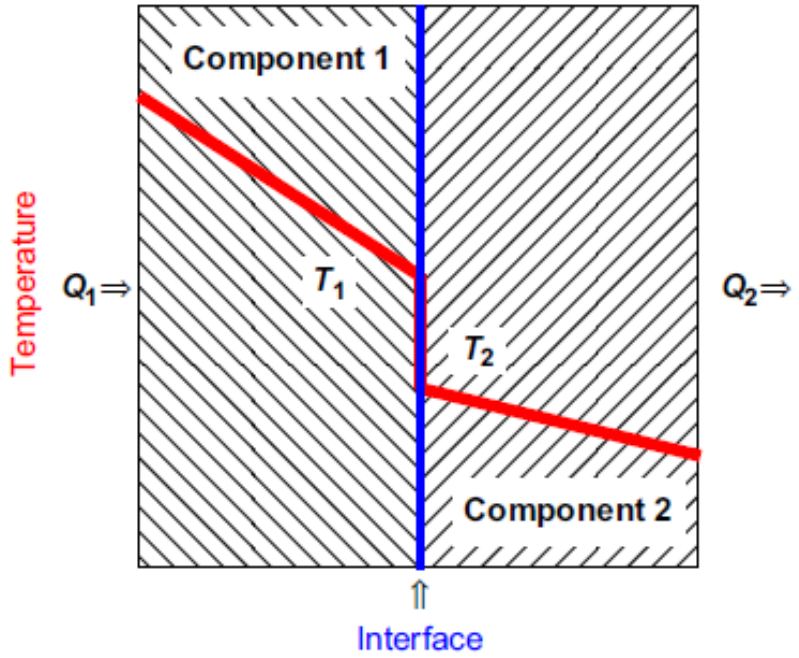

Figure 7.17: Thermal Contact Resistance (Tirovic, 2013).

Q1 is the heat entering component 1 and Q2 is the heat leaving component 2. It is assumed that both components are insulated and steady-state conditions have been established, so that:

$$Q_1 = Q_2 \qquad (7.36)$$

The rate of heat transfer through the solid ($\dot{Q}_{cond}$) is governed by the material thermal conductivity (k), the cross-sectional area (A) and the thermal gradient, and can be defined as:

$$\dot{Q}_{cond} = -kA\mathrm{d}\theta/\mathrm{d}x \qquad (7.37)$$

Since in the steady state the conductive heat transfer is identical for both components:

$$Q_1 = Q_2 = Q_{cond} \tag{7.38}$$

Thermal gradients can be determined as:

$$d\theta/dx = -Q_{cond}/kA \tag{7.39}$$

The contact area (A) is identical for both components, and the difference in the thermal gradients through components 1 and 2 in Figure 7.17 is the result of the difference in the materials' thermal conductivities.

Figure 7.18 and Equations (7.37)e(7.39) assume conduction-only heat transfer at the interface. Where there is no intimate contact, i.e. between the asperities, heat transfer may be achieved by convection and radiation, which may not be as effective as conduction, and hence the overall interface contact resistance to heat flow may be increased

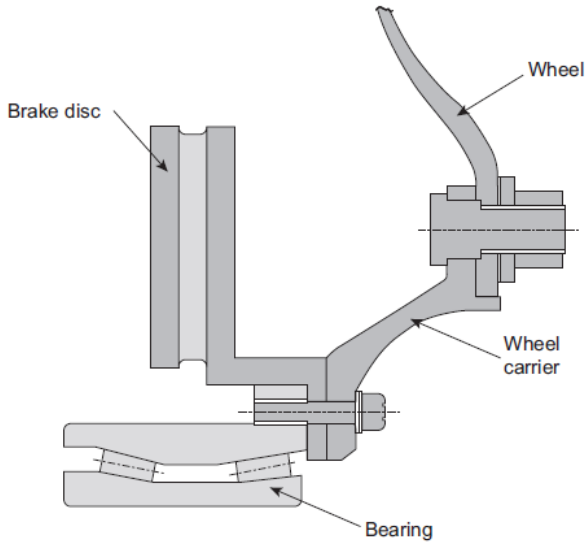

Figure 7.18: Cross-Sectional View Though a Typical Commercial Vehicle Front Wheel, Hub and Brake Assembly (Tirovic, 2013).

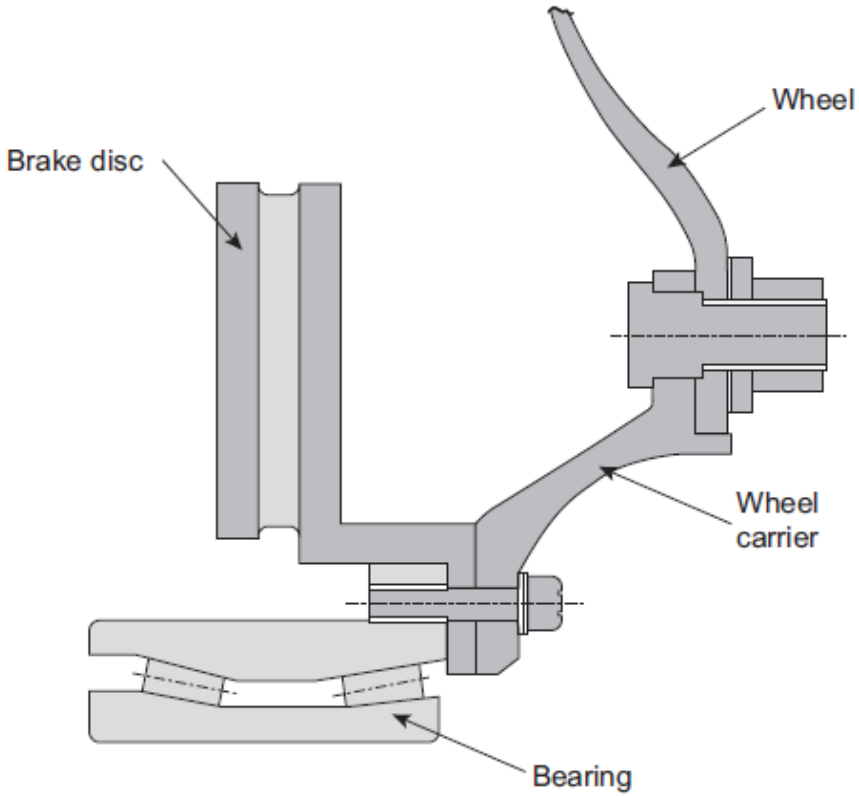

Figure 7.18: Cross-Sectional View Though a Typical Commercial Vehicle Front Wheel, Hub and Brake Assembly (Tirovic, 2013).

In FE modelling it is more convenient to use thermal conductance (the reciprocal of thermal contact resistance) expressed in the form of (conductive) heat transfer coefficient h_{cond} (W/m^2 K), with the additional benefit that by using the same nominal heat transfer coefficients and units (m^2 K/W) for all three heat transfer modes, the rate of heat transfer for each mode can be directly compared. The conductive heat transfer can be calculated using:

$$Q_{cond} = h_{cond} A \Delta\theta_{int} \qquad (7.40)$$

where:

$$\Delta\theta_{int} = \theta_1 - \theta_2 \qquad (7.41)$$

The effect of interface pressure in the form of bolt-up torque was more significant; in the used condition the relationship shown in Equation (7.40) can be used to calculate average thermal conductance as a function of interface pressure:

$$h_{cond} = 150P + 1560 \qquad (7.42)$$

where the units of thermal conductance are h_{cond} W/m^2 K and of interface pressure P are MPa.

Radiative Heat Transfer

The heat transferred by radiation from the surfaces of a brake disc and other brake components (Q_{rad}) is determined by Equation (7.43), which predicts a substantial increase of radiative heat dissipation at elevated temperatures:

$$Q_{rad} = \varepsilon \sigma A_s \left(\theta_D^4 - \theta_0^4 \right) \tag{7.43}$$

where:

ε is the emissivity of the surface;
σ is the Stefan–Boltzmann constant ($W/m^2/K^4$);
A_s is the area of radiative heat emission (m^2);
θ_D is the surface temperature of the disc (K);
θ_0 is the ambient (air) temperature (K).

Equation (7.43) for radiative heat transfer can be rewritten in a form similar to Equation (7.26) for convective (or conductive) cooling:

$$\dot{Q}_{rad} = -h_{rad} A_s (\theta_{st} - \theta_0) \qquad (7.44)$$

The radiative heat transfer coefficient h_{rad} is defined as:

$$h_{rad} = \frac{\varepsilon\sigma\left(\theta_{st}^4 - \theta_0^4\right)}{(\theta_{st} - \theta_0)} \qquad (7.45)$$

which can be further reduced to:

$$h = \varepsilon\sigma\left(\theta_{st}^3 + \theta_0^3 + \theta_{st}\theta_0^2 + \theta_0\theta_{st}^2\right) \qquad (7.46)$$

The most difficult aspect of radiation heat transfer modelling and analysis relates to the value of emissivity; the material, the condition of the surface and its temperature all influence the value of emissivity.

Using an average emissivity of 0.55 in Equation (7.45), radiative heat transfer coefficient (h_{rad}) values were calculated and are shown in Figure 7.19 (Tirovic, 2013).

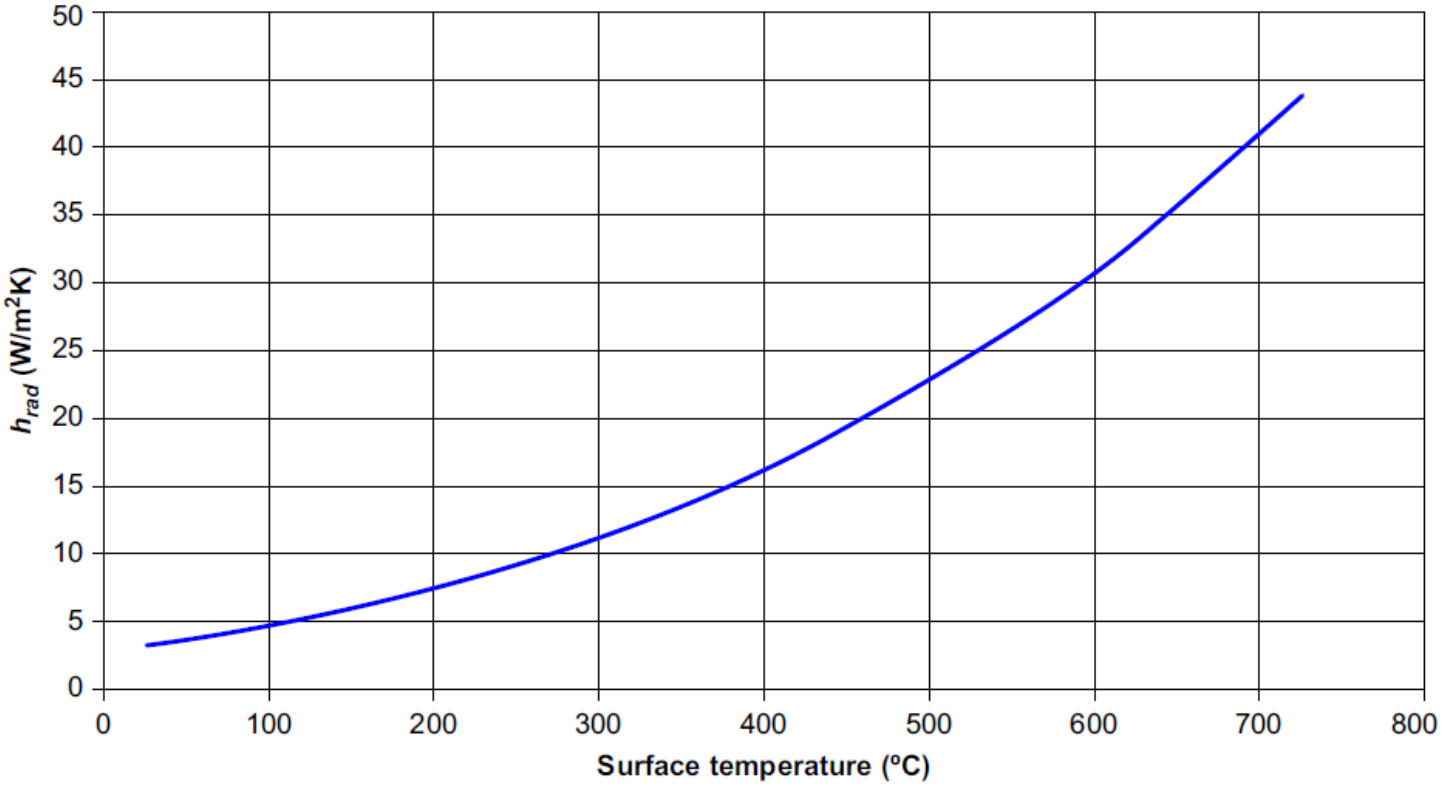

Figure 7.19: Radiative Heat Transfer Coefficient h_{rad} Increase with Surface Temperature for Emissivity $\varepsilon = 0.55$ (Tirovic, 2013).

As shown in Figure 7.20, heat radiated from the brake disc is partly reflected back from the wheel and wheel carrier (on a commercial vehicle disc brake assembly) to the disc, and under heavy-duty, repeated or drag brake applications, radiative heat reflection can result in an increase of over 20^0C in brake disc temperatures.

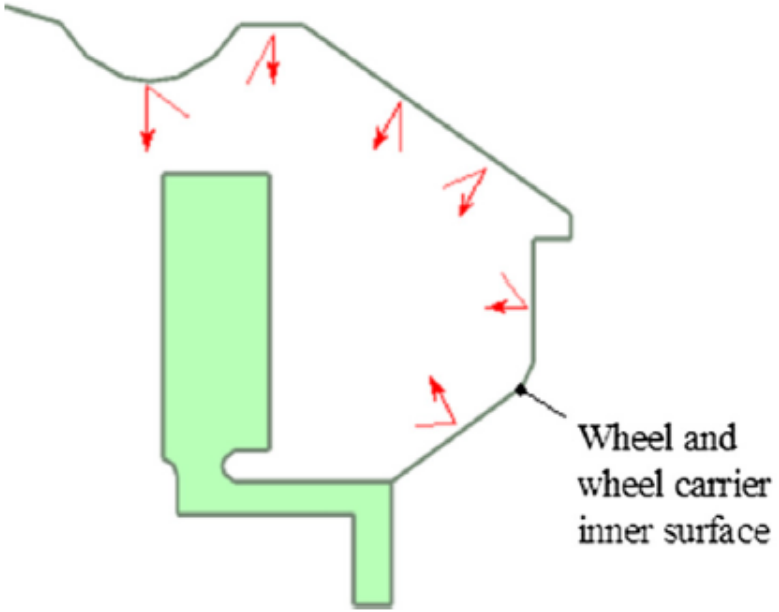

Figure 7.20: Radiative Heat Reflection in a Brake Disc, Wheel Carrier and Wheel Environment (Tirovic, 2013).

Figure 7.21 shows the contribution of individual modes of heat transfer to the braking power heat dissipation from the disc at this temperature; a wheel rotational speed of 150 rev/min corresponds to a road speed of 30 km/h.

At a disc temperature of 100^0C (Figure 7.21(a)), the total braking power heat dissipation was about 11.5 kW and the contributions of the individual modes of heat dissipation were approximately:

Conduction 2 kW (18%);

Convection 4.5 kW (39%);

Radiation 5 kW (43%).

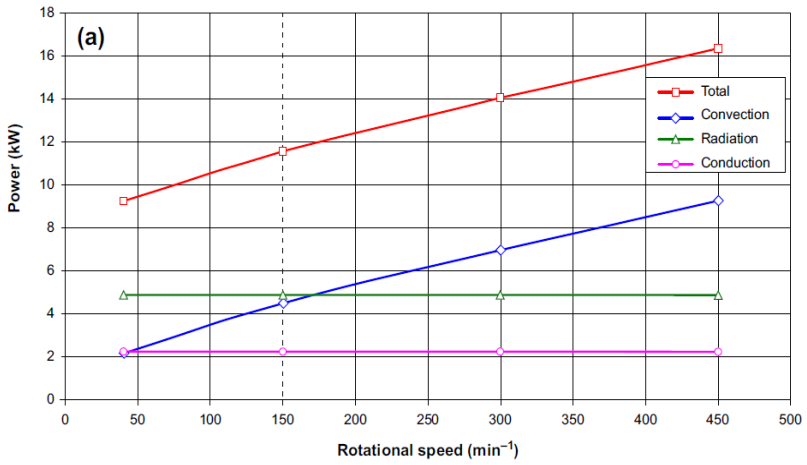

Conductive and radiative heat dissipation were not affected by speed but convective cooling varied from 2 kWat 40 rev/min to over 8 kWat maximum speed (450 rev/min). At a disc temperature of 100^0 C (Figure 7.21(b)) the total heat dissipation was about 700 W, and over 80% is by convective heat transfer.

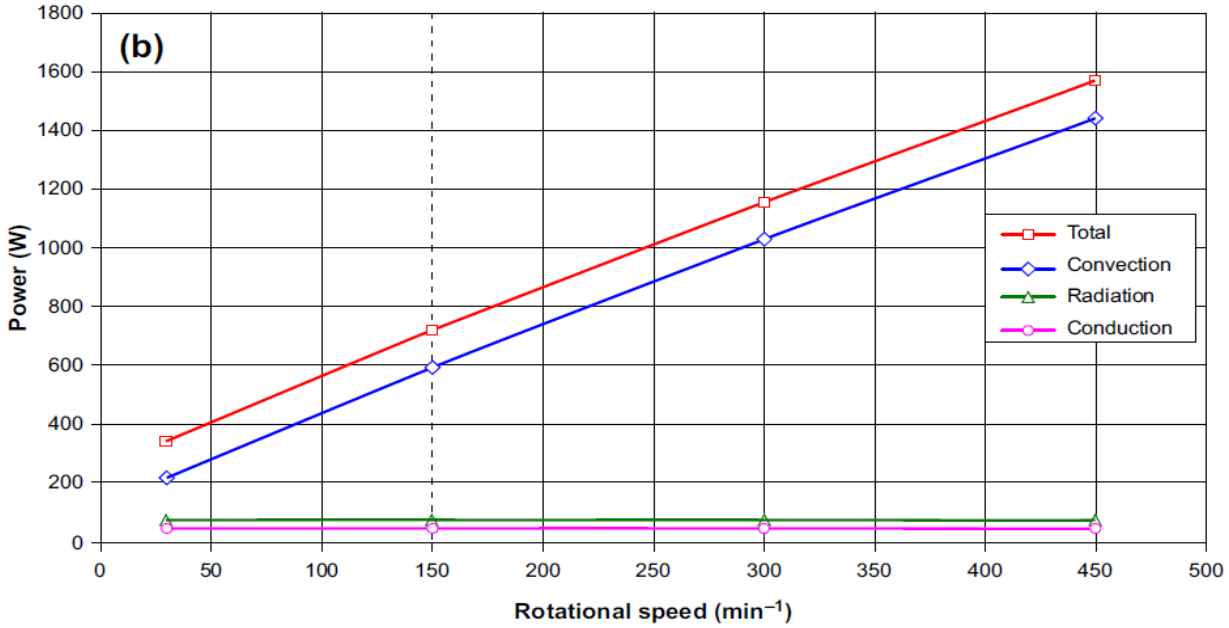

Figure 7.21: Braking Power Dissipated by Each Mode of Heat Transfer for the Brake Disc at 600°C (a) and 100°C (b) (Tirovic, 2013).

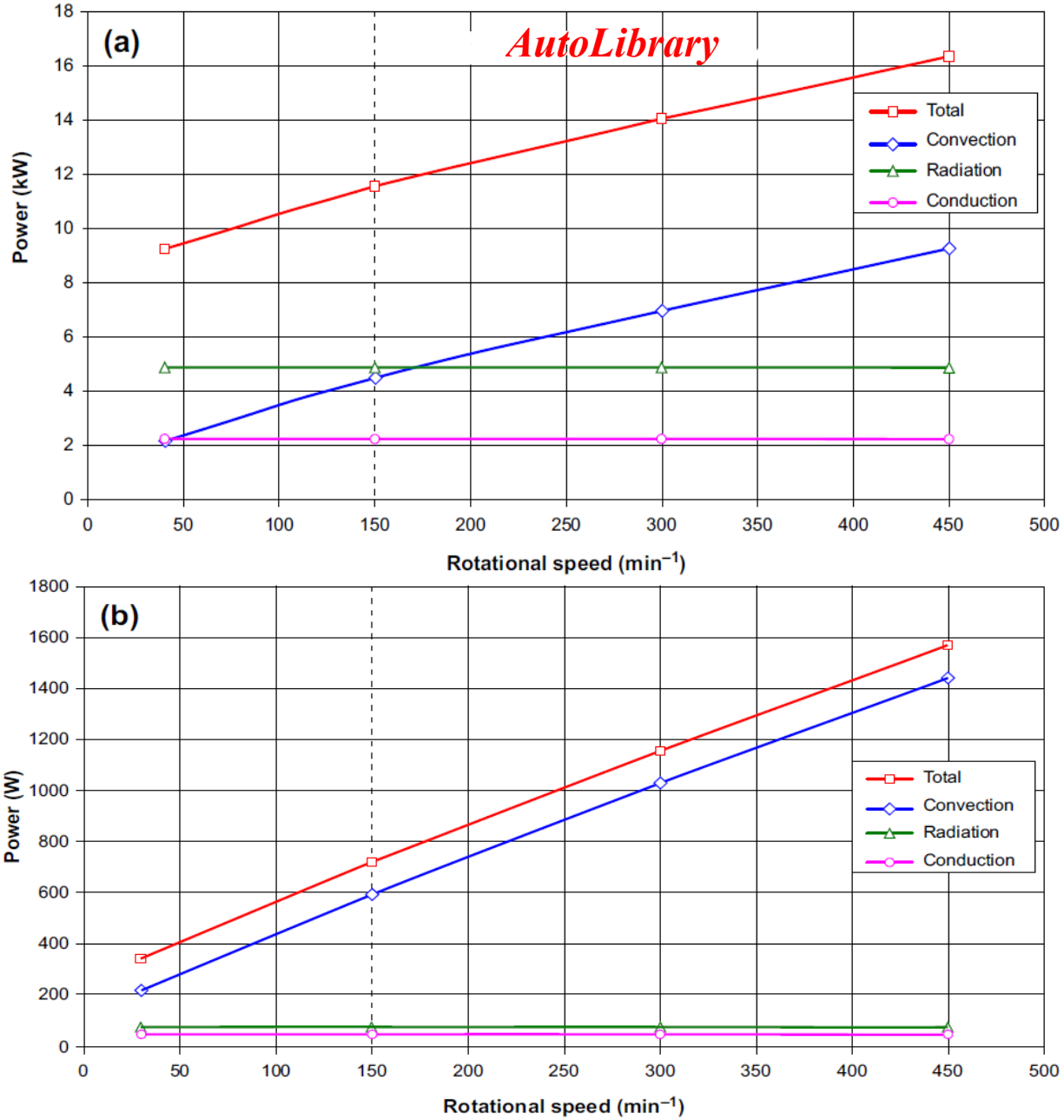

Figure 7.21: Braking Power Dissipated by Each Mode of Heat Transfer for the Brake Disc at 600°C (a) and 100°C (b) (Tirovic, 2013).

Chapter eight

Braking Legislation

Effective and efficient braking systems are fundamental to the safety of all road vehicles, and for this reason the braking of road vehicles is very closely controlled by law in most countries across the world to ensure that road vehicles are designed and constructed to brake safely and efficiently under all conditions of operation. The purpose of braking legislation is to ensure the provision and maintenance of safety standards for road vehicles and their braking equipment in terms of minimum safety standards and performance requirements in order to ensure that the public is protected against unreasonable risk of accidents.

The main way in which braking legislation is applied in practice is through Regulations and Directives, which are part of a comprehensive legal framework for all aspects of road vehicles in terms of their construction and use. The major world regions that enforce road vehicle legal standards and the associated legislative bodies are:

- Europe: EC (European Community), EU (European Union) and UN (United Nations).

- United States and Canada: Federal Motor Vehicle Safety Standards (FMVSS) and Canadian Motor Vehicle Safety Standards (CMVSS).
- Australia: Australian Design Rules (ADR).
- Japan and eastern Asia: type approval test procedures (TRIAS) (refer to the Japanese National Traffic Safety and Environment Laboratory (JNTSEL)).

European Legislation for Road Vehicle Braking

Within the European Community, legislation relating to the braking of road vehicles is defined in terms of Regulations that are mandatory, and Directives that are not mandatory but may be adopted into national law by member states to which they are addressed.

In the EU, a Regulation is binding in its entirety and is directly applicable in all member states, and this chapter concentrates on UNECE Regulations. The legislation covers three broad classes of vehicles with a design road speed exceeding 25 km/h:

- Road vehicles and their trailers
- Two- and three-wheel road vehicles and quadricycles.
- Agricultural and forestry vehicles.

Road vehicles and their trailers are categorized as follows:

Category M, passenger vehicles that are defined as motor vehicles with at least four wheels designed and constructed for the carriage of passengers:

- Category M1: passenger vehicles comprising no more than eight seats in addition to the driver's seat.
- Category M2: passenger vehicles comprising more than eight seats in addition to the driver's seat, and having a maximum mass not exceeding 5 tones.

Category M3: passenger vehicles comprising more than eight seats in addition to the driver's seat, and having a maximum mass exceeding 5 tones.

Category N, goods vehicles that are defined as motor vehicles with at least four wheels designed and constructed for the carriage of goods:

- Category N1: goods vehicles having a maximum mass not exceeding 3.5 tones.
- Category N2: goods vehicles having a maximum mass exceeding 3.5 tones but not

exceeding 12 tones.

- Category N3: goods vehicles having a maximum mass exceeding 12 tones

Category O, trailers, including semi-trailers:

- Category O1: trailers with a maximum static combined wheel loading not exceeding 0.75 tones.
- Category O2: trailers with a maximum static combined wheel loading exceeding 0.75 tones but not exceeding 3.5 tones.
- Category O3: trailers with a maximum static combined wheel loading exceeding 3.5 tones but not exceeding 10 tones.
- Category O4: trailers with a maximum static combined wheel loading exceeding 10 tones.

Note that for full (chassis) trailers the combined axle load is equal to the trailer mass but not for center axle trailers and semi-trailers, as the load transmitted to the towing vehicle is not included.

Category L, motor bicycles, tricycles and quadricycles:

- Category L1eL5: two- and three-wheel vehicles.
- Category L6, L7: quadricycles.
- Categories T and C: agricultural tractors.
- Categories R and S: agricultural trailers

The GSR also introduces new definitions relating to braking as listed below, and defines fundamental provisions for the type approval of motor vehicles relating to the following new braking-related requirements.

- Electronic Stability Control Systems (ESC)
- Advanced Emergency Braking Systems (AEBS)
- Lane Departure Warning Systems (LDW)
- Tyre Pressure Monitoring Systems (TPMS)
- Tyres, with regard to wet grip, rolling resistance and rolling noise.

Individual Vehicle Approval (IVA) is usually used for the type approval of:

- Vehicles for use on construction sites or in quarries, ports or airports.
- Vehicles for use by the armed services, civil defense, fire services and forces responsible for maintaining public order.
- Mobile machinery.
- Vehicles intended exclusively for racing on roads.
- Prototypes of vehicles used on the road under the responsibility of a manufacturer to perform a specific test programme provided they have been specifically designed and constructed for this purpose.

Braking Regulations

The European UN Regulations 13 and 13H (UNECE March 2014, UNECE February 2014) form the basis of the road vehicle braking legislation covered in this chapter. The US FMVSS Rules and Regulations Standard No. 135 (Light vehicle brake systems) (US FMVSS 135) and Standard No. 121 (Air brake systems) (US FMVSS 121) are also considered. The UN Regulation 90 for replacement or 'aftermarket' brake system components (UNECE, 2012) is also discussed. UN Regulations 13 and 13H concern the 'adoption of uniform technical prescriptions for wheeled vehicles, equipment and parts which can be fitted and/or be used on wheeled vehicles and the conditions for reciprocal recognition of approvals granted on the basis of these prescriptions.'

They specify procedures for type approval including specifications and tests, and many Annexes, which

for example relate to:

- Braking tests and performance of braking systems, including energy consumption (pneumatic systems), the procedure for monitoring the state of battery charge, and provisions relating to energy sources and energy storage devices.
- Braking distribution between vehicle axles, including a wheel-lock sequence test procedure and a torque wheel test procedure.

- Test requirements for vehicles fitted with ABS systems, including symbols and definitions and the utilization of adhesion (see Chapter 11), performance on differing adhesion surfaces, and method of selection of the low-adhesion surface.
- Inertia dynamometer test method for brake linings (see Chapter 9).
- Electronic stability control systems and brake assist systems, and special requirements that apply to the safety aspects of complex electronic vehicle control systems (see Chapter 11).

UN Regulation 13H (Category M1 and N1 Vehicles)

Road vehicle brakes must comply with the requirements of UN Regulation 13H (UNECE, February 2014) in normal use, including being resistant to deterioration, e.g. by wear and corrosion, and the effects of magnetic or electrical fields. The braking system must provide the basic functions summarized below, and the reader is referred to the Regulation documents for full details (UNECE, February 2014).

- Service braking. To control the movement of the vehicle and to bring it safely and quickly to rest under all conditions of operation in a ‘graduable’ action by the driver without the removal of his/her hands from the steering control. Automatic wear adjustment is required for the service braking system.

- Park braking. To hold the vehicle stationary on an up or down gradient even in the absence of the driver, with the brakes held in the locked position by a purely mechanical device. Again, the driver must be able to achieve this braking action from the driving seat.

- Secondary braking. If a failure occurs in the service braking system, it must be possible by application of the service brake control to bring the vehicle safely to rest within a reasonable distance under all conditions of operation in a ‘graduable’ action. The driver must be able to obtain this braking action from the driving seat without the removal of his/her hands from the steering control. It is assumed that not more than one failure of the service braking system can occur at one time.

The tests may include up to six stops, and the general behavior of the vehicle during braking must be checked, especially at high speed. The tests include:

- Type-0 test. Ordinary performance test with engine disconnected with cold brakes (Table 8.3(a)).
- Type-0 test. Ordinary performance test with engine connected with cold brakes (Table 8.3(a); this test is not run if the maximum speed of the vehicle is 125 km/h).
- Type-I test: fade and recovery test (Table 8.3(b)).

- Type-0 test. Ordinary performance test with engine disconnected with cold brakes (Table 8.3(a)).

Table 8.3(a): Summary of Test Conditions and Minimum Service and Secondary Braking System Performance Requirements for Type-0 Tests for Category M_1 and N_1 Vehicles in UN Regulation 13H

		Service Braking	Secondary Braking
Type-0 test with engine disconnected	V	100 km/h	100 km/h
	$s \leq$	$0.1V + 0.0060V^2$ (m)	$0.1V + 0.0158V^2$ (m)
	$J_m \geq$	6.43 m/s^2	2.44 m/s^2
Type-0 test with engine connected	V	80% $V_{max} \leq$ 160 km/h	
	$s \leq$	$0.1V + 0.0067V^2$ (m)	
	$J_m \geq$	5.76 m/s^2	
	F_d	6.5–50 daN	6.5–50 daN

- Type-I test: fade and recovery test (Table 8.3(b)).

Table 8.3(b): Summary of Test Conditions and Minimum Service and Secondary Braking System Performance Requirements for Type-I Tests for Category M_1 and N_1 Vehicles in UN Regulation 13H

Type-I Test (Fade and Recovery Test)	V_1 (km/h)	V_2 (km/h)	Number of Brake Applications (n)
	80% $V_{max} \leq$ 120 km/h	$0.5V_1$	15

V = vehicle road (test) speed (km/h).
s = stopping distance (m).
J_m = mean fully developed deceleration (m/s^2).
F_d = Force applied by the driver to the brake pedal, also termed force applied to foot control (daN).
V_{max} = maximum vehicle road speed (km/h).

The service braking system performance is verified using these tests, and then the performance of the secondary braking system is tested using the Type-0 test with the engine disconnected. The test conditions and minimum service and secondary braking system performance requirements for category M1 and N1 vehicles in UN Regulation 13H are summarized in Table 8.3(a). The response time of a hydraulic braking actuation system must not exceed 0.6 s.

Stopping distance (s) is defined as the distance travelled from the moment the brake pedal is actuated until the vehicle comes to rest. MFDD (J_m) is calculated over part of the brake application as the deceleration averaged with respect to distance over the interval V_b to V_e, according to:

$$J_m = \frac{(V_b^2 - V_e^2)}{25.92(s_g - s_b)} \text{ m/s}^2 \qquad (8.1)$$

where:

V_1 = initial vehicle road speed (km/h);
V_b = vehicle speed at $0.8V_1$ (km/h);
V_e = vehicle speed at $0.1V_1$ (km/h);
s_b = distance travelled between V_1 and V_b (m);
s_e = distance travelled between V_b and V_e (m).

Prior to the addition of stopping distance into the European braking legislation, only the time-related deceleration was used, but this is not now regarded as an objective measure of the MFDD because by averaging the deceleration over time, the effect of a low deceleration at high speed at the beginning of the braking event is proportionally under-weighted and a high deceleration at low speed at the end of the braking is proportionally over-weighted, as illustrated in Figure 8.1.

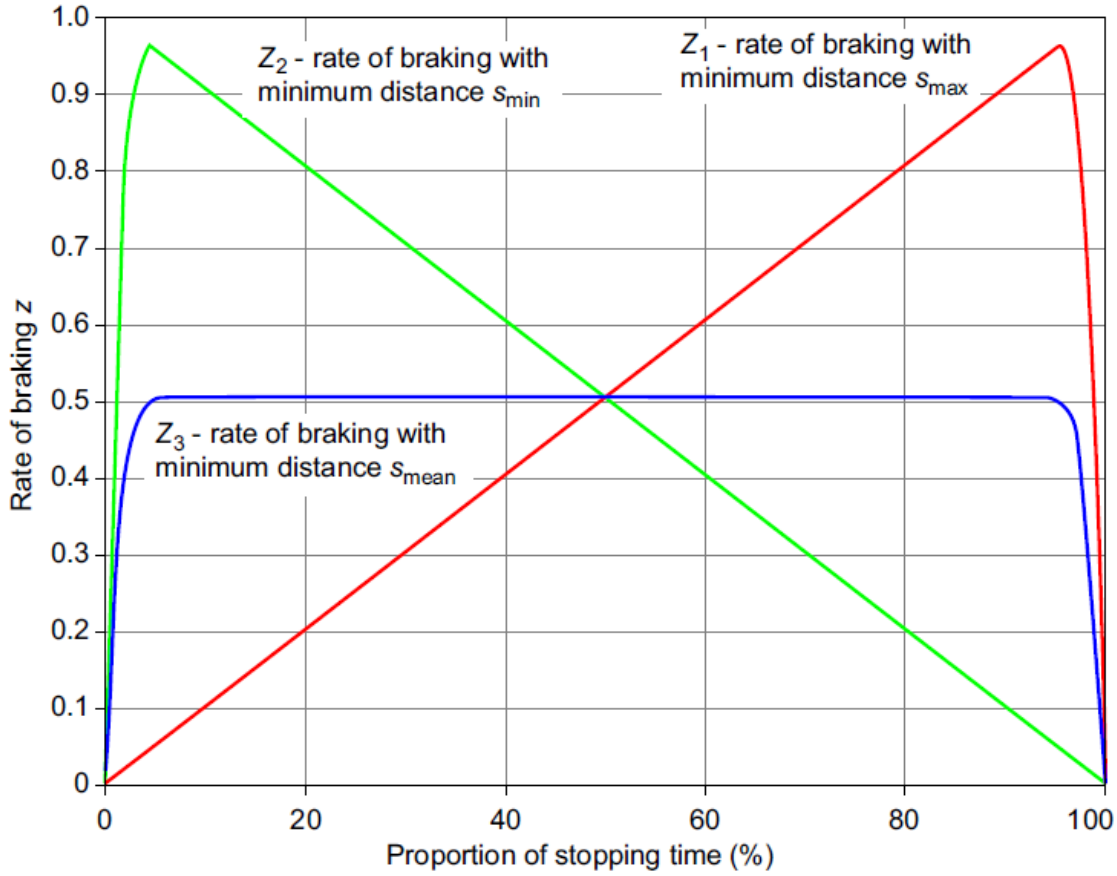

Figure 8.1: Different Examples of Rate of Braking vs. Time (Gaupp, 2013).

This demonstrates in theory that the three rate-of-braking curves z1, z2 and z3 result in very different stopping distances, although their time-averaged decelerations are all 50% g:

z1: the braking force is linearly increasing until the vehicle comes to rest, which gives the longest stopping distance.

z2: the braking force is linearly decreasing until the vehicle comes to rest, e.g. because of fade, which gives the shortest stopping distance.

z3: the braking force is constant until the vehicle comes to rest, which gives a stopping distance between z1 and z2.

The minimum Type-0 service braking performance of a motor vehicle towing an unbraked trailer must not be less than 5.4 m/s^2 in both laden and unladen conditions, and must beverified by calculation using:

$$J_{M+R} = J_m \frac{M_{laden}}{M_{trailer\ max}} \qquad (8.2)$$

where:

J_{M+R} = the calculated MFDD of the motor vehicle coupled to an unbraked trailer (m/s^2);

J_m = maximum MFDD of the solo motor vehicle achieved during the Type-0 test with engine disconnected (m/s^2);

M_{laden} = mass of the laden motor vehicle (kg);

$M_{trailer\ max}$ = maximum mass of the unbraked trailer.

The park braking system must be capable of holding the laden vehicle stationary on a 20% up or down gradient. If coupled to an unbraked trailer, the park braking system of the motor vehicle must be capable of holding the combination stationary on a 12% up or down gradient. Where the park brake control is manual, the operating force must not exceed 40 daN, or 50 daN if it is foot operated.

One of the most important features of UN braking legislation is adhesion utilisation and basic braking stability based on wheel-lock sequence (see Chapter 3). For vehicles that are not equipped with ABS, UN Regulation 13H Annex 5 requires that for all states of load of the vehicle, the adhesion utilisation curve of the rear axle must not lie above the curve for the front axle for all braking rates between 0.15 and 0.8, and for tyre/road adhesion values (k) between 0.2 and 0.8. For k values between 0.2 and 0.8, the required minimum rate of braking is determined from:

$$z \geq 0.1 + 0.7(k - 0.2) \qquad (8.3)$$

Braking stability is verified by a wheel-lock sequence test in the laden and unladen conditions with the engine disconnected at a test road speed of 65 km/h for z 0.50 or 100 km/h for z > 0.50. Neither rear wheel must lock before both front wheels lock for braking rates between 0.15 and 0.8, as indicated by:

1. No wheels lock
2. Both wheels on the front axle and one or no wheels on the rear axle lock
3. Both axles simultaneously lock.

UN Regulation 13 (Category M, N and O Vehicles)

As with UN Regulation 13H, road vehicle brakes must comply with the requirements of UN Regulation 13 (UNECE, March 2014) in normal use, and must provide the basic functions summarized previously for UN Regulation 13H in terms of service braking, secondary braking and park braking with the addition of residual braking (in UN Regulation 13H requirements for residual braking performance are not explicitly stated, being part of the secondary braking performance requirements). The braking must be controlled by the driver from the driving seat, and must be graduable, including the braking of the trailer in a vehicle combination.

Service, secondary and residual braking performance are defined below, and the reader is referred to the UN Regulation 13 document for full details (UNECE, March 2014).

- ‘Service braking performance’. The defined performance is required when no faults are present and must be achieved when the driver has both hands on the steering control.
- ‘Secondary braking performance’. The defined performance is required when a ‘single’ defect is present and must be achieved when the driver has at least one hand on the steering control.
- ‘Residual braking performance’. In UN Regulation 13 this is defined as the braking performance required when there is a failure within one service braking circuit (service braking performance is when no faults are present and secondary braking performance is when a single defect is present).

Tests to verify braking performance for EU type approval must be carried out in the laden and unladen conditions at the speeds prescribed for each type of test. In the laden condition the distribution of mass among the axles must be that stated by the manufacturer. Where several arrangements of the load on the axles is possible, the distribution of the maximum mass among the axles must ensure that the load on each axle is proportional to the maximum permissible load for each axle

The prescribed speeds in the tests depend on the vehicle category, as indicated in Tables 8.4, 8.5 and 8.6.

Table 8.4(a): Service and Secondary Braking Performance Requirements for Solo Vehicles (Categories M and N) Based on UN Regulation 13 (Type-0 Test with Engine Disconnected; Refer to the UN Regulation 13 Document for Full Details)

	Service		Secondary			
	N_1	M_2, M_3, N_2 and N_3	M_2 and M_3	N_1	N_2	N_3
Initial vehicle road speed, V_1 (km/h)	80	60	60	70	50	40
Stopping distance, s (m)	$0.15V + (V^2/130)$		$0.15V + (2V^2/130)$	$0.15V + (2V^2/115)$		
	≤61.2	≤36.7	≤64.4	≤95.7	≤51.0	≤33.8
MFDD (m/s^2)	5		2.5		2.2	
Control force, F_d (daN)	≤70		≤70			

- Type-0 test. Ordinary performance test with engine disconnected (see Table 8.4) with cold brakes.

Table 8.4(b): Residual Braking Performance Requirements for Solo Vehicles (Categories M and N) Based on UN Regulation 13 (Type-0 Test with Engine Disconnected; Refer to the UN Regulation 13 Document for Full Details (UNECE, March 2014))

	Residual				
	M_2	M_3	N_1	N_2	N_3
Initial vehicle road speed, V_1 (km/h)	60	60	70	50	40
Laden Stopping distance, s (m)	$0.15V + ((100/30) \times (V^2/130))$		$0.15V + ((100/30) \times (V^2/115))$		
	≤101.3	≤101.3	≤152.5	≤80.0	≤52.4
Laden MFDD (m/s^2)	1.5	1.5	1.3	1.3	1.3
Unladen Stopping distance, s (m)	$0.15V + ((100/25) \times (V^2/130))$	$0.15V + ((100/30) \times (V^2/130))$	$0.15V + ((100/25) \times (V^2/115))$		$0.15V + ((100/30) \times (V^2/115))$
	≤119.8	≤101.3	≤180.9	≤94.5	≤52.4
Unladen MFDD (m/s^2)	1.3	1.5	1.1	1.1	1.3
Control force, F_d (daN)	≤70				

- Type-0 test. Ordinary performance test with engine connected (see Table 8.5) with coldbrakes.

Table 8.5: Service Braking Performance Requirements for UN Regulation 13 Type-0 Test with Engine Connected, for Category M and N Vehicles (Refer to Regulation 13 Document for Full Details (UNECE, March 2014))

		Category				
	Type of Test	M_2 0, I	M_3 0, I, II, or IIA	N_1 0, I	N_2 0, I	N_3 0, I, II
Type 0 test with engine connected	$V = 0.80V_{max}$ but not exceeding:	100 km/h	90 km/h	120 km/h	100 km/h	90 km/h
	Stopping distance (s)	$\leq 0.15V + \frac{V^2}{103.5}$				
	J_m	≥ 4.0 m/s^2				
	Control force (F_d)	≤ 700 N				

Type-I test. Fade test with repeated braking (see Table 8.6) followed by a hot performance test (measured at the same conditions as the Type-0 test), which must demonstrate braking performance not less than 80% of that prescribed for the motor vehicle category, or less than 60% of the Type-0 test performance with the engine disconnected. For trailers, the hot brake force at the periphery of the wheels when tested at 40 km/h must not be less than 36% of the maximum stationary wheel load, or less than 60% of the figure recorded in the Type-0 test at the same speed (see Table 8.7).

Table 8.6: Test Conditions for UN Regulation 13 Type-I Test (Fade Test with Repeated Braking), for Category M and N Vehicles (Refer to Regulation 13 Document for Full Details (UNECE, March 2014))

Type-I Test (Fade and Recovery Test) Vehicle Category	Conditions			
	V_1 (km/h)	V_2 (km/h)	Time Interval Δt (s)	Number of Brake Applications (n)
M_2	80% $V_{max} \leq$ 100 km/h	$0.5V_1$	55	15
N_1	80% $V_{max} \leq$ 120 km/h	$0.5V_1$	55	15
M_3, N_2, N_3	80% $V_{max} \leq$ 60 km/h	$0.5V_1$	60	20

Table 8.7: Braking Performance Requirements for Trailers Based on EC Regulation 13 (Refer to Regulation 13 Document for Full Details (UNECE, March 2014))

	Semi-Trailer	Full (Chassis) Trailer	Centre Axle Trailer
	Minimum Braking Force is Based on a Percentage of the Static Axle/Bogie Load		
Initial vehicle road speed, V_1 (km/h)	60	60	60
Braking force (%)	≥45	≥50	≥50
Maximum coupling head pressure (bar)	6.5	6.5	6.5
Supply line pressure (bar)	7.0	7.0	7.0

For trailers that are equipped with a single circuit braking system (note that in the case of trailers with EBS the electrical transmission cannot be a purely 'single circuit braking system'), two additional requirements apply:

- 'Automatic braking performance'. Braking performance of 13.5% of the maximum laden static axle load is required when a failure in the supply line is present.
- 'Auxiliary equipment'. The braking system may supply air for the function of auxiliary systems, e.g. air suspension, but the braking system must be protected so that in the event of a failure within the auxiliary system the braking system must be able to achieve a performance of 80% of that prescribed for the specific vehicle.

The effect of Equations (8.4) and (8.5) is therefore to simulate the effect on the tractor of the vertical and horizontal forces imposed on the fifth wheel coupling by a laden semi-trailer; both M_s and ham increase as z increases. It should be noted that any retarding force produced by an endurance brake (retarder) is not taken into consideration when defining the compatibility performance.

$$M_s = M_{so}(1 + 0.45z) \tag{8.4}$$

$$h_{am} = (hM + h_3M_s)/(M + M_s) \tag{8.5}$$

where:

M_{so} represents the difference between the maximum laden mass of the tractor and its unladen mass (M), i.e. the maximum allowable static load on the kingpin;
h is the height of centre of gravity of the solo tractor;
h_3 is the height of the coupling (kingpin or fifth wheel);
M is the unladen mass of the solo tractor.

Requirements for the distribution of braking between vehicles' axles, and requirements for compatibility between towing vehicles and trailers, are detailed in UN Regulation 13. First, the 'threshold' actuation must avoid erratic brake operation at low actuation pressures, and it is required that the development of braking force on the axles of each independent axle group is within the pressure ranges summarized below:

(a) Laden vehicles. At least one axle must start to develop a braking force when the pressure at the coupling head is 20e100 kPa, and at least one axle in every other axle group must start to develop a braking force when the pressure at the coupling head is 120 kPa.

(b) Unladen vehicles. At least one axle must start to develop a braking force when the pressure at the coupling head is 20e100 kPa.

UN Regulation 13 requires that for all states of loading of two-axle motor vehicles that are not equipped with ABS, the rate of braking shown in Equation (8.6) must be achieved for k values between 0.2 and 0.8. (A tractor without ABS that is designed to operate with a semi-trailer would also need to meet the adhesion utilization requirements outlined above when operating solo.)

For all states of load of the vehicle, the adhesion utilization curve of the rear axle must not lie above the curve for the front axle, but with qualifications depending on the vehicle category.

This means that the requirements for adhesion utilization and wheel-lock sequence depend upon the type of vehicle. These relate to the state of load of the vehicle, and include for example that in the case of category N1 vehicles with a laden/unladen rear axle loading ratio not exceeding 1.5 or having a maximum mass of less than 2 tones, in the range of z values between 0.3 and 0.45, an inversion of the adhesion utilization curves is permitted provided that the adhesion utilization curve of the rear axle does not exceed the line defined by k = z by more than 0.05 (UN Regulation 13 Annex 10 para 3.1.2.1 for two-axled vehicles).

This is the line of ideal adhesion utilization shown in Diagram 1A of Annex 10 (see Figure 8.2). Refer to UN Regulation 13 (UNECE, March 2014) for full information.

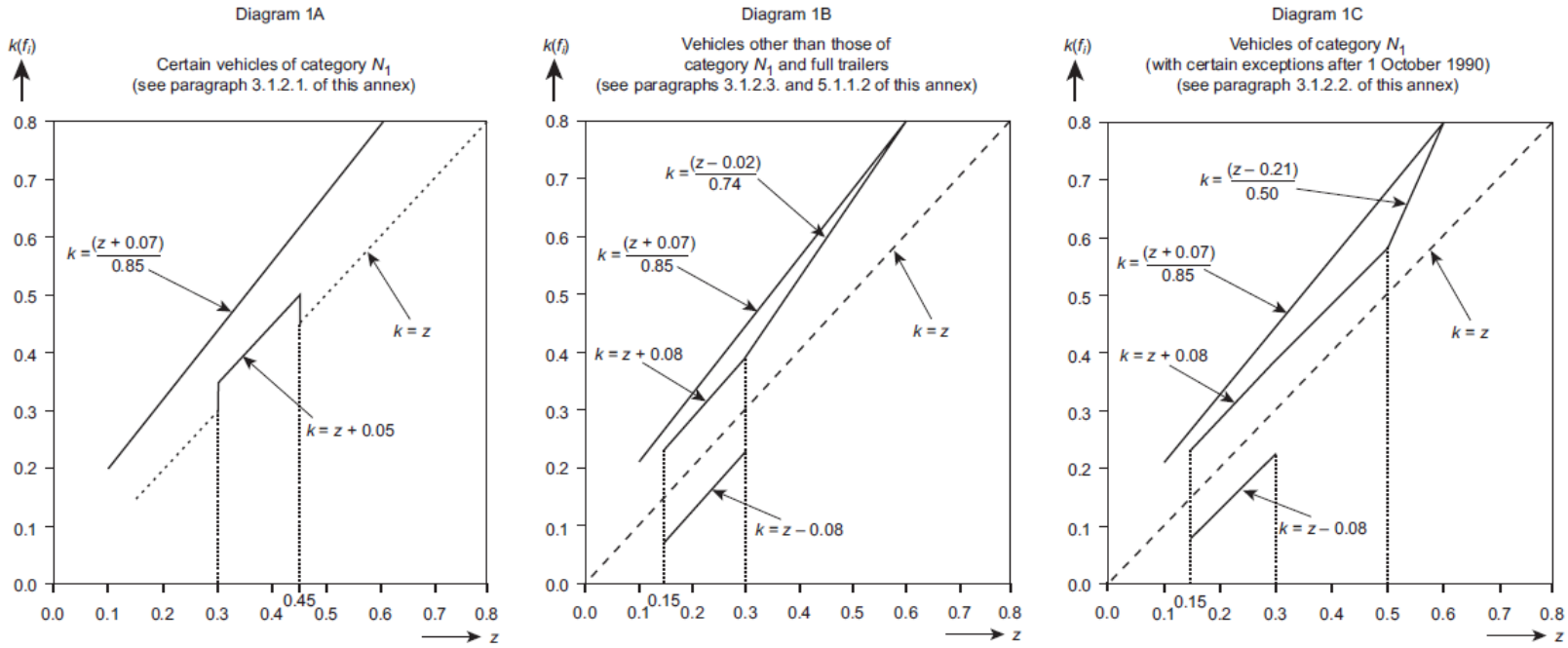

Note: The lower limit $k = z - 0.08$ is not applicable for the adhesion utilisation of the rear axle.

Figure 8.2: Diagrams 1A to 1C of Annex 10 of UN Regulation 13 (UN, March 2014).

$$z > 0.10 + 0.85(k - 0.20) \qquad (8.6)$$

For category O2, O3 and O4 trailers, the total braking forces at the tyre/road interface of the wheels must be at least the proportion of the maximum static normal wheel load as indicated below (category O1 trailers are generally unbraked but if they are equipped with a braking system they must fulfil the requirements of a category O2 trailer):

Full trailer, laden and unladen:	50%
Semi-trailer, laden and unladen:	45%
Centre-axle trailer, laden and unladen:	50%

US Road Vehicle Braking Legislation

Braking legislation in the USA requires that manufacturers must confirm with the National Highway Traffic Safety Agency (NHTSA) that their products conform to the relevant Federal Motor Vehicle Safety Standards (FMVSS) through the process of self-certification. The NHTSA can inspect any product at any time to evaluate whether a vehicle or equipment item conforms to the performance requirements. The relevant standards include FMVSS 135 for light vehicle brake systems (US FMVSS 135), FMVSS 121 for air brake systems (performance and equipment requirements for braking systems on vehicles equipped with air brake systems) (US FMVSS 121), and FMVSS 105 for hydraulic and electric brake systems (requirements for hydraulic and electric service brake systems, and associated park brake systems) (US FMVSS 105).

The classes of road vehicles specified by the US Department of Transportation, Federal Highway Administration (FHWA 13) are outlined in Table 8.8. These classes can be compared with the EU vehicle categories summarized earlier, noting the following differences:

- EU categories for passenger-carrying vehicles are dependent on vehicle mass and number of seats.
- All EU categories of commercial vehicles and combinations are dependent on vehicle mass.
- Vehicle combinations of more than one motor vehicle and one trailer of any type (FHWA classes 11, 12, 13) are not permitted in EU legislation (except in the case of special purpose vehicles).

The service and emergency braking performance requirements defined in FMVSS 121 depend upon the type of vehicle and road speed, and are specified in terms of stopping distance (FMVSS 121, Table 2). The control forces to achieve these are not defined. The calculated approximate average decelerations from these values (which show slight variations depending on the vehicle road speed) are summarized in Table 8.9.

Table 8.9: Service and Emergency Braking Performance Requirements in Terms of Calculated Average Deceleration from Table 2 of FMVSS 121 (US FMVSS 121)

	Calculated (Approximate) Average Deceleration (m/s^2)	
Type of Vehicle	Service Braking	Emergency Braking
Loaded and unloaded buses	4.2	1.9
Loaded single-unit trucks	3.8	1.9
Loaded tractors with two axles, or with three axles and GVWR $\leq$ 31.8 tonnes, or with four or more axles and GVWR $\leq$ 38.6 tonnes	4.7	1.9
Loaded tractors with three axles and GVWR $>$ 31.8 tonnes or with four or more axles and GVWR $>$ 38.6 tonnes	3.8	1.9
Unloaded single-unit trucks	3.5	1.9
Unloaded tractors (solo)	3.5	1.6

There are several functions for commercial vehicle braking systems that are defined in FMVSS 121 but are not defined in UN Regulation 13, e.g. the preparation of brakes prior to testing, and trailer braking only (not permitted in Regulation 13). There are more functions that are defined in UN Regulation 13 but not in FMVSS 121, e.g.:

- Specific fade tests for vehicles (FMVSS defines less stringent dynamometer procedures)
- Towing vehicle and trailer compatibility

- Wheel lock (prescribed braking performance must be achieved without wheel lock although directly controlled wheels may lock below 15 km/h and for brief periods above this speed)
- Split-m stability
- Vehicle stability control
- AEBS.

UN Regulation 90

UN Regulation 90 (UNECE, 2012) relates to the approval of replacement brake lining assemblies, drum brake linings and rotors (discs and drums). It was introduced in 1995 to control the manufacture, sale, distribution and installation of replacement brake pad assemblies and lined shoe assemblies, and sets minimum performance standards for replacement brake rotors and stators for vehicles of categories M, N and O. With the exception of replacement drum brake linings (i.e. linings without the metal shoe) for vehicles of categories M3, N2, N3, O3 and O4, brake lining materials alone (i.e. not part of a stator assembly) are not approved.

Complex Electronic Vehicle Control Systems

The incorporation of complex electronic vehicle control systems into road vehicle braking systems started with ABS and has been extended to electronic brake control (EBS) and vehicle stability control (VSC or ESC) e see Chapter 11. Automatic brake applications are defined by two functions: automatically commanded braking (the main purpose being to decelerate rather than to stabilize the vehicle) and selective braking (the main purpose being to stabilize rather than to decelerate the vehicle).

Electronic Stability Control (ESC) systems are explained in Chapter 11, and apply selective braking with the main purpose of stabilizing the vehicle. Under UN Regulation 13H, category M1 and N1 vehicles must be fitted with an ESC system that meets the functional and performance requirements as measured by prescribed test procedures. These include a ‘sine with dwell test’, which defines a steering pattern of a sine wave at 0.7 Hz frequency with a 500 ms delay beginning at the second peak amplitude, as shown in Figure 8.3.

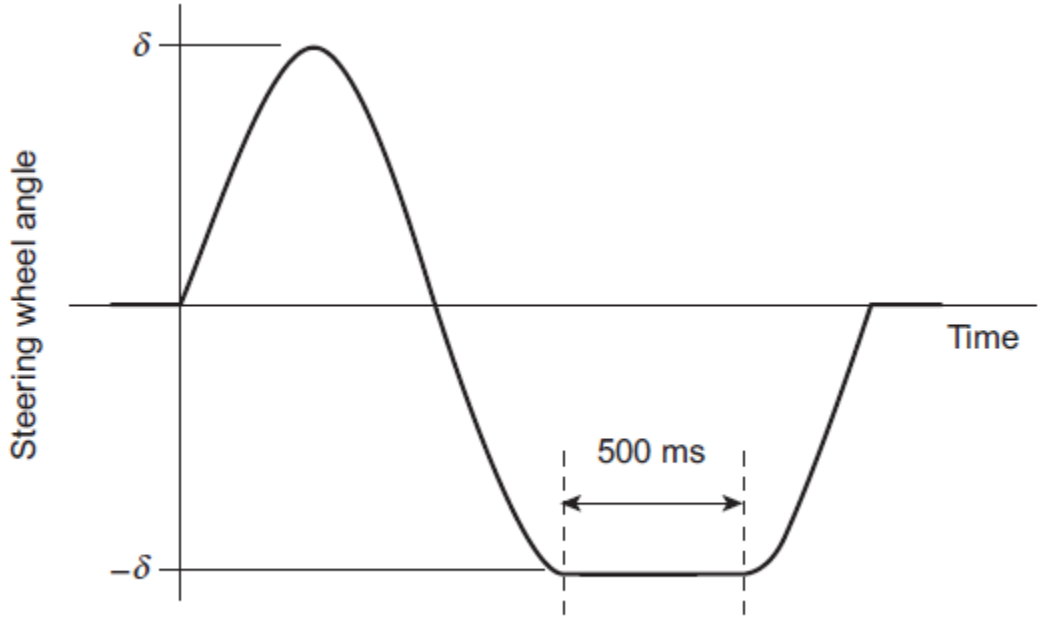

Figure 8.3: Sine with Dwell Test for ESC (UN Regulation 13H Annex 9 (UN, Feb 2014)).

For vehicles of categories other than M_1 and N_1, the GSR through UN Regulation 13 makes ESC mandatory for type approval and thus for registration, sale and entry into service of new vehicles (see Table 8.1).

Table 8.10: Dynamic Manoeuvres to Demonstrate the Vehicle Stability Function for Commercial Vehicles (UN Regulation 13 Annex 21 (UNECE, March 2014))

Directional Control	Rollover Control
Reducing radius test	Steady state circular test
Step steer input test	J-turn
Sine with dwell	
J-turn	
μ_t-split single lane change	
Double lane change	
Reversed steering test or 'fish hook' test	
Asymmetrical one period sine steer or pulse steer input test	

A vehicle stability function can be tested and evaluated in terms of a ‘vehicle framework’, covering for example:

- Trailer type (semi-trailer, center-axle trailer, full trailer), axle configuration, steering axles, lift axles, suspension type, wheelbase, track and wheel type.
- Braking system, anti-lock braking system configuration and foundation brake type.
- Vehicle stability function components including sensors, controllers and modulators

In order to meet this requirement a motor vehicle with an electric brake control transmission might be fitted with a ‘wake-up’ function activated by applying the brake pedal. Other requirements include:

- A control transmission failure must be indicated to the driver by a warning signal; a red warning signal is used to indicate when the prescribed service braking performance (attained without wheel lock) has not been reached.
- A red warning signal is required if excessive voltage drop of the battery is detected.
- A red warning signal is also required in the event of failure in a trailer braking system, failures due to insufficient energy and/or service brake performance.
- A test must be included to verify that the battery has enough energy capacity by requiring a given number of full brake applications.

For commercial vehicles the full actuation of the trailer brakes must remain ensured in the event of a failure in the electric control transmission of the service braking system of a towing vehicle equipped with an electric control line. This requirement is more stringent than for a towing vehicle with conventional air actuation, where in the case of a circuit failure only partial actuation of the trailer brakes is required. The vehicle manufacturer has two options to show a 'red signal failure' of the trailer on the dashboard:

- Two lamps option: red (towing vehicle signal) and yellow (trailer signal).
- One lamp option: separate red warning signal (to specifically indicate trailer faults that require a red signal).

because of the complexity of the technology, two levels of approval have been defined as summarized in Table 8.11.

Table 8.11: Two Level Approvals for Category M_2, M_3, N_2 and N_3 Vehicles with AEBS (Appendix 1 of Annex II to EC Regulation 347/2012) (see Table 8.1 for Implementation Dates Under the GSR)

	Level 1 Approval	Level 2 Approval
Scope	Vehicles of categories M_2 and M_3, and types of category N_2 vehicle with a maximum mass exceeding 8 tonnes, provided that these types of vehicle are equipped with pneumatic or air-over-hydraulic braking systems and with pneumatic rear axle suspension systems	Level 1 vehicles plus vehicles with hydraulic braking systems and non-pneumatic rear axle suspension systems. Will also include category M_2 and N_2 types of vehicle with a maximum mass not exceeding 8 tonnes
Speed reduction of subject vehicle	Not less than 10 km/h	Not less than 20 km/h
Target speed	32 ± 2 km/h	12 ± 2 km/h

Brake Assist Systems

Brake Assist Systems (BAS) were developed to improve the braking performance of drivers of M_1 vehicles in emergency situations. Many drivers do not make effective use of the full capability of the braking system in such circumstances, they do not apply sufficient pedal force to reach maximum braking during an emergency stop and they do not act quickly enough. The BAS detects when a driver might be intending to make an emergency stop and will reduce the brake actuation time and boost the brake pedal effort, e.g. by actuating the ABS pump.

Accordingly UN Regulation 13H Supplement 9 was mandated for M1 category vehicles from November 2011 for new types and will be from November 2014 for existing types. UN Regulation 13H defines two different BAS categories:

- Category A Brake Assist System. A system that detects an emergency braking condition based primarily* on the brake pedal force applied by the driver, e.g. it may be triggered at pedal force actuation rate of approximately 550 N/s.
- Category B Brake Assist System. A system that detects an emergency braking condition based primarily* on the brake pedal speed applied by the driver, e.g. it may detect an emergency braking condition triggered at a pedal speed 300 mm/s.

(*As declared by the vehicle manufacturer.)

A conventional dual-rate brake booster can also be capable of meeting the definition of a BAS and especially for heavier vehicles a dual-rate brake booster can also qualify (under the Regulations) as an acceptable category A BAS if its pedal force characteristic is similar to that shown in Figure 8.4.

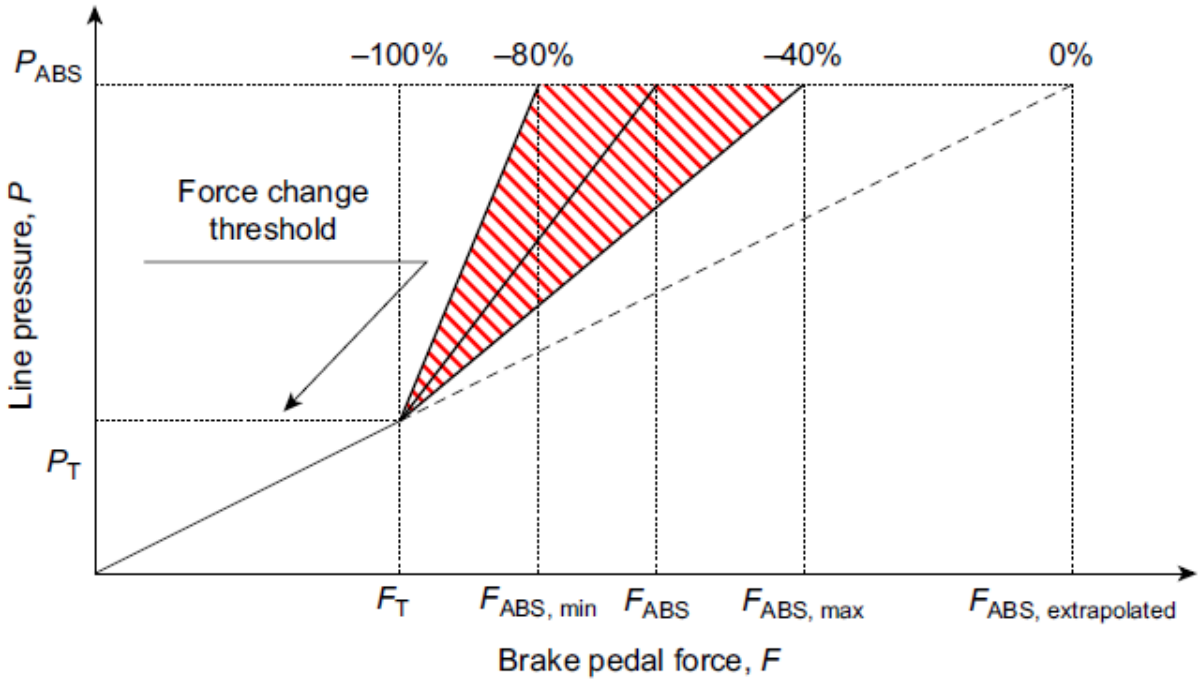

Figure 8.4: Pedal force Characteristic for Category A BAS (UN Regulation 13H Annex 9 (UN, Feb 2014)).

Regenerative Braking Systems

As described in Chapter 11, vehicles that incorporate regenerative braking are equipped with devices to convert the vehicle's kinetic energy into a form of energy that can be stored onboard and reused. Typically such vehicles use a generator or pump to convert kinetic energy into another form of energy and store it in batteries, ultracapacitors, hydraulic reservoirs, flywheels, etc.

In the UN Regulations 13 and 13H, 'electric regenerative braking' means a braking system which, during deceleration, provides for the conversion of vehicle kinetic energy into electrical energy. 'Electric regenerative braking control' means a device that modulates the action of the electric regenerative braking system. Electric regenerative braking systems are separated into two categories:

- Category A: an electric regenerative braking system that is not part of the service braking system.
- Category B: an electric regenerative braking system that is part of the service braking system.

The contribution from other sources of braking may also be phased to allow the regenerative braking system alone to be utilized, provided that both of the following conditions are met:

- Intrinsic variations in the torque output of the electrical regenerative braking system, e.g. from the state of charge (SoC) of the traction batteries, are automatically compensated by a suitably graduated reduction of the phasing setting, i.e. the friction braking is introduced to make up for any reduction in the regenerative braking torque.
- The braking distribution requirements on low-adhesion roads are met or the ABS operates to prevent wheel lock at all times.

The precise design of the phasing should permit the majority of normal braking applications to be achieved by regenerative braking alone; this is typically achieved by controlling regenerative braking alone up to a preset level of vehicle retardation since this braking is usually applied through a single drive axle. Figure 8.5 illustrates the concepts.

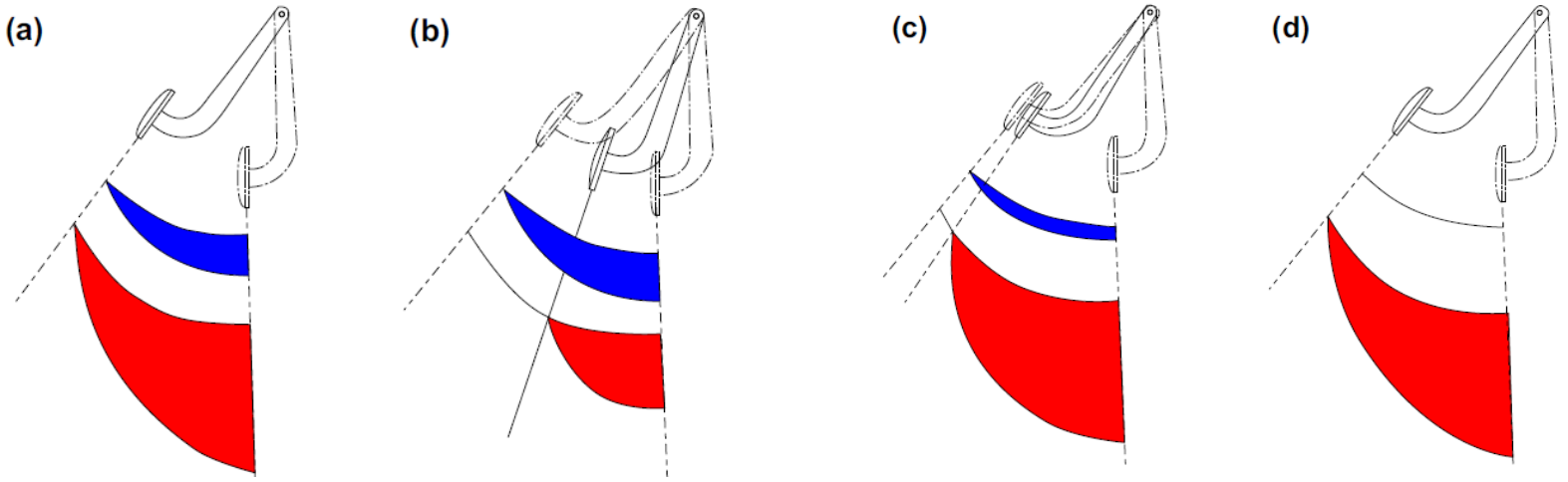

Figure 8.5: Examples of Phased Movement for Electrical Regenerative Brake Actuation Controls (Gaupp, 2013).

(a) Non-phased operation. (b) Maximum phased operation. (c) Intermediate phased operation. (d) Zero phased with no regenerative braking.

Chapter nine

Brake Testing

Brake testing for road vehicles traditionally takes many forms, ranging from large fleet user trials of complete braking systems through the laboratory dynamometer testing of foundation brakes, to small sample component testing. However, the increase in the capability and sophistication of computer-based modelling and simulation over the last 20 years has improved the accuracy of predictive design analysis methods and has enabled many aspects of brake testing for design optimization and verification to be carried out in the form of 'virtual' testing.

Once a vehicle has been manufactured and sold, it passes into the customer domain, where the manufacturer has no control over how it is used but retains product liability in the event of a failure that can be attributed to any deficiency in the design or manufacturing process. If a suspected deficiency is found, experimental testing will be required to confirm or deny its existence and, if confirmed, containment actions and countermeasures would usually be verified experimentally as part of a structured procedure for failure mode investigation. Any form of testing is a costly activity, and experimental testing, especially that which involves whole vehicles, is particularly expensive so there should always be compelling and valid purposes for brake testing.

These could typically include:

- Design optimization, e.g. computer-based virtual 'experiments' to iterate to an efficient and optimal design.
- Verification of system and component performance, including durability and reliability.
- Verification of vehicle braking performance for the vehicle manufacturer's and the legislative bodies' requirements, principally deceleration and stability, efficiency, actuation forces, system part-fail, etc., but also including durability and reliability.
- Measurement of material properties for brake design.

- Characterization of friction material tribological properties for (a) material formulation and development purposes, and (b) brake design purposes.
- Investigation of vehicle braking characteristics for failure mode investigation and countermeasure development.

Instrumentation and Data Acquisition in Experimental Brake Testing

Parameters that can be measured in experimental brake testing include:

- Temperature
- Deceleration
- Torque
- Force
- Pressure
- Displacement and distance
- Vibration frequency, amplitude and phase.

Temperature

Because friction brakes work by converting kinetic energy into heat energy, the single most important parameter to measure and control in experimental brake testing is temperature. As explained in Chapter 7, the effect of the heat generated is to create temperature distributions in the foundation brake, and because of the effect of the heat on the friction and wear performance of the friction material and the contact relationship between the rotor and stator components, changes in the temperature distribution and magnitude can dominate the measured brake performance.

A temperature difference across the contact will always exist, but careful experimental technique can minimize this. Usually the force holding the skid against the rotor surface is adjusted until the temperature measured is the same whether the rotor is moving or stationary; too low contact force will indicate a low temperature and too much contact force will cause the skid to generate frictional heat, which will indicate a high temperature during operation. Examples of skids are illustrated in Figure 9.1.

A comparison of temperatures measured by two different types of thermocouple and skid is shown in Figure 9.1(c); the older 'bare wire' thermocouple unit with the copper button skid (Figure 9.1(a)) is less responsive than the modern sheathed thermocouple unit (Figure 9.1(b)) because of its higher thermal mass.

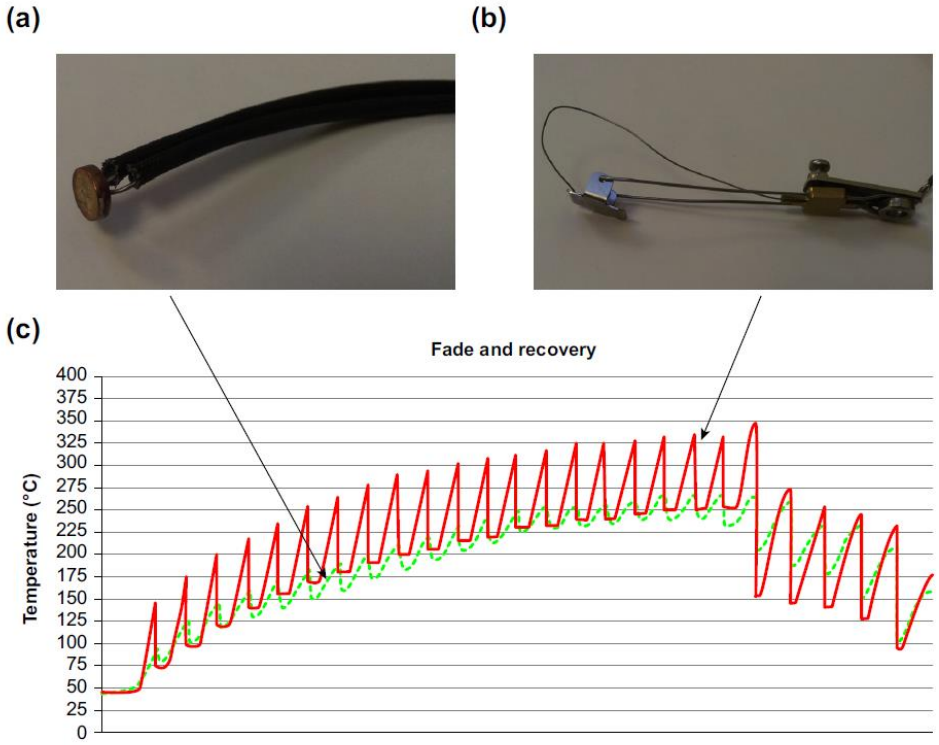

Figure 9.1: Comparative Performance of Two Types of Rubbing Thermocouple (McLellan, 2012).
(a) Bare wire rubbing thermocouple with copper button. (b) Sheathed rubbing thermocouple with steel skid. (c) Comparative performance of the two types of rubbing thermocouple.

Deceleration

Since the required function of a vehicle braking system is deceleration, its measurement is very important in the experimental testing of vehicle brakes and braking systems. By recording the instantaneous deceleration as a time series, variation during a brake application can be examined so that in-stop characteristics can be quantified. Traditional methods of measuring vehicle deceleration included portable decelerometers, which were mounted inside the vehicle and read by an observer.

Torque

There are two methods used to measure the torque generated by a brake, namely a torque sensor and a 'torque arm'. The former is fitted 'in-line' with the shaft or component that is transmitting the torque, and works by sensing a torque-sensitive parameter such as the 'twist' of the shaft or the relative angular displacement of the sensing elements of the device. Such devices are able to sense dynamic torque up to frequencies in excess of 1 kHz, and may be used on laboratory equipment such as dynamometers or on actual vehicles.

Where experimental determination of individual brake performance or braking balance between individual wheels on full vehicles is required, torque sensors in the form of ‘torque wheels’ are used. These are road wheels fitted with strain gauges or similar sensing devices, which provide a direct indication of wheel torque on a vehicle on a test track; torque wheels are generally not considered to be safe for use on public roads.

Force

Many different types of load cells and other force transducers are available for use in experimental brake testing. On vehicles the measurement of the actuation force at the brake is avoided if possible because of the high temperatures, restricted space and hostile environment. It is used only where necessary, e.g. to confirm actuation system function and efficiency, and instead brake actuation force is usually calculated from the actuation pressure, which is easier to measure accurately.

A recent development in the controlled measurement of driver effort is the ‘robot driver’, which is an actuation device that can be fitted to the driver’s seat and connected to the brake pedal via an actuation rod, while still allowing a human driver to operate the vehicle. This device can achieve very accurate programmable force applications to the brake pedal at exactly the correct angle of force to represent the driver’s foot and leg actuation.

Pressure

Brake actuation pressure downstream of all valves, boosters, ABS pump, etc., whether pneumatic or hydraulic, is a fundamentally important parameter that must be measured accurately in experimental brake testing. A traditional Bourdon tube pressure gauge can be used to provide an immediate indication of line pressure, but the gauge and the associated piping does affect the actuation characteristics, especially in hydraulic system fluid consumption and pedal travel, and Bourdon tube pressure gauges should not be used whenpedal feel assessment is required.

Displacement and Distance

Displacement measurement is required to investigate and confirm system actuation. Linear variable displacement transducers (LVDT) are used to measure large displacements such as brake pedal travel or pneumatic actuator displacement, and an alternative is a ‘string potentiometer’ where a linear displacement is converted to a rotary displacement for measurement and can be easier to fit into confined spaces. Very small displacements need to be measured to assess circumferential variations in rotational precision, e.g. the concentricity and ‘ovalising’ of brake drums and ‘coning’, ‘runout’’ and thickness variation of brake discs.

Vibration Frequency, Amplitude and Phase

Experimental techniques and instrumentation for the measurement of noise and vibration represent a very specialized area of activity, which is covered in more detail in Chapter 10. A portable ‘noise meter’ (which may actually measure sound pressure level) can be used to measure the frequency of specific noises and identify frequency components of complex waveforms. Noise can be recorded on a hand-held voice recorder for subsequent analysis, and both these are very useful during the experimental brake testing of a vehicle whether on a test track or on the public road, since they are completely self-contained and do not require installation on the vehicle.

The fundamental performance of a friction braking system for road vehicles is defined by the friction pair, which forms the core of the foundation brake. The lowest level of brake component that would normally be considered for experimental testing is included in the foundation brake package illustrated in the boundary diagram in Figure 9.2.

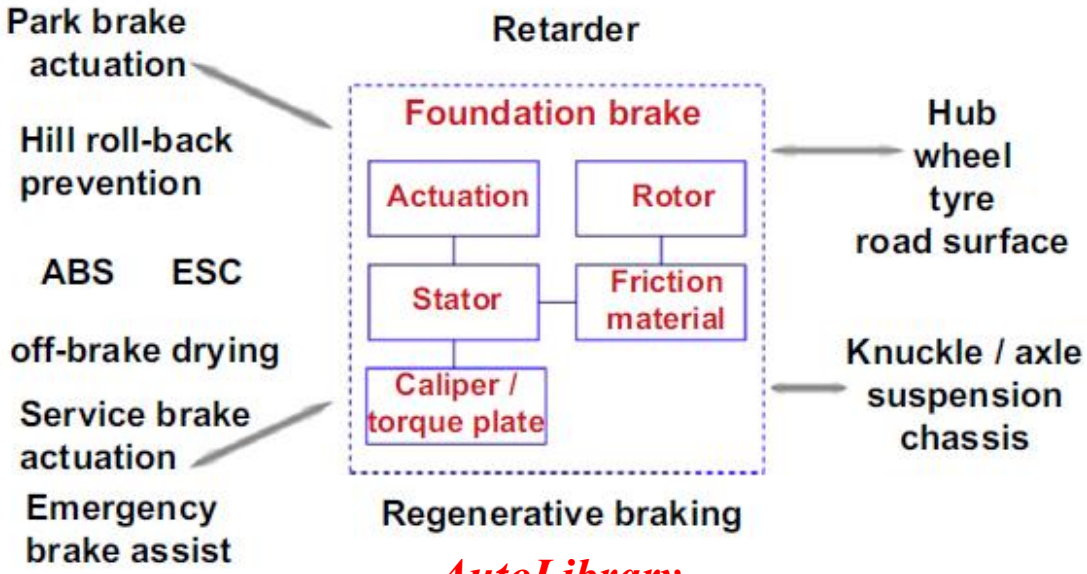

Figure 9.2: Foundation Brake Boundary Diagram (After McLellan, 2012).

The actuation force is applied to the stator as explained in Chapter 5. Outside the boundary are examples of other vehicle components and systems that interact with the foundation brake. Depending upon the purpose of the test, these components and systems may or may not need to be included. From the boundary diagram illustrated in Figure 9.2, a 'P-diagram' can be generated showing the driver's viewpoint as illustrated in Figure 9.3, which helps to identify some of the issues that might provide reasons for brake testing.

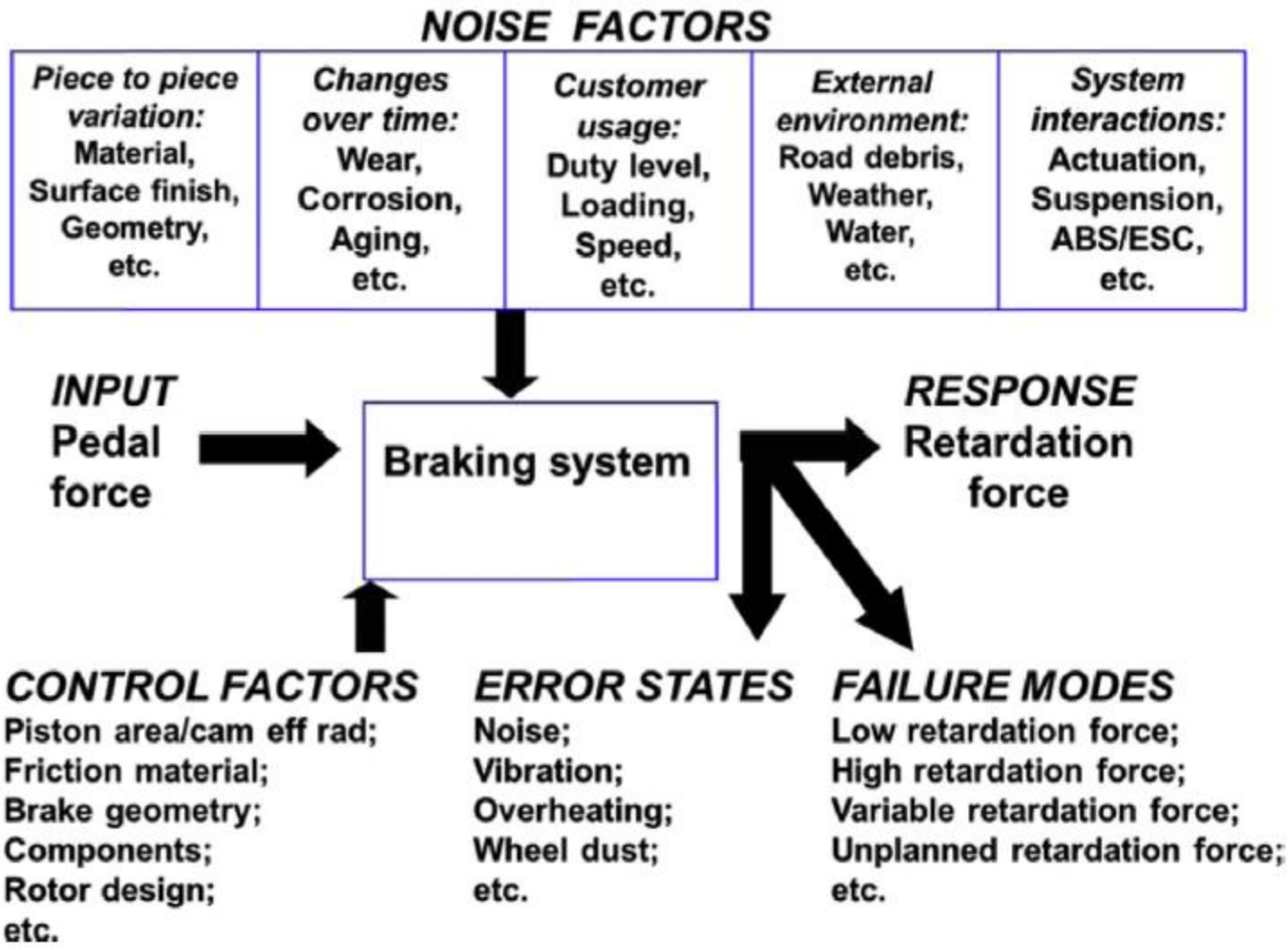

Figure 9.3: Braking System P-Diagram (After McLellan, 2012).

Test Vehicles, Dynamometers and Rigs

There are many options for testing brakes and braking systems, and a wide range of machines, rigs and devices exists for the experimental testing of brakes, from full vehicles to ‘scale’ test machines. A complete vehicle can be instrumented with sensors as described above, fitted with data acquisition equipment, and driven on a test track to undertake specific test procedures, or on public roads as ‘field testing’ for general ‘real-world’ data gathering. The very large capability of modern data acquisition systems for on-board data collection, processing and storage means that data from entire journeys of several hours’ duration can be recorded for subsequent analysis.

The most widely used laboratory-based machine in experimental brake testing is the inertia dynamometer. Shaft-type inertia brake dynamometers (see Figure 9.4) are designed so that the brake rotor is attached to a driven shaft (usually by an electric motor) on which flywheels are mounted to simulate the appropriate part of the vehicle inertia and kinetic energy.

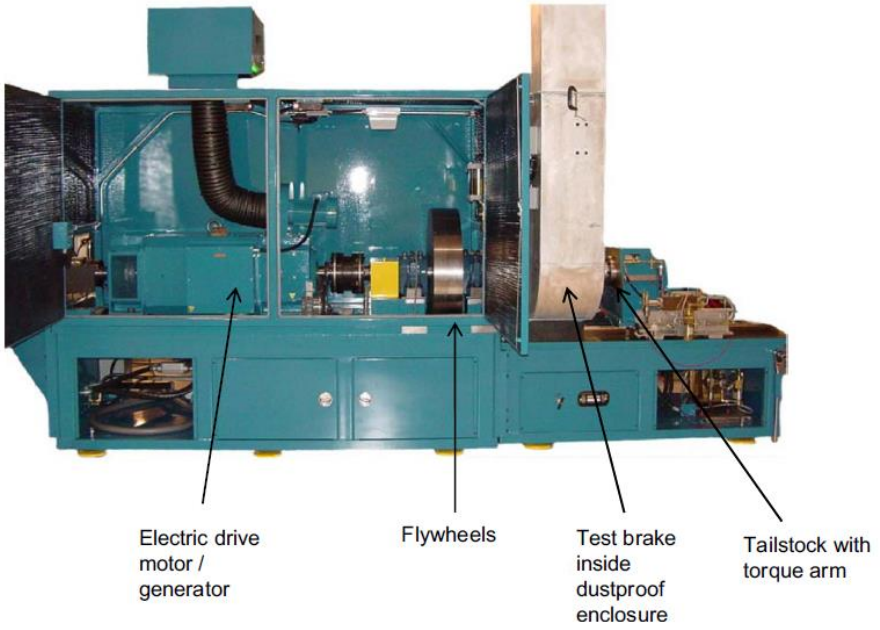

Figure 9.4: Inertia Dynamometer for Brake Testing (Courtesy of Link Engineering).

An example of a purpose-designed small-sample scale friction research test rig is shown in Figure 9.5.

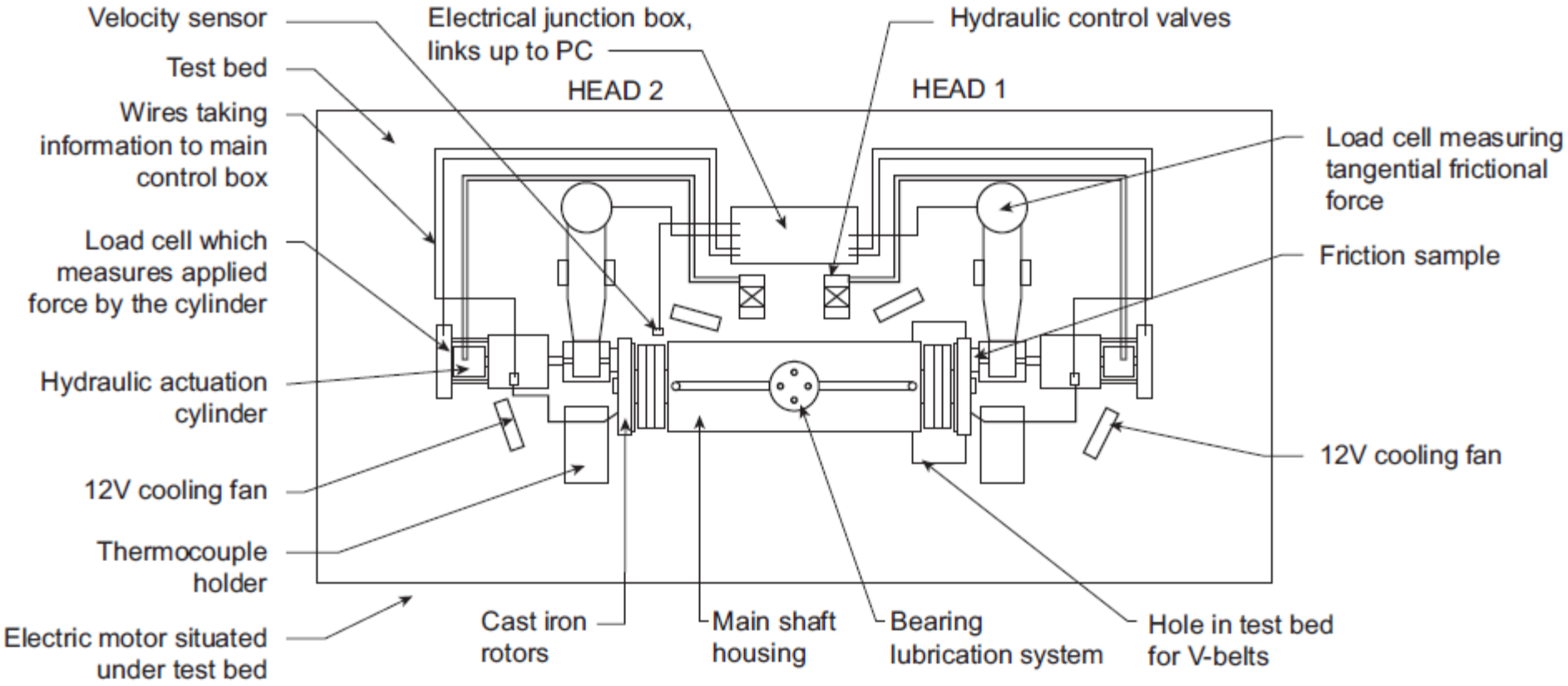

Figure 9.5: Purpose-Designed Small-Sample Scale Friction Research Test Rig.

This machine has two working heads, each comprising a 125 mm diameter disc manufactured from the desired rotor material and a sector-shaped specimen of approximately 625 mm^2 (1 square inch). The actuation force is applied via a hydraulic piston and measured by an electronic load cell. Torque is measured by a torque arm arrangement with another electronic load cell. The machine is fully computer controlled and can be fitted with an environmental chamber for ambient temperature control. It can be used for both friction material performance mapping and wear mapping at power densities up to 5 W/mm^2.

Brake Experimental Test Procedures

Preparation, Bedding and Burnishing

With all brake experimental testing it is essential to take account of the preparation and conditioning history of the brake system and friction pair before critical measurements are taken. Unless the purpose of the test is to evaluate a brake installation in its operational condition from new, consistency and repeatability of results that are representative of the stabilized performance of brake friction pairs will only be obtained if the friction pair is carefully prepared through a process of bedding and burnishing (see Chapter 2).

The friction surfaces of brake discs or drums can be prepared for bedding/burnishing before performance testing as follows:

1. Clean the rotor friction surface with a degreasing agent.
2. Use medium (grade 60) emery paper to lightly abrade the surface in a random fashion.
3. Wipe with a clean lint-free cloth to remove dust.
4. Clean again with a degreasing agent.
5. Wipe again with a clean lint-free cloth to remove all traces of preparation.

Braking Performance

‘Braking performance’ (sometimes known as ‘effectiveness’) experimental testing may take many forms, including noise and vibration, water recovery, salt recovery, ambient temperature, humidity, static/parking, partial system fail and vehicle compatibility/overload. It is essential to determine the purpose of a braking performance test before a suitable test procedure can be selected or designed.

ABS/ESC is usually disabled for basic brake performance testing. A basic brake performance test procedure is outlined below:

1. Commence each braking event only when the initial temperature of the brake (as indicated by a rubbing thermocouple or an embedded thermocouple as explained earlier) has reached the specified ‘start of stop’ temperature, e.g. 100C. If the indicated temperature is too low, drive while gently applying the brakes to increase the temperature to the set value.

2. Drive the vehicle at constant road speed 5e10 km/h above the set speed, select neutral gear and coast until the set speed is reached, and then apply the brake to achieve the required deceleration or pressure.

3. When the vehicle comes to rest (or nearly to rest), immediately release the brake actuation pressure and accelerate gently to a predefined road speed to facilitate brake

cooling.

4. The vehicle should then be driven at constant speed without the use of the brakes until the indicated temperature has declined to reach the specified temperature.

5. Repeat the procedure (steps 1e4) at different settings (speed, temperature, deceleration, actuation pressure) until the test is complete.

Some typical ‘raw data’ test results are shown in Figures 9.6 and 9.7 from a basic brake performance test on a small car with hydraulically actuated brakes.

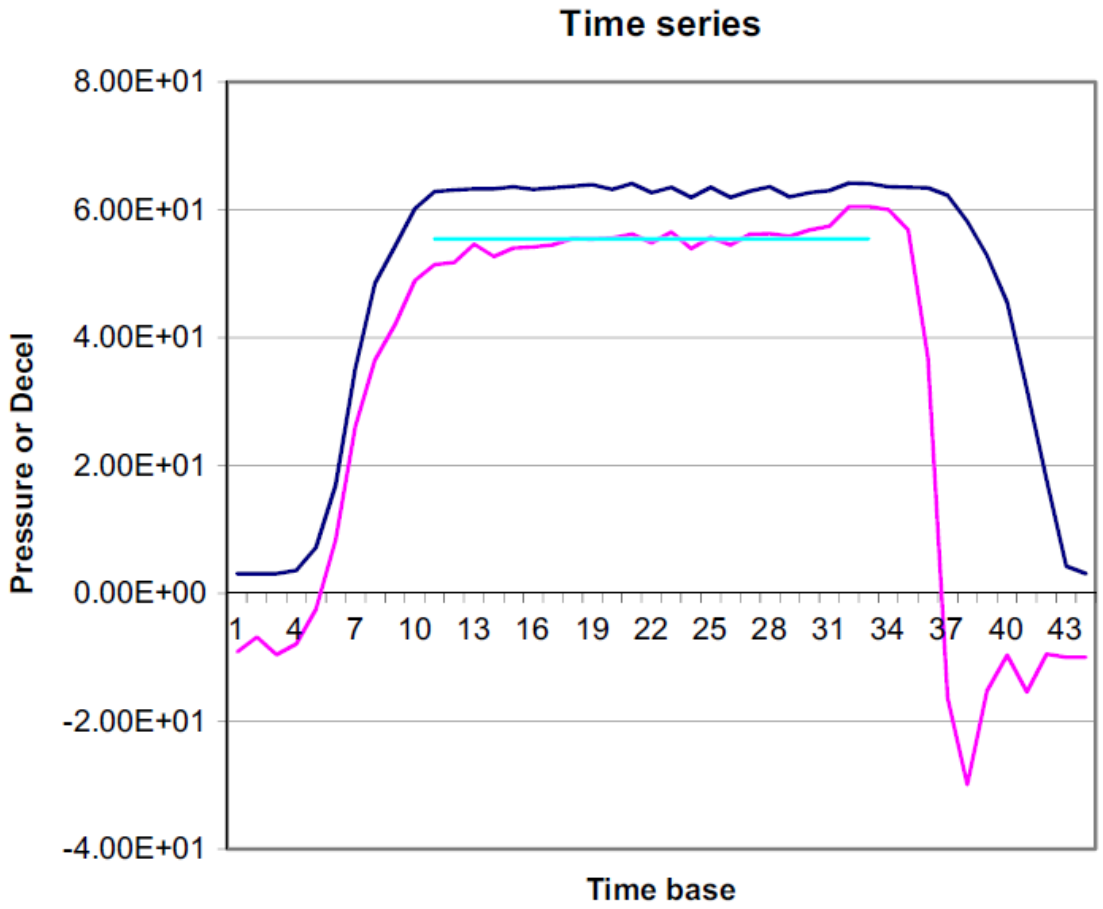

Figure 9.6: Example of Brake Pressure and Vehicle Deceleration Data vs. Time.

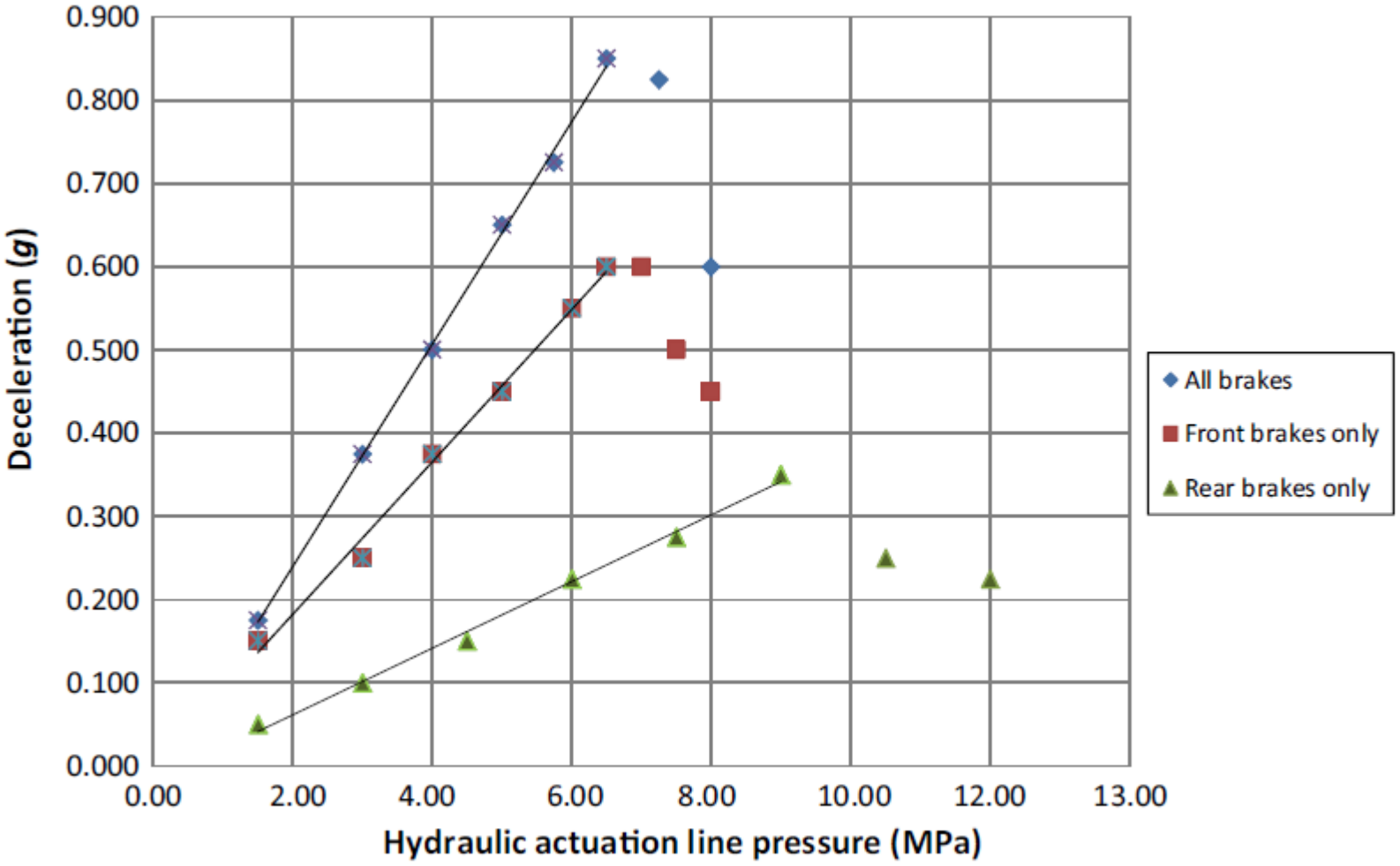

Figure 9.7: Brake Performance Graph (Data from Marshall, 2008).

Actuation pressure and deceleration are plotted as time series in Figure 9.6, from which the points below are highlighted:

1. There is a slight zero offset for both the pressure and the deceleration transducers, which would normally be corrected in the data processing.

2. Both the deceleration and the pressure traces show an initial ‘ramp-up’ section and a final ‘ramp-down’ section. The deceleration reaches zero before the actuation pressure (brake pedal) is released, and the deceleration indicates a reversal after the vehicle has come to rest. This is caused by torque reversals on the wheels and is the main reason why some testers only bring the vehicle ‘nearly to rest’.

3. The purpose of this particular test was to hold the deceleration constant and evaluate the ‘in-stop’ performance of the friction pair from the variation in actuation pressure. An estimate of the average deceleration over the ‘steady’ part of the brake application is indicated, which has been calculated as the arithmetic mean over the central portion. The selection of this ‘central portion’ can be difficult, especially if there is substantial in-stop variation caused either by an inexperienced test driver or by variable friction. There are various definitions of ‘trigger’ points for the start and end of averaging, which can include for the start pressure/deceleration above zero, 95% of fully developed deceleration, and for the end road speed within 5% of start speed, deceleration reduces to 90% of fully developed deceleration, or actuation pressure is reduced to zero. None of these is foolproof, but consistency in the data helps all of them to be utilized effectively if required

Figure 9.8 highlights the effect of threshold pressure and rolling resistance around the origin of the graph

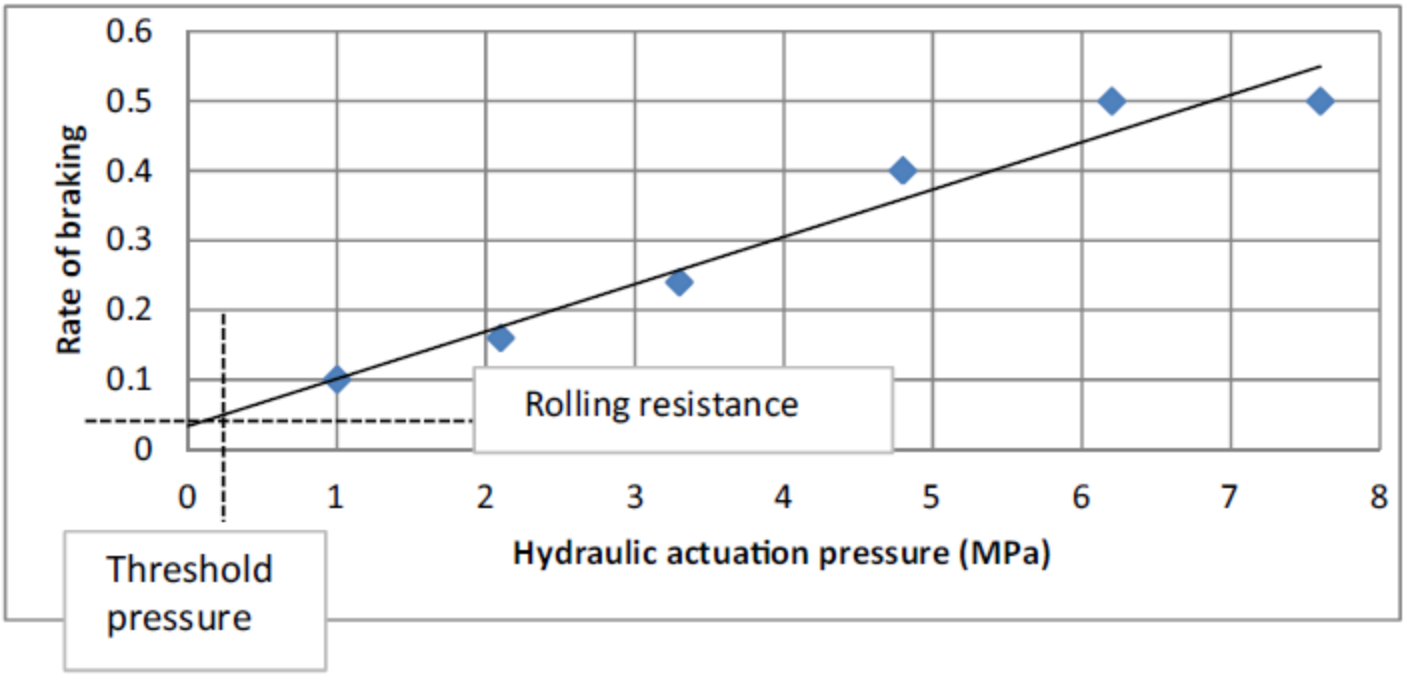

Figure 9.8: Brake Performance Graph Highlighting Threshold Pressure and Rolling Resistance at The Origin.

Rolling resistance generates deceleration without actuation pressure, which is represented on the ordinate, while threshold pressure is the offset on the abscissa (actuation pressure but no deceleration). The straight-line fit of brake performance data should not be expected to pass through the origin and a common mistake in data analysis for system verification is to use individual data points or a line fit forced through the origin. This will give incorrect results and waste a lot of time chasing reasons for an apparently declining brake factor with actuation pressure!

Wear Test Procedures

The ultimate test of wear and durability of a road vehicle braking system is through ‘normal’ service operation on actual vehicles driven by their owners or users. As previously explained, this approach is generally unacceptable because of the time and cost so accelerated (shorter duration) tests must be adopted to replicate real-world usage to estimate the likely wear life of the friction pair at the design stage, if possible using laboratory-based rather than vehicle-based methods.

Standardized Test Procedures

Many different brake performance tests following standardized test procedures can be carried out on vehicles and on dynamometers; an excellent overview is given by Agudelo and Ferro (2005), who summaries the publicly available test procedures used by the automotive industry worldwide to assess brake and vehicle braking performance. These are:

- Federal Motor Vehicle Safety Standards (FMVSS) and the National Highway Traffic Safety Administration (NHTSA) Regulations
- Standards or Recommended Practices from the Society of Automotive Engineers (SAE)
- International Standards from the International Organization for Standardization (ISO)
- Regulations from the United Nations Economic Commission for Europe (UNECE).

An example of measured temperature time during a fade test is shown in Figure 9.9 (McLellan, 2012).

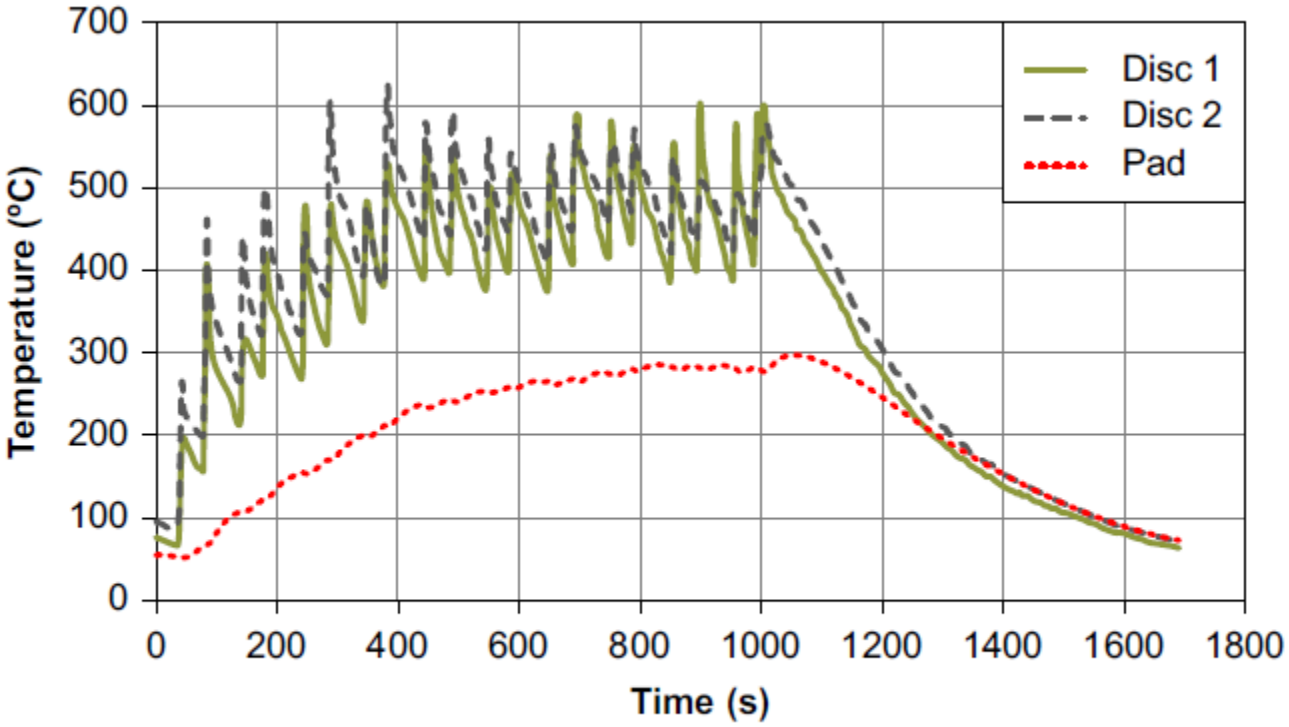

Figure 9.9: Example of Temperature–Time During a Fade Test (McLellan, 2012).

Brake Test Data Interpretation and Analysis

The universal use of computer-based data acquisition systems in brake experimental testing provides very large amounts of data, which requires close and careful analysis. Since the most critical wearing component in a conventional braking system is the friction material, which is a highly complex and constantly changing composite, established experimental procedures that recognize this inherent variation in performance must always be followed. Fundamentally this means understanding the statistical basis of variation, and testing a large enough number of samples from a suitable population.

Chapter ten

Brake Noise and Judder

Noise and judder from the braking systems of road vehicles are of major concern to manufacturers and users. Audible noise causes environmental pollution, especially in urban areas, and is regarded by vehicle owners and users as symptomatic of a fault in the braking system, i.e. an ‘error state’ (see Figure 9.3). Whilst judder may also create audible noise, the main problem from brake judder is the mechanical vibration that is sensed by the vehicle users and is also regarded as a fault.

Within the broad definitions of brake noise and judder, there are many sub-categories of brake noise and judder, which were defined by North (1976), and subsequently by Lang and Smales (1983) and several more researchers. In ascending order of frequency some of the original sub-categories of brake noise are listed below:

- Judder is a speed-related non-resonant vibration with a low frequency (typically around 10 Hz), which is a multiple of the rotor rotational speed. It creates wheel and brake torsional vibration about the suspension or chassis, and vibration in the actuation system that can be transmitted back to the driver, e.g. via the brake pedal on passenger cars with hydraulic braking systems.

The actual judder frequency is a multiple of the rotor speed and becomes intrusive when the frequency coincides with resonant frequencies in the vehicle's suspension, steering or structure. There are two distinct categories of brake judder, namely cold judder and hot judder (sometimes termed 'high-speed' judder).

Cold judder is associated with the mechanical effects of nonuniformity of the rotor rubbing path for which there can be several causes, e.g. noncircular or eccentric brake drums, runout or swash of brake discs, disc thickness variation (DTV) caused by off-brake wear, or circumferential friction variation, which might occur with uneven coatings or transfer films on the rotor friction surfaces.

Hot judder is also a speed-related non-resonant vibration usually of a higher frequency (typically 200 Hz) because of the greater circumferential non-uniformity of the rotor surface, which is caused by thermomechanical interactions between the friction pair.

• Groan is a semi-resonant vibration, typically <100 Hz, which is most prevalent at lower speeds and is usually considered to be caused by 'stick-slip' arising from a negative $\mu - v$ characteristic (i.e. μ decreases with increasing sliding speed). Groan usually displays a vibration mode of rigid body axial rotation of the disc brake caliper and the adjacent suspension components.

- Hum is a resonant sinusoidal vibration that generally occurs under ‘off-brake’ conditions, is independent of rotor speed, and occurs at frequencies between 100 and 400 Hz. It is associated with disc brakes that have a low caliper mounting torsional stiffness.
- Moan is a higher frequency vibration often associated with disc brake caliper whole body movement, which usually occurs at frequencies of 600e700 Hz.
- ‘Low-frequency’ squeal is the most intrusive type of brake noise that occurs with disc and drum brakes and usually has a frequency between 1 and 4 kHz, which is in the part of the audible spectrum to which the human ear is particularly sensitive.

- High-frequency squeak in disc brakes involves higher order disc vibrational modes in the frequency range 4e15 kHz, which have typically five to 10 nodal diameters. The nodal spacing is therefore less than the pad length and the squeak natural frequencies are now higher than the fundamental pad bending mode. Squeak is a major problem for single-piston sliding calipers with high aspect ratio pads.
- Squelch in disc brakes is an amplitude modulated version of squeak noise with a ‘beating’ effect caused by general asymmetry in the disc.
- Wire brush is a non-resonant noise at a very high frequency (up to 20 kHz) with random amplitude modulation, and is often heard immediately prior to the development of a true unstable squeak.

This chapter explains the features and principles of brake noise and judder, summarizes some of the approaches to modelling and analyzing the physical mechanisms, and suggests best practice design rules to minimize brake noise and judder propensity. In this context ‘noise propensity’ and/or ‘judder propensity’ are terms used to describe the likelihood that a given brake design will suffer from noise or judder problems.

For example, it is suggested from published work and experience that the following approaches can be beneficial in influencing brake noise propensity; however, some seem to conflict with others.

- Practical methods for reducing brake noise propensity depend on the individual nature of the noise, e.g. frequency, likely instability mechanism and the type of brake involved.
- Brake noise propensity tends to increase with coefficient of friction (m), so the noise propensity of a particular brake may be reduced by the substitution of a lower m friction material.
- Brake noise propensity tends to increase on cooling after heavy-duty and/or repeated brake applications.

- The contact between the friction material and the rotor, e.g. heel and toe contact on the leading shoe of drum brakes, and leading contact on disc brake pads, often increases noise propensity:

- Drum brake noise can often be reduced by reducing the leading shoe factor, by grinding the lining to give crown contact, or shortening or chamfering the linings.

- Disc brake squeal can often be eliminated by moving the contact between the piston and the pad backplate towards the trailing end, e.g. by a shim.

- In disc brake calipers with two or more actuation pistons, stability can be increased (and noise propensity reduced) by utilizing piston seal damping in the pad rotational mode, e.g. using shims to encourage contact between the pistons and the backplate extremities.

- Squeal in disc brakes that have leading and trailing abutments can be reduced by locating the abutment at the leading end.

- Decoupling the piston and pad motions in the tangential direction by grease or a low friction coating and using the piston as a mass damper can reduce squeal noise propensity.

- Damping of a brake drum can be increased by fitting a band lined with friction material around its mouth, although the band tension is critical, and allowance must be made for drum expansion and centrifugal effects. The addition of friction damping to the rotor with a loose peripheral ring may similarly help to reduce brake noise propensity, but all such devices are adversely affected by corrosion in use.

• Damping the pad bending mode, e.g. by removing slots in the friction material, incorporating a high loss interlayer between the friction material and backplate, or applying a damping layer to the back of the pad, can reduce certain types of brake noise propensity. A thin viscoelastic layer between the backplate and a separate steel shim helps by converting small bending strains into large shear strains in the viscoelastic layer.

Brake Noise Review

There is an enormous body of knowledge associated with brake noise that has been developed over the last 60 years, and gaining an understanding of the significant advances is a daunting prospect. As a starting point, some conclusions and observations from four significant reviews of brake noise published in the last 40 years are summarized here. These show a development of approach from understanding the nature and characteristic features of vibration associated with brake noise (frequencies, mode shapes), through lumped-parameter models, mathematical models, stability criteria, to modelling and simulation, all supported by increasingly sophisticated experimental measurement and research techniques such as laser holographic interferometry.

In (Nanticipation of this work, his review of published work on vibrations in braking systems orth, 1969) noted the characteristic features associated with drum brake squeal, which are listed below:

- ✓ The frequency of squeal is independent of the rubbing speed.
- ✓ Brake torque increases while the brake is squealing.
- ✓ Squeal tendency increases with increased actuation pressure.
- ✓ Drum vibration is ‘bell-like’ with six to 14 modes measured.
- ✓ Squeal is most likely to occur after high-temperature and high-pressure operation, which could be a friction interface contact effect or a recovery effect in the friction material.
- ✓ Squeal is most prevalent at temperatures below 100C.
- ✓ Squeal is most likely to occur when the brake linings have high m, e.g. with cold brake usage (North’s term was ‘early morning sharpness’).

For disc brakes, North noted the following:

- ✓ The disc vibrates with an even number of radial nodes, the spacing of which is widest at the position of the pads and approximately equal over the rest of the disc.
- ✓ The pads are positioned approximately on an antinode and vibrate with the disc.
- ✓ An increase in temperature causes a decrease in squeal frequency.
- ✓ Squeal frequency is independent of disc speed.
- ✓ Squeal is again most likely after high-temperature and high-pressure operation.
- ✓ Pad thickness has no effect on squeal frequency or the likelihood of squeal.
- ✓ Squeal is again likely as a result of high m (early morning sharpness).

The review of disc brake squeal by Kinkaid et al. (2003) presents a thorough analysis of a large number of significant publications covering every aspect of the brake noise problem, from which they summarized the conclusions relating to brake squeal listed below:

- A braking system can generate squeal noise at several distinct frequencies.
- Higher m and variation of m with speed and actuation pressure may all be associated with higher squeal noise propensity (the effect of any decreasing mespeed characteristic on squeal noise occurrence is still not agreed; see recent work by Eriksson et al. (2002) and Yuan (1995)).

- Pad/disc contact in a disc brake is important in squeal noise propensity.
- Vibration amplitudes during brake squeal noise occurrence are very small (microns).
- Knowledge of the modal characteristics of individual uncoupled disc brake system components does not necessarily indicate squeal noise propensity.
- Squeal noise is generated by coupled vibrations of a disc brake system.
- Squeal noise frequency is not necessarily close to any resonant frequency of the brake rotor.
- It is likely that the contributions of different brake components to squeal noise generation depend on the squeal noise frequency.

- Out-of-plane and in-plane vibrations of the brake disc are generated with brake squeal noise, and the coupling between them is important.
- The vibration of a squealing disc brake assembly rotating at constant speed may be a standing wave or a travelling wave, and if a travelling wave, its speed is not the same as the squeal noise frequency.
- During the generation of squeal noise, disc brake pads vibrate with various bending and torsional modes, and disc mode shapes are based on an even number of radial nodes.
- The amount of squeal noise increases when the natural frequencies of the pads, caliper and disc are close together.
- Detailed tribological phenomena, e.g. the size of 'contact plateaux' at the brake friction interface (Eriksson et al., 2002), may also contribute to the generation of brake squeal noise.

The review also considered methods to eliminate brake squeal noise. Some of these methods are often referred to as ‘fixes’, indicating that they are applied post-design, usually to solve brake noise problems that have occurred in the customer domain (the ‘field’). Commonly used fixes include:

- Grease or viscous layer between the pad backplates and caliper
- ‘Shims’ between the pad backplate and the actuation piston or mechanism
- Chamfers or slots in the brake pad material
- ‘Refreshing’ the disc friction surfaces, which may take the form of cleaning, lightly abrading or re-machining
- Lubrication of moving parts, e.g. the pin slides of a sliding caliper.

The Source of Brake Noise

Frictionally induced dynamic instabilities in the brake may be generated by asperity contact and the physical mechanisms of friction as introduced in Chapter 2, which in turn create time-varying frictional forces at the friction interface to act as the source function for brake noise. As previously explained, stick-slip or the μ -speed characteristic of the friction material was thought to contribute to the source instability of brake noise and although they can be the source of certain types of brake noise (e.g. groan) they are not the source of most types of brake noise, especially squeal.

If μ is assumed to decrease linearly with sliding velocity, the equations of motion of the pad will be as indicated in Equation (10.1), which can be rewritten in the form of Equation (10.2):

$$M\ddot{x} + c\dot{x} + kx = \mu_D P = [\mu_S - \alpha(V - \dot{x})]P \quad (10.1)$$

$$M\ddot{x} + (c - \alpha P)\dot{x} + kx = (\mu_S - \alpha V)P \quad (10.2)$$

The damping term (c - α P) would be negative, representing instability, if α P > c and the amplitude of the pad vibration would then increase, although the instability could be controlled by reducing α or increasing the damping coefficient (c).

Spurr's sprag-slip model (Spurr, 1961) proposed a basis for time-varying friction force variation. Figumechanicalre 10.1(a) shows a rigid strut $0'$ P pivoted at $0'$, which is the free end of a cantilever $0'$-$0''$, where $0''$ meets an abutment. Taking moments about $0''$ the friction drag force *F* is calculated from:

$$F = \frac{\mu L}{(1 - \mu \tan \theta)} \qquad (10.3)$$

The strut 'sprags', i.e. *F* tends to infinity when 1-$\mu tan\theta = 0$, which Spurr associated with the onset of squeal noise when the 'sprag angle' (q) was close to the limit indicated in Equation (10.2).

$$\theta = \cot^{-1} \mu \qquad (10.4)$$

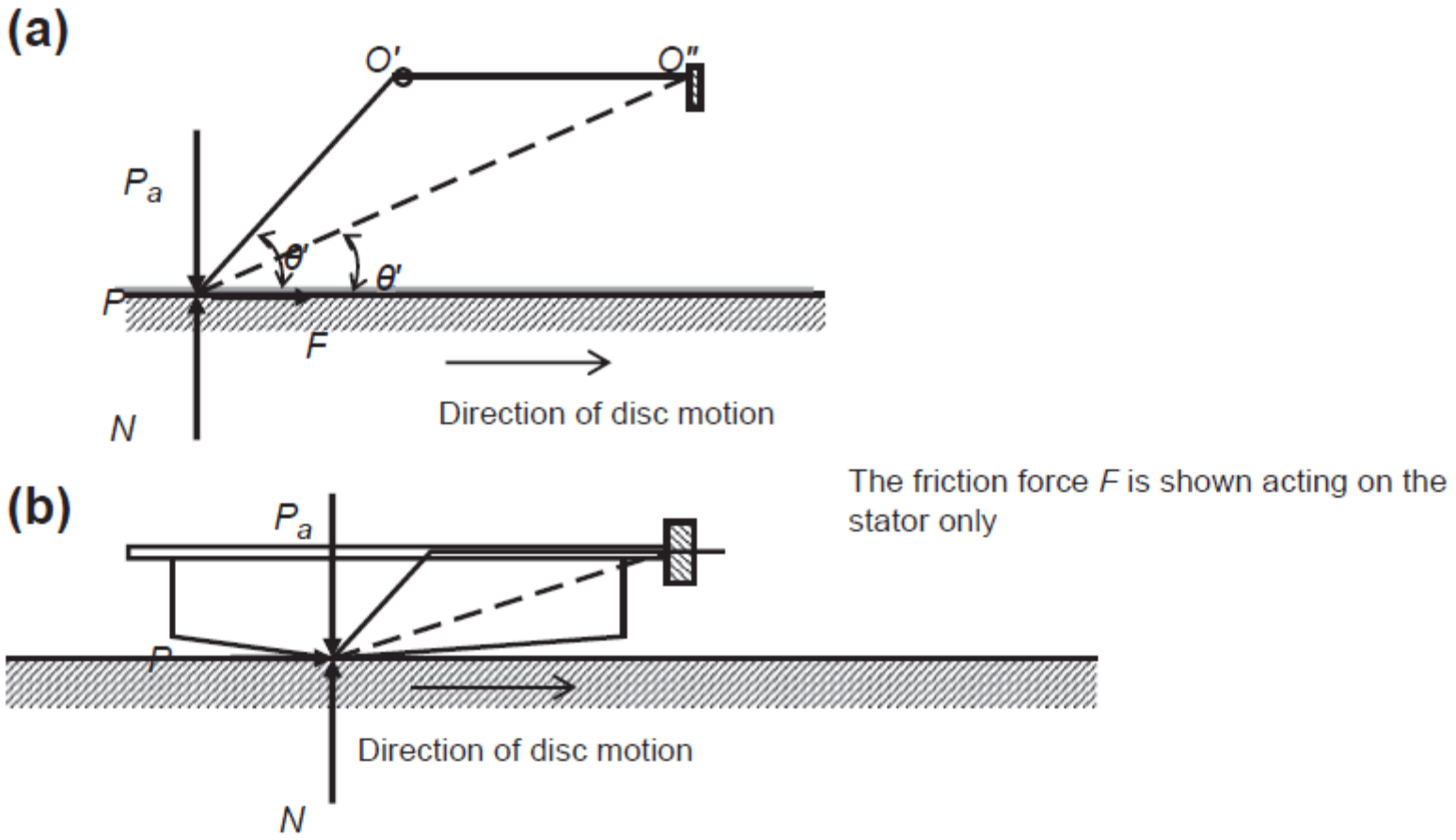

Figure 10.1: (a) 'Sprag-Slip' Model (Spurr, 1961) (Upper). (b) 'Sprag-Slip' Model in a Disc Brake Scenario (Lower).

System Response

The response of the brake to the source vibration defines the nature (modes and frequencies) of the generated brake noise. A friction brake is a complicated assembly of components that are connected by a variety of linear and non-linear devices and physical phenomena such as springs, contact interfaces and sliding friction, which couple various parts of the brake system together. Thus it can vibrate as a system of rigid bodies or as a system of flexible bodies, or both, coupled by linear and non-linear contact interfaces, forces, springs and dampers.

Eigenvalue stability analysis has been widely reported in the published literature relating to brake noise, and can be demonstrated on simple lumped parameter models, e.g. the dynamic response of a single degree of freedom (DoF) mass/spring/damper system subjected to a sinusoidal input ($f = f_o \sin(\omega t)$), as illustrated in Figure 10.4. The frequency response can be calculated from the system transfer function:

$$\frac{X}{f_o} = \frac{1}{-\omega^2 m + i\omega c + k} \qquad (10.5)$$

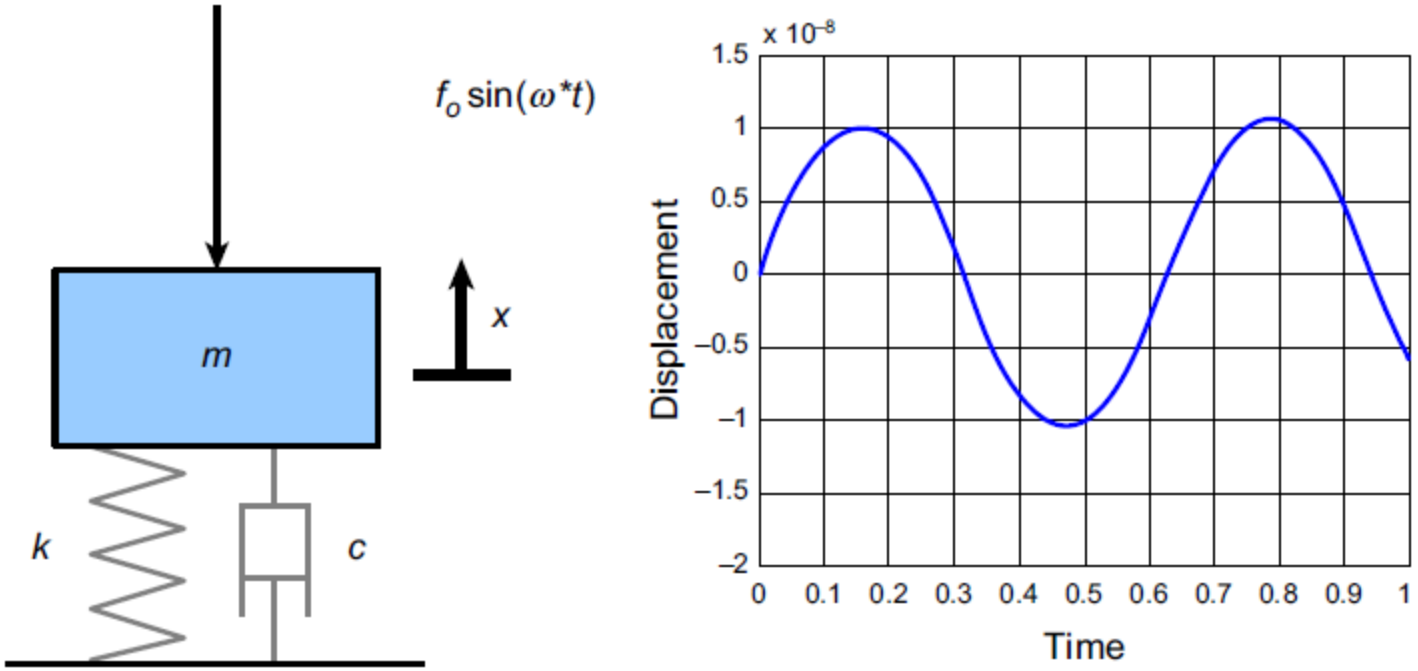

Figure 10.4: Single Degree of Freedom System Vibrational Response (Displacement vs. Time).

$$\frac{X}{f_o} = \frac{1}{-\omega^2 m + i\omega c + k} \tag{10.5}$$

The system stability can be analyzed by calculating the roots or eigenvalues of the characteristic equation (10.6); a negative real part indicates stability.

$$-\omega^2 m + i\omega c + k = 0 \qquad (10.6)$$

Extending this to a 2DoF coupled system as illustrated in Figure 10.5, where one mass has two coupled vibration modes of bounce and pitch, shows the effect of damping on stability.

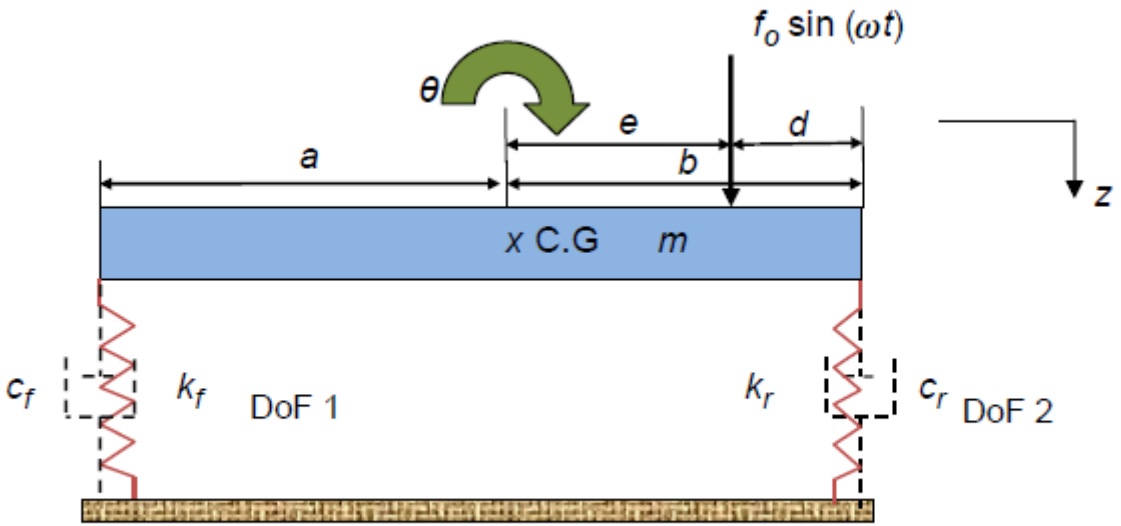

Figure 10.5: 2DoF Coupled System.

$$-\omega^2 m + i\omega c + k = 0 \tag{10.6}$$

The frequency response is calculated from the transfer function for each DoF, which can be done by evaluating the determinant of the nominator and denominator of the matrix equations (10.5):

$$\frac{X_1}{f_o} = \frac{\begin{bmatrix} 1 & -\left[(k_f a - k_r b) + (c_f a - c_r b)i\omega\right] \\ 0 & \left[(k_f a^2 + k_r b^2) - \omega^2 I + (c_f a^2 + c_r b^2)i\omega\right] \end{bmatrix}}{\begin{bmatrix} \left[(k_f + k_r) - \omega^2 m + (c_f + c_r)i\omega\right] & -\left[(k_f a - k_r b) + (c_f a - c_r b)i\omega\right] \\ -\left[(k_f a - k_r b) + (c_f a - c_r b)i\omega\right] & \left[(k_f a^2 + k_r b^2) - \omega^2 I + (c_f a^2 + c_r b^2)i\omega\right] \end{bmatrix}} \tag{10.5a}$$

$$\frac{X_2}{f_o} = \frac{\begin{bmatrix} \left[(k_f + k_r) - \omega^2 m + (c_f + c_r)i\omega\right] & 1 \\ -\left[(k_f a - k_r b) + (c_f a - c_r b)i\omega\right] & 0 \end{bmatrix}}{\begin{bmatrix} \left[(k_f + k_r) - \omega^2 m + (c_f + c_r)i\omega\right] & -\left[(k_f a - k_r b) + (c_f a - c_r b)i\omega\right] \\ -\left[(k_f a - k_r b) + (c_f a - c_r b)i\omega\right] & \left[(k_f a^2 + k_r b^2) - \omega^2 I + (c_f a^2 + c_r b^2)i\omega\right] \end{bmatrix}} \tag{10.5b}$$

The modal frequencies for zero damping are shown in Figure 10.6 and the effect of damping at each of the degrees of freedom is illustrated in Figures 10.7 and 10.8 for the two system natural frequencies ω_1 and ω_2.

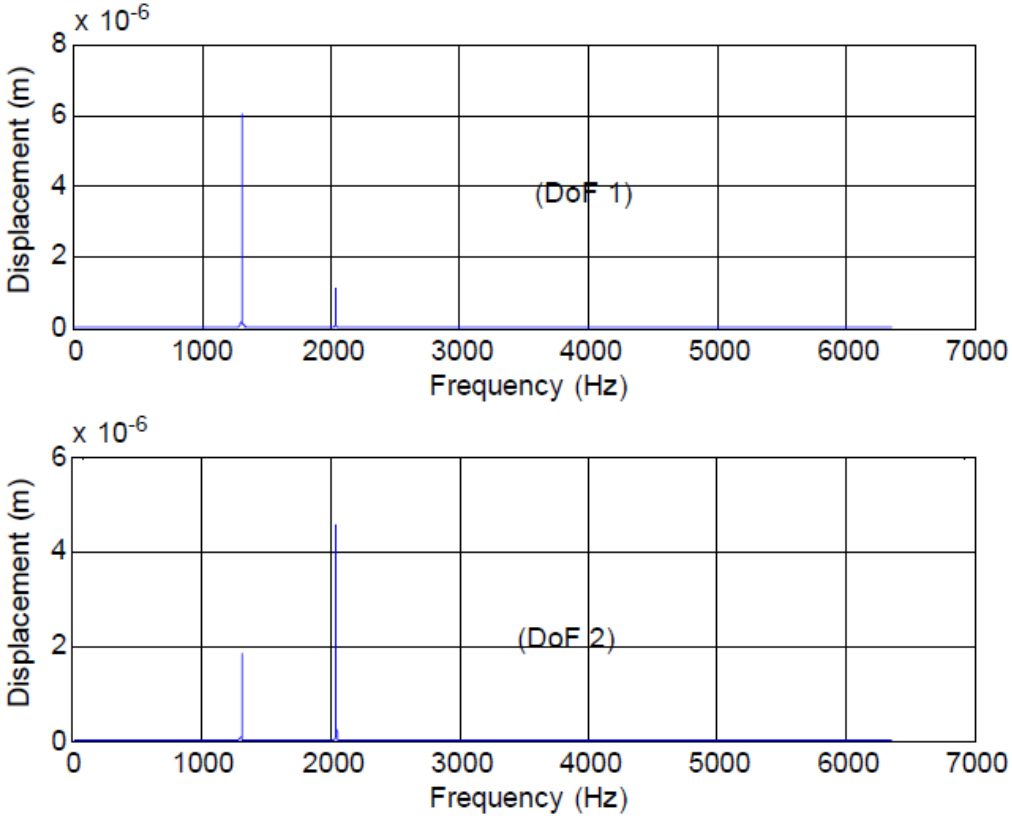

Figure 10.6: Frequency Response for Zero Damping (DoF 1 and 2).

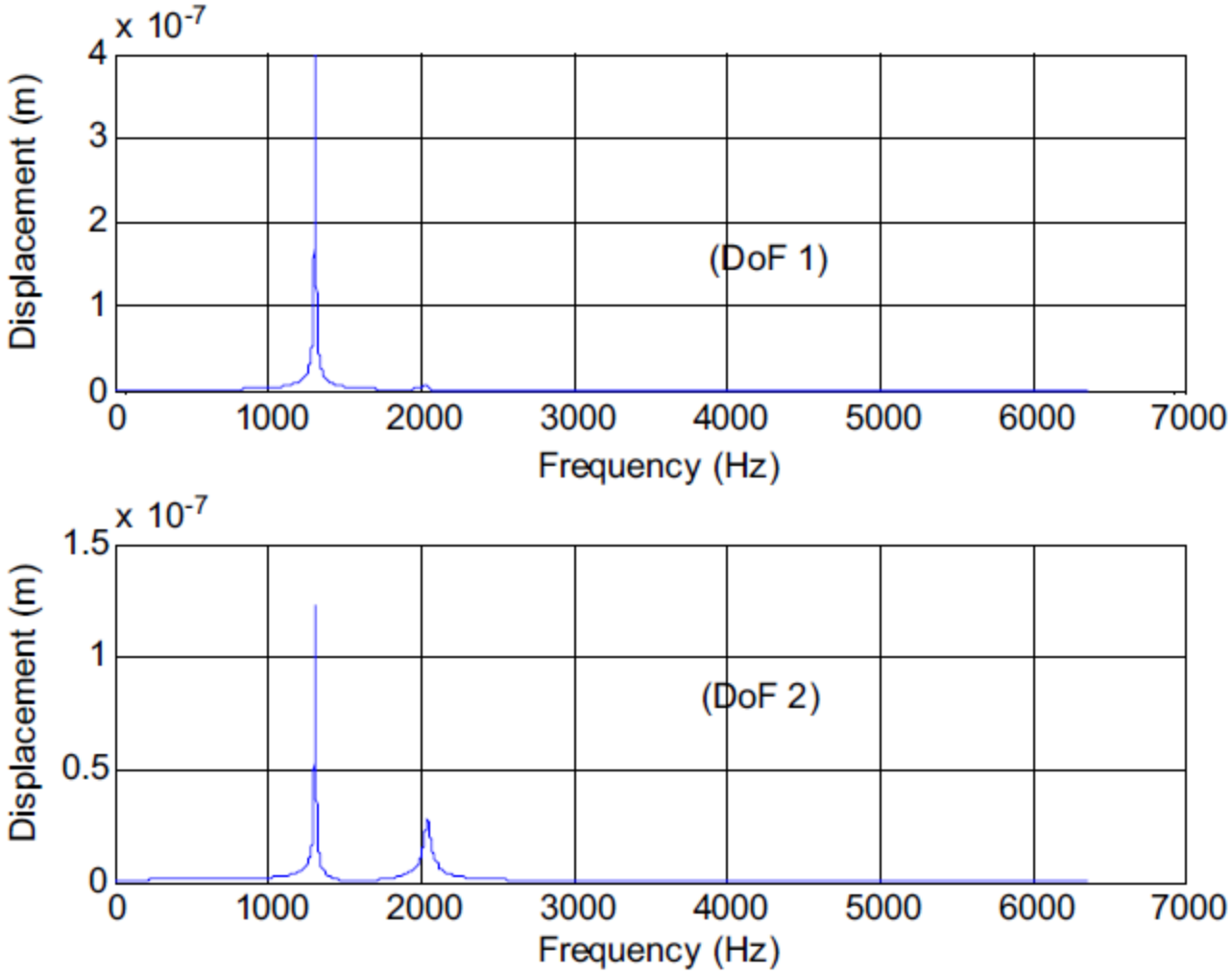

Figure 10.7: Frequency Response With High Damping At DoF 1 (DoF 1 and 2).

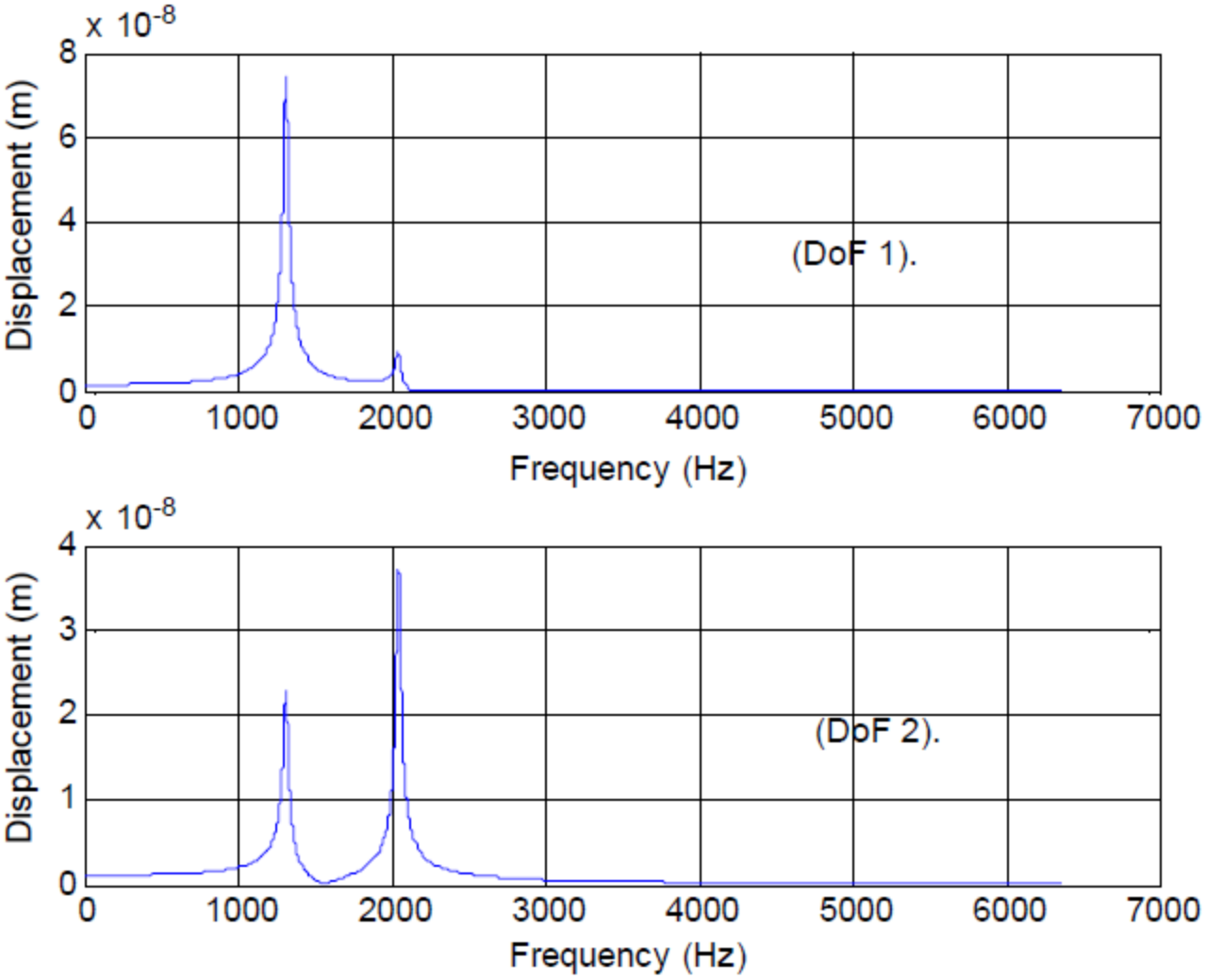

Figure 10.8: Frequency Response with High Damping at DoF 2.

The mode shapes are shown in Figure 10.9; both modes represent a combined translation and rotation.

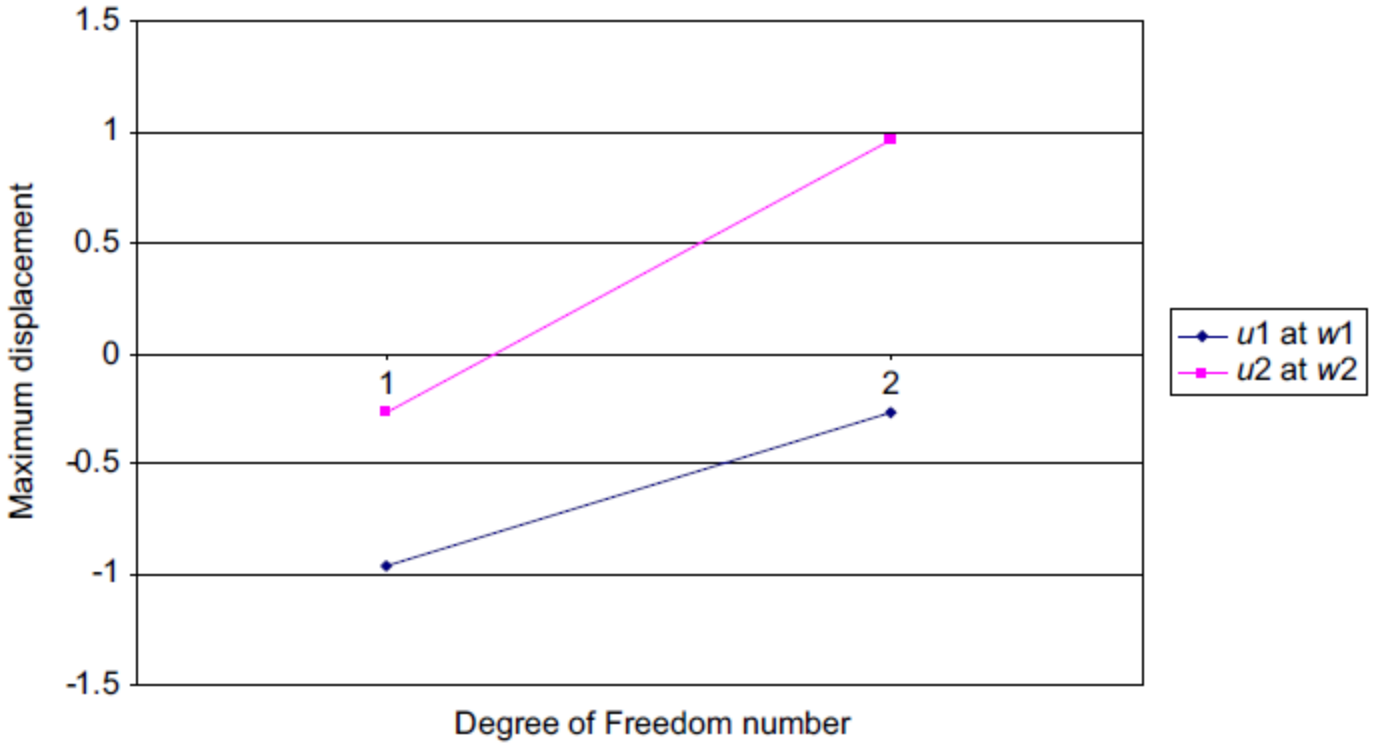

Figure 10.9: Coupled 2DoF Mode Shapes.

For this 2DoF system the stability can be assessed as shown in Table 10.1 for three cases of zero damping and high damping at each of the two masses.

Table 10.1: Roots of the Characteristic Equation for the Coupled 2DoF System

Roots	Values		
	Zero Damping	High Damping at #1	High Damping at #2
s_1	$0 + 2046.0i$	$-120 + 12{,}854i$	$-90 + 12{,}853.0i$
s_2	$0 - 2046.0i$	$-120 - 12{,}854i$	$-90 - 1285.0i$
s_3	$0 + 1313.2i$	$-18 + 8251i$	$-99 + 8252.0i$
s_4	$0 - 1313.2i$	$-18 - 8251i$	$-99 - 8252.0i$

The principles demonstrated in these simple 1DoF and 2DoF system models are only intended to help understand some basics of the dynamic behavior of vibrating mechanical systems. Real vibrating systems have distributed properties such as mass, stiffness and damping, which can be linear and/or non-linear. They can be modelled by decomposing them into degrees of freedom representing the key elements and interconnections, which was the approach taken by researchers including North (1976) and Millner (1976, 1978). The analytical solution of the equations of motion for such systems is in principle possible but computer methods are quicker.

Figure 10.10 shows a multiple (four) DoF linear model, which for the example properties shown in Table 10.2 generates the results summarized in Figures 10.11-10.13.

Table 10.2: Example Properties for Model Parameters in Figure 10.11

Parameter	Values
k_1 (N/m)	10^8
k_2 (N/m)	10^7
k_3 (N/m)	10^8
k_4 (N/m)	3.5×10^7
k_5 (N/m)	5×10^7
m_1 (kg)	12.3
m_2 (kg)	0.4
m_3 (kg)	0.26
m_4 (kg)	8.8
c_1 (kg/s)	0
c_2 (kg/s)	0
c_3 (kg/s)	0
c_4 (kg/s)	0
c_5 (kg/s)	0
f_1 (N)	$f_o\sin(\omega t)$
f_2, f_3 and f_4	0

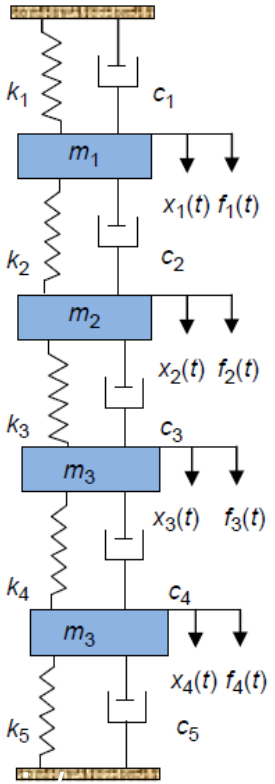

Figure 10.10: Example Multiple (Four) Degree of Freedom Lumped Parameter Mechanical Model.

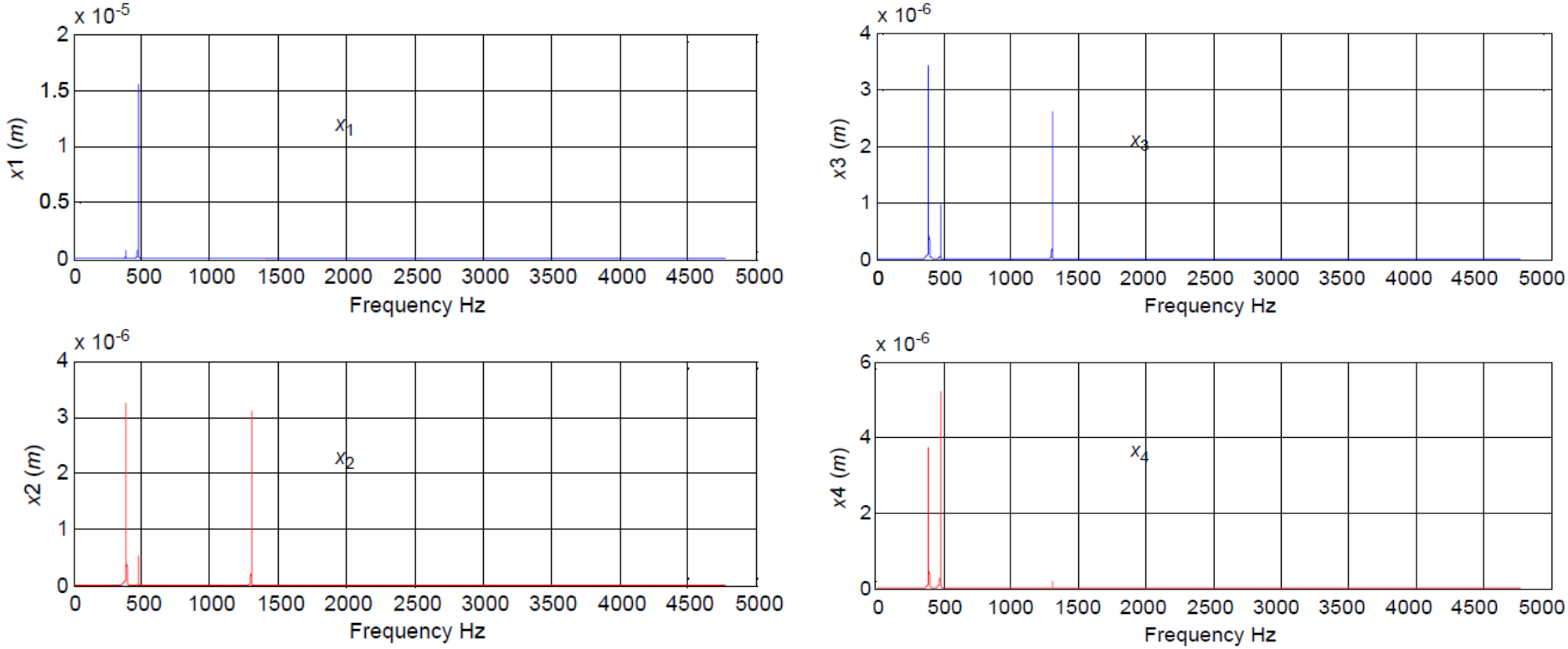

Figure 10.11: Frequency Response of the System for Damping Coefficients (c_1—c_5) = 0.

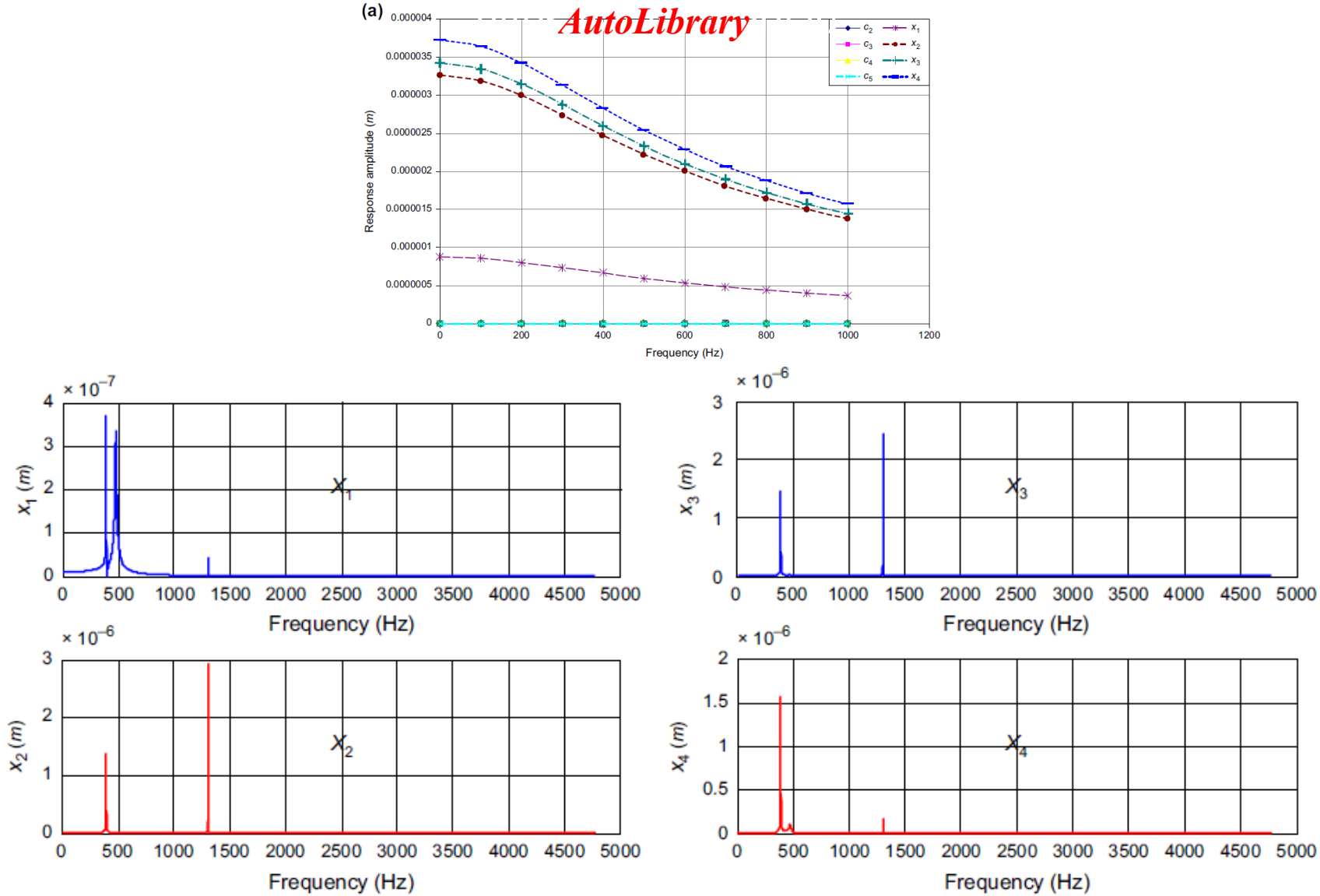

Figure 10.12: (a) Effect of Changing c_1 on the System Amplitude Response. (b) Frequency Response when $c_1 = 1000$ kg/s.

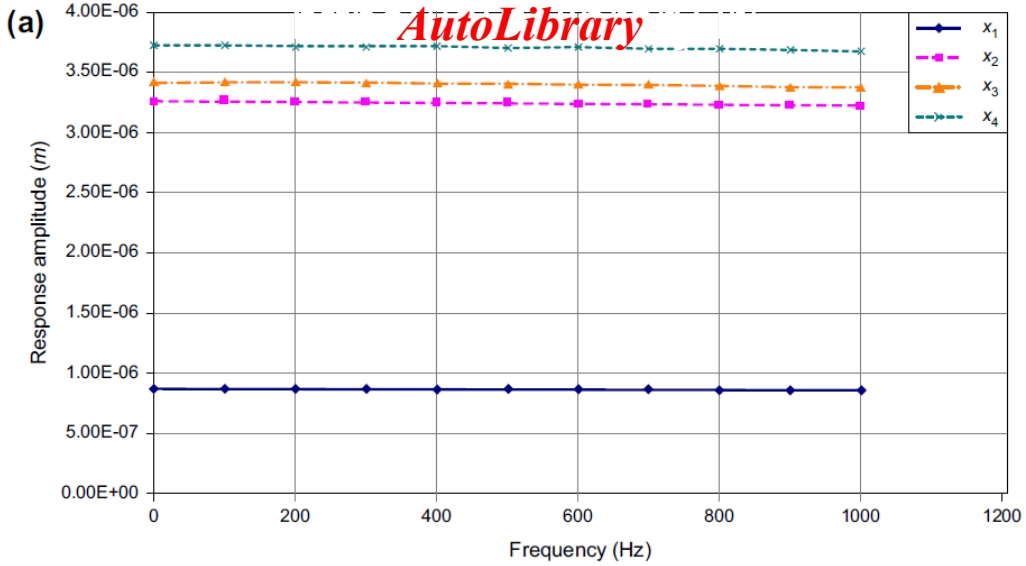

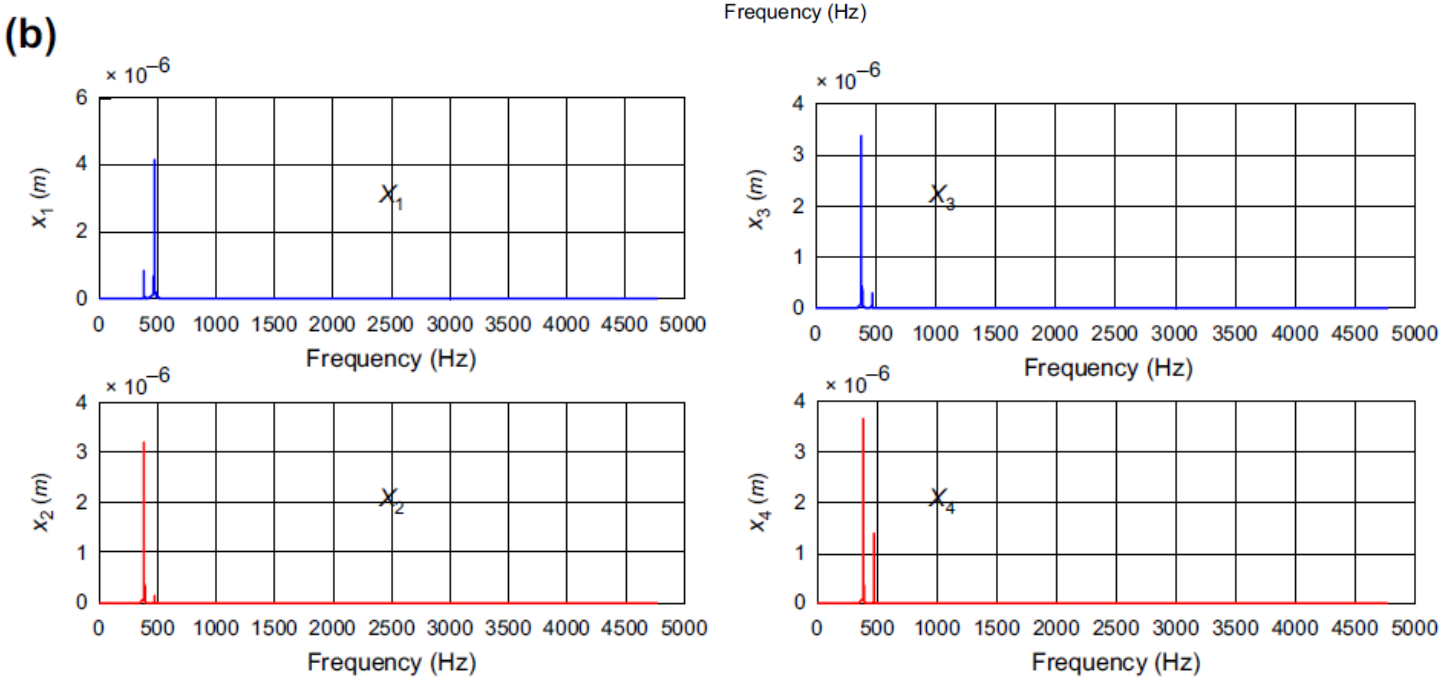

Figure 10.13: (a) Effect of Changing c_4 on the System Amplitude Response. (b) Frequency Response when $c_4 = 1000$ kg/s.

A multiple DoF lumped parameter model for low-frequency ‘hum’ noise on a disc brake (200e400 Hz) with constant m, which occurs under ‘off-brake’ conditions with only one pad touching the disc, is illustrated in Figure 10.14 (Lang and Smales, 1983).

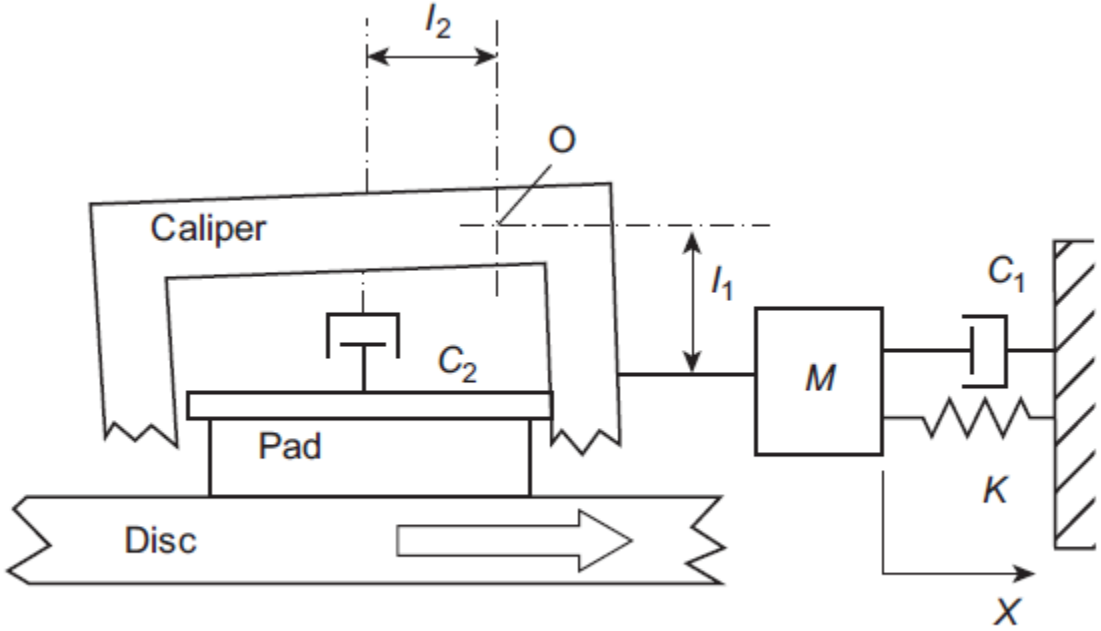

Figure 10.14: Lumped Parameter Disc Brake ‘Hum’ Noise Model (Lang and Smales, 1983).

The caliper oscillates as a rigid body on its mounting of stiffness K about a node at O, with damping c_1. The actuator (piston in the cylinder bore) provides further damping c_2 attributed to the piston seal, and the disc does not vibrate because the frequency of interest is below its first flexural mode so that the piston is effectively stationary. An initial pad velocity of $\dot{x}$ in the direction of disc rotation produces a relative velocity in the damper c_2 of $(l_2/ l_1)\ \dot{x}$ and hence a normal force at the friction face of $c_2(l_2/ l_1)\ \dot{x}$.

The resulting friction force of $\mu c_2(l_2/l_1)\dot{x}$ is a damping force acting in the same direction as $\dot{x}$, and acts as a negative damping force leading to instability. The equation of motion is:

$$M\ddot{x} + \left[c_1 + c_2\left(\frac{l_2}{l_1}\right)\left(\frac{l_2}{l_1} - \mu\right)\right]\dot{x} + kx = 0 \qquad (10.7)$$

and hence unstable oscillation occurs when:

$$\mu > \frac{l_2}{l_1} - \frac{c_1 l_1}{c_2 l_2} \qquad (10.8)$$

The stability of this model can be increased by decreasing μ and/or increasing the caliper mounting damping c_1, which was verified experimentally with a mass damper fitted on the suspension. Equation (10.8) also indicates that instability does not occur if l_2/ l_1 is negative, i.e. if the caliper mounting is designed with O positioned towards the leading end of the brake.

In particular, flexural vibrations of the rotor occur and the natural frequencies of the disc or drum appear to have some influence on the noise frequency. The 1 kHz lower frequency for squeal noise is defined by the frequency of the fundamental mode of vibration of discs and drums of passenger cars, although this can be lower for large commercial vehicle brake drums so squeal noise on CV brakes can be lower than 1 kHz.

A typical flexural (out-of-plane) mode of a brake disc is shown in Figure 10.15

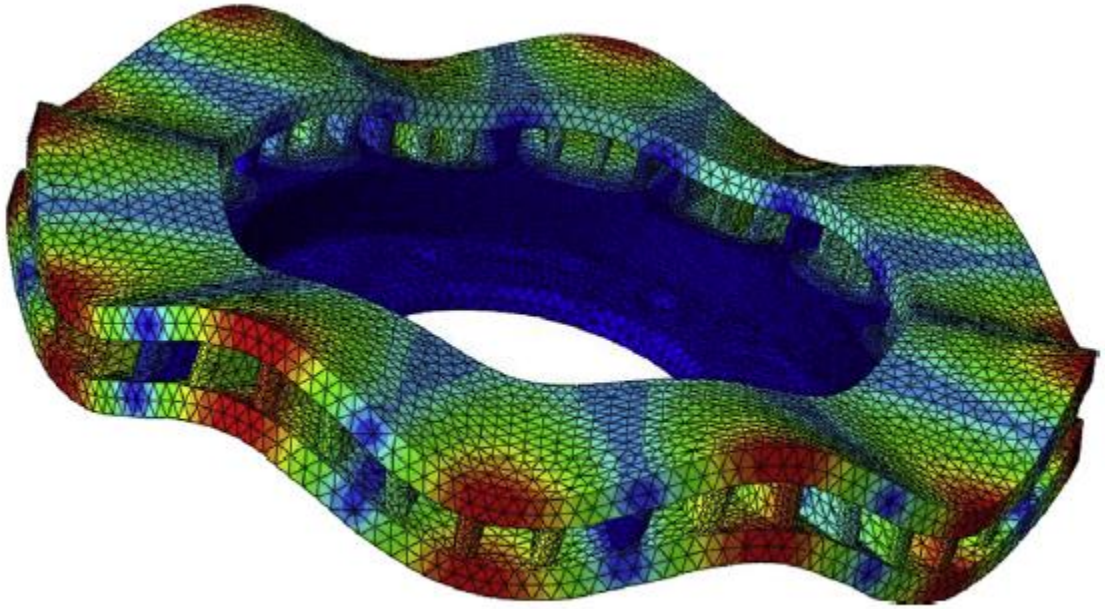

Figure 10.15: Typical Flexural (Out-of-Plane) Mode Shape of a Brake Disc (Bryant, 2013).

A lumped parameter model of binary flutter is shown in Figure 10.16

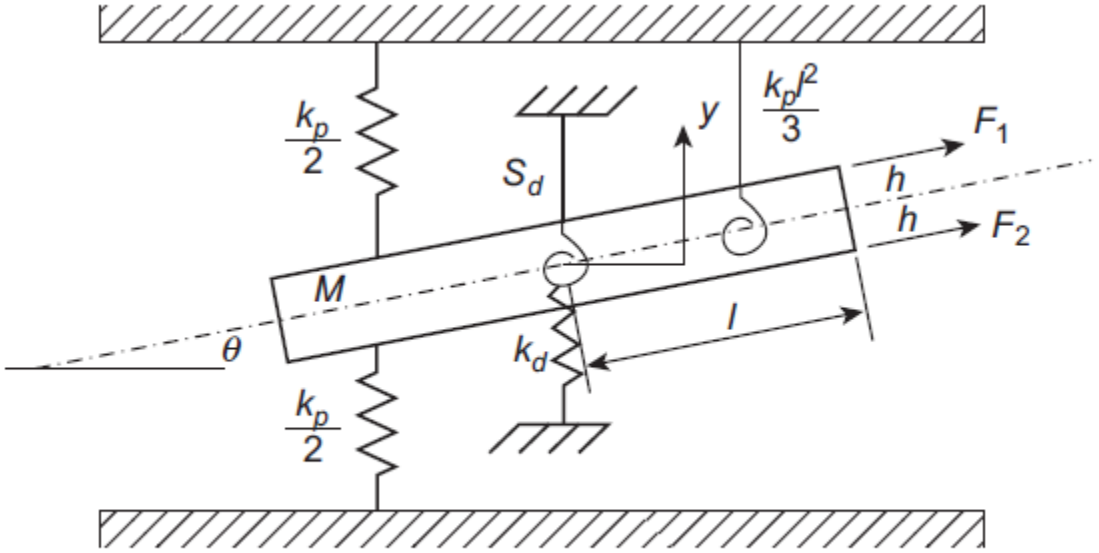

Figure 10.16: Binary Flutter Model (North, 1976).

comprising a 2DoF disc section interfacing with a spring representation of the friction material with the backplate fixed. The two equations of motion are:

$$M\ddot{y} + (k_d + k_p)y + F\theta = 0 \tag{10.9}$$

$$I\ddot{\theta} - \mu h k_p y + \left(S_d + k_p \frac{l^2}{3}\right)\theta = 0 \tag{10.10}$$

These can be written in matrix form (see Equations (10.5)):

$$[M]\{\ddot{X}\} + [K]\{X\} = 0 \tag{10.11}$$

The solutions are of the form $y = y_0 e^{xt}$ and $\theta = \theta_0 e^{xt}$ and hence $\{\ddot{x}\} = \lambda^2\{x\}$, which on substitution into the equations of motion gives the eigenvalue equation:

$$\lambda^2\{X\} + [A]\{X\} = 0 \qquad (10.12)$$

where [A] = $[M]^{-1}$[K].

If the associated characteristic equation in the eigenvalue λ has complex conjugate solutions (p + iq) the solution for y and θ is oscillatory (y = $y_0 e^{pt}\cos(qt)$). The stability criterion can be applied again; as previously explained a positive value of the real part of λ indicates instability (the imaginary part indicates the frequency of oscillation), which gives the condition for instability as:

$$\frac{4MIF\mu h}{\left(I - M\frac{r^2}{3}\right)^2} > k_p > 0 \qquad (10.13)$$

FE analysis for brake noise tends to concentrate on the time domain, while multi-body dynamics (MBD) computer simulation can predict the vibration behaviour of the brake parts in the time domain. Recent work on brake noise modelling using MBD has presented a full dynamic model of an opposed piston passenger car disc brake that includes 3D flexible body modelling of the disc, pads, pistons and caliper, plus the hub and steering knuckle as shown in Figure 10.17 (Alasadi et al., 2013).

modelling of the disc, pads, pistons and caliper, plus the hub and steering knuckle as shown in Figure 10.17

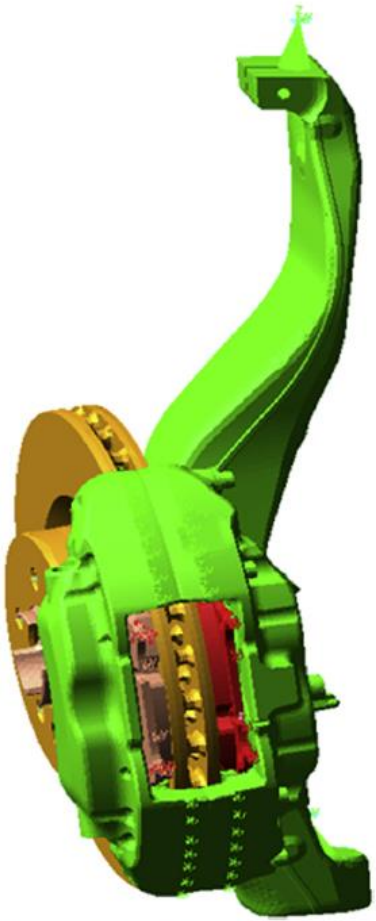

Figure 10.17: MBDS Model for Brake Noise Investigation (Alasadi et al., 2013).

The predominant frequency identified from the simulation varied between 2.6 and 2.8 kHz over a range of different actuation pressures and friction coefficients. Other frequencies were also predicted, in particular the onset of 5.7 kHz over 15e30 bar hydraulic actuation pressure and with a friction coefficient of 0.55. The predicted vibrational response of the brake disc, caliper, and the inner and outer brake pads is illustrated in Figure 10.18 and shows that 2.7 kHz was the predominant frequency that appeared on the disc, pads and caliper.

The predicted vibrational response of the brake disc, caliper, and the inner and outer brake pads is illustrated in Figure 10.18

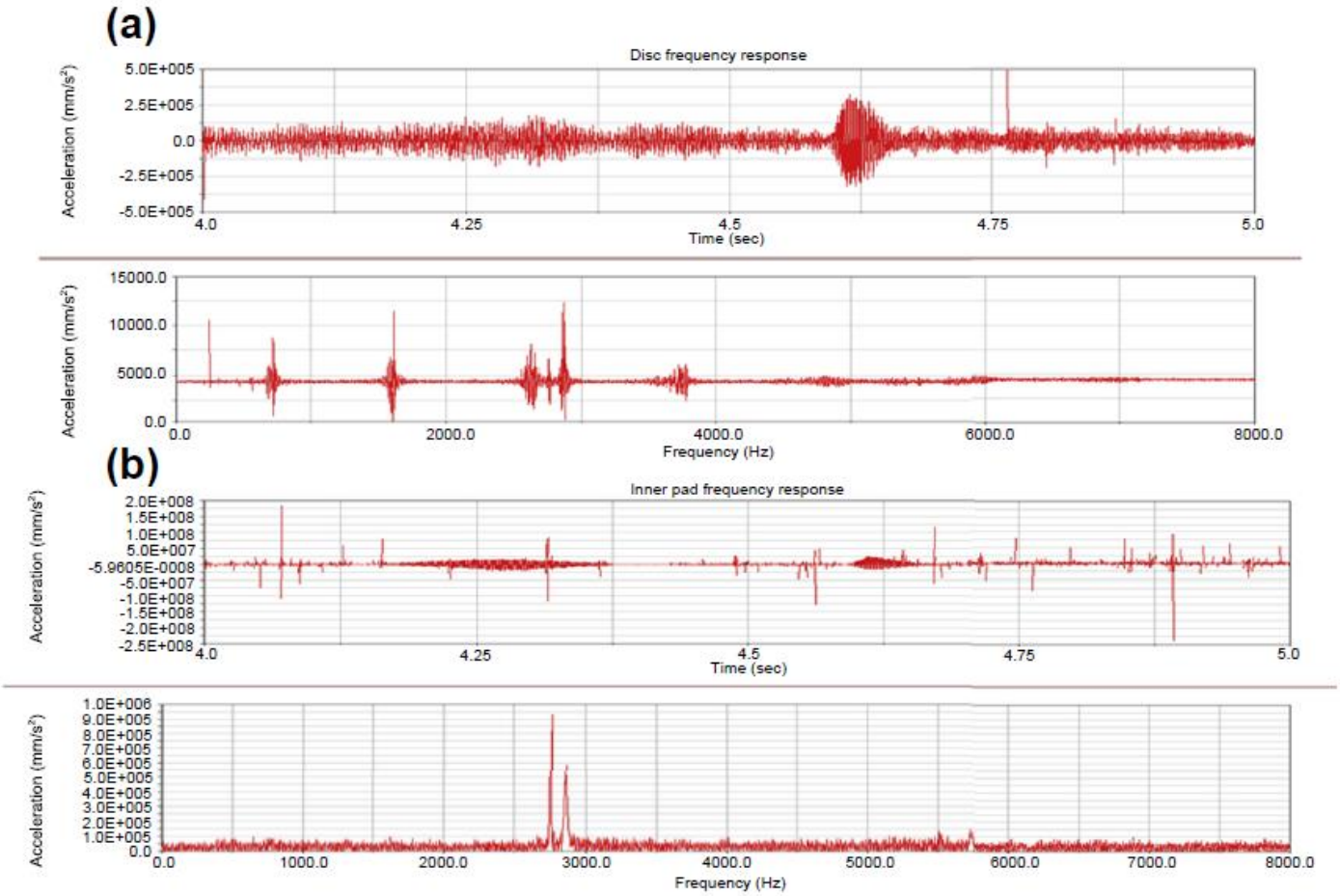

Figure 10.18: (a) Predicted Disc Frequency Response. (b) Predicted Inner Pad Frequency Response. (c) Predicted Outer Pad Frequency Response. (d) Predicted Caliper Frequency Response (Alasadi et al., 2013).

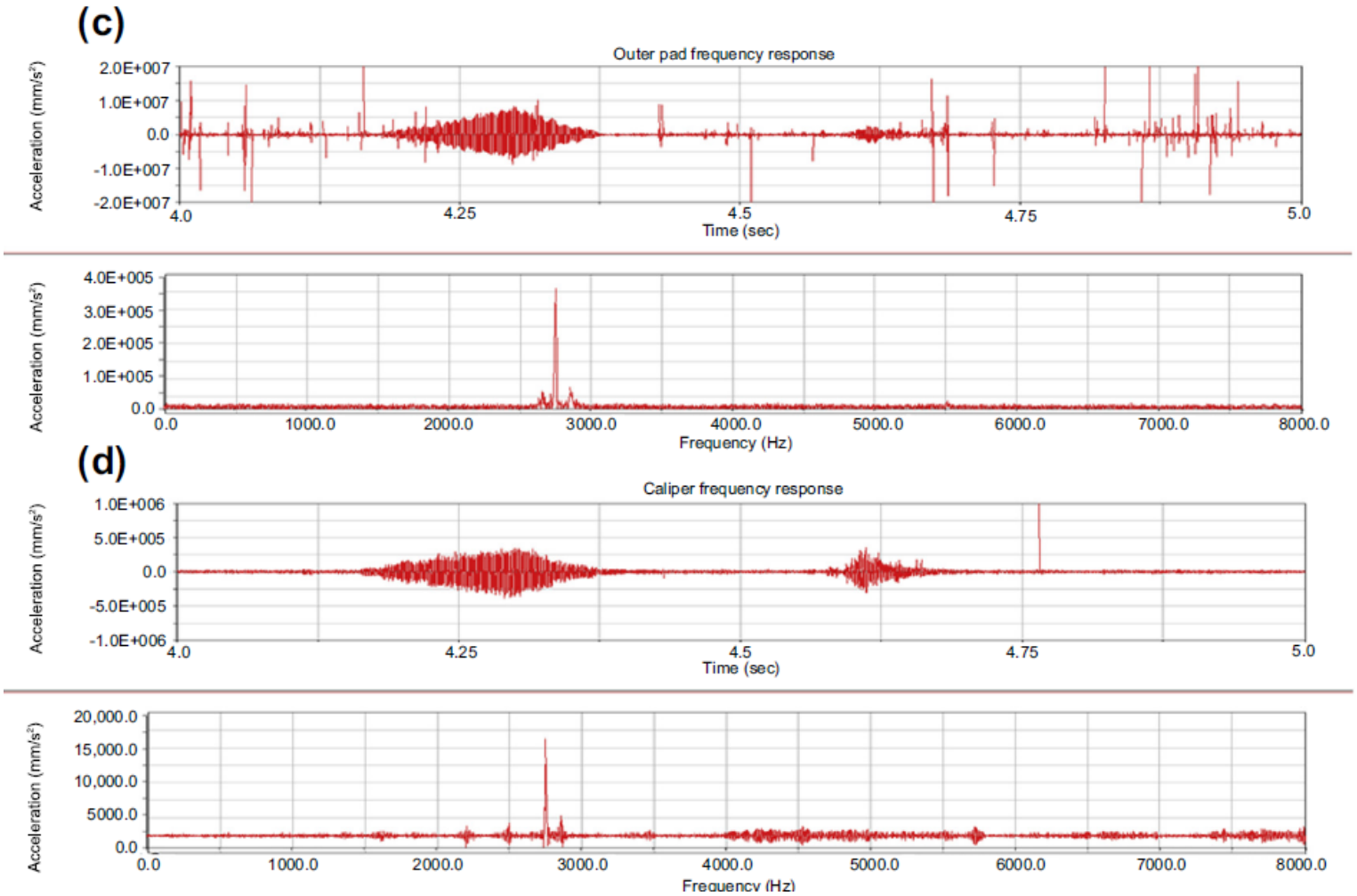

Figure 10.18: (a) Predicted Disc Frequency Response. (b) Predicted Inner Pad Frequency Response. (c) Predicted Outer Pad Frequency Response. (d) Predicted Caliper Frequency Response (Alasadi et al., 2013).

Drum brake noise now tends to be associated with commercial vehicles where problems of noise in drum brakes are still all too evident. Brake drum mode shapes associated with noise have similar characteristics to brake disc mode shapes in that they form a wave around the rubbing path with an even number of nodal lines across the rubbing path, as illustrated in Figure 10.19.

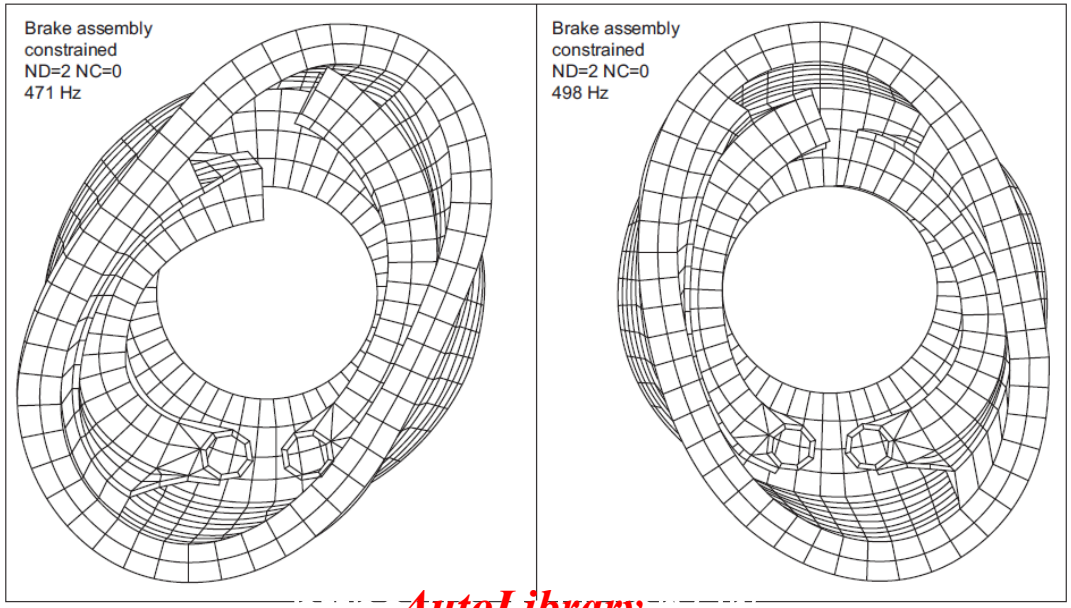

Figure 10.19: Example of Drum Brake Mode Shape Associated With Squeal Noise (Day and Kim, 1996).

Modal Analysis in Brake Noise

Modal analysis studies the mode shapes of vibrating bodies and systems when they are vibrating at a resonant frequency, i.e. the response to a time-varying forcing vibration is significant. A mode shape can be defined as a graph that shows the deflected form of the body or the system when the displacements are at a maximum, and there is one mode shape for each mode of vibration (e.g. Figure 10.9). There are two approaches to modal analysis, namely experimental modal analysis where mode shapes are measured using sensors and transducers for, say, acceleration and displacement, and theoretical modal analysis where the mode shapes are predicted, e.g. by FE-based eigenvalue extraction, or MBD analysis of the vibration behaviour of the brake assembly.

All experimental modal parameters are obtained from measured operating deflection shapes (ODSs) while artificially exciting the body or system. An ODS describes the forced motion of two or more points on a body. The most widely used experimental modal analysis method is impact testing, which excites the body or system by an impact.

For impact testing the body is usually supported in the ‘freeefree’ condition, e.g. by suspending it on lowstiffness ‘bungee’ cords, and the equipment listed below is required:

- An impact hammer with a load cell attached to its striking face (‘head’) to measure the input force.
- An accelerometer to measure the response; this may be achieved by transducers mounted on the body or a laser accelerometer device.
- An FFT analyser to compute the frequency response functions (FRFs).
- Post-processing software for identifying modal parameters and displaying the mode v shapes.

An example FRF from a brake disc impact test is shown in Figure 10.20.

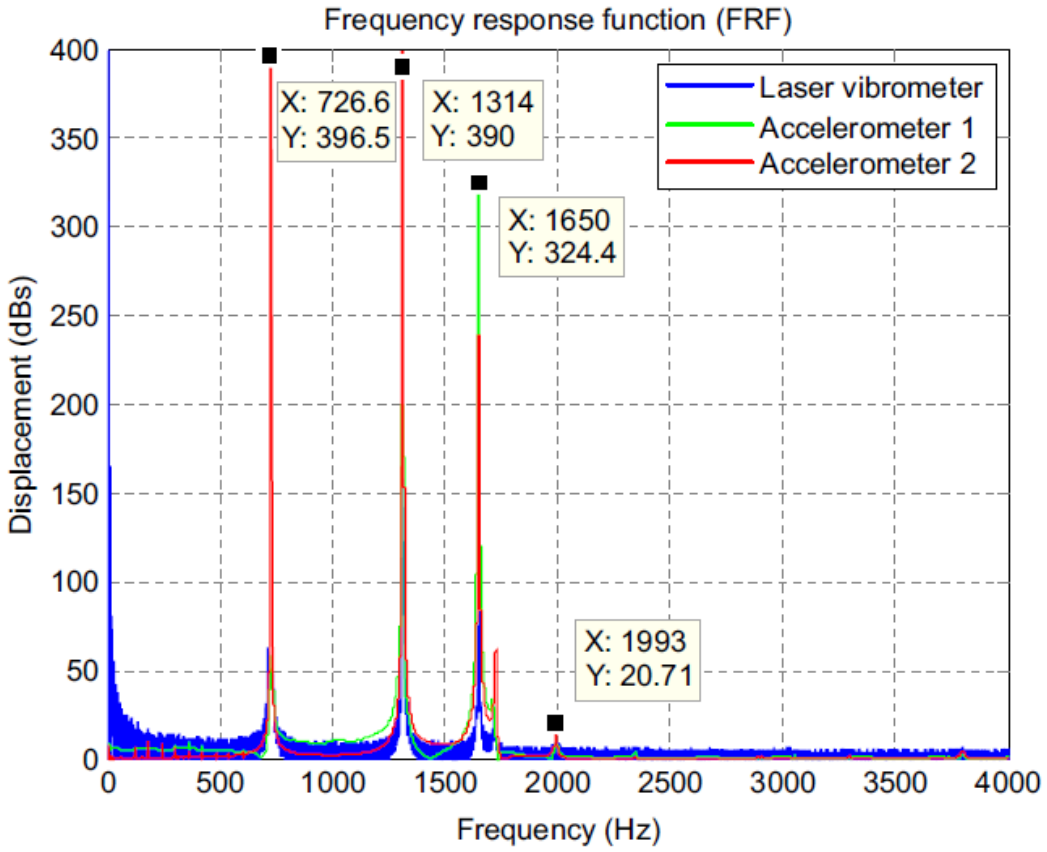

Figure 10.20: Example FRF from a Brake Disc Impact Test.

Figure 10.21 shows different vibration mode shapes in a brake disc with stinger attached; the mode shapes are indicated by grains of sand (the disc is horizontal), which agglomerate at the nodal lines.

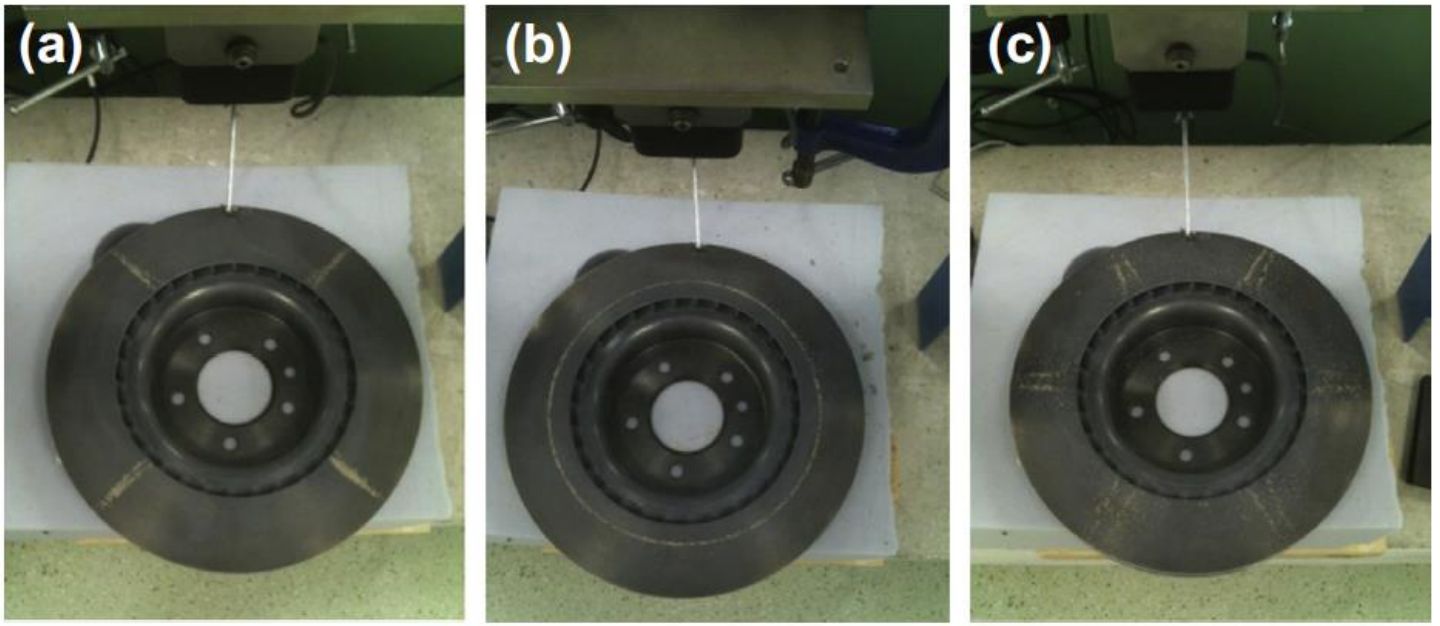

Figure 10.21: Example Brake Disc With Stinger Attached Showing Different Vibration Modes.

In this case Figure 10.21(a) indicates a two nodal diameter mode of vibration that is associated with a re Figure 10.21(b) indicates a circumferential mode associated with a resonant frequency of about 1.3 kHz, and Figure 10.21(c) indicates a three nodal diameter mode with a resonant frequency of about 1.7 kHz. sonant frequency of about 700 Hz,

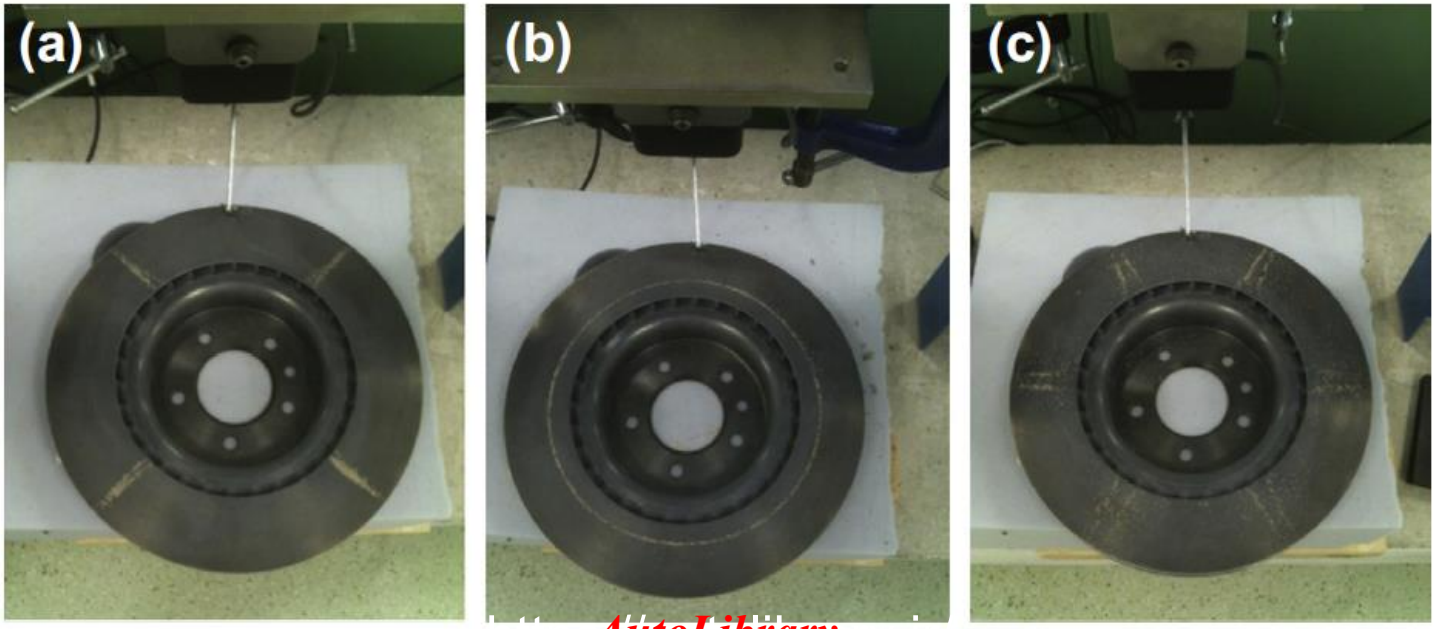

Figure 10.21: Example Brake Disc With Stinger Attached Showing Different Vibration Modes.

While a disc brake is generating noise, experimental modal analysis has shown that the disc vibrates with a diametral mode of vibration that may be stationary or rotate around the disc axis at an angular velocity determined by the quotient of the frequency and the mode order. It has been shown (Fieldhouse, 2013) that there is a well-defined relationship between disc diametral vibration modes and frequency, which can be written in the form shown in Equation (10.14), where a is the node pitch angle and g and b are constants for the particular disc design:

$$\text{Frequency (Hz)} = \gamma\alpha^{-\beta} \qquad (10.14)$$

In practice there is always circumferential asymmetry in a brake rotor because of manufacturing imperfections and tolerances, and it has been found that increasing the circumferential asymmetry by, for example, adding equally spaced concentrated masses to a rotor periphery (while maintaining balance) can reduce or eliminate noise by separating the pair modes (Lang et al., 1983). The number of concentrated masses required is indicated by:

$$\frac{2M}{R} = \text{positive integer} \qquad (10.15)$$

where:

M = mode order;

R = number of equally spaced masses.

The parametric study showed that the parameters listed below increased the separation of pair modes of two nodal diameters, 471 and 498 Hz (see Figure 10.19), both frequencies close to an observed squeal noise of 480e490 Hz:

- Increasing coupling stiffness between the brake linings and the brake drum, e.g. by increasing lining stiffness or contact pressure (actuation force).
- Uniform or crown contact of the linings with the drum friction surface.

Referring to Figure 10.22 (Talbot and Fieldhouse, 2002), diagonal fringes can be seen along the edge of the brake disc (upper part of the image) that represent combined rotational motion, in plane vibration and out-of-plane vibration.

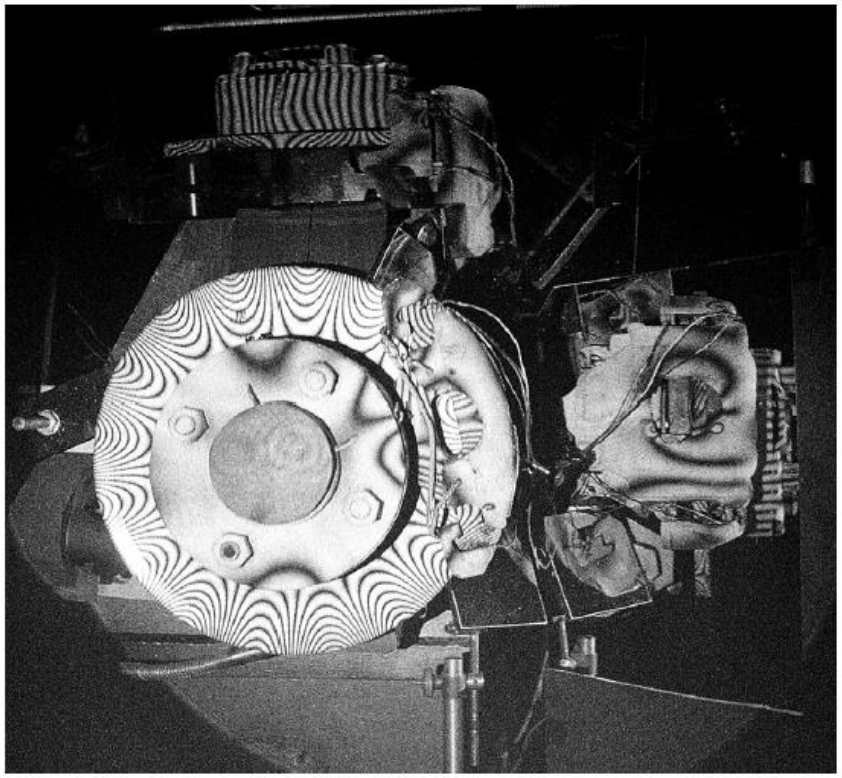

Figure 10.22: Photograph of Mode Shapes Using Laser Holographic Interferometry (Fieldhouse, 2015).

This effect could be controlled by careful design of the pad effective length. They summarized five basic criteria associated with this effect:

- The system tries to fit a whole number of antinodes along the pad friction interface.
- The pad effective length can be between 80% and 100% of its design length.
- The antinode will generally compress to fit under the pad friction interface.
- Antinode compression will be a maximum of 60% of the original free mode angle.
- For frequency to be considered a problem the free mode antinode subtended angle must be greater than that of the pad.

Variability in Brake Noise

One of the most interesting (and frustrating) features of brake noise is its fugitive nature; it is well known that even across different vehicles of the same make and model with the same brake installation, some exhibit brake noise, while others do not. Given the complexity of the underlying physical principles of brake noise generation that have been outlined above and the emphasis on instability, it appears that relatively small changes in one or more of the many design and operational parameters associated with friction brakes can tip a brake installation from quiet to noisy.

Brake Judder

As previously described, brake judder is a mechanical instability that creates a nonresonant forced vibration usually with a low frequency (typically up to 200 Hz) related directly to rotor speed. It may be caused by circumferential variations or imperfections in the rubbing path of the brake rotor, which cause wheel and brake torsional vibration at a frequency that is a multiple of the rotor speed. The vibration can be transmitted through the vehicle suspension, brake actuation system, steering and the structure.

Hot judder is more problematic because it is fundamentally a thermally induced phenomenon, and it occurs in disc and drum brakes, though it is particularly a problem in large heavy-duty disc brakes, e.g. on commercial vehicles and certain types of large high performance passenger cars. Permanent thermoplastic rotor deformation results from localised yielding of cast iron under thermal cycling, the same mechanism that causes thermal cracks (see Chapter 7) and is also relevant to hot judder. The main cause of hot judder though is considered to be ‘hot spotting’ or ‘blue spotting’ (see Figure 10.23)

The main cause of hot judder though is considered to be ‘hot spotting’ or ‘blue spotting’ (see Figure 10.23)

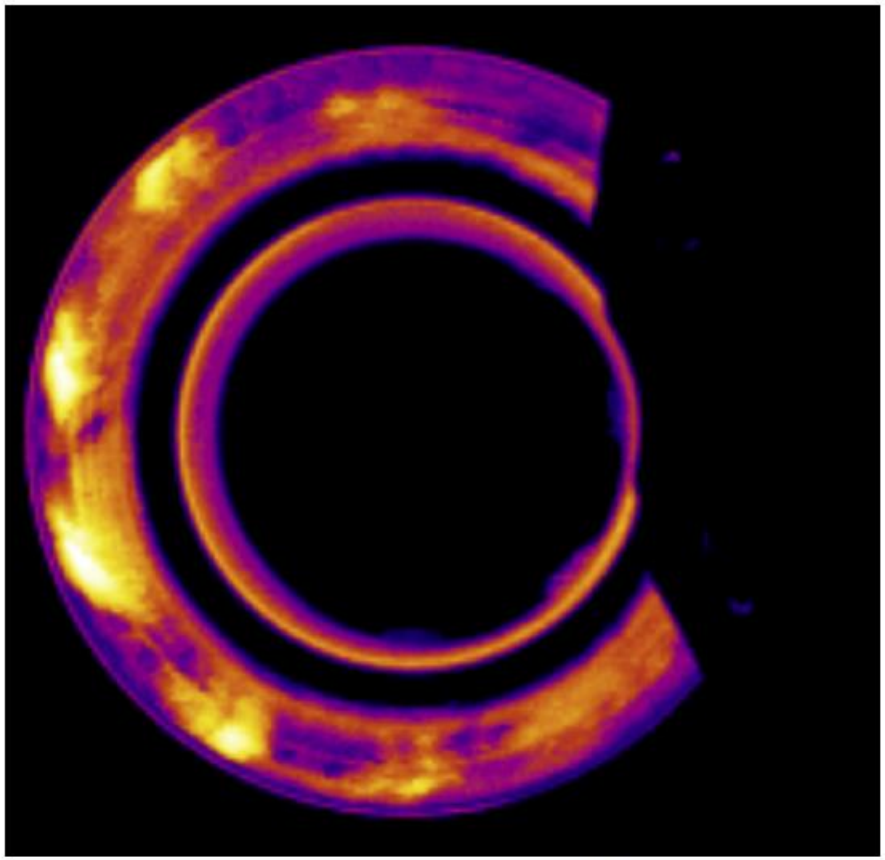

Figure 10.23: Hot Spots on a Brake Disc Rubbing Surface (Bryant, 2010).

Panier et al. (2004) used an IR camera to investigate hot spot formation on a brake disc and concluded that the energy flow into the disc brake pads was significant in their formation of MHS. They identified five types of hot spot formation on the brake disc, as illustrated in Figure 10.24:

- Type 1: the asperity type hotspot with only small areas of rapid temperature rise.
- Type 2: temperature gradients along a hot band that create small contact areas from a single rubbing path.
- Type 3: hot bands then forming from pad expansion causing larger circumferential contact patches in the plane.
- Type 4: buckling effects creating large, distinct hot spots.
- Type 5: the type 4 hot spots coalescing to form hot contact areas over most of the rubbing path, usually evident at the end of a braking application.

They identified five types of hot spot formation on the brake disc, as illustrated in Figure 10.24:

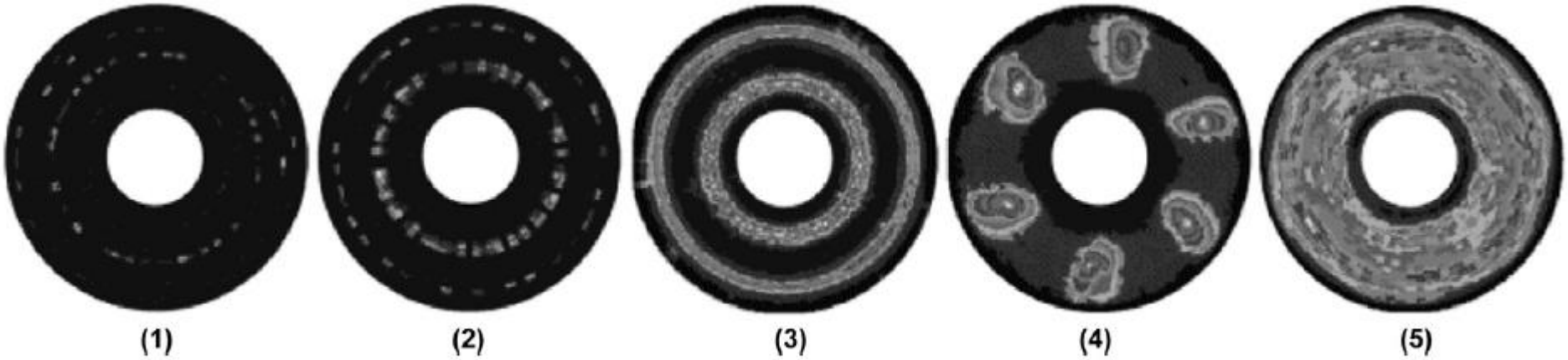

Figure 10.24: Hot Spot Formation Types (Panier et al., 2004).

Kubota et al. (1998) recommended four design rules to minimize disc brake drone noise (and the underlying hot judder):

- Design the rotor to minimize thermal deformation and maintain uniform pad/disc contact.
- Use a low-compressibility friction material to ensure more uniform pad/disc contact.
- Specify high thermal conductivity rotor materials to minimise surface temperatures and circumferential temperature variations.
- Design discs with a narrow rubbing path width.

The factors that Bryant ascribed to the development of judder included:

- Thermoelastic deformation due to rapid heat dissipation through the brake disc, causing buckling in the rubbing path.
- The clamping action of the brake pads causing the buckling form to change as it passes between them.
- Thermoplastic deformation from stress relieving allowing the disc to relax back to a state of cold deformation after cooling; after different brake applications, the states of cold deformation after cooling could be different.

He concluded that minimizing thermoelastic deformation will reduce brake judder and can be achieved by adopting a disc design with:

- Higher buckling stiffness to resist circumferential buckling
- Lower buckling stiffness to promote higher order circumferential buckling
- Reduced thermal gradients to allow greater thermal expansion to avoid buckling
- More uniform distribution of the heat to reduce maximum temperature (and temperature gradients).

Chapter eleven

Electronic Braking Systems

The term ‘electronic braking systems’ used in this chapter covers the use of electrical, electronic and computer technology in the actuation and control of road vehicle brakingsystems, and includes aspects of regenerative braking that depend heavily on electronic control technology for its effective implementation. Electronic braking systems have made it possible to utilise the brakes to enhance road vehicle safety through technologies such as antilock braking (ABS) and Electronic Stability Control (ESC), and in this waythe brakes of a road vehicle have become ‘active safety’ devices.

Antilock Braking System (ABS)

ABS was the first active safety technology to utilise the vehicle's braking system. It aims to detect the potential occurrence of wheel lock, e.g. by comparing the wheel speed with vehicle speed, and cyclically releasing and reapplying the brake so that the wheel continues to rotate and thus provide maximum braking force (based on adhesion coefficient rather than sliding tyre/road friction) and directional stability. The first road vehicle antilock braking system to be put into production in Europe was the Dunlop Maxaret 'anti-skid' device, a mechanical system fitted to a Jensen car in 1966. The first electronic antilock braking system was a Bosch system fitted to a Mercedes production car in 1978, and with this the term 'ABS' (which comes from the German term 'Anti Blockier System') came into general use to mean an antilock braking system.

A diagram of the forces and torques on a road wheel ‘i’ which is rotationally accelerating while the brake is ‘off’ under ABS cycling is shown in Figure 11.1.

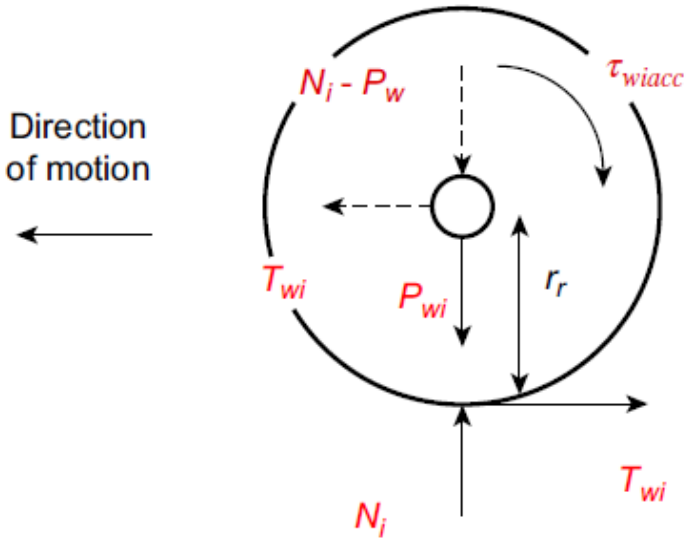

Figure 11.1: Forces and Torques Acting on a Road Wheel Under Braking.

If the coefficient of adhesion between the tyre and the road is k, the maximum force (Ti) that can be generated at the tyre/road interface of the wheel is $T_{wi} = k\ N_i$ (Equation 3.9, Chapter 3). Equation [11.1] demonstrates that the wheel can accelerate rotationally only if $T_{wi}\ r_r > \tau_{wiacc}$

$$T_{wi} \cdot r_r - \tau_{wiacc} = I_{zzi} \cdot \dot{\omega}_i \qquad (11.1)$$

T_{wi} = Braking force at axle 'i' (N);
τ_{wiacc} = Torque to accelerate rotationally the wheel and brake rotor assembly (Nm);
P_{wi} = Weight of the wheel and associated rotating parts ('unsprung' weight) (N);
ω_i = Angular (rotational) velocity of the wheel (Rad/s).
$\dot{\omega}_i$ = Angular (rotational) acceleration of the wheel (Rad/s^2).
I_{zzi} = Polar moment of inertia of the wheel and hub assembly (kgm^2).

This demonstrates how the ABS controller must take account of the acceleration of the wheel back up to speed. Sufficient wheel torque is needed and thus the coefficient of adhesion (k) must be high enough to achieve this within the ABS cycle time, but in the case where the coefficient of adhesion (k) is very low (see Figure 11.2), e.g. on snow or ice, or the wheel dynamic normal reaction is very small, this may be a problem.

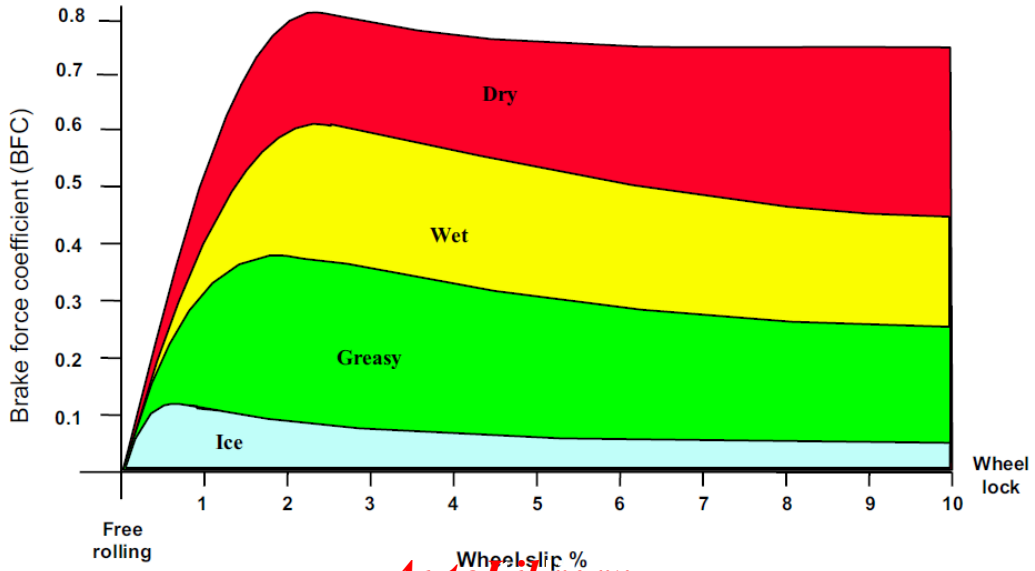

Figure 11.2: Brake Force Coefficient (BFC) vs. Wheel Slip: Example Characteristics for Different Road Surfaces (Ross, 2013).

Figure 11.2: Brake Force Coefficient (BFC) vs. Wheel Slip: Example Characteristics for Different Road Surfaces (Ross, 2013).

ABS Technology and Control Strategy Options

The basic components of an ABS control system include the following components and technology (refer to Figures 11.3 and 6.19):

- With hydraulically actuated braking systems as fitted to passenger cars and similar vehicles, an ABS pump is required to maintain hydraulic pressure during ABS operation. In a pneumatically actuated braking system, actuation pressure is already provided by the compressor.
- Wheel speed sensors provide wheel rotational speed information to the ABS controller at the required cycling speed; all ABS control decisions are based on this information. All two-axle rigid vehicles have one per wheel but other types of vehicle may not.

- The main functions of the ABS electronic controller are:
  - • Monitor wheel speed data
  - • Calculate the vehicle reference speed (Vref)
  - • Make decisions when to release and reapply the brakes
  - • Control the pressure modulators and cycling valves
  - • Monitor general system integrity.

• There is usually one pressure control valve per wheel on two-axle rigid vehicles, although this can depend on the installation and the ABS control strategy, particularly for multi-axle commercial vehicle combinations. In pneumatic systems each pressure control valve can deliver states of pressure reduction, pressure hold or pressure increase. In hydraulic systems each pressure control valve switches between the driver (‘muscular’) applied pressure and ABS generated pressure, which is controlled not to exceed the driver intent.

Pressure cycling (ABS) valves: these are designed to cycle the actuation pressure on and off at the required frequency, and may be fitted one per wheel or one per axle depending on the control strategy, which is discussed later.

The basic components of an ABS control system include the following components and technology (refer to Figures 11.3 and 6.19): next page

Figure 11.3(a)) the hydraulic actuation pressure is transmitted through open pressure control valves to the wheel cylinders and the ABS valves are closed.

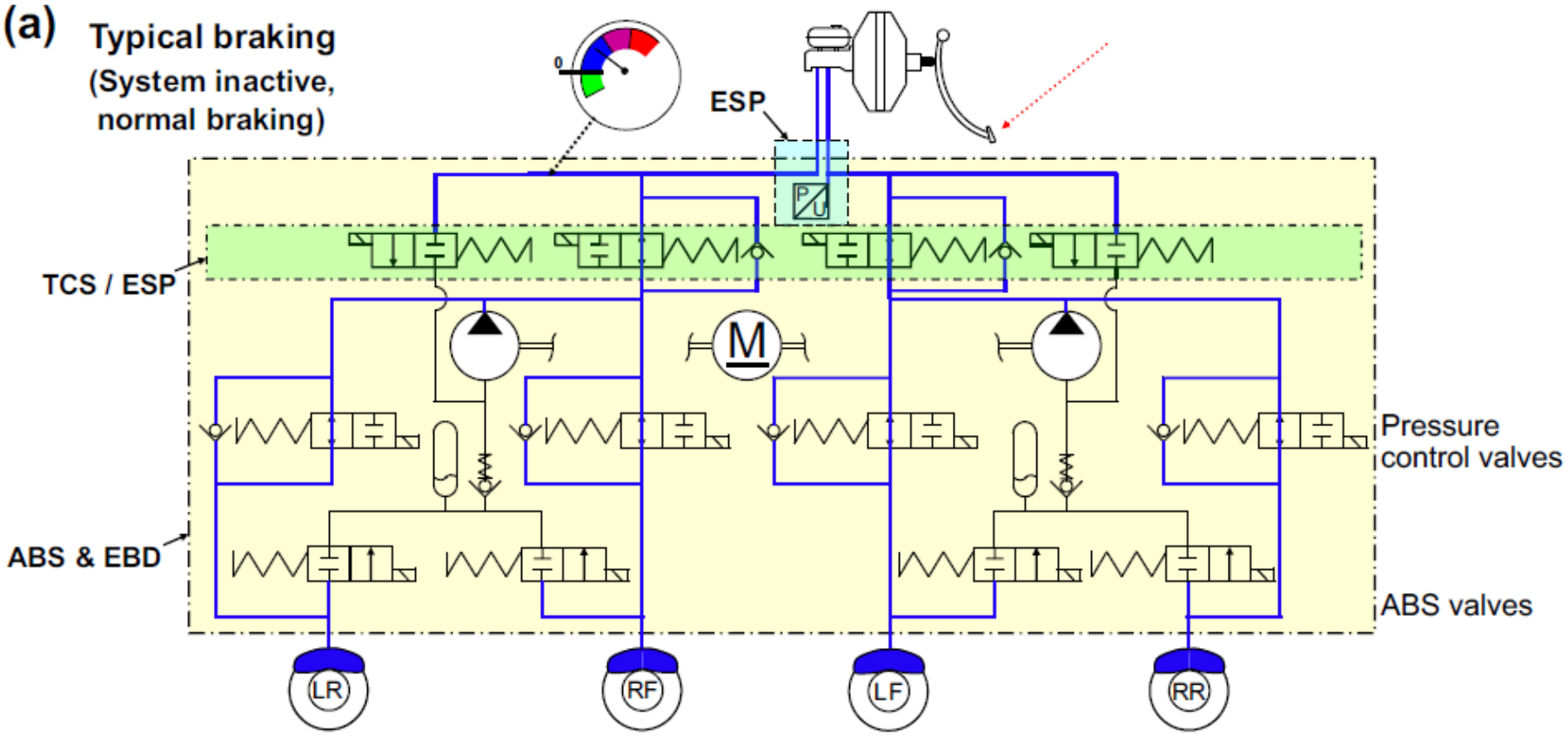

Figure 11.3: (a) Car Braking System (Hydraulic Actuation); Brakes Applied, ABS Inactive.
(b) Car Braking System (Hydraulic Actuation); Brakes Applied, ABS Active (Moore, 2013).

Figure 11.3(b) illustrates how the pressure control valves are closed and the ABS valves are opened, allowing the ABS pump to provide hydraulic actuation pressure to the individual wheel cylinders, which can be modulated as required.

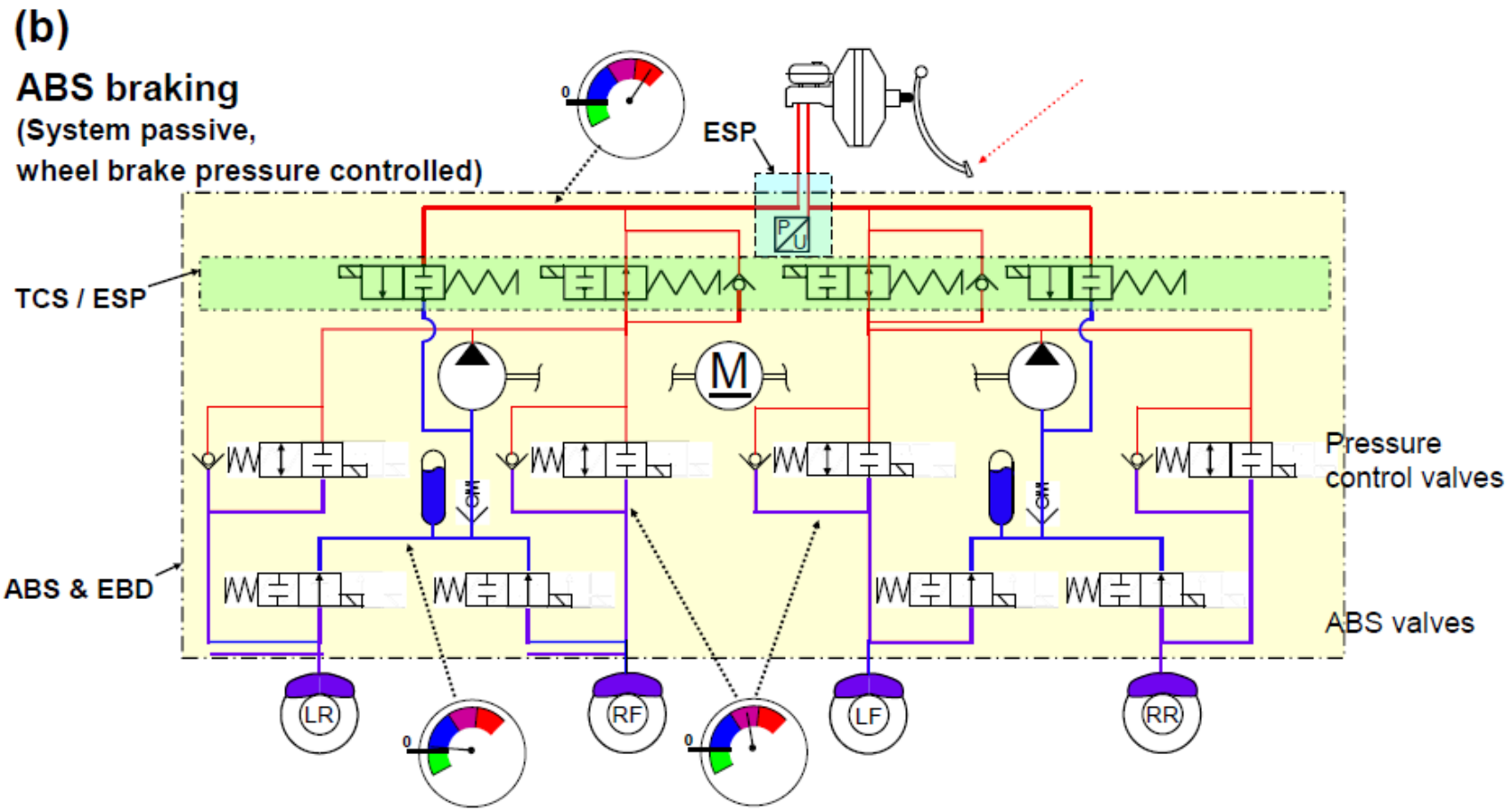

Figure 11.3: (a) Car Braking System (Hydraulic Actuation); Brakes Applied, ABS Inactive. (b) Car Braking System (Hydraulic Actuation); Brakes Applied, ABS Active (Moore, 2013).

All brakes have hysteresis, the amount of which is dependent on the brake type, its design and how well the brake is maintained. Brake hysteresis can be defined as the difference in the input (actuation) torque required to produce either an increase or decrease in generated brake torque when changing state from increasing brake demand to reducing brake demand, and vice versa. Figure 11.4 illustrates this effect for commercial vehicle (air-actuated) systems.

Figure 11.4 illustrates this effect for commercial vehicle (air-actuated) systems.

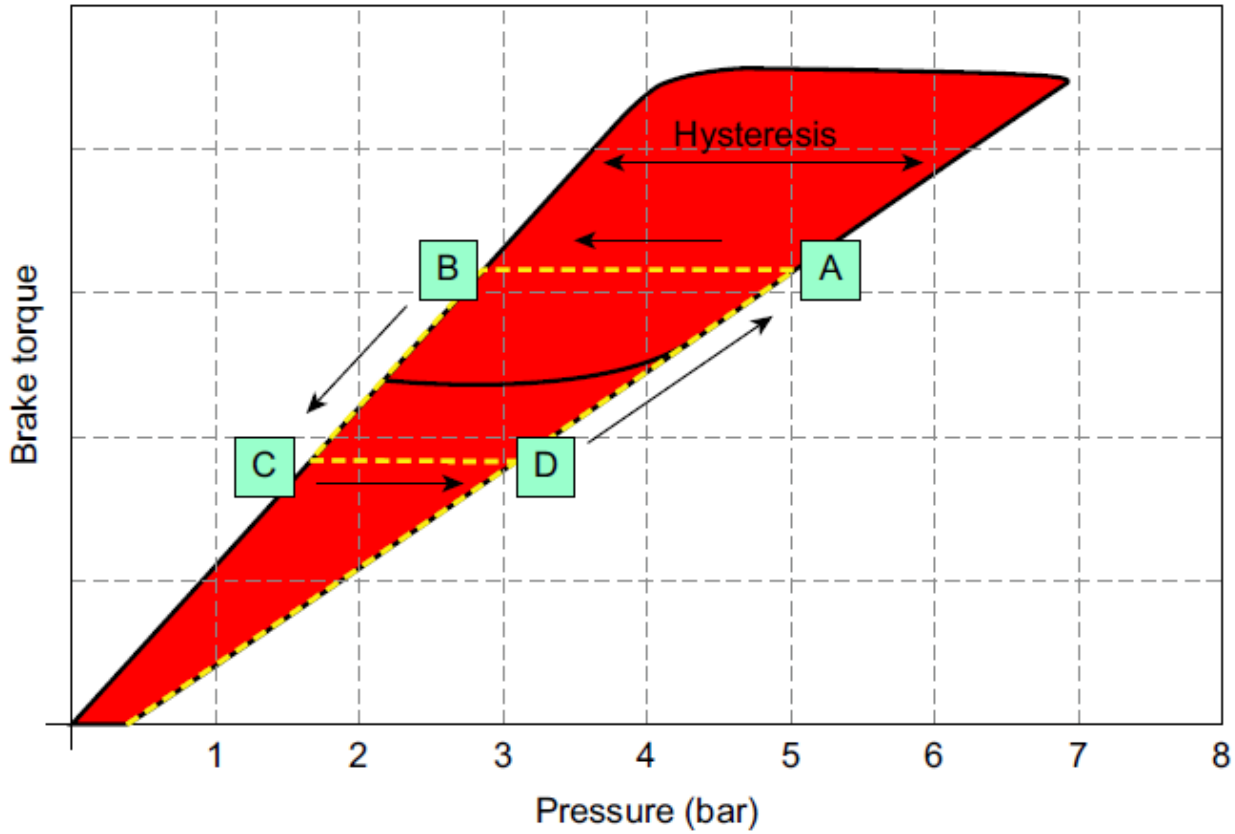

Figure 11.4: Hysteresis in Pneumatic Brake Operation on a Commercial Vehicle (Ross, 2013).

When brake pressure increases there is a corresponding increase in brake torque generated. When ABS cycling commences (point A), actuation pressure is reduced; however, the brake torque generated remains the same until a reduction from 5 to 2.8 bar (point A to B) has been produced, which is equivalent to 44% hysteresis. Equally when the brakes are reapplied, the applied brake pressure must increase from 1.6 to 3.1 bar (point C to D) before there is an increase in the generated brake torque.

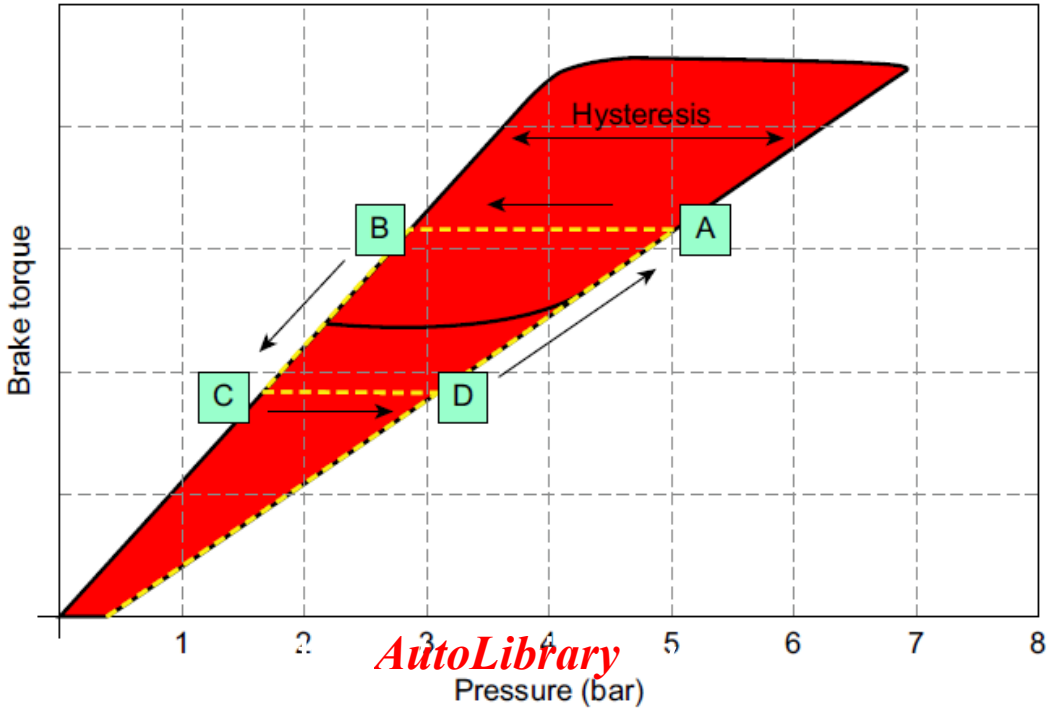

To minimize the effect of brake hysteresis in ABS operation, actuation pressure modulators must be designed for high flow, especially those used in pneumatic braking systems because air is compressible. Also, to ensure that the flow capability of the pressure modulator is fully utilized the flow from the pressure modulator(s) to the brake actuator(s) must be maximized.

During brake reapply with pneumatic systems, one way of allowing for system hysteresis is a rapid pressure rise (primary rise) followed by a slower pressure rise (secondary rise) to move through the optimum slip band relatively slowly, as illustrated in Figure 11.5.

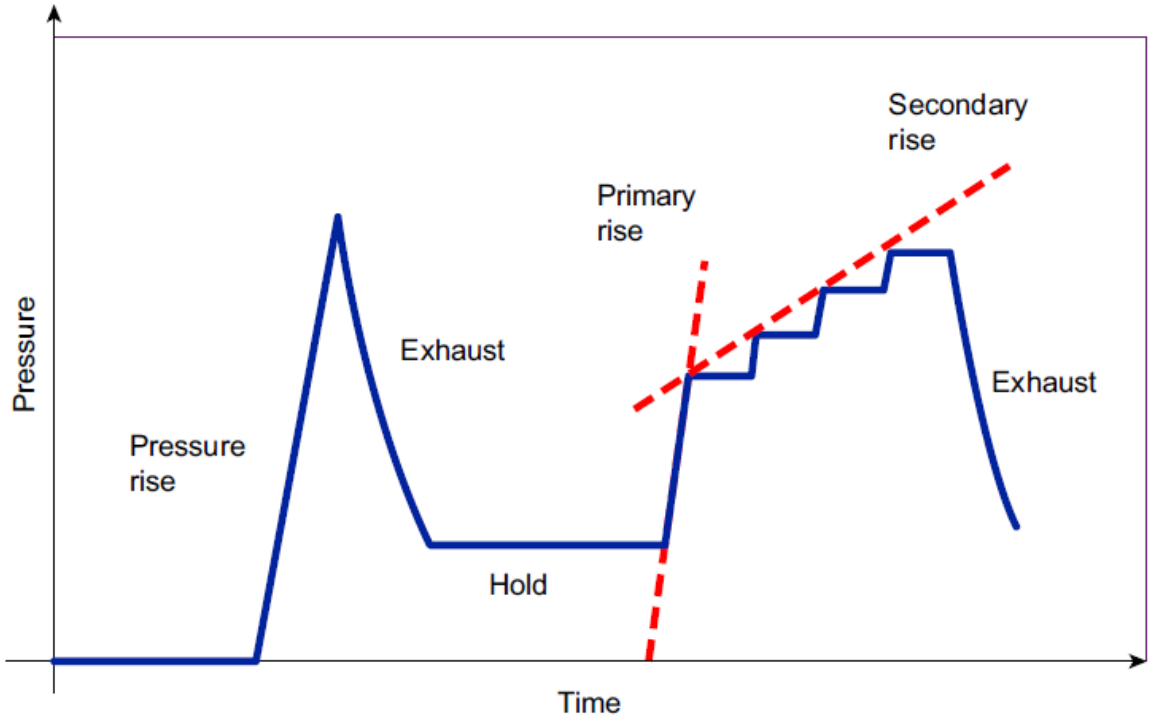

Figure 11.5: 'Ideal' Pneumatic Actuation Pressure Characteristic Showing a Rapid Primary Rise Followed by a Slower Secondary Rise (Ross, 2013).

Measurement of ABS Efficiency

The braking performance of a road vehicle is usually defined in terms of minimum stopping distances and/or minimum mean fully developed deceleration (MFDD), but neither of these criteria is suitable to define the braking performance of a road vehicle when the ABS is operating. This is because both stopping distance and MFDD assume that the tyre/road adhesion is sufficient to generate the r the vehicle's braking performance depends upon the vehicle braking system design and specification.equired rate of braking and thus

A basalt surface is usually used for low-adhesion ABS tests; this requires water to reduce the adhesion but near 100% wheel slip the adhesion increases as illustrated in Figure 11.6. As a result the ratio of the peak adhesion to the adhesion at 100% wheel slip is often very close to the minimum value of 1.

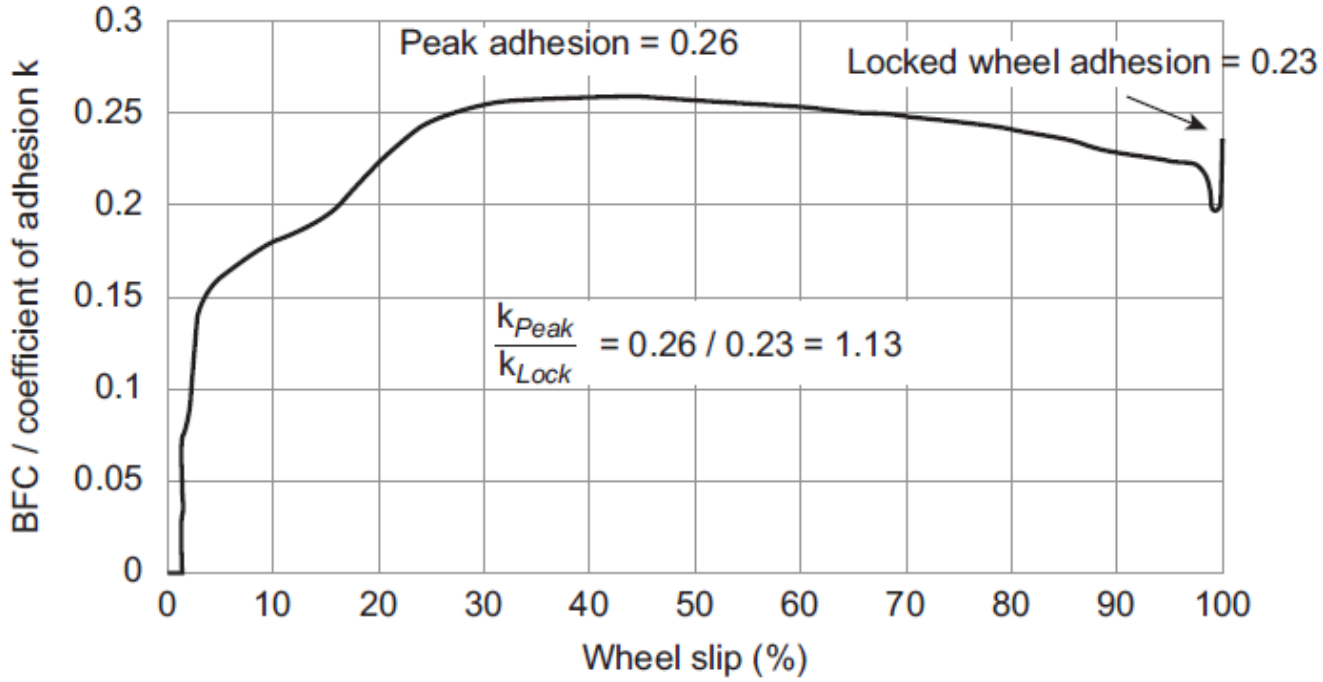

Figure 11.6: Tyre/Road Characteristics of Wet Basalt (Ross, 2013).

A methodology for measuring the ABS efficiency of any road vehicle is presented here which has two parts: measurement of the ABS braking performance of the road vehicle, and measurement of the peak adhesion value. When measuring the ABS performance, only that part of the braking event when the ABS is in control of the wheels must be considered; when the brakes are first applied the ABS is not in control because the actuation pressure rise at the start of the brake application is very rapid, which results in high wheel deceleration and slip.

After the ABS has reacted to the condition and started to control the wheels, assessment of the system performance can be commenced. Similarly, when the vehicle road speed approaches zero, wheel slip cannot be accurately evaluated (see Figure 11.7), and so this part of the braking event should also not be included.

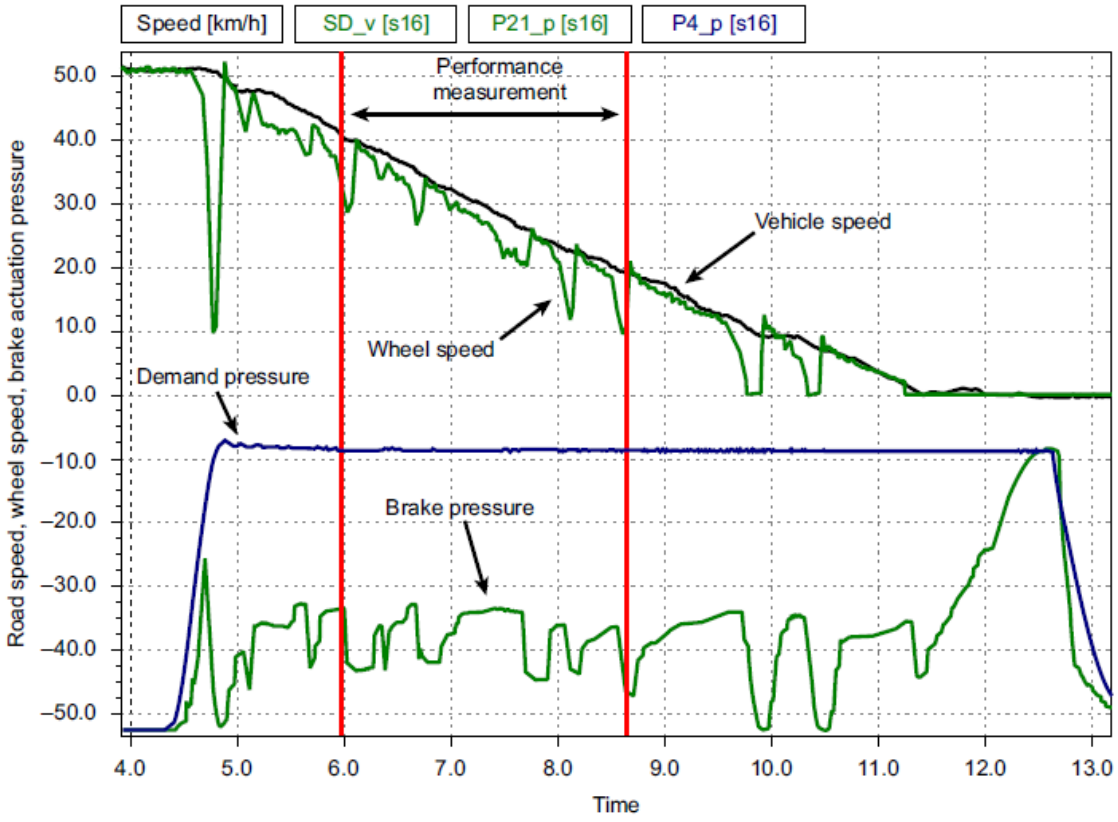

Figure 11.7: Vehicle Speed, Wheel Speed and Brake Actuation Pressure vs. Time During ABS Operation (Ross, 2013).

The test procedure for measuring ABS performance is summarized below, with the set speed parameters listed in Table 11.1.

Table 11.1: Speed Parameters for ABS Performance Measurement

ABS Performance; Measured Speed Parameters	Solo or Towing Vehicles	Trailers*
Speed at which the brakes are first applied (km/h)	55	50
Speed at which ABS performance measurement commences (km/h)	45	40
Speed at which ABS performance measurement ceases (km/h)	15	20

*Trailers have different test measurement speeds as only the trailer is braked and must also decelerate the unbraked mass of the towing vehicle.

The level of deceleration produced must allow the ABS to cycle fully, e.g. a front axle may commence ABS cycling but as dynamic load transfer occurs the load on that axle increases and slip is reduced.

- • Approach the test area at a speed above the brake apply speed.
- • Disengage the engine (select neutral gear) and coast to the required brake apply speed (Table 11.1).
- • Apply the brakes.

The data to be recorded include:

- • Vehicle speed
- • Wheel rotational speed (all wheels)
- • Driver demand (e.g. hydraulic or pneumatic actuation system pressure at the control)
- • Actuation pressure at each brake actuator.

Measurement of the peak adhesion value for the vehicle (k_M) starts with measuring the peak adhesion for the front and rear axles independently. The actuation pressure to the braked axle is gradually increased until the time to decelerate between two speeds (as shown in Table 11.2) without wheel lock is minimized.

Table 11.2: Speed Parameters for Peak Adhesion Measurement

ABS Performance Measurement Speed Parameters	Solo or Towing Vehicles	Trailers
Speed at which the brakes are first applied (km/h)	50	50
Speed at which peak adhesion measurement commences (km/h)	40	40
Speed at which peak adhesion measurement ceases (km/h)	20	20

The adhesion utilization at each wheel on any axle will always be different because of side-to-side differences in the adhesion coefficient (k), the actual brake performance the ABS performance measurement individual actuation pressure adjustment to each brake on the axle is needed. The test procedure is:

- For all vehicle types apply the brakes at an initial speed of 50 km/h.
- Record the time to decelerate the vehicle from 40 to 20 km/h without wheel lock.

An example of the type of data recorded during peak adhesion measurement on a commercial vehicle fitted with pneumatic brake actuation is illustrated in Figure 11.8.

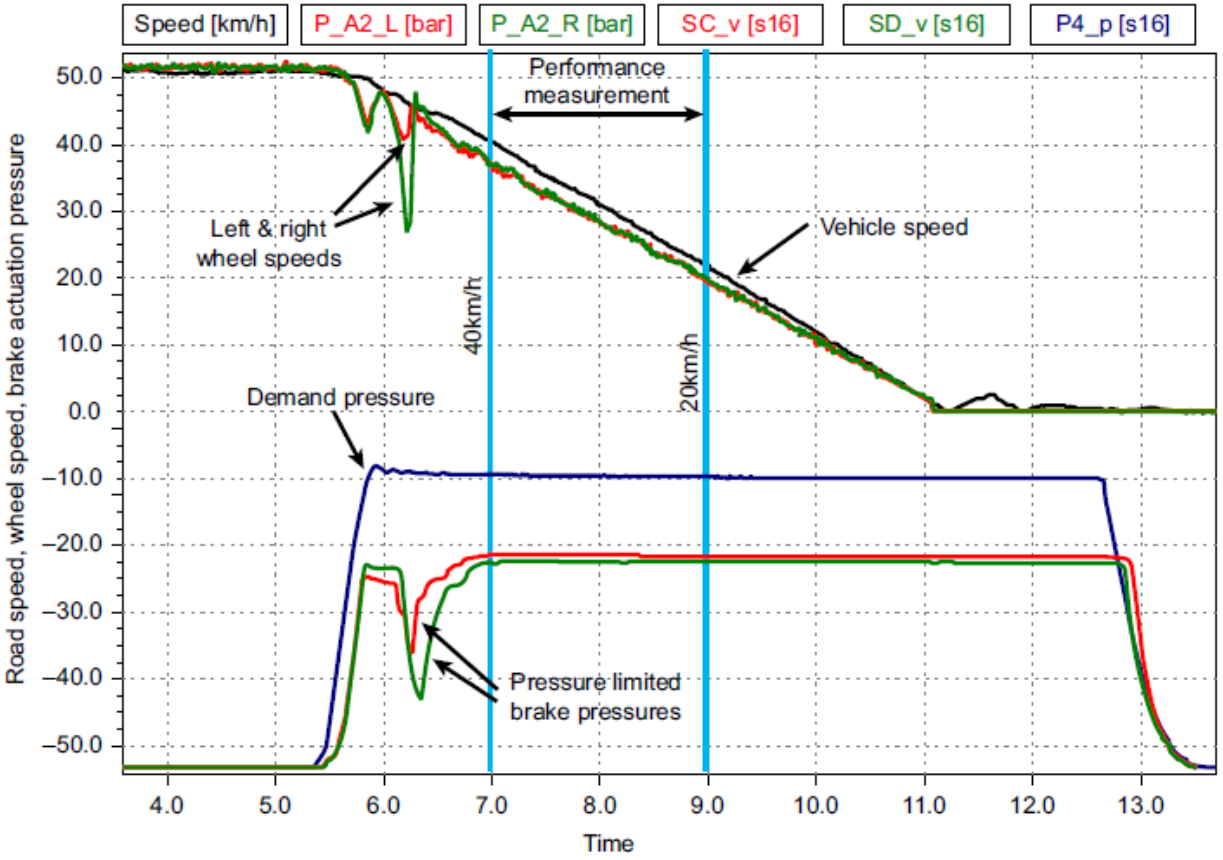

Figure 11.8: ABS Operates to Control Initial Wheel Deceleration on Brake Application but is not Operating Between the Speeds ABS Performance is Measured (Ross, 2013).

In comparison, Figure 11.9 illustrates a situation where ABS cycling restarts below 20 km/h, but again the ABS is not operating during the 20-40 km/h speed measuring range.

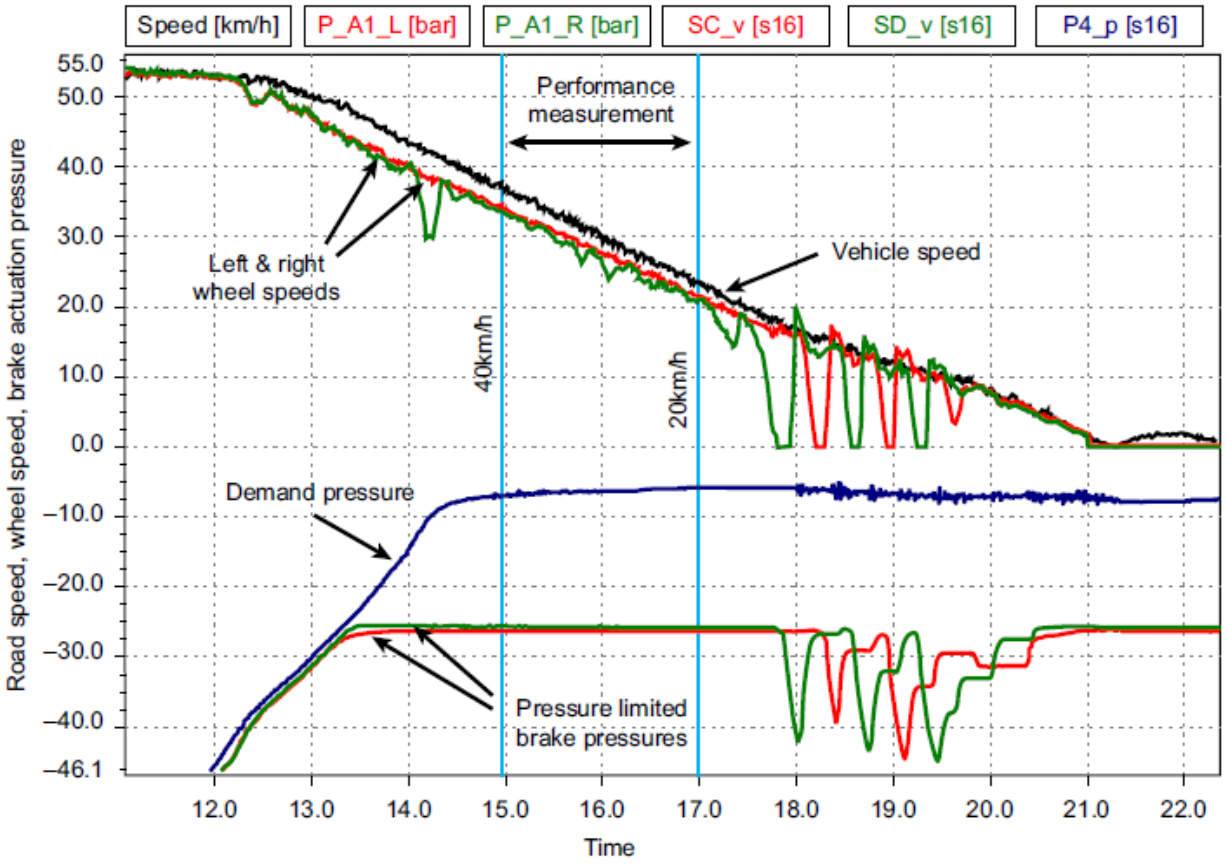

Figure 11.9: ABS Operates Below 20 km/h but is not Operating Between the Speeds ABS Performance Is Measured (Ross, 2013).

The peak adhesion deceleration for each axle can be calculated as follows:

$$z_m = 0.566/t_m \qquad (11.3)$$

where:

z_m is the rate of braking of the vehicle;

t_m is the minimum deceleration time measured between 40 and 20 km/h.

To determine the peak adhesion rate of braking from the vehicle rate of braking (z_m) the rolling resistance of the unbraked wheels and the dynamic load transfer to or from the axle under test must be taken into account. For a front axle:

$$k_f = \frac{\left[z_m Mg - (\text{Rolling resistance of unbraked rear axle} \cdot P_2)\right]}{\left[P_1 + \left(\frac{h}{E}\right) z_m Mg\right]} \qquad (11.4)$$

And for a rear axle:

$$k_r = \frac{\left[z_m Mg - (\text{Rolling resistance of unbraked front axle} \cdot P_1)\right]}{\left[P_2 - \left(\frac{h}{E}\right) z_m Mg\right]} \qquad (11.5)$$

The rolling resistance is specified as the rate of braking (z) of the vehicle attributed to each axle, which is defined in UN Regulation 13 as:

- Driven axle =0.015
- Non-driven axle

To determine the ABS efficiency, the times from three tests for the vehicle to decelerate from 45 to 15 km/h are averaged (t_m) and the average rate of braking (z_{AL}) is calculated from: = 0.010.

$$z_{AL} = \left(\frac{0.849}{t_m}\right) \qquad (11.6)$$

Using the braking rate (zAL) the respective dynamic axle loads are calculated using Equations (11.7) and (11.8) (see Equations (3.2) and (3.3)):

$$\text{Front axle:} \qquad N_1 = P_1 + P z_{AL} \frac{h}{E} \qquad (11.7)$$

$$\text{Rear axle:} \qquad N_2 = P_2 - P z_{AL} \frac{h}{E} \qquad (11.8)$$

The peak adhesion braking rates for the front axle (k_f) and rear axle (k_r) are then weighted according to the dynamic load distribution using Equation (11.9) to produce a peak adhesion braking rate for the whole vehicle (k_M):

$$k_M = \frac{k_f N_1 + k_r N_2}{P} \qquad (11.9)$$

The ABS braking efficiency (h) is then determined from Equation (11.10), and must be at least 0.75 (laden and unladen) e see Equation (11.2).

$$\eta = \frac{z_{AL}}{k_M} \qquad (11.10)$$

Traction Control System (TCS)

Traction control (TCS) is a stability control feature closely associated with ABS. It allows brake actuation pressure to be generated to brake a driven wheel to prevent it spinning when peak adhesion has been lost during acceleration, and thus maintain traction by transferring the drive torque to another drive wheel that does have full adhesion. Communication with the engine control unit is essential, so the ESC controller also requests engine torque reduction during a traction control event; thus TCS control is more complicated than ABS control.

The advantage of TCS is that it allows optimized vehicle acceleration, but the disadvantage is that it increases brake usage, which can in turn increase friction material and rotor wear, reducing brake life. The operation of TCS is illustrated in Figure 11.10 for a front wheel drive (FWD) car; in the event of wheel spin the pressure control valves to the front brakes are closed and the ABS valves are opened, allowing the ABS pump to provide hydraulic actuation pressure to the front brake wheel cylinders, which can be modulated as required.

The operation of TCS is illustrated in Figure 11.10 for a front wheel drive (FWD) car

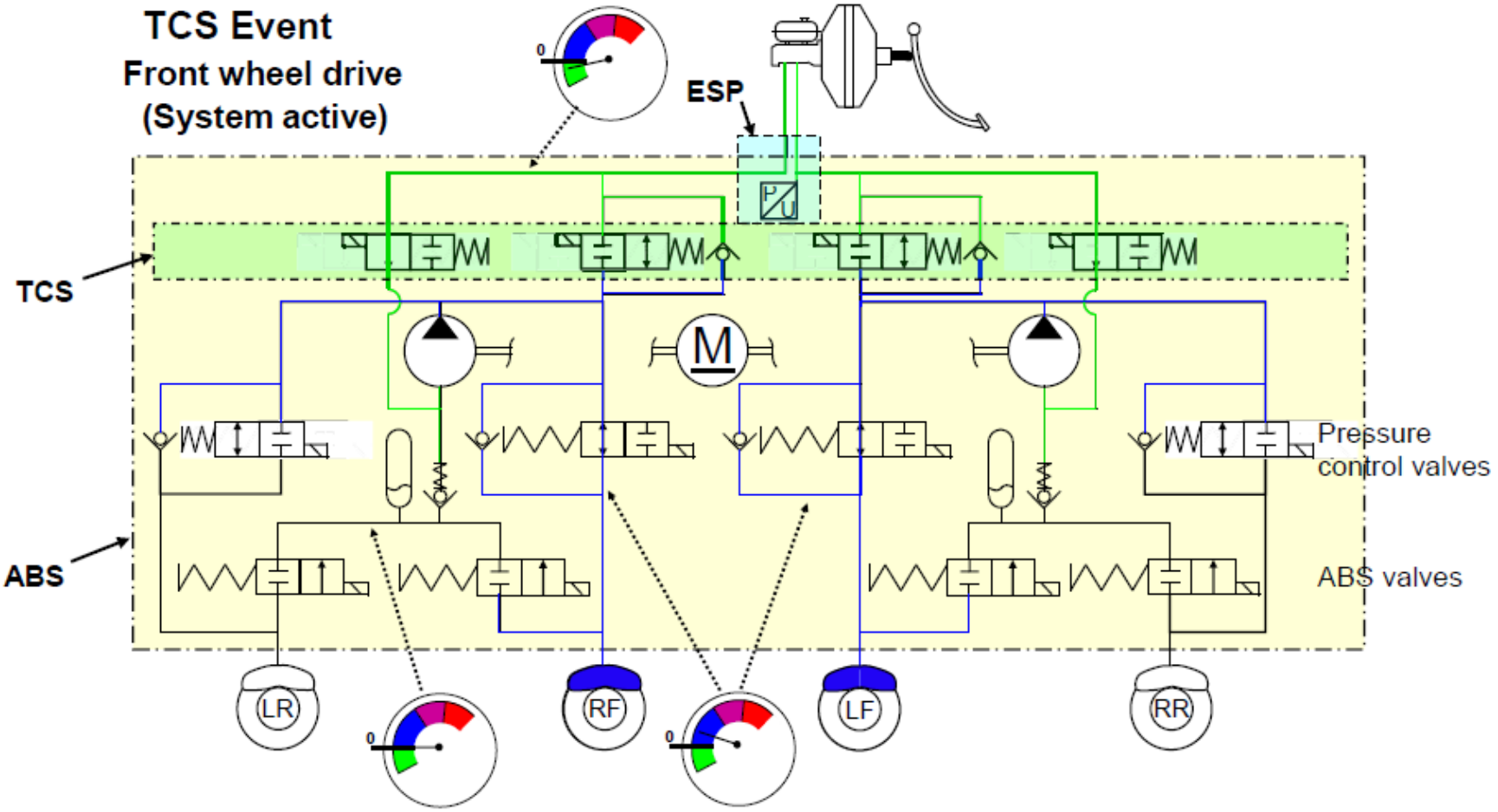

Figure 11.10: Car Braking System (Hydraulic Actuation), TCS Active (Moore, 2013).

The basic TCS logic to control wheel spin is therefore as follows:

Single spinning wheel (split-m surface):

- Apply brake to spinning wheel to bring wheel under control
- Use a combination of engine control and brake to prevent either wheel from spinning.

Single spinning wheel (uniform adhesion surface):

- Control wheel slip by engine control only (applying the brake to the spinning wheel simply causes the opposite wheel to spin).

Two spinning wheels (homogeneous surface):

- Control wheel slip by engine control only.

Electronic Stability Control (ESC)

Following recommendations of many studies and statistics, stability control has become a standard feature in Europe, North America and Canada. The North American FMVSS126 legislation mandated ESC by September 2011 for all new vehicles with a mass less than 4.5 tones, and in Europe standard requirements for stability control will be fully implemented in 2014 (see Table 8.1). Many passenger cars have already had some form of ESC or 'roll stability control' (RSC) fitted as standard to improve their dynamic stability, especially to prevent rollover of high center of gravity vehicles such as MPVs and SUVs.

In terms of vehicle handling, specifically directional control, if a road vehicle does not respond to the commands of the driver then at least one of the following parameters has been exceeded:

- High wheel slip that indicates that the braking force has exceeded the tyre/road adhesion.
- High wheel slip that indicates that the traction force has exceeded the tyre/road

adhesion.

- High slip angle that indicates that the sideways forces have exceeded the available lateral adhesion.

The first two can be controlled by ABS and TCS respectively but the third requires stability control. The maximum lateral and longitudinal forces that can be generated at any tyre/road interface are limited by the total adhesion as illustrated in Figure 11.11

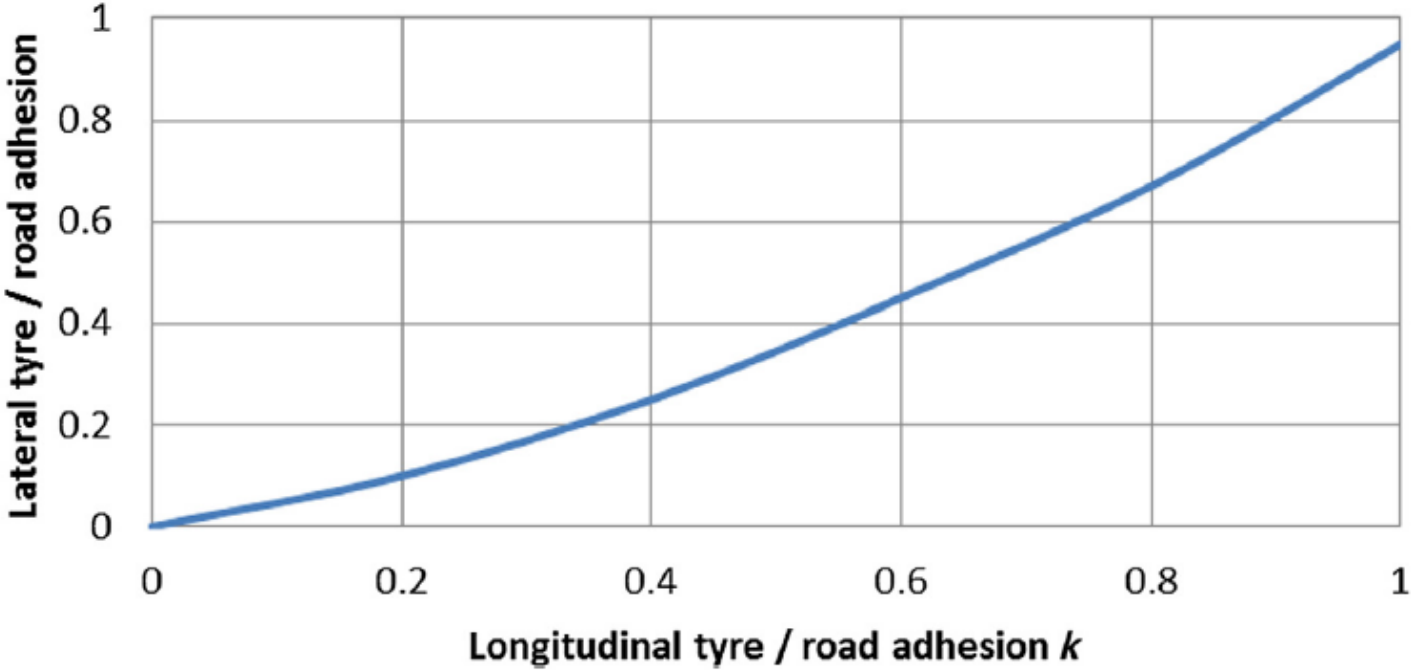

Figure 11.11: Illustration of the Relationship Between Maximum Lateral and Longitudinal Tyre/Road Adhesion.

Figure 11.12 illustrates how an ESC system on a two-axle rigid vehicle addresses understeer; as the vehicle drifts outwards while cornering, the brake on the inside rear wheel is actuated to provide an opposing yaw moment, which returns the vehicle to the desired trajectory.

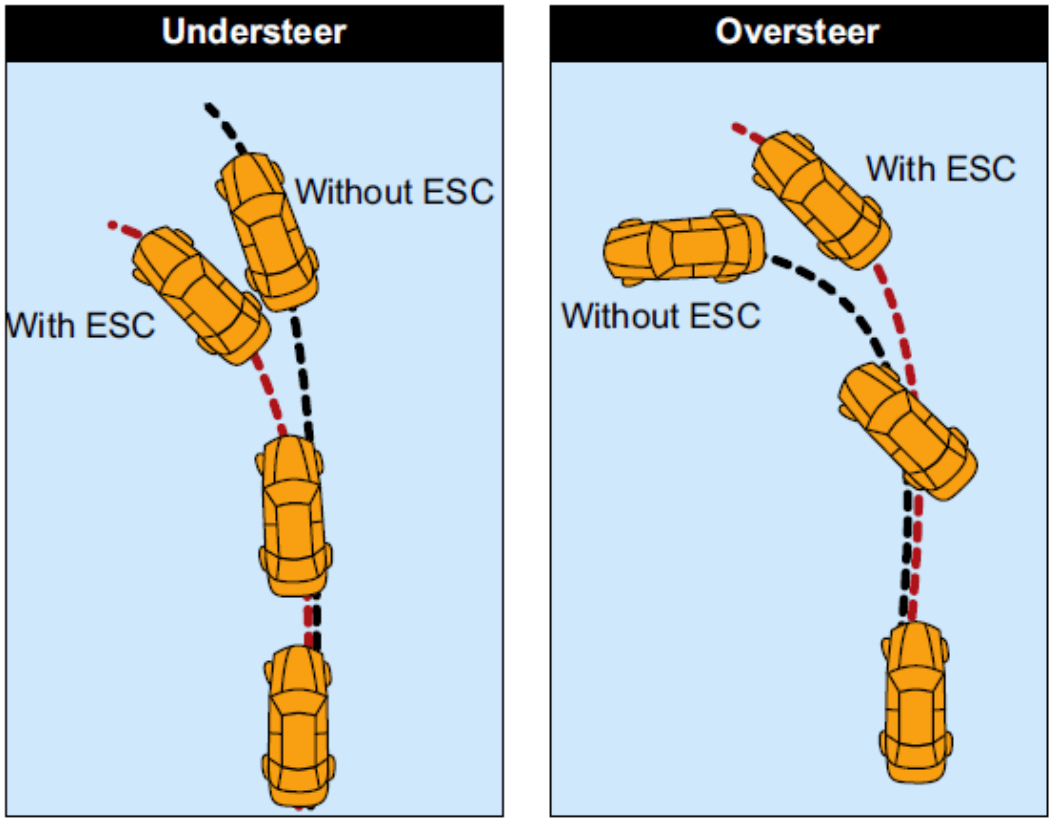

Figure 11.12: ESC Operation To Correct Oversteer And Understeer. *(Adapted from Continental)*

Additional capabilities that can be provided by the ESC function include:

- Emergency brake assist: increasing brake pressure when emergency actuation is detected.
- Adaptive cruise control interface: smooth pressure modulation according to cruise control requirements.
- Failed booster support/cold start support/overboost by pressure increase by ESC in the cases of insufficient or no vacuum, recognised for example by a vacuum sensor or differential travel sensor.

The operation of ESC on a passenger car with a hydraulic braking system is illustrated in Figure 11.13.

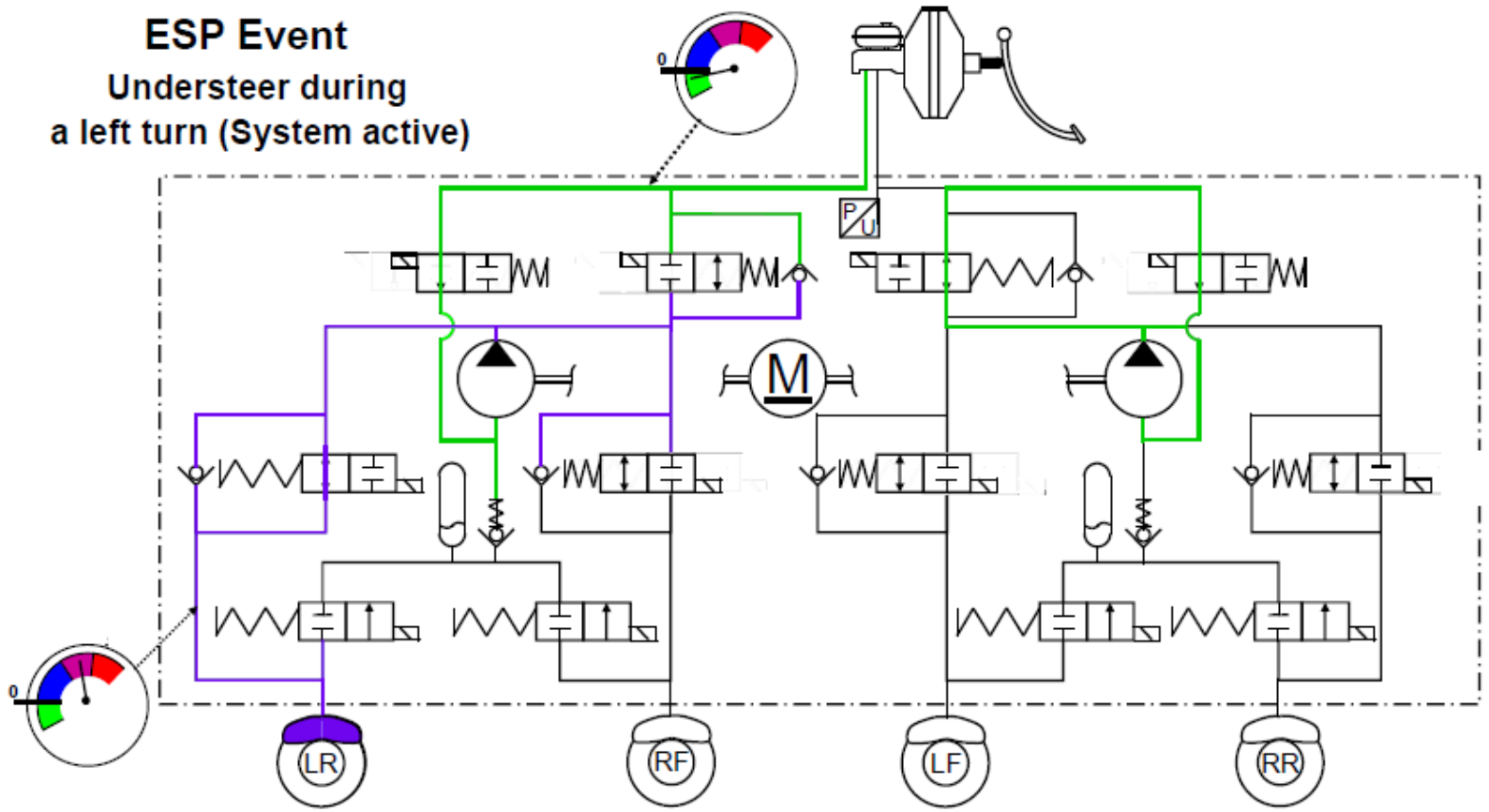

Figure 11.13: Car Braking System (Hydraulic Actuation), ESC Active (Moore, 2013).

This illustrates how the pressure control valves to the brakes are open to allow the driver to apply the brakes, but in the case illustrated no actuation pressure is generated by the driver's muscular effort. However, the ECU has detected that a brake intervention is required (to the left rear brake) and the hydraulic pump is activated, which creates the required hydraulic pressure.

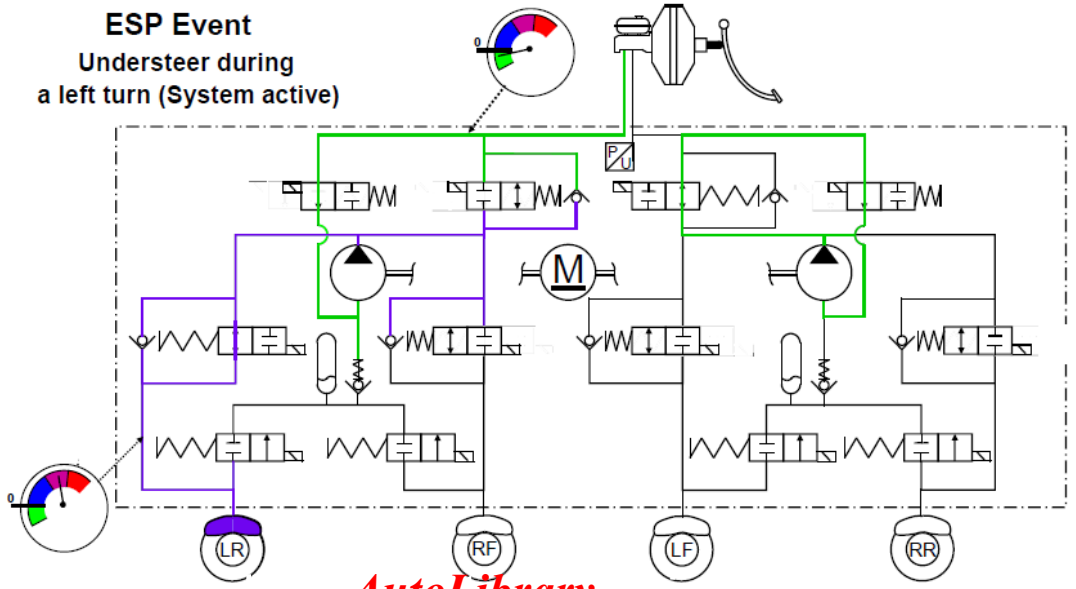

Figure 11.13: Car Braking System (Hydraulic Actuation), ESC Active (Moore, 2013).

On commercial vehicles with pneumatic brake actuation and electronic control, an ESC system (often termed ‘Electronic Stability Program’ or ESP on commercial vehicles) has a central ECU, which receives the driver demand from a footbrake module as illustrated in Figure 11.14.

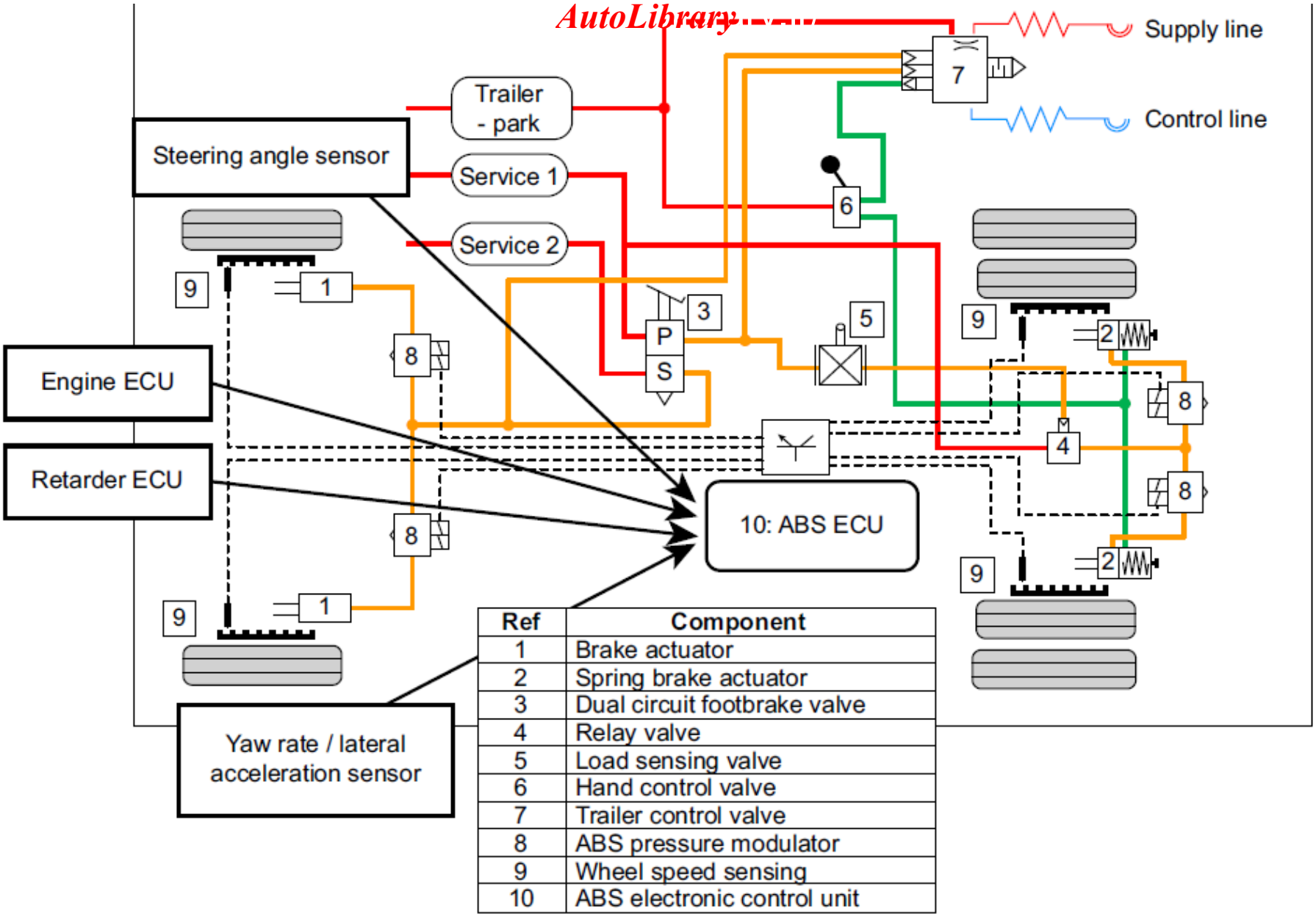

Ref	Component
1	Brake actuator
2	Spring brake actuator
3	Dual circuit footbrake valve
4	Relay valve
5	Load sensing valve
6	Hand control valve
7	Trailer control valve
8	ABS pressure modulator
9	Wheel speed sensing
10	ABS electronic control unit

Figure 11.14: Commercial Vehicle Pneumatic Braking ESC System (Compare with Figure 6.19(a)) (Ross, 2013).

This controls, via a controller area network (CAN) databus, the 'brake apply' modules at each axle, which perform the following functions:

- Ensure air pressure is available to actuate the brakes (from the pressure supply/reservoir/ storage system)
- Specify and generate the required actuation brake pressure at the selected brake
- Hold or exhaust actuation pressure at the selected brake
- Measure brake pressures and wheel speeds.

The correction of the loss (or imminent/anticipated loss) of directional control by the driver of a commercial vehicle is similar to the ESC control actions outlined previously for a passenger car. Oversteer and understeer correction in a commercial vehicle tractor/semi-trailer articulated combination is illustrated in Figures 11.15 and 11.16.

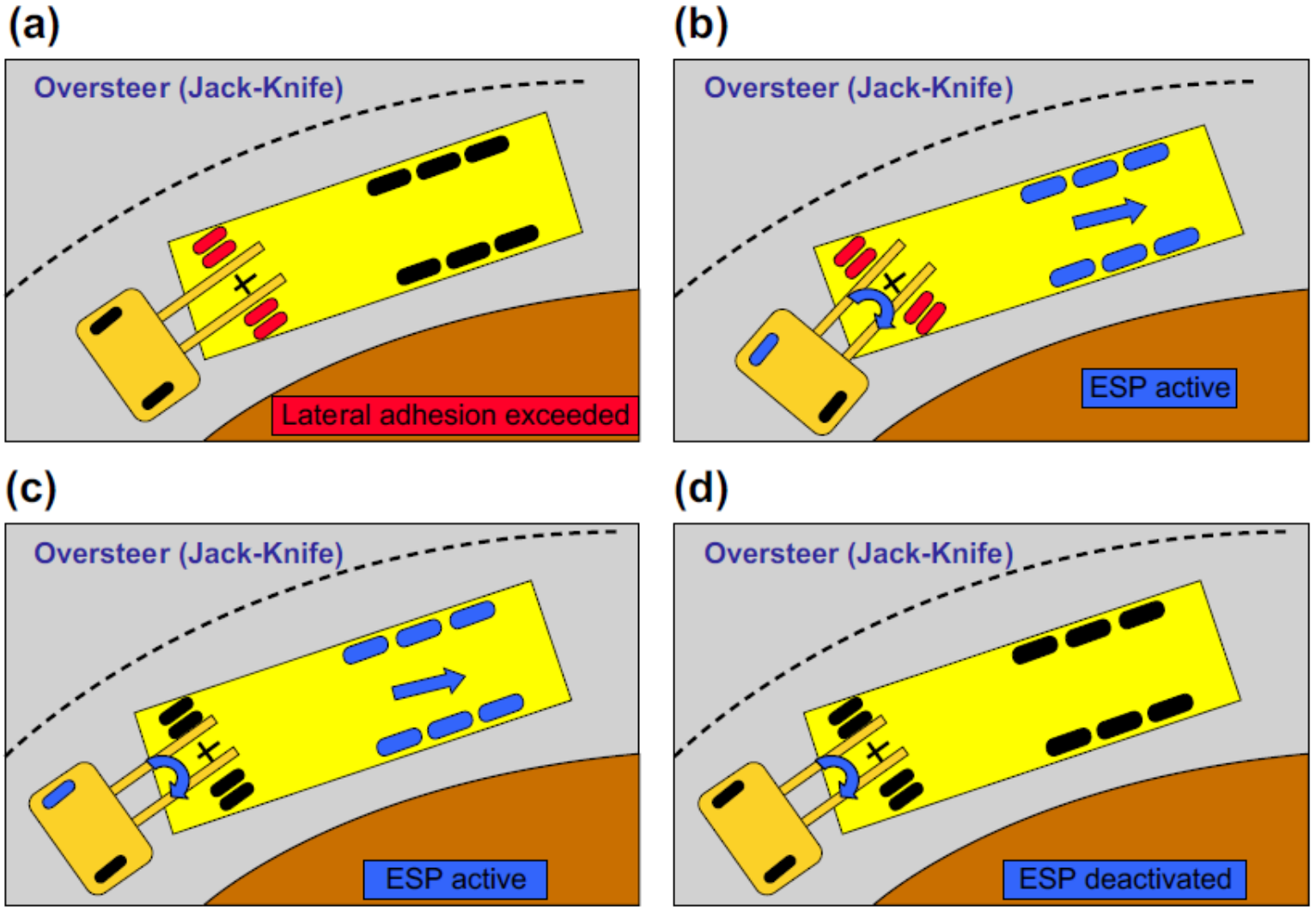

Figure 11.15: Correction of Oversteer by ESC/ESP in a Commercial Vehicle Tractor/Semi-Trailer Articulated Combination (Ross, 2013).

Semi-trailer tractors generally have a short wheelbase that, combined with the effect of the trailer, makes them very sensitive to oversteer once lateral adhesion of the tractor drive axle has been exceeded. The ESC correction phase sequence for oversteer (see Figure 11.15) is:

(a) Vehicle sensors detect oversteer

(b) ESP active, tractor front right brake applied to counter initial yaw, trailer brakes

applied to stretch combination

(c) Brake intervention stabilizes tractor and reduces combination speed

(d) Stability retained, ESP deactivated.

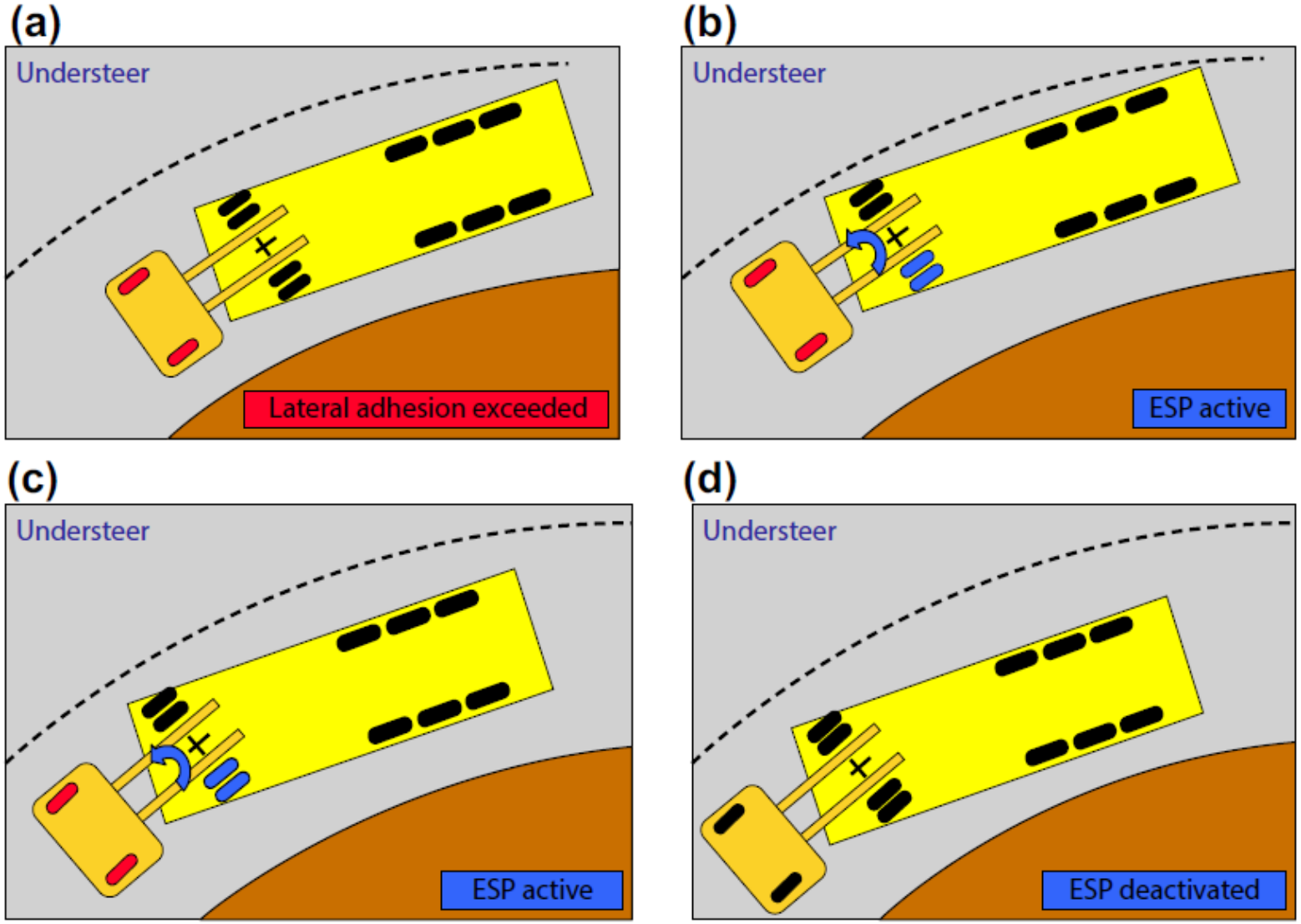

Figure 11.16: Correction of Understeer by ESC/ESP in a Commercial Vehicle Tractor/Semi-Trailer Articulated Combination (Ross, 2013).

The ESC correction phase sequence for understeer (see Figure 11.16) is:

(a) Vehicle sensors detect understeer

(b) ESP active, tractor rear left brake applied to induce opposing yaw moment

(c) Brake intervention modifies vehicle behaviour to maintain directional control

(d) Stability retained, ESP deactivated.

Rollover Stability Control (RSC)

ESC sensors can also be used to recognize conditions that might lead to vehicle rollover, and initiate brake interventions to prevent it as far as possible, thus providing rollover protection. This feature is known by various names including Roll Stability Control (RSC), Roll Stability Program (RSP), Active Rollover Mitigation (ARM) and Rollover Mitigation (ROM). The purpose is to detect a potential vehicle rollover condition and reduce the risk of rollover occurring by slowing down the vehicle and generating understeer via brake intervention to reduce the vehicle's radial acceleration and hence lateral forces, e.g. by applying the brakes on the outside front wheel.

Commercial vehicles with a high center of gravity are particularly susceptible to rollover, and semi-trailer combinations are most at risk of rollover initiated from the trailer. Additionally, as in the case of semi-trailer combinations, the driver can be remote from what is happening at the trailer and therefore unlikely to become aware of impending instability until it is too late. Rollover of a heavy commercial vehicle is very serious and can have very severe consequences in terms of danger to life, effect on the environment and traffic flow, and repair costs.

Sideways inertia forces act through the vehicle's center of gravity and are resisted by the lateral adhesion forces at the tyre/road interfaces, as illustrated in Figure 11.17 (see also Figure 3.6).

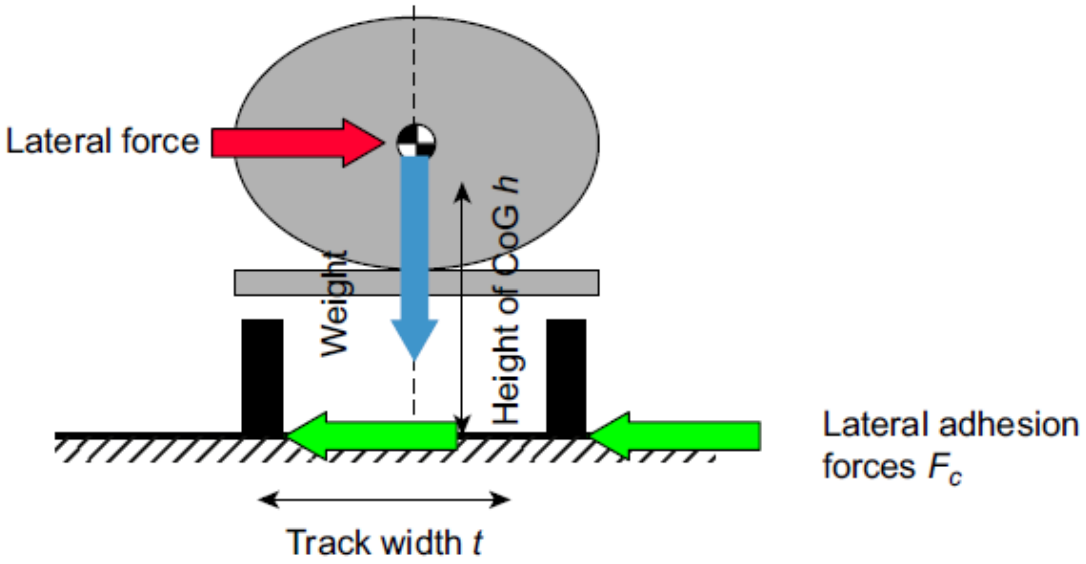

Figure 11.17: Force System in Vehicle Rollover.

If the lateral force exceeds the maximum lateral adhesion force at the wheels, the vehicle will skid rather than roll. The rollover susceptibility therefore depends on three design parameters: height of the center of gravity, longitudinal position of the center of gravity (position of the load center of gravity) and the 'effective track'. Because semi-trailers are coupled to the tractor via the coupling (kingpin or fifth wheel), the effective track depends upon the position of the trailer center of gravity, as illustrated in Figure 11.18.

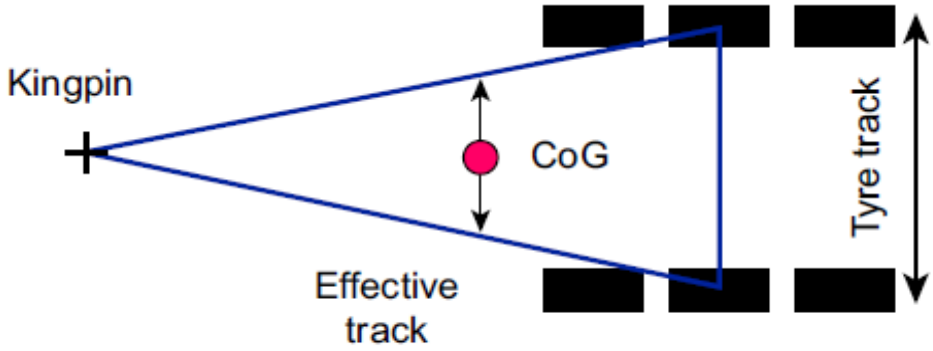

Figure 11.18: Effective Track of a Semi-Trailer.

The most stable condition to reduce the possibility of rollover is for the CoG to be over the rear of the trailer with no load on the coupling, but this is an undesirable arrangement that could have an adverse effect on the dynamic handling and stability of the combination during normal driving and braking because of the increased possibility of yaw oscillations and jack-knife.

Other factors that affect the susceptibility of articulated semi-trailer vehicle combinations to rollover include:

- Road camber
- Coupling position and design
- Suspension roll stiffness
- Chassis torsional stiffness
- Tyre pressures
- Load shift
- Roll center position.

Any automatically commanded brake control system must have at least one threshold to pass before it can become active. If the threshold is set too low the system will intervene prematurely and cause driver dissatisfaction, and if it is set too high the intervention may be too late. Many ESC and RSC systems incorporate some learning function in their control logic, e.g. to establish the load distribution or position of the center of gravity, in order to be able to improve the interpretation of the sensor data, as illustrated below:

- ✓ System passive: continuously monitors information from vehicle sensors, checks for potential rollover and compares with predefined threshold.

- ✓ Detect potential rollover: the indicated lateral acceleration has exceeded the threshold value.
- ✓ Automatic brake application: automatically generates a low actuation pressure in the brakes.
- ✓ Check wheel response: ABS wheel speed sensors provide information to decide whether the vehicle is approaching a critical rollover state, involving either of the following:
  - ➢ No wheel response: the inside wheels are not decelerating, which indicates that the trailer is not in a critical rollover condition. The detection threshold is modified and the system returns to passive mode.
  - ➢ Wheel response: the inside wheel(s) decelerate due to lateral load transfer, reducing the inside wheel load, indicating imminent rollover.

- ✓ Brake application: the brakes of the tractor and/or trailer are automatically applied. In the case of motor vehicle systems engine power is also reduced.

- ✓ Speed reduction: the reduction in speed due to the application of the brakes reduces the lateral acceleration.

- ✓ Stability maintained: the reduction in lateral acceleration results in the stability of the vehicle/trailer being maintained.

- ✓ System passive: after the brake intervention and reduction in lateral acceleration the brakes that have been applied are released and the system returns to a passive mode.

Electronic Brakeforce Distribution (EBD)

EBD systems control the balance between the brake forces on different axles to optimize braking efficiency across all vehicle loading and driving conditions. It has the advantage of being able to sense and control the amount of braking applied to an axle more accurately in proportion to the dynamic axle load. Wheel speed sensor information is used to detect circumferential tyre slip on the front and rear axles, and when a defined rear tyre slip level is exceeded, the actuation pressure to the rear wheels is limited or reduced.

The way EBD works can be explained as follows for the simplest case of a two-axle rigid vehicle. If the rotational speeds of the front and rear wheels are ω_1 and ω_2 respectively, the differential slip (dQ) can be calculated from:

$$dQ = (\omega_1 - \omega_2)/\omega_1 \qquad (11.12)$$

A braking control system based on differential slip would then individually control the actuation pressure (pneumatic or hydraulic) applied to the brakes on each axle to minimize the differential slip, thereby ensuring that the wheels are operating in the same region of the adhesion/slip curve; i.e. they are being braked in proportion to the dynamic normal forces on the wheels.

Emergency Brake Assist (EBA)

As discussed above with RSC, reducing the vehicle speed as quickly as possible has many advantages in avoiding or reducing the severity of dynamic instabilities in motor vehicles; if nothing else it will reduce the kinetic energy prior to a collision. Brake interventions initiated by an ESC system operate at a much faster response time than can be achieved by a human driver, and Emergency Brake Assist (EBA) is a generic name for the way in which some of the features of ESC can be utilized to help the driver brake faster and more effectively in an emergency.

The requirement for brake assist is a part of the European pedestrian protection legislation, and recognizes that often in a panic situation the driver may brake quickly but insufficiently (see Figure 11.19).

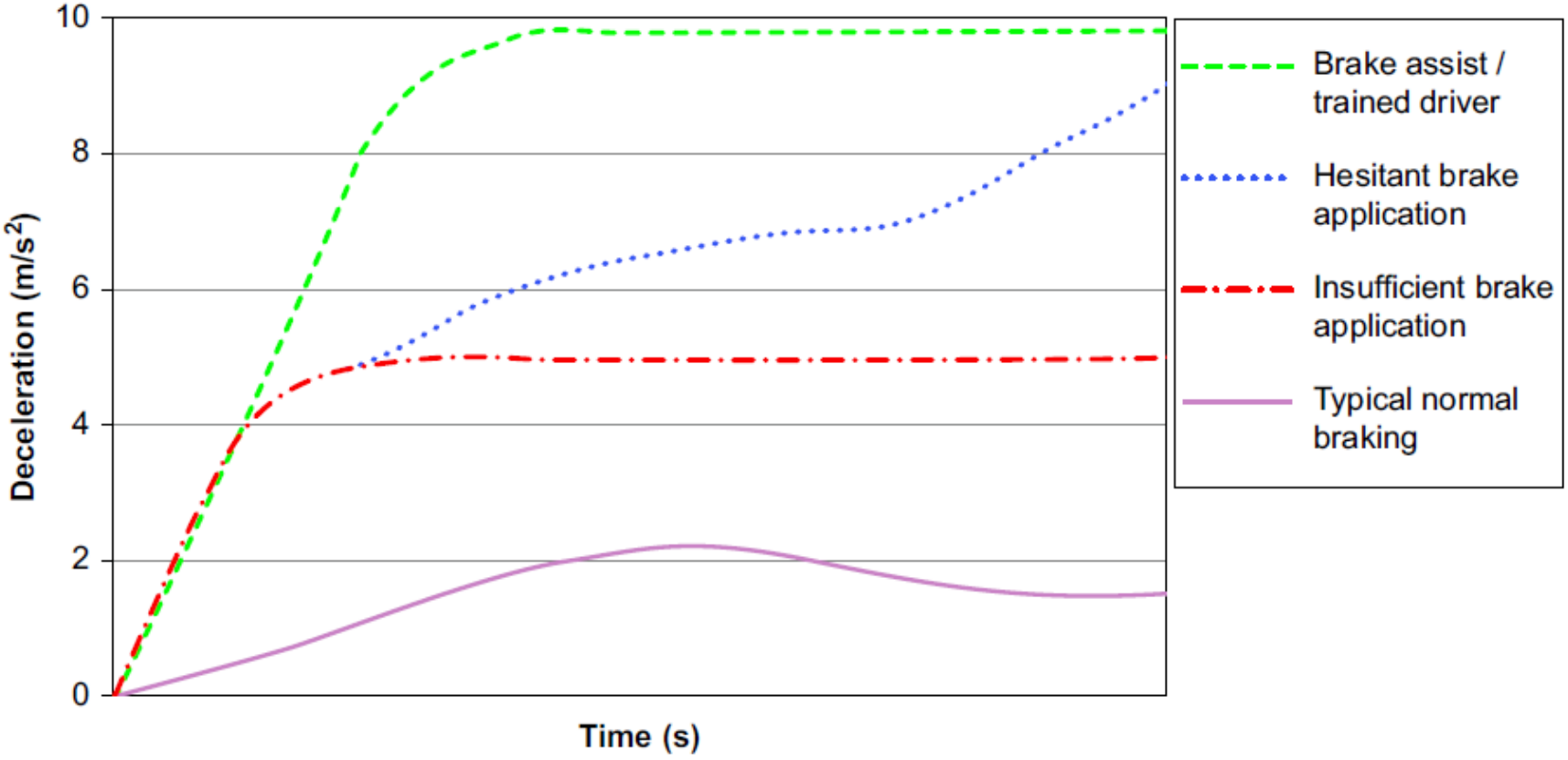

Figure 11.19: Effectiveness of Emergency Brake Assist (Moore, 2013).

Applying the brakes quickly can be recognized by the EBA function, which can use the ABS/ESC system to increase the brake actuation pressure to maximize adhesion utilization and force ABS operation; if ABS is active then the vehicle is also steerable. Alternatively, and especially for vehicles with ABS but not ESC, a spring mechanism in the brake master cylinder can trigger the required increase in brake pressure.

Adaptive Cruise Control (ACC)

Adaptive Cruise Control (ACC) combines constant speed cruise control with the automatic positioning of a road vehicle with respect to another vehicle in front. It uses the vehicle's engine and transmission to maintain the set speed, and the vehicle's braking system as necessary to maintain a safe distance behind the vehicle in front. The primary components of ACC are a microprocessor controller and a range finding sensor, which scans the road ahead and reports the location and rate of approach of a vehicle or obstacle in front.

The controller then determines the safest course of action for the vehicle and the driver and implements it. The possible responses include:

- No intervention
- Request a vehicle speed and/or engine torque decrease
- Request the brakes to be applied
- Warn the driver of a potentially critical stop situation.

An ACC system can request a vehicle deceleration to match the speed of the preceding vehicle and then will resume the preset speed and distance once the road in front of the vehicle is clear. Requests to reduce vehicle speed or engine torque, or to apply the brakes, are passed to the engine controller, and to the ESC module if the requested vehicle speed reduction cannot be achieved via engine/transmission braking alone.

Collision Mitigation by Braking (CMbB)

As explained in Chapter 8, a 'Collision Mitigation Braking System' (CMBS) is a type of 'Advanced Emergency Braking System' (AEBS) that can autonomously apply emergency braking in order to mitigate the severity of a collision that has become unavoidable. In comparison, a 'Collision Avoidance Braking System' (CABS) can autonomously apply emergency braking in order to avoid a collision.

An ACC forward sensing system automatically controls the vehicle to decelerate the vehicle gently to match the vehicle's speed with that of a preceding vehicle if slower than the set cruise speed. The same system can also detect a potential collision if the relationship between the vehicle closing speed and the distance predicts it, and take appropriate control action including a brake pre-fill and emergency braking typically up to 8 m/s^2.

Electric Parking Brake (EPB) Systems and Hill Start Assist (HSA)

Current EPB systems take the form of either a cable-operated device consisting of a single electromechanical actuator with an electronic controller (part of the brake ECU), which actuates the parking brakes via bowden cables, or an electric motor directly attached to the disc brake caliper. The latter type of EPB system saves package space but the caliper may have a weight penalty, which may not be acceptable because of the increased unsprung mass.

The caliper may also be pre-actuated using hydraulic actuation pressure via the ESC module and then locked electromechanically. Combining an EPB system with ESC can provide the following optional additional functions:

- Hydraulic support for the parking brake (e.g. on a grade)
- Hill Start Assist
- Automatic Vehicle Hold.

Trailer Sway Control (TSC)

Trailer sway or ‘snake’ is a dynamic instability where the trailer (usually centre axle types, especially caravans) sways from side to side with increasing amplitude while travelling, and can be initiated by side winds, track ruts, fast steering movements or a badly configured trailer load (drivers should always ensure that there is a small downward tow hitch force to minimize the potential for instability). It is extremely difficult to recover from trailer sway once it has started, and the end result is usually an overturned trailer and possibly the towing vehicle as well.

Torque Vectoring by Braking (TVbB)

Torque vectoring is a feature that is now often installed on high-performance vehicles to actively direct the drive torque at the road wheels to maximize adhesion utilization during acceleration. Torque Vectoring by Braking (TVbB) provides some of the benefits of TVbD through the use of the vehicle's brakes. Brake torque is applied to one driven wheel on a drive axle, which directs ('vectors') drive torque to the opposite wheel via the differential. Excessive wheel spin is prevented and more importantly yaw rate during manoeuvres can be controlled before stability control thresholds are reached and TCS or ESC intervenes.

Engine Drag Control (EDC)

On some very low friction surfaces (e.g. ice) a vehicle may become unstable when the throttle is closed and the residual drag torque from the engine prevents the driven wheels from rotating sufficiently. To avoid this phenomenon the brake control system requests a positive torque (torque increase) from the powertrain control system to compensate for the engine drag and powertrain losses during specific driving manoeuvres. This feature is of particular benefit for RWD vehicles, but can also be usefully installed on FWD vehicles.

ESC Mode Switching

It can sometimes be beneficial for the driver to have more than one stability control setting. Some passenger car manufacturers fit an on/off ESC switch while others choose not to; such a switch may be a physical switch or a software switch. ESC is fitted to vehicles to assist with the control of their dynamic stability in use, and there can be situations where ESC is not required (e.g. driver choice), tyre/road adhesion settings need to be changed (e.g. driving on grass), or its operation aggravates problems that can occur in certain types of driving conditions, e.g. deep snow.

Some of the options that are currently available on passenger cars are summarized in Table 11.3.

Table 11.3: Examples of ESC Switch Modes

ESC Modes	No ESC Switch	ESC Switch with 'Get out of Deep Snow' Function	Cars with a 'Sport Heritage'	Cars Designed also for the 'Racetrack'
ABS, EBD, BAS	Active	Active	Active	Active
ACC interface	Active	Active	Off	Off
CMbB interface	Active	Active	Off	Off
Engine TCS	Active	Off	Extended tuning	Off
Brake TCS	Active	Active	Extended tuning	Off
Stability control	Active	Active	Extended side slip	Off

Regenerative Braking

The increasing functionality of electronic braking control systems to enhance road safety for road vehicles has also been associated with alternatives to the use of friction brakes for retarding the vehicle. For many years it has been accepted that a vehicle's kinetic energy dissipated during braking is lost to the environment. Even the provision of retarders (or endurance brakes) to augment the braking power of the friction (foundation) brakes on a road vehicle has not changed the accepted practice that the heat energy from braking is generally dissipated to the environment.

Challenges for road vehicle regenerative braking systems therefore include:

- The provision of two types of braking system, namely friction and regenerative, necessary to meet legislative requirements under all operating conditions.
- Transition between and distribution of regenerative and friction braking.
- Stability and response time under low road adhesion conditions and emergency braking.

Brake system technologies that have been described in this book and that could be suitable for vehicles with regenerative braking include:

- Electrohydraulic brake (EHB)
- Electromechanical brake (EMB)
- Conventional brake with active booster and electric vacuum pump
- Electromechanical rear and conventional front brake.

Regenerative braking systems aim to recover, store and reuse some of the vehicle's braking energy to improve fuel efficiency or boost the range of electric and hybrid vehicles (FEV/HEV). Energy storage media include electric batteries and/or ultra capacitors, flywheels and hydraulic accumulators. Some form of motor/generator augments the friction braking (from the foundation brakes) where possible; as the driver applies the brakes through a conventional pedal, the motor/generator creates braking torque that may provide sufficient retarding force to meet the driver demand, or may supplement the friction braking.

An example layout for a passenger car is shown in Figure 11.20.

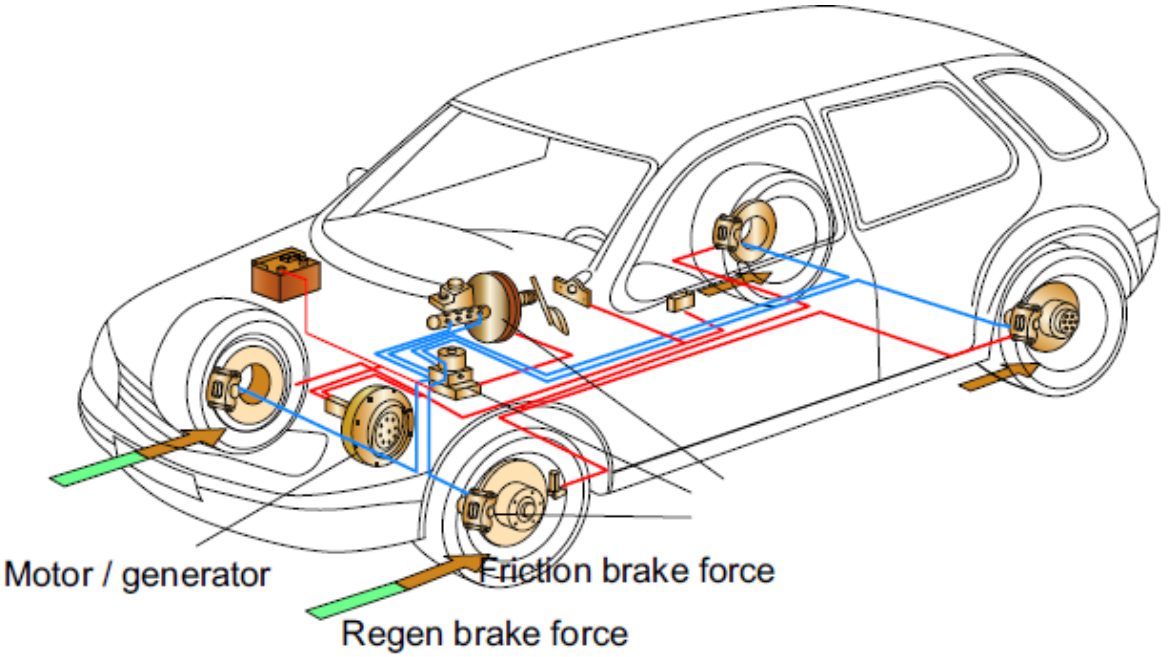

Figure 11.20: Hybrid Vehicle Regenerative Braking System (Continental).

There are different levels of 'hybrid' road vehicles:

- ✓ Micro hybrid. Some form of alternative power source in the vehicle provides low levels of energy conversion and reuse, e.g. providing regenerative braking by using the vehicle alternator to charge the vehicle battery, or drive ancillary equipment only during vehicle deceleration.
- ✓ Mild hybrid. Some form of alternative power source in the vehicle provides sufficient power to drive the vehicle to some extent, e.g. by augmenting the internal combustion engine (ICE) during acceleration.
- ✓ Full hybrid. Some form of alternative power source in the vehicle provides sufficient power to drive the vehicle without assistance from the ICE.
- ✓ Plug-in hybrid. The vehicle's batteries can be recharged by connecting an external power source to further decrease the reliance on the ICE.

Standard legislative drive cycles are now used extensively by vehicle manufacturers to define vehicle operation in the operating domain. These are intended more for evaluating engine usage and fuel consumption, and as a result their applicability to braking events is very limited. If such cycles are used to evaluate regenerative braking systems, the indicated results may not be representative of real-world usage, performance and benefits. For this reason regenerative braking systems should be evaluated based on field driving data rather than legislative drive cycles. On flat roads it has been possible to define the work done by the brakes in terms of a duty factor D_k as shown in Equation (11.13)

D_k describes the energy dissipated during braking per unit time after allowing a correction factor for drag losses, and can be related to the mean journey road speed V and a parameter V_0 that relates to the route and represents the maximum speed that the test route could be driven without applying the brakes (and without engine braking).

$$D_k = A\left[\frac{\overline{V}}{V_0^{0.75}}\right]^B \qquad (11.13)$$

Values for the constants A and B were found to be 9.61 $*10^{-6}$and 6.3 respectively. The mean journey speed can be related to the maximum road speed V_{max} of the vehicle used, as shown in Equation (11.14):

$$\overline{V} = \beta V_0^{0.62} V_{max}^{0.45} \qquad (11.14)$$

The value of the parameter β depends upon the manner in which the vehicle is driven: 0.93 for normal driving and 1.17 for fast driving.

The legislative aspects of the control and performance of 'blended' brake systems on vehicles with regenerative braking are covered in Chapter 8 of this book. As explained there, in EU braking legislation regenerative braking systems are separated into two categories:

- Category A: a regenerative braking system that is not part of the service braking system; typically regenerative braking is introduced when the accelerator pedal is released.
- Category B: a regenerative braking system that is part of the service braking system.

An example of a brake system blending profile required during a brake application is illustrated in Figure 11.21.

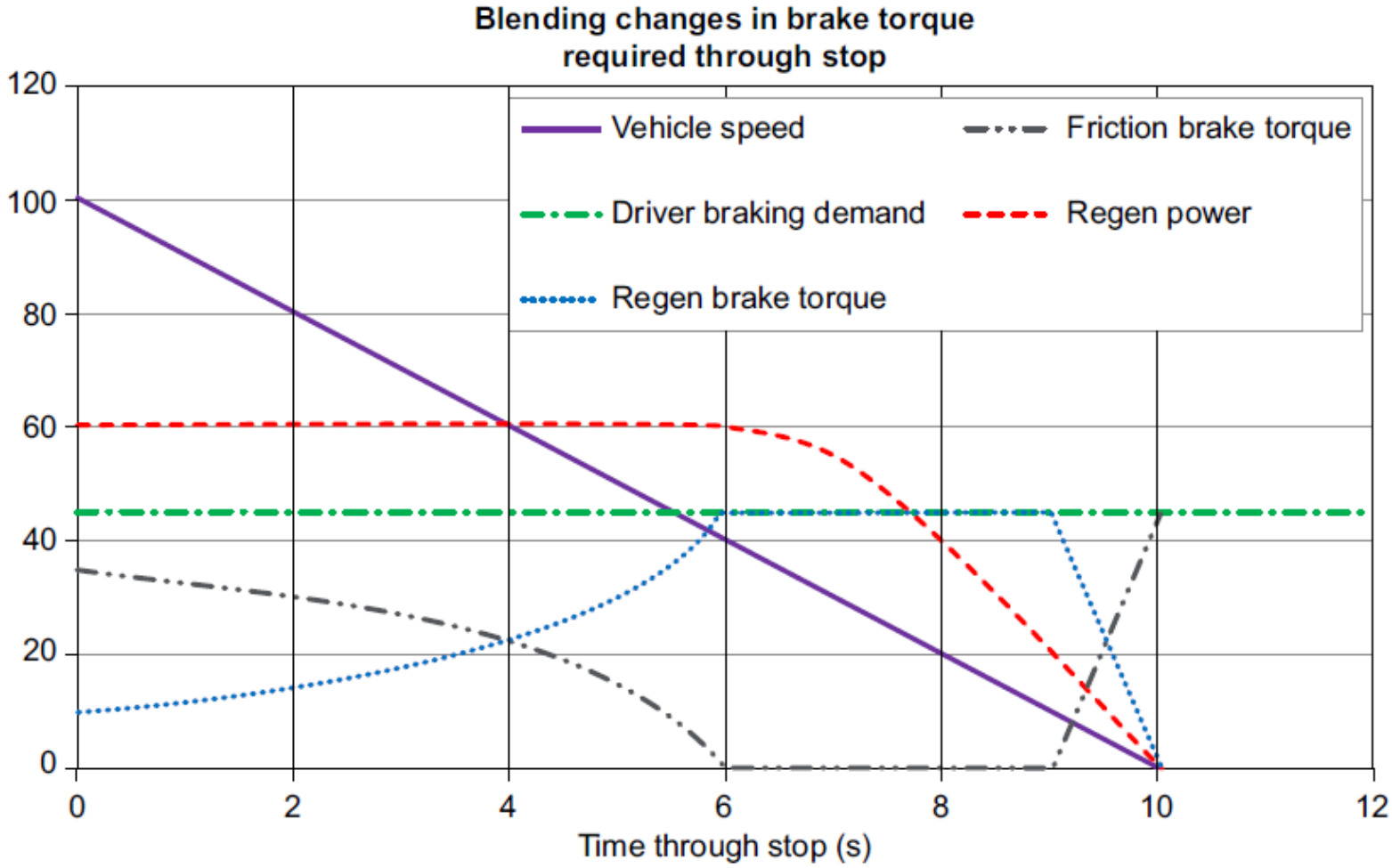

Figure 11.21: Example of a Brake System Blending Profile During a Brake Application (Curry, 2013).

System Warnings and Driver Interfaces with Electronic Braking

The modern vehicle braking system has many electronic functions and capabilities and it is essential that the driver is aware firstly of which functions are being utilized, and secondly if any particular function has failed or is not working properly. The requirements for braking system warnings and indicators are included in the UN Regulations 13 and 13H, which means that requirements and symbols are well standardized across different vehicles.

Red warning lights typically represent a brake symbol in the instrument cluster, which must illuminate under specified conditions including:

- When the parking brake is applied (manual parking brake or EPB)
- When a low level of the brake fluid in the reservoir is detected
- When EBD is disabled due to a system failure.

Chapter twelve

Case Studies in the Braking of Road Vehicles

The chapters in this book have presented some of the basic theory and practice of road vehicle braking, and some examples of design calculations have been included to demonstrate how the theory is applied. The purpose of this chapter is to present and discuss some examples that illustrate firstly an experimental verification of a braking system design by comparison of measured braking performance (in terms of deceleration vs. actuation hydraulic line pressure for the basic braking system of an example passenger car), and subsequently how and why the actual performance of brakes and braking systems can vary from the design performance.

As explained in previous chapters and referring particularly to Figure 9.3, the input to a vehicle braking system is the driver effort, i.e. the force applied to the brake pedal, and the desired response is retardation force to decelerate the vehicle. Drivers expect consistent and reliable performance from the braking system, therefore variations from the design performance can be regarded as failure modes, and as indicated in Figure 9.3 these can include:

- Retardation force too low
- Retardation force too high
- Variable retardation force
- Unplanned or unintended retardation force.

Brake System Design Verification

In Chapters 3 and 4 the theory relating to the braking dynamics of rigid vehicles with two or more axles and vehicle/trailer combinations with more than two axles was presented, and examples were shown to illustrate braking performance parameters such as efficiency and adhesion utilization. In Chapter 6 braking system design and actuation layout was explained and examples were presented for a passenger car (specification in Table 6.2) and a commercial vehicle (specification in Table 4.6).

In Chapter 9 methods of experimental brake testing were presented, describing how the braking performance of a road vehicle could be evaluated. An example is presented here (Marshall, 2007) to illustrate the verification of a passenger car braking system design by comparing the calculated (predicted) braking performance with that measured experimentally on the vehicle. The vehicle design specification is summarized in Table 12.1 and the brake system design data are summarized in Table 12.2.

Table 12.1: Passenger Car Design Specification (Marshall, 2007)

Design Parameter	Specification	
Loading Condition:	DoW	Test Weight (Partially Laden)
Wheelbase, E (mm)	2754	2754
Vehicle mass (kg)	1486	1710
Vehicle weight (N)	14,575	16,780
Dynamic radius of tyres (mm)	307	307
Centre of gravity height (mm)	565	570
Position of centre of gravity behind the front axle, L_1 (mm)	1132	1243
Position of centre of gravity in front of the rear axle, L_2 (mm)	1622	1511
Front axle weight, N_1 (N)	8585	9205
Rear axle weight, N_2 (N)	5990	7575
GVW (N)	18,394	18,394
Vehicle maximum speed (km/h)	210	210

Table 12.2: Brake System Design Data (Marshall, 2007)

Design Parameter	Specification	
	Front – Single Piston Sliding Caliper Disc Brake	Rear – Single Piston Sliding Combined Caliper Disc Brake
Caliper piston diameter (mm)	57	38
Threshold pressure (bar)	0.75	1.5
Pad friction coefficient	0.4	0.38
Effective radius of rotor (mm)	125	119
Actuation system efficiency (η)	0.95	0.95

The measured brake performance, although close, is slightly lower than the calculated values, as illustrated in Figure 12.1 in the region where wheel lock does not occur.

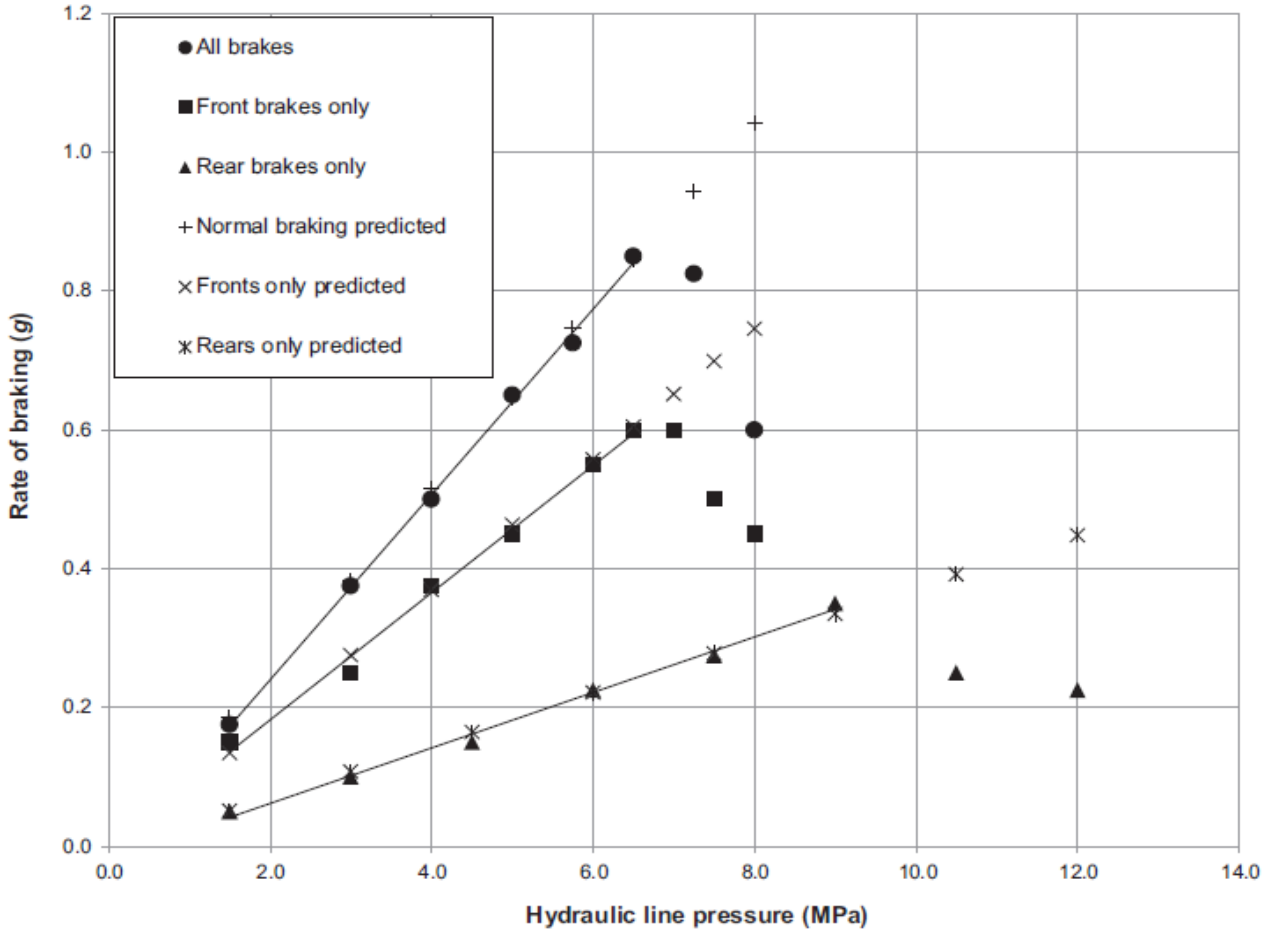

Figure 12.1: Comparison of Measured and Predicted Brake Performance (see Table 12.3).

Figure 12.1 indicates that front wheel lock (FWL) occurred at 7 MPa and because this data point lies well away from the linear characteristic it can be assumed that the maximum deceleration occurred at about 6.5 MPa, when the predicted rate of braking is z = 0.605. Similarly rear wheel lock (RWL) occurred at 9 MPa but this data point lies on the linear characteristic; therefore it can be assumed that the maximum deceleration occurred at this actuation pressure, for which the predicted rate of braking is z = 0.335.

On this vehicle the actuation system design data was:

- Pedal ratio = 3.26:1
- Master cylinder piston diameter = 23.89 mm
- Boost ratio = 4.5:1.

Using Equation (6.21c), the driver effort required to achieve z = 0.25 in the 'servo-fail' condition at GVW (= 18,394 N) would be approximately 300 N.

The design calculation does not include the tyre/road coefficient of adhesion so the effect of wheel lock has not been covered. The reasons for the difference between the calculated and measured values could include:

- ✓ The assumed actuation system efficiency is too high (estimated at 95%).
- ✓ The coefficient of friction m between the brake pads and discs may be different (lower) than the design values (0.4 front, 0.38 rear) because of heat generation and temperature.
- ✓ There may be experimental error, e.g. arising from wind or incline (which cannotalways be excluded even with repeat testing in opposite directions).
- ✓ Calibration of the instrumentation may be imperfect.

Braking Performance Variation

In the previous section the measured performance of a vehicle braking system was shown to be close to the design performance. The measurement of the vehicle's braking performance was made under carefully controlled test conditions in the 'as new' condition. It is good practice to quantify the magnitude of any such variation and evaluate its effects on the vehicle's braking performance at the design stage so that top and bottom limits to the design operation can be set. Working to a $\pm$10% tolerance on friction materials (see Chapter 2) the braking performance range is illustrated in Figure 12.2.

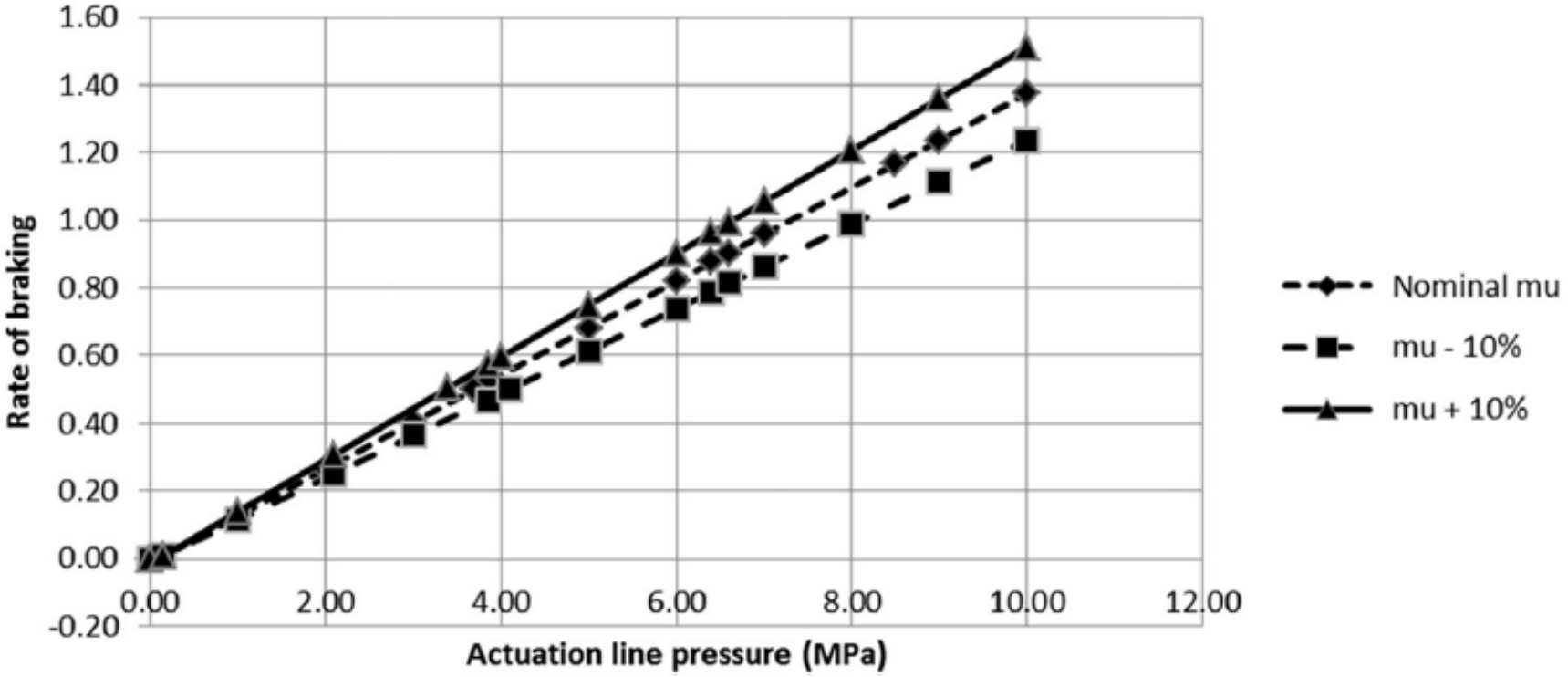

Figure 12.2: Braking Performance Range at 10% μ.

Figure 12.3 shows photographic images of one of a pair of badly corroded brake discs taken from the rear axle of a sports utility vehicle (SUV) on which a thick layer of rust had built up over a region towards the inner radius of the rubbing path on the inner face of the brake disc.

Figure 12.3: Corroded Brake Disc.

Another example of brake performance variation over time was reported by Day and Harding (1983) relating to an S-cam drum brake as used on an articulated vehicle semitrailer. Figure 12.4 shows the specific torque of a 420 mm * 180 mm S-cam drum brake measured on an inertia dynamometer over nearly 4000 brake applications, to investigate the cause of brake performance variation on semi-trailers reported by operators in the field (4000 brake applications were estimated as possibly representing as much as 32,000 km on long-distance haulage operation).

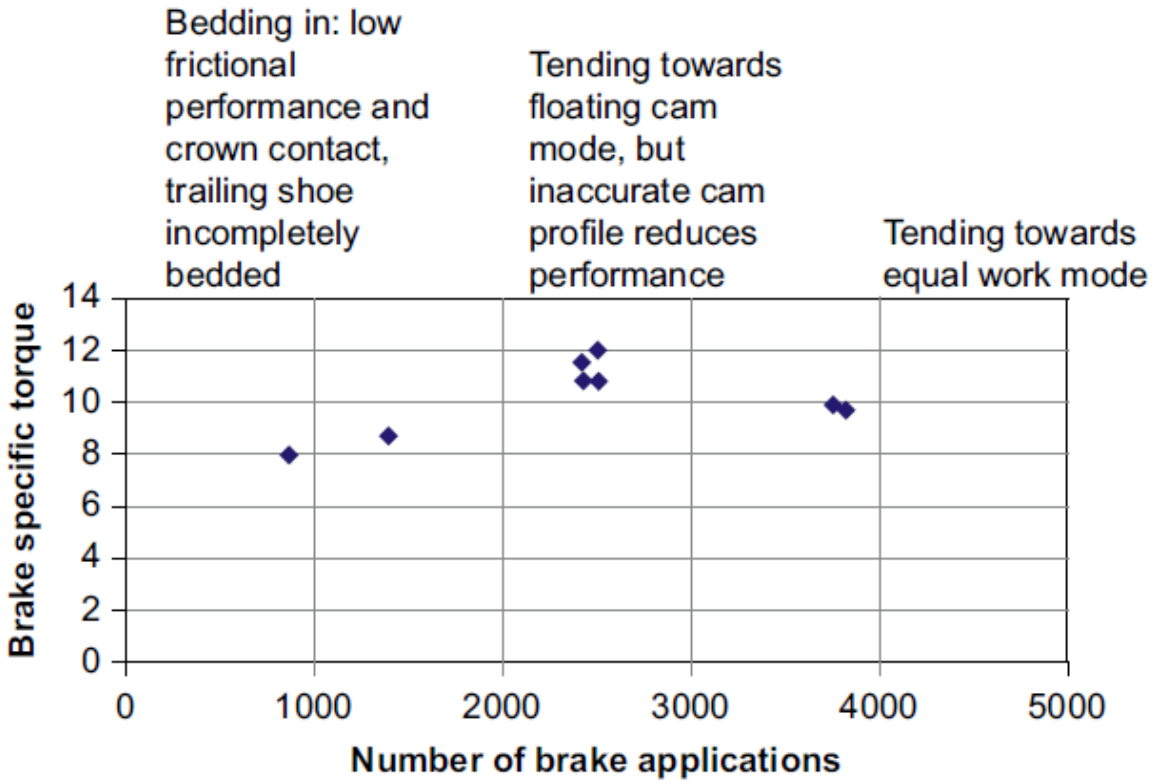

Figure 12.4: Measured S-cam Drum Brake Specific Torque vs. Time (Day and Harding, 1983).

The residual torque from the front disc brake of a passenger car exhibiting the symptoms of a dragging brake was measured under quasi-static conditions at ambient temperature, and found to be approximately 30 Nm. An FE thermomechanical analysis was conducted in which a circumferentially uniform steady-state heat flux input equivalent to a constant torque of 30 Nm at a vehicle speed of 50 km/h was applied to the rubbing surfaces of the friction ring of a simple FE model. A surface heat transfer boundary condition was applied to the exposed surfaces of the disc using values of heat transfer coefficient derived for the specific brake installation from brake cooling curves on an actual vehicle.

The calculated steady-state temperature distribution is shown in Figure 12.5.

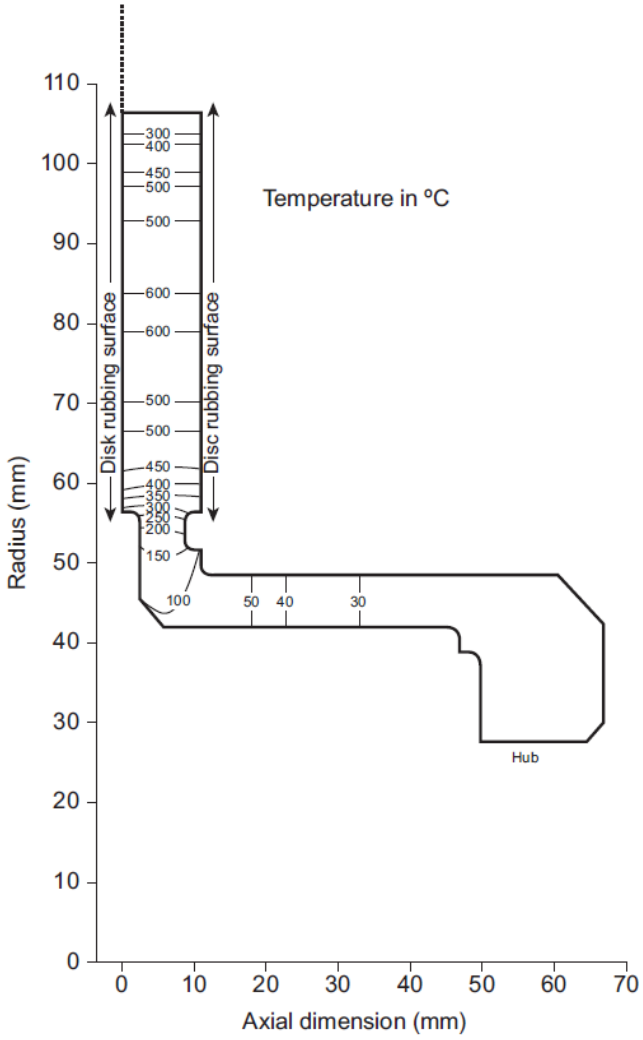

Figure 12.5: Temperature Distribution of a Brake Disc Subject to a Constant 30 Nm Drag

Interaction Between the Brakes and the Vehicle

There are many interactions that occur between a vehicle and its brakes, either by structural connections, e.g. the suspension, or the actuation system, or by the transmission of heat and noise to the vehicle's driver and other occupants. Brake judder, for example, has been shown to be more of a problem where the effect is transmitted to the driver (and passengers), e.g. by steering shake, cabin shake or noise, and less where the judder at the brake is just the same but is attenuated rather than transmitted by the vehicle's structure. The consistency of a vehicle's braking performance not only extends to longitudinal braking performance, but also to lateral stability and consistency.

The kinematics of vehicle suspension systems can introduce ‘compliance steer’ because lateral or longitudinal forces at the tyre contact patch deflect the suspension bushings and change the camber and toe angles (Momoiyama and Miyazaki, 1993). Compliance exists in all road vehicle suspension systems because they may include elastomeric suspension pivot bushes, cross-member mounts, steering rackmounts, and the elastic deformation under the application of braking forces of components such as suspension and steering links, and subframes.

Compliance in the suspension system is viewed as essential to achieve a good ride characteristic, but compliance steer is considered to be one of the biggest contributors to straight-line stability during braking. As an example, when the steering control arms move because of elastomeric bush deflection a change in steering angle can result, and if this is different side to side, the vehicle can steer to one side while braking. Klaps and Day (2003) reported a series of experiments to investigate steering drift during braking on a 1.2 km straight test track.

The car had a MacPherson strut design of front suspension, in which a lower suspension arm provided lateral and longitudinal location (Figure 12.6), and was known to demonstrate a small amount of steering drift during braking.

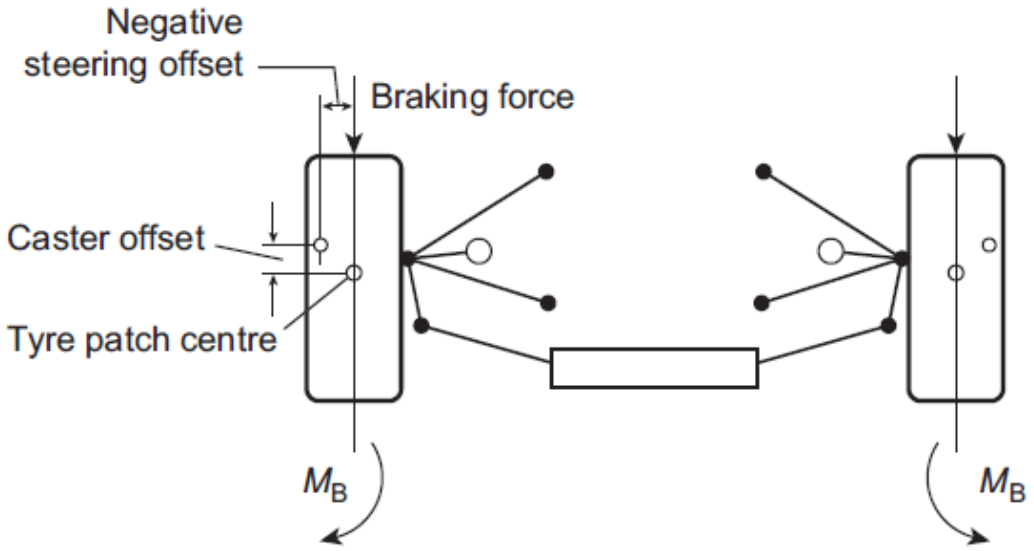

Figure 12.6: Test Car Steering Geometry (Klaps and Day, 2005).

The following parameters were investigated:

A. Tyre and brake temperature

B. Suspension geometry toe steer curve

C. Steering gear housing/engine subframe reinforcement cover

D. Front suspension lower wishbone rear bush stiffness

E. Wheel offset (y-direction).

Having established that the suspension compliance and steering offset had a significant effect on steering drift during braking, further vehicle tests were carried out to investigate how steering drift during braking could be reduced or eliminated. Steering drift during braking to the left occurred as shown in Figure 12.7; under fixed control (the driver held the steering wheel in the straight-ahead position) the yaw velocity initially increased and then decreased towards the end of the deceleration, but remained positive throughout, indicating a continuous drift to the left.

Steering drift during braking to the left occurred as shown in Figure 12.7;

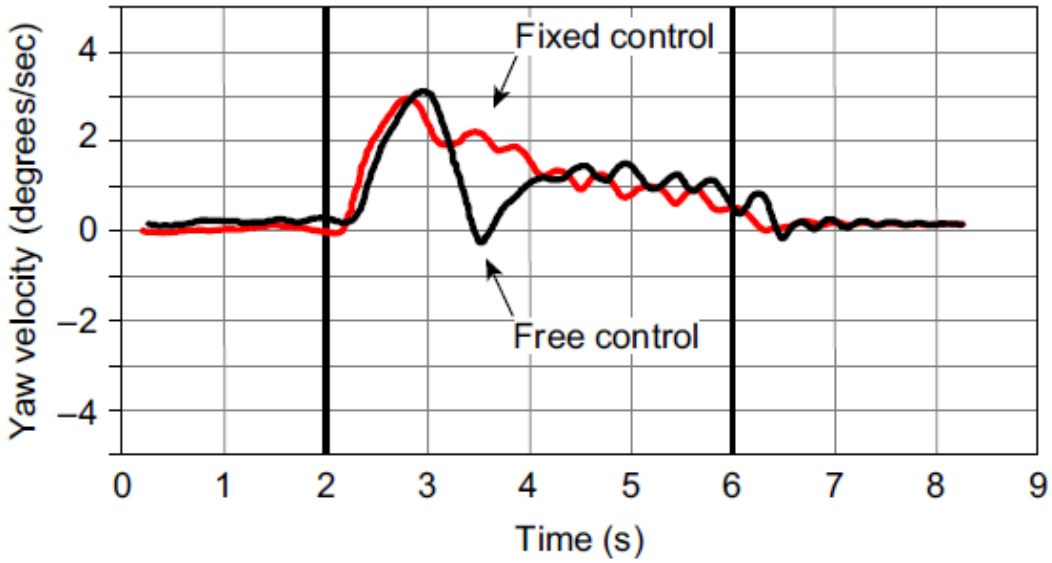

Figure 12.7: Typical Yaw Velocity Measurements, Fixed and Free Control (Klaps and Day, 2005).

Under free control (hands off the steering wheel) the yaw velocity characteristic also remained positive throughout, showing an initial increase, then a sharp decrease and then an increase before decreasing towards the end of the deceleration. Again this represented a drift to the left, but was less continuous. The brake pressures were measured and found to be higher at the left front wheel than at the right front wheel, but when the brake pipe connections were swapped from left to right, the steering drift to the left remained.

Figure 12.8(a) and (b) illustrate the improvement in terms of toe steer changes during the braking event from the original to the new design.

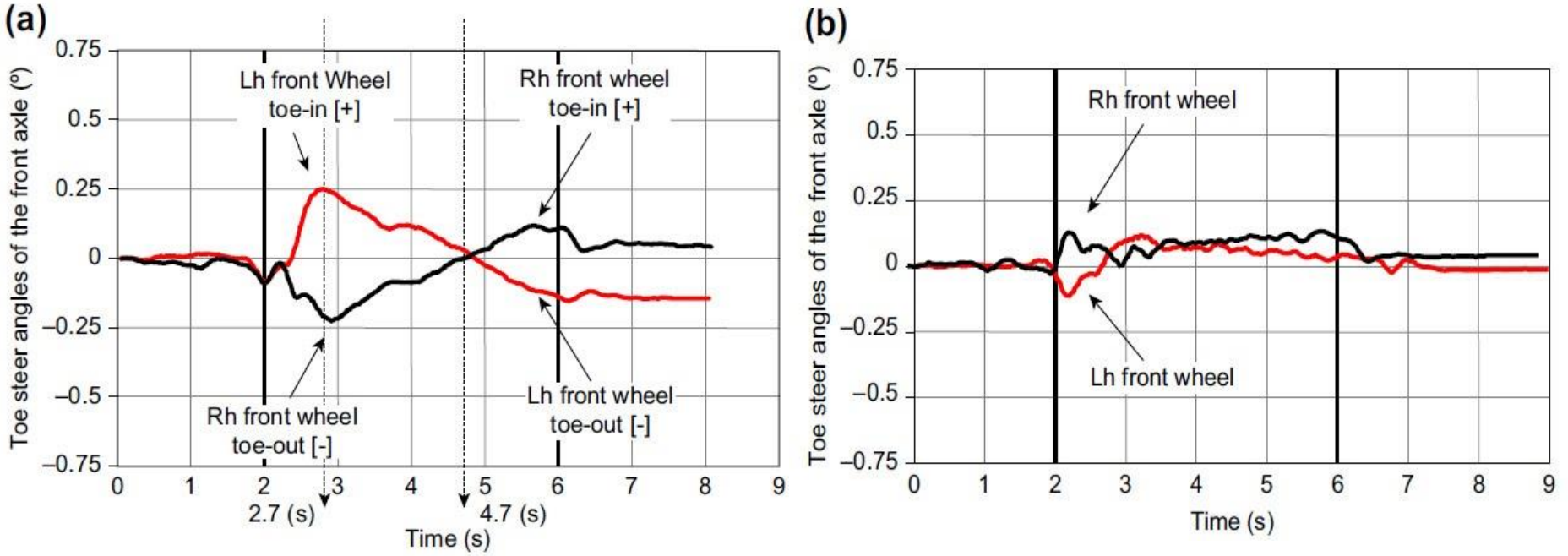

Figure 12.8: (a) Toe Steer Angles, Original Bushes. (b) Toe Steer Angle, Redesigned (Stiffer) Bushes (Klaps and Day, 2005).

From the work reported, the major cause of steering drift during braking was found to be side-to-side dynamic variation in the deformation and deflection of suspension and steering components and not any form of side-to-side variation in braking forces. The most significant effect was the stiffness of the rear bush in the lower suspension arm. The deflections and compliance arising from this component generated large changes in the side-to-side camber and steering offset, changing toe steer angles during braking, which actually reversed during the braking event.

Mixed-Mode Braking Systems

Road vehicles that are fitted with other types of braking systems such as endurance braking (retarders) and regenerative braking in addition to conventional friction foundation brakes are called ‘mixed-mode’ braking systems. They need to have actuation control systems that integrate or blend the function of each type to provide consistent and reliable braking under all conditions of operation. As stated in Chapter 10, the challenges of blending regenerative braking with friction brakes so that brake operation is completely transparent to the driver are considerable.

The basic design of a mixed-mode braking system needs to start with the same considerations of adhesion utilization and braking distribution between the axles of the vehicle, as were introduced in Chapters 3 and 4 of this book, and an example based on a passenger car vehicle with regenerative braking is introduced here.

The total braking force on a two-axle rigid road vehicle is defined by Equation (3.16), assuming no lateral variation:

$$Pz = T_1 + T_2 \tag{3.16}$$

In a mixed-mode braking system the brake forces may comprise a friction brake force component and a 'second mode' brake force component, e.g. from a retarder or from regenerative braking, so Equation (3.16) can be rewritten as:

$$Pz = (T_{1fb} + T_{1rb}) + (T_{2fb} + T_{2rb}) \qquad (12.1)$$

where the subscript '*fb*' refers to friction brake force and '*rb*' refers to regenerative brake force. As explained in Chapter 3, the ratio of the braking force generated by the front wheels to the braking force generated by the rear wheels of a two-axle rigid road vehicle is defined in Equation (3.19a) as the ratio X_1/X_2, where X_1 and X_2 are the proportion of the vehicle's total braking force generated at the front and rear axles respectively. Therefore:

$$\left(T_{1fb} + T_{1rb}\right) / \left(T_{2fb} + T_{2rb}\right) = X_1/X_2, \text{ and } X_1 + X_2 = 1 \qquad (12.2)$$

In many designs of hybrid (HEV) or electric (FEV) vehicles, regenerative braking operates only on the drive axle, so for an FWD car, only friction braking applies at the rear wheels, i.e. $T_{2rb} = 0$. Despite having two drive axles, some 4WD vehicles also apply regenerative braking only on one axle, e.g. the rear axle, in which case only friction braking applies at the front wheels, i.e. $T_{1rb} = 0$. From a basic braking stability point of view, the limiting rate of braking (z) for a specified adhesion coefficient (k) is still defined by the vehicle's dimensions as in Equations (3.26) and (3.27), and adhesion utilization (Equation (3.40)) is defined in the same way.

Thus, the design of a road vehicle's braking system can still follow the procedure set out in Chapters 3 and 4, which uses considerations of adhesion utilization to ensure that a good basic design is achieved, provided that all modes of braking (as appropriate) are included in the calculation of brake forces at each axle.

$$f_i = \left(T_{ifb} + T_{irb}\right)/N_i \qquad (3.40)$$

A major challenge with regenerative braking is that the brake force developed by the regenerative braking system is highly variable, e.g. it depends upon road speed and the capacity of the energy storage system to receive and hold the recuperated energy (e.g. the state of charge of the batteries of an HEV). Therefore, in operation, the vehicle's brake control system must blend the brake force from the regenerative braking system with the brake force from the friction brakes so that the total brake force at each wheel creates thetotal vehicle braking force, which matches the driver's demand.

The detail of brake blending control systems is beyond the scope of this book, but the principle is illustrated in the following example of an HEV as specified in Table 12.5.

Table 12.5: Vehicle and Braking System Data

Electric Vehicle and Braking System Data	
Wheelbase	2700 mm
Position of centre of gravity (behind front axle)	1444 mm (driver only) 1512 mm (GVW)
Height of centre of gravity	690 mm (driver only) 750 mm (GVW)
Effective radius of tyres	355 mm
Unladen mass	2192 kg
Front axle static weight	10,000 N (driver only) 11,000 N (GVW)
Rear axle static weight	11,200 N (driver only) 14,000 N (GVW)
Maximum speed	140 km/h

Table 12.5: Vehicle and Braking System Data

Brake data	
Front Disc Brakes – Single Piston Sliding Caliper	
Piston diameter	59 mm
Threshold pressure	0.5 bar
Pad friction coefficient	0.40
Effective radius of rotor	160 mm
Rear Disc Brakes – Single Piston Sliding Combined Caliper	
Piston diameter	47 mm
Threshold pressure	0.8 bar
Pad friction coefficient	0.38
Effective radius of rotor	160 mm

This vehicle has regenerative braking on the rear axle only, i.e. $T_{1rb} = 0$, provided by the 60 kW electric motor/generator, and for the purposes of this example 60 kW can be assumed to be the maximum available regenerative braking power $\dot{Q}_{rb}$(ignoring losses and inefficiencies in the system). The regenerative braking torque at the rear axle is calculated from Equation (12.3),

$$\tau_{2rb} = \dot{Q}_{rb}/\omega \qquad (12.3)$$

and the torque road speed characteristic is shown in Figure 12.9.

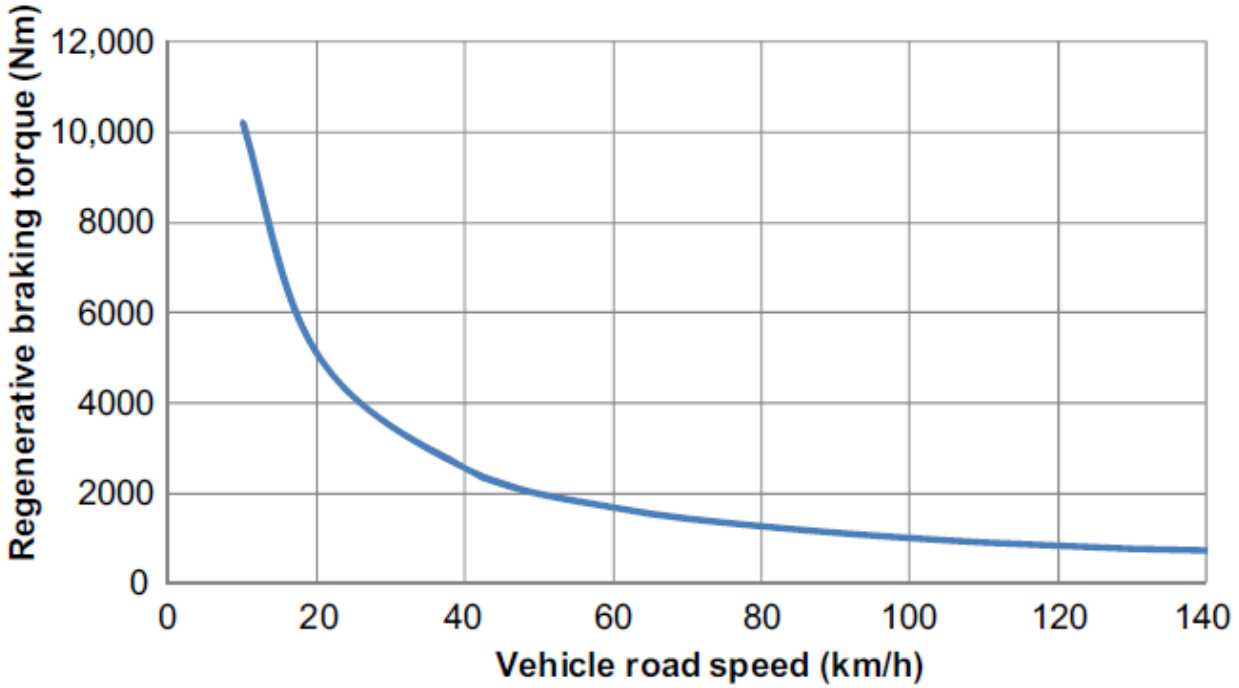

Figure 12.9: Regenerative Brake Torque vs. Road Speed for the Example Vehicle (Rear Axle Only).

The brake torque shown in Figure 12.9 represents the maximum regenerative braking torque (ignoring losses and inefficiencies in the system) available at any road speed. It is clear that the regenerative brake torque and hence brake force is lowest at high road speeds and greatest at low road speeds, although regenerative braking is normally disabled at very low speeds. In practice, electric motor/generators are torque limited and speed limited to avoid damage, and their operational power rating is usually specified in terms of transient, intermittent and continuous power modes, the highest being transient mode.

At road speeds of 40 and 140 km/h (maximum speed), two extremes of mixed-mode braking system operation have been examined on this example vehicle: no regenerative braking and maximum regenerative braking. The purpose is to illustrate the effect on the vehicle braking performance and the difficulties involved. Using Equations (3.38) and (3.39), the ideal braking ratio (X_1/X_2) to achieve optimum braking (100% braking efficiency) can be shown to vary from 47/53 at z = 0.1 to 70/30 at z = 1 for the vehicle fully laden (GVW).

Using Equation (6.27) the hydraulic actuation pressure required at the front and rear brakes is shown in Figure 12.10, which represents the condition with no regenerative braking. The other extreme (maximum regenerative braking) could be achieved in several ways, but two are considered here to illustrate the options.

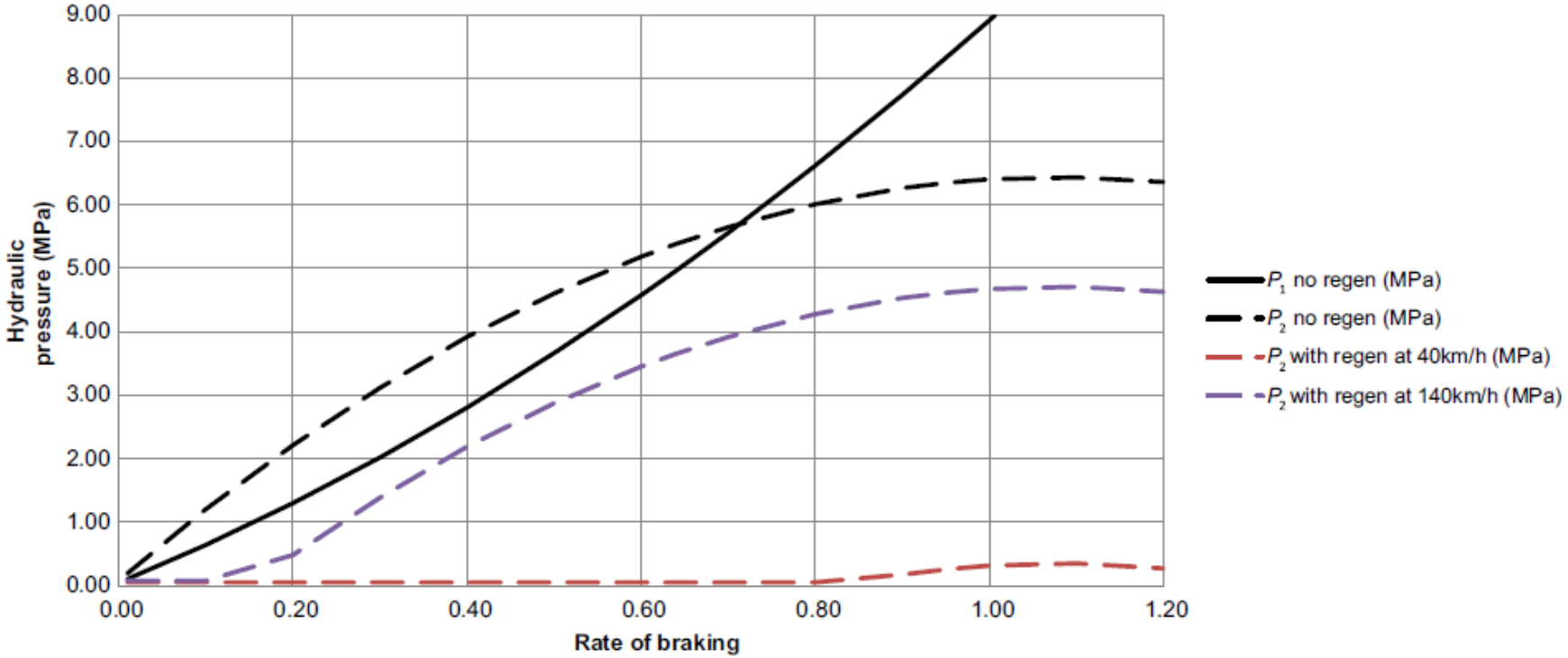

Figure 12.10: Required Hydraulic Actuation Pressure to Achieve Optimum Adhesion Utilisation vs. Rate of Braking (Vehicle at GVW).

First, the regenerative braking on the rear axle of the vehicle could take precedence over front axle braking until the limit of adhesion were approached. At this point the front brakes would be actuated. This would have the advantage of maximizing braking energy recovery, but operating the rear wheels at significant levels of braking slip and the front wheels at zero braking slip with the potential for a sudden change being required could introduce handling peculiarities that would probably be unacceptable.

The second approach would be to use the regenerative braking to achieve ideal braking, which is also illustrated in Figure 12.10. The regenerative braking contributions at two speeds, 40 km/h (representing low-speed operation) and the vehicle's maximum speed of 140 km/h to represent high-speed operation, are shown. This illustrates that at low speed the friction brakes are not required below a rate of braking of about 0.8, and even at high speed the front brakes define the actuation pressure requirement.